IFITMs & Immunity to Respiratory Viruses in the Ferret Model

William Samuel James Horman

Submitted in total fulfilment of the requirements of the degree of Doctor of Philosophy

September 2021

Department of Microbiology and Immunology

at the Peter Doherty Institute for Infection and Immunity,

The University of Melbourne

Abstract

Respiratory virus outbreaks pose a major threat to human health, with many of these zoonotic threats having potential for global pandemics. In order to gain a greater understanding of these viruses, considerable research into the immune responses elicited against these pathogens occurs in the ferret model for human disease. This PhD focussed on using this model to assess two of these pandemic threats in the ferret model, whilst gaining valuable insight into the immune mechanics at work within this understudied animal model.

An infection study in the ferret model was used to assess the cellular immune response against A/Anhui/1/2013(H7N9) avian influenza virus in Chapter 3. This study found ferrets to have variable disease outcomes towards H7N9 infections, with severe disease marked by time dependent increases in two pro-inflammatory cytokines, IL-6 and IFNγ. Unlike other studies investigating severe avian influenza, this study did not see any marked decreases in T cells other than an initial, transient lymphopenia, though there was evidence for T cell trafficking to the site of infection. The study also provided insight into the maturation and trafficking of antigen-presenting cells, giving new insight into immune cell dynamics in the ferret model.

Chapter 4 took what was learned in the H7N9 study and applied it on a larger scale, using the ferret model to assess the immune response to an ongoing pandemic virus, SARS-CoV-2. This study primarily aimed to assess the immune response to a vaccine candidate against this virus, the AstraZeneca ChAdOx1-nCoV-2019 adenoviral-vectored vaccine. A prime-boost regime was found to be more effective at producing an immune response following SARS-CoV-2 infection than one dose of the vaccine, with the prime-boost ferrets producing greater B cell responses in the blood and tissues. Two doses of the vaccine also elicited a greater $CD8^+$ T cell responses in the blood. As such, this study helps to guide the future application and administration of the vaccine to help overcome the effects of this wide-spreading virus.

In order to gain greater insight into the immune genes that play a role in the protection against respiratory viruses, Chapter 5 sought to identify and classify and important family of interferon-stimulated genes, the Interferon-Inducible Transmembrane (IFITM) protein family, in the ferret model. The IFITM locus was found in the ferret to be of high similarity to the loci previously classified in other species, with this work having a particular focus on *IFITM1*, *IFITM2*, and *IFITM3* due to their intrinsic anti-viral activity in other species. These genes were found to be expressed at a basal level across multiple tissues in the ferret, whilst also

being highly upregulated in the presence of both IFNα and influenza virus. These results, along with sequence alignment confirmation, identify these genes as interferon-stimulated genes of the IFITM family, filling in an important piece of missing information for the ferret model.

Overall, this thesis furthers our knowledge of the ferret model and the immune responses that occur within, providing a framework for future studies aiming to assess the immunology of respiratory viruses and their vaccine candidates.

Declaration

This is to certify that

i. the thesis comprises only my original work towards the PhD except where indicated,

ii. due acknowledgement has been made in the text to all other material used,

iii. the thesis is fewer than 100,000 words in length, exclusive of tables, maps, bibliographies and appendices

William Horman

Acknowledgements

This PhD has been a long and difficult one, but I am incredibly thankful for this opportunity. Firstly, thank you to The University of Melbourne and CSIRO for taking a chance on me, awarding me the OneHealth Scholarship to complete this work.

I would like to thank my supervisors at the university, Prof Katherine Kedzierska and Dr Oanh Nguyen for all their support, often from afar as I worked down in Geelong, it has truly been a privilege to work with you both. You have always believed in me, even if in the early days I was more a ghost who floated through every six months with an update. I may have felt a black sheep at times, but you made sure to make me feel like part of the flock. To the other Kedzierska lab members, in particular Dr Louise Rowntree for helping me with my experiments and putting up with my inane talking when sitting next to me, and Dr Marios Koutsakos for experiment help and a wealth of advice. To my fellow students, Luca, Xiaoxiao and Maria who I started with and watched from afar, I'm proud of you all and so glad you embraced me when I was there, if only I could have spent more time with you in the Doherty! Also, to Jen, Wuji and Lily who may as well be a student, thank you for your help and making my time on level 7 enjoyable.

I extend my gratitude to my PhD committee, Prof Kanta Subbarao, Prof Lorena Brown and her replacement Dr Sarah Londrigan, and to my chair Prof Patrick Reading who has been one of the biggest influences on my scientific career and always a calm and caring mentor to talk to when needed.

The work in this thesis would not be possible without the countless hours of help and support given to me by the Bean team down at CSIRO ACDP. A massive thank you to Dr Andrew Bean and Dr Daniel Layton, Dan in particular took on the bulk of my supervisory work and helped morph this thesis into what it is today. Thank you for all your support and help, and with getting me onto the numerous ferret trials and the COVID-19 team, it's thanks to you I now have a CSIRO Chairman's Medal to look fondly upon. To all the Bean team members, but in particular, Tamara Gough, Kerri Bruce, Christina Rootes, Leon Tribolet, Kostlend Mara and Meiling Dai for all their help across my various projects and experiments, most of which could not have been completed without your significant input. I also must thank the ACDP animal house staff who assisted and ran the numerous PC3 animal trials I conducted, and to all the ferrets that bravely sacrificed their lives for the scientific cause. Lastly, to my student brethren down in Geelong, you made all the travel so much more fun – Sam Jasinski, Alix Spahn, and my disciple in the church of Peanit, Meg McDonald.

To my friends who have supported me, thank you for everything. Dr Jonno Jacobson, you sent me down this path, so thanks for that! And to my fellow potatoes Phil, Tiff and Kai, thank you for all being doctors and Phil. Special thanks to Jono for the ice-cream, and Campbell for the support from afar, good luck with yours! And to the PDubz crew, especially Keit, Miku, Catriona, and Rachel for always being there and for doing this whole thing as well.

Thank you to my family, Mum and Dad you've been so supportive, thanks for the house! I can finally become the most qualified person in our family. A big thank you to Dr Jude for the love and support. And of course, to my partner Zoe. It has been a long and tumultuous journey, but it's finally over. You've been the most amazing support through the many long nights away at Aireys and the 150,000 kilometres of driving, I love you so much and this could not have been done without you, really.

"The sea of stupidity can only be crossed by the boat of knowledge."

Research Output

The following research output has been generated as part of work conducted during the duration of this thesis.

Refereed Journal Articles:

Horman WSJ, Nguyen THO, Kedzierska K, Bean AGD, & Layton DS (2018) "The Drivers of Pathology in Zoonotic Avian Influenza: The Interplay Between Host and Pathogen" ***Frontiers in Immunology*** doi: 10.3389/fimmu.2018.01812

Horman WSJ, Nguyen THO, Kedzierska K, Butler J, Shan S, Layton R, Bingham J, Payne J, Bean AGD, & Layton DS (2020) "The Dynamics of the Ferret Immune Response During H7N9 Influenza Virus Infection" ***Frontiers in Immunology*** doi: 10.3389/fimmu.2020.559113

Horman WSJ, Kedzierska K, Rootes CL, Bean AGD, Nguyen THO, & Layton DS (2021) "Upregulated expression of ferret Interferon-Inducible Transmembrane genes by IFN-α and influenza virus infection" ***Journal of Virology***, doi: 10.1128/JVI.00111-21

Marsh GA, McAuley AJ, Au GG, Brown S, Riddell S, Layton R, Payne J, Durr PA, Bender H, Barr JA, Bingham J, Boyd V, Bruce M, Burkett K, Edwards S, Gough T, Holmes C, Horman WSJ, Jansen van Vuren P, Layton DS, Lowther S, Maynard K, McAuley KD, Neave MJ, Poole T, Paradkar P, Rootes CL, Rowe B, Soldani E, Stevens V, Stewart C, Suen W, Tachedjian M, Todd S, Trinidad L, Walter D, Watson N, Drew TW, Gilbert SC, & Vasan SS (2021) "ChAdOx1 nCoV-19 (AZD1222) Vaccine Candidate Significantly Reduces SARS-CoV-2 Shedding in Ferrets" ***npj Vaccines*** doi**:** 10.1038/s41541-021-00315-6

Awards & Scholarships:

2017 – CSIRO/University of Melbourne OneHealth PhD Scholarship

2018 - AAHL Student Presenter of the Year award

2020 - CSIRO Chairman's Medal as part of the COVID-19 team

Poster Presentations:

Horman WSJ*, Nguyen THO, Kedzierska K, Bean AGD, & Layton DS "*Analysis of variable immune cell phenotypes in avian and mammalian hosts following infection with avian influenza viruses*" **Lorne Infection and Immunity Conference 2019**, Lorne, Australia

Table of Contents

List of Tables

CHAPTER 1: INTRODUCTION

CHAPTER 4: THE IMMUNOGENICITY OF PRIME/BOOST VACCINATION WITH THE SARS-COV-2 VACCINE CANDIDATE CHADOX1-NCOV-2019 IN THE FERRET MODEL

Tables from publications not listed

List of Figures

CHAPTER 1: INTRODUCTION

CHAPTER 4: THE IMMUNOGENICITY OF PRIME/BOOST VACCINATION WITH THE SARS-COV-2 VACCINE CANDIDATE CHADOX1-NCOV-2019 IN THE FERRET MODEL

Figures from publications not listed

Abbreviations

A – Alanine

AAHL – Australian Animal Health Laboratory

ACDP – Australian Centre for Disease Preparedness

ACE2 – Angiotensin-converting enzyme 2

AF – AlexaFluor

AI – Avian Influenza

APC – Antigen presenting cells *or* Allophycocyanin

ATCC – American Type Culture Collection

B4GALNT4 – β-1,4-N-Acetyl-Galactosaminyltransferase 4

BSA – Bovine serum albumin

BSL – Biosafety level

BV421 – Brilliant Violet 421

C – Constant region *or* Cysteine

CD – Cluster of differentiation

cDC – Conventional dendritic cell

cDNA – Complementary DNA

ChAdOx1-nCoV-2019 – Chimp Adenovirus Oxford 1 novel Coronavirus 2019 vaccine

CoV – Coronavirus

COVID-19 – Coronavirus infectious disease of 2019

CRISPR – Clustered regularly interspaced short palindromic repeats

CSIRO – Commonwealth Science and Industrial Research Organisation

Ct – Comparative threshold

DC – Dendritic cell

DMEM – Dulbecco's Modified Eagle Medium

DMSO – Dimethyl sulfoxide

DNA – Deoxyribonucleic acid

E – Envelope protein *or* Glutamic acid

EID_{50} – 50% egg infectious dose

ELISA – Enzyme-linked immunosorbent assay

ELISpot – Enzyme-linked immunospot

FACS – Fluorescence-activated cell sorting

FADD – Fas-associated death domain

FAM – Fluorescein amidite

FBS – Foetal bovine serum

FITC – Fluorescein isothiocyanate

FRL – Ferret Lung Epithelial cells

Gal – Galactose

gDNA – Genomic DNA

H – Histidine

H/HA – Haemagglutinin

HBSS – Hanks Buffered Salt Solution

HEPES – 4-(2-hydroxyethyl)-1-piperazineethanesulfonic acid

HI – Hemagglutination inhibition

HI-FCS – Heat-Inactivated Fetal Calf Serum

HLA – Human Leukocyte Antigen

HPAI – Highly Pathogenic Avian Influenza

I – Isoleucine

ICOS – inducible co-stimulator

IFITM – Interferon-induced transmembrane protein

IFN – interferon

Ig – Immunoglobulin

IL – Interleukin

ILI – Influenza-like illness

IM – Intramuscular

IN – Intranasal

IRF3 – interferon-regulatory factor 3

K – Lysine

KO – Knockout

L – Leucine

LPAI – Low Pathogenicity Avian Influenza

M – Membrane protein *or* Methionine *or* Mock-infected

M1 – Matrix 1

M2 – Matrix 2

MBCS – Multi-basic cleavage site

MDCK – Madin-Darby Canine Kidney cells

MERS – Middle East Respiratory Syndrome

MHC – Multi-Histocompatibility Complex

MOI – Multiplicity of infection

mRNA – Messenger RNA

N – Nucleocapsid protein *or* Asparagine

N/NA – Neuraminidase

NS1 – Non-Structural 1

ORF – Open reading frame

P – Proline

PA – Polymerase Acidic

PB1 – Polymerase Basic 1

PB2 – Polymerase Basic 2

PBS – Phosphate buffered saline

PCA – Principal component analysis

PCR – Polymerase chain reaction

PD-1 – Programmed cell death protein 1

pDC – Plasmacytoid dendritic cell

pdm09 – 2009 pandemic

PE – Phycoerythrin

PerCP-Cy5 – Peridinin chlorophyll-cyanine 5

PFA – paraformaldehyde

PGGHG – Protein-Glucosylgalactosylhydroxylysine Glucosidase

PIKFYVE - phosphatidylinositol 3-phosphate 5-kinase

Q – Glutamine

qPCR/qRT-PCR – Qualitative real-time PCR

RACE – Rapid amplification of cDNA ends

RDE – Receptor destroying enzyme

RNA – Ribonucleic acid

ROX – Carboxyrhodamine

RT-PCR – Real-time PCR

rV_{K627E} – K627E mutation

S – Spike protein *or* Switch region *or* Serine

SARS – Severe Acute Respiratory Syndrome

SD – Standard deviation

SEM – Standard error of the mean

sgRNA – Single guide RNA

SNP – Single nucleotide polymorphism

SOCS3 – Suppressor of cytokine signalling 3

SPF – Specific pathogen free

T – Threonine

$TCID_{50}$ – 50% tissue culture infectious dose

T_{CM} – Central memory T cell

TCR – T Cell receptor

T_{EM} – Effector memory T cell

T_{EMRA} – Terminally differentiated memory T cell

T_{FH} – Follicular helper T cell

Th1 – T helper type 1

Th2 – T helper type 2

TNF – Tumour necrosis factor

T_{SCM} – Stem cell memory T cell

TSS - Thrombosis with thrombocytopenia syndrome

T_{RM} – Tissue-resident memory T cell

V – Variable region *or* Valine

VIC01 – SARS-CoV-2 hCoV-19/Australia/VIC01/2020

VIDRL – Victorian Infectious Diseases Reference Laboratory

vRNP – Viral genome segments

WHO - World Health Organization

WHO CC – World Health Organization Collaborating Centre

Y – Tyrosine

Chapter 1: Introduction

1.1 Global burden of respiratory viruses

Respiratory viruses are viral pathogens which infect the respiratory tract of their hosts, often causing some degree of respiratory distress. An estimated 200 million people contract viral pneumonia each year, with the rapid spread and high transmissibility in the community contributing to respiratory viruses being a major global health burden (1, 2). In Australia alone, over AUD$404 million of the disease burden expenditure is taken by respiratory illnesses, making these viruses one of the leading causes of infectious disease burdens on our health system (3). One European study estimated the mean cost of keeping a patient in hospital to treat influenza-like illness (ILI) to be €3353 per patient, or upwards of AUD$5000, putting the global cost of treating these diseases in the trillions of dollars every year (4).

Of these respiratory viruses, one major group of viruses of concern are those in the influenza virus family. Influenza viruses are highly contagious pathogens of the respiratory tract, with symptoms of influenza disease ranging from mild coughing and fever, to severe morbidity and death due to respiratory distress (5). Influenza viruses are estimated to infect between 3-5 million people each year but account for a large portion of respiratory illness-related deaths, with an estimated 400,000 mortalities each year attributed to these viruses due to severe respiratory illness during seasonal epidemics (6-8). While these strains have a maximal mortality rate of 16% in elderly patients (9), some strains that zoonotically infect people can have mortality rates of greater than 40% even in healthy adults, making these viruses of great concern for future outbreaks (6).

Further to these zoonotic influenza virus strain, respiratory viruses derived from other species have been shown to have great human consequence, which is particularly the case for severe acute respiratory syndrome (SARS) coronaviruses (CoV). The recent COVID-19 pandemic, as declared by World Health Organization (WHO) in March 2020, is caused by the

SARS-CoV-2 virus and has infected 88 million people worldwide, resulting in nearly 2 million deaths, as of January 2021 (10). These viruses highlight the impact that highly contagious respiratory viruses can have on a global scale, and as such, this review will focus on these two virus groups of particular human consequence, influenza viruses and SARS-coronaviruses.

1.2 Influenza viruses

1.2.1 Influenza virus subtypes

Influenza viruses belong to the *Orthomyxoviridae* family, and are split into four sub-types based on differences in their structural proteins: types A, B, C, and D. Types A, B, and C are capable of causing severe disease in human hosts (11). Of these, types A and B are the main viruses of human concern, as type C, though capable of causing epidemics, has been shown to only present with mild disease when studied in children (12, 13). Influenza type D viruses are typically respiratory pathogens of bovine ruminants, with seroconversion towards these viruses only regularly seen in people in close contact with cattle (14-16).

Influenza A viruses are classified into subtypes based on differences in their haemagglutinin (HA, H when used for subtyping) and neuraminidase (NA, or N), with notation written as HxNx where x is the designated subtype number (for example, H1N1 and H1N2 share the same HA, but not NA) (5, 17). Human-infecting strains typically have odd-numbered HA subtypes, with H1N1 and H3N2 being the main seasonal influenza A virus strains and only influenza A virus strains to circulate in humans alongside swine-origin H1N2 (18, 19). Whilst infections in humans are less common, avian viruses such as H5N1, H7N9, and H9N2 have all been shown to zoonotically infect humans sporadically, adding to the repertoire of human-infecting influenza A viruses (20-22). Influenza B viruses conversely show less genetic diversity compared to their Influenza A counterparts, and are separated into two antigenically distinct lineages known as the B/Victoria-like and B/Yamagata-like, which have co-circulated since the delineation of the B/Victoria/2/87 and B/Yamagata/16/88 strains in the late 1980s (23, 24).

1.2.2 Influenza epidemics and pandemics

Influenza viruses are primarily transmitted from host to host via respiratory droplet transmission, allowing these viruses to be transmitted across relatively great distances while also being stable in the environment for lengthy periods of time (25). This property allows influenza to cause widespread transmission as seasonal epidemics, though this human-to-human transmission is predominantly caused by certain subtypes of influenza A (notably, H1N1 and H3N2 subtypes) and the two influenza B lineages (11). As these circulating strains are constantly interacting with their hosts in order to replicate and transmit, these influenza viruses have two mechanisms by which they evolve that hinder efforts to protect against them. The first mechanism is called antigenic drift, which is caused by the viral polymerase, wherein mutations to the viral gene segments, in particular the surface proteins HA and NA, lead to viral strains that maintain the fitness of previous strains but are unable to be inhibited by host factors such as antibodies due to accumulation of minor structural changes (26). The second mechanism is called antigenic shift, which results in much larger genomic changes compared to antigenic drift. Antigenic shift occurs when two influenza strains co-infect a single host, and due to this co-infection, genome segments from both strains are able to be packaged into a single virion creating a new virus that may be a hybrid of the two infecting strains. These strains often retain the more desirable fitness qualities of the previous strains, and thus may be able to effectively avoid immunity in many hosts due to their relatively novel nature, and it is these strains which often lead to more severe and widespread outbreaks, or pandemics (5).

Influenza vaccinations primarily target the HA protein due to its high conservation, though vaccine mismatch may occur when antigenic drift allows a virus to attain enough mutations for vaccine escape, resulting in annual checks to confirm that vaccines against influenza viruses continue to be effective (27). Vaccines against influenza are typically one of three forms: inactivated, attenuated, or recombinant HA (28). All three of these vaccines trigger immune responses specifically against the HA of the strains in the vaccine, with modern vaccines often

being trivalent against circulating H1N1, H3N2, and influenza B virus strains, though some vaccines now also incorporate both influenza B lineages (29). While these vaccines typically form strong immune responses against seasonal strains which mutate through antigenic drift, producing vaccines against newly emerging influenza viruses that arise due to antigenic shift remains difficult, as these viruses usually contain completely novel HA proteins.

Of particular concern are zoonotic influenza viruses which, through antigenic shift, gain the ability to infect humans which have very little immunity to them, in which case these viruses often have severe consequences to accompany their rapid spread. This was the case for the A(H1N1)pdm09 virus, colloquially known as “swine flu” due to its zoonotic origins in pigs. This virus reassorted a swine-origin H1N1 with a human-infecting, circulating H3N2 strain, while also gaining genes from an avian influenza strain in a triple-reassortment event leading to a novel, human-infecting H1N1 virus, which subsequently resulted in over 200,000 influenza-related deaths across the globe in 2009 (30-33). Major outbreaks of influenza viruses have been common throughout modern history, from large scale pandemics such as the 1918 and 2009 H1N1 outbreaks (34), to smaller outbreaks such as avian influenza outbreaks in 1997, 2005 and 2013 (35-38), and as such it is of high importance to understand how these viruses infect their hosts and make themselves transmissible on such a large scale, particularly when a universal vaccine that can protect against most strains is not yet available.

1.2.3 Virus structure and life cycle

Influenza viruses are typified by their single-stranded, negative-sense RNA genome which is present in eight segments that encode twelve viral proteins (39). As reviewed by Dou and colleagues, viral entry into host cells is mediated by the viral HA protein, which binds to sialic acid receptors on the cell surface to initiate attachment and entry into the respiratory epithelium (40). The virus enters via an endosome, and the lowering of the endosome pH activates the viral Matrix 2 (M2) ion channel protein, which acidifies the viral particle. This allows for the release of the packaged viral genome segments (vRNPs) from the Matrix 1 protein, with a pH-dependent conformational change in the HA allowing for viral hemifusion

with the endosomal membrane and thus viral genome escape. The vRNPs are then transported using host machinery to the cell nucleus, where the genome is replicated using the viral RNA-dependent RNA polymerase comprised of the Polymerase Basic 1 and 2 (PB1 and PB2) subunits, and the Polymerase Acidic (PA) protein (40). These new viral RNAs then facilitate the production of new viral proteins, both for novel virion assembly and genome amplification, and also for immune evasion, such as the Non-Structural 1 (NS1) protein which plays a role in dampening the host interferon (IFN) response (40, 41). Viral envelope proteins HA and NA are synthesised in high quantities and are used to form the virion alongside the other proteins. Viral gene segments are trafficked towards the cell membrane for packaging into the virion by host Rab11 protein, which associates with PB2 (40). These new virions bud-off from the cell and are released by NA which cleaves the sialic acids that HA binds to, allowing for infection of other cells.

1.2.4 Avian influenza viruses

Influenza A viruses have consistently posed a major threat to human health, both through seasonal infections and pandemic outbreaks (42). Avian influenza (AI) viruses have contributed significantly to this, and in recent years highly pathogenic AI (HPAI) viruses have emerged as a major zoonotic threat. AI viruses naturally circulate in wild bird populations, including but not limited to, ducks and waterfowl, and can spill over to poultry birds such as chickens, with one study finding wild ducks to be a source of transmission for the H5N8 HPAI virus in poultry farms in the United Kingdom (43). Other than a few novel strains isolated in bats, all influenza A subtypes have been found in aquatic birds, which act as natural reservoirs for the viruses (44). These viruses typically replicate in the gastrointestinal and upper respiratory tract of both these natural hosts and chickens, and typically present as subclinical to mild disease (45, 46). Based on these clinical signs in chickens, these influenza viruses are classified as ‘low pathogenicity AI’ (LPAI) infections (47). Although many AI viruses circulate without causing serious disease, other viral subtypes can lead to more severe outbreaks within birds. Birds infected with these subtypes have more severe pathogenesis and rapid disease

progression, often as the result of dissemination of the virus into tissues peripheral to the gastrointestinal and respiratory tracts. This type of infection in chickens defines the subtypes as HPAI (47). Highlighting the importance of HPAI viruses, recent outbreaks of HPAI H5N6 in China and the Philippines have caused approximately 37,000 bird deaths and 400,000 more culled at an economic cost of nearly $USD40 million (48, 49). While such outbreaks represent a significant economic burden to the poultry industry, of greater concern is the potential for HPAI viruses to cross the species barrier into mammals, especially humans.

Despite there being a broad range of AI subtypes, fortunately, only a very select subset of these have been shown to infect humans with highly pathogenic consequences. The first known HPAI infections in humans were highlighted by the outbreak of H5N1 avian-derived influenza in Hong Kong in 1997, leading to 6 deaths from 18 confirmed cases (38). Since then, sporadic outbreaks of H5N1 have had highly pathogenic consequences in humans, resulting in over 450 deaths from approximately 900 cases and thus becoming the first major human-infecting AI virus (50-52). While H5N1 remains a threat to human health, the emergence of the avian-derived H7N9 strain infecting humans, first described in March 2013 in China's Yangtze River Delta, has since caused 613 deaths out of 1,568 human cases throughout most of China as of January 2021 (53). This viral subtype is of a particular concern, as unlike H5N1, which is highly pathogenic in chickens and humans, H7N9 typically presents as a LPAI in chickens, but causes a high mortality rate in humans (40%), similar to that seen for H5N1 infections. H7N9 is one of several LPAI viruses in the H7 family capable of human infections, with viral transmission usually only acquired through close contact with host species. However, for reasons that are still unclear, H7N9 has greater transmissibility and more severe disease outcomes in humans than any other H7 viruses (54, 55). Thus, differences in clinical presentation across species, coupled with the potential of viruses such as H7N9 to cause a pandemic outbreak via evidence of human-to-human transmission (37), makes understanding the mechanisms by which these viruses cross the species barrier and become highly pathogenic in humans a critical area of investigation.

Human cases of AI infection have become increasingly common since outbreaks of H5N1 in the late 1990s and accentuated by a dramatic increase in H7N9 infections during the recent "fifth wave" of epidemic infections in China (56-58). These viruses were commonly contracted by people in regular close contact with live poultry markets (59, 60), where outbreaks of AI viruses in chickens can be common yet go largely unnoticed, especially in the case of H7N9 infections, and the pathways of human infection with avian influenza are shown in **Figure 1.1**. Despite the vast diversity of AI viruses, predominantly only viruses from three haemagglutinin (HA) subtypes have been recorded to naturally infect humans: H5Nx viruses, most notably H5N1; H7Nx viruses such as H7N9; and H9Nx viruses, commonly H9N2. H9Nx strains present as LPAI infections in birds and have less severe symptoms in human hosts compared to H5 and H7 strains (20, 61-63). Despite this, as H9N2 viruses are regularly found co-circulating with H5N1 and H7N9 with assortment frequently occurring between these viruses in poultry there is a real possibility of a novel HPAI strain emerging from these subtypes (64, 65). While there have been isolated cases of human infections with other subtypes, such as H6 (66) and H10 (67), the H5/H7/H9-subtypes of AI remain of greatest concern for human infections and potential pandemics. Thus, understanding the clinical manifestations of these viruses in avian hosts is needed for our understanding of why these viruses are considered such a threat.

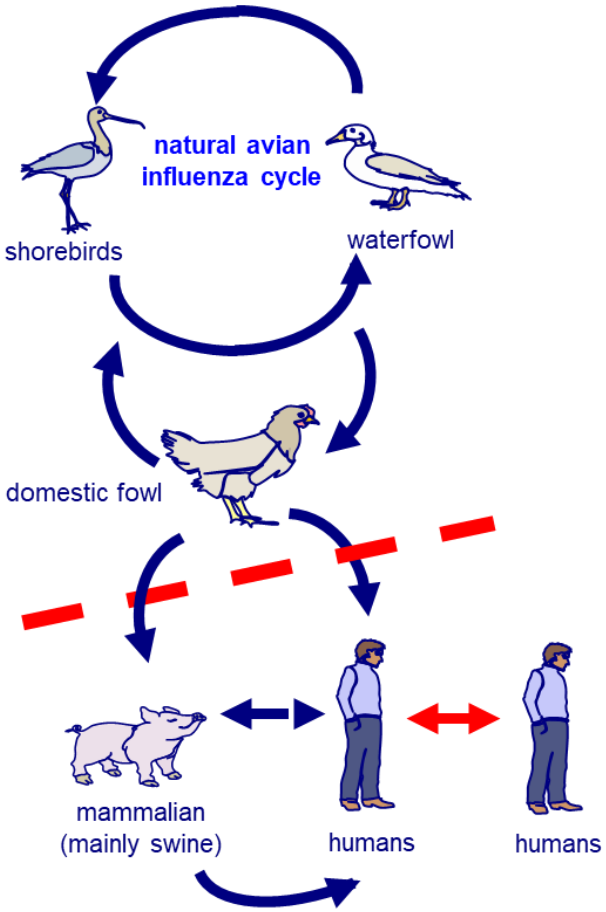

Figure 1.1. Pathways of avian influenza transmission
AIVs typically circulate among shorebirds, though have the ability to spread into poultry flocks. It is through close contact with the birds that AIVs can cross the avian-mammalian threshold (red dotted-line) into other mammalian species such as pigs or directly into humans. While possible, direct human-to-human spread is rare, signified by the red arrow.

1.2.5 Low and highly pathogenic AI viruses in avian hosts

In the case of LPAI, infections tend to localize in the mucosal surfaces of the gastrointestinal tract of infected birds and although often asymptomatic, chickens may present with mild clinical signs following infection. These include excess mucus and congested tracheae, watery droppings and mild respiratory inflammation, with rarely any other signs of respiratory disease associated with influenza infections (45, 61, 68, 69). Highest viral titres typically occur two-to-three days after infection with limited gross lesions evident, allowing the virus to replicate and be excreted into the environment with little to no effect on the host animal (70, 71). Interestingly, ducks can exhibit even more limited clinical signs following LPAI infection than chickens, with Wang and colleagues showing less severe clinical signs and histopathological

lesions in ducks compared to chickens infected with LPAI H9N2 virus (72). Thus, it is interesting to note that even in avian hosts, there is a range of clinical severity to LPAI viruses, with chickens showing more moderate/severe signs compared to waterfowl infected with LPAI.

In contrast to LPAI viruses, HPAI viruses have the ability to induce severe disease and cause devastating outbreaks with high mortality rates in poultry (73, 74). In chickens, H5N1 causes acute illness with high levels of viral shedding and clinical signs such as dehydration, nasal discharge, and lesions in many tissue types (75-77). While LPAI infections tend to remain within the faecal-oral tract of infected birds, HPAI infections are often identified by virus spreading systemically to multiple tissues (78). Suzuki and colleagues (2009) described the pathology of H5N1 infections in chickens, finding that clinical signs progressed from milder signs such as feather ruffling and depression behaviour, to the more severe outcomes of haemorrhaging and oedema in multiple tissues. These birds also showed severe respiratory distress not seen in LPAI infections (79). In contrast, ducks can present with a wider range of symptoms following infection with HPAI H5N1, with experimentally infected ducks having clinical signs as mild as depressive behaviour without any other complications (80). Ducks may also show severe signs such as those seen in chickens, with common outcomes including neurological spread and haemorrhaging in the body extremities. Additionally, Yamamoto and colleagues (2016) have also found that domestic ducks, unlike chickens, show corneal opacity following H5N1 infection and less severe haemorrhaging compared to chickens (81, 82). Likewise, wild ducks have been shown to exhibit less severe signs following H5N1 infection compared to other gallinaceous birds including domestic ducks, despite showing high levels of viral shedding consistent with an HPAI infection, which may suggest their role as a key reservoir species (77).

1.2.6 Clinical manifestations of AIV in mammalian hosts

AI viruses can also infect pigs, which are housed in close proximity to human populations. Pigs often act as a ‘mixing vessel’ for influenza viruses, allowing multiple stains to co-infect and reassort leading to strains that are capable of human infection (83, 84). While this is

particularly the case for low pathogenicity viruses, there has been little evidence to suggest that pigs can contract highly pathogenic strains such as H5N1 and H7N9 to a great extent, with H5N1 strains isolated from pigs in China found to be attenuated from the HPAI form due to a mutation in their NS1 gene, with these viruses activating lessened interferon response when returned into chickens compared to avian-derived variants of the virus (85). Although there have been no confirmed cases of H7N9 infection in pigs (86), H7N9 can replicate, cause pathology amongst pigs during *in vivo* studies at low levels, though multiple studies have shown pigs infected with H7N9 have little to no clinical signs or viral shedding, and no transmission between infected pigs and sentinel animals (87-89). However, the fact that these viruses replicate in swine respiratory tissue *in vitro* reinforces the idea that pigs could still act as an important reservoir species for mammalian-adapted H7N9, if only sporadically (90). While H7N9 currently has limited transmission in pigs, of particular concern are reports of other H7Nx infections in pigs, with Kwon and colleagues identifying a H7N2 strain that was a genetic reassortant between avian H7N2 and H5N3 viruses (91). This reassortment event suggests that as the frequency of H7Nx cases increase in pigs, so too does the likelihood of an H7N9 virus infecting pigs and potentially gaining stable mammalian transmissibility through reassortment between the H7N9 virus and a mammalian transmission competent virus.

Studies in ferrets as a model for human infection have shown that mammalian-adapted AI viruses typically localise to the respiratory tract (92), however these viruses can have a limited ability to transmit via droplets (93-95). This model has been used to study high consequence AI viruses such as H5N1, which cause acute illness in the upper respiratory tract of ferrets. Clinical signs of H5N1-infected ferrets include nasal discharge, high temperatures and weight loss due to dehydration, and worsened pathogenesis as highlighted by lung damage due to extensive infiltration of the lung tissue by inflammatory cells (54, 96, 97). H7N9 can also cause severe respiratory distress in this way, with lengthened time until viral clearance contributing to the substantial inflammation in the lungs of ferrets. Severe infections may cause complications such as viral pneumonia due to the breakdown of lung endothelial barriers, which contributes to this systemic spread and may lead to encephalitis or other neurological

issues (54, 98). This is of particular importance as systemic spread to the central nervous system is more commonly associated with HPAI H5N1 than LPAI viruses (97), making H7N9 a unique threat to human health due to its ability to cause HPAI-like disease symptoms.

Symptoms following human infection with AI are similar to those observed in the ferret model. Less severe cases present as more typical influenza infections, with symptoms such as fever and coughing among those commonly associated with influenza-related illness (22, 99). However, these viruses can cause severe respiratory illness following infection in the lungs, which may manifest as atypical viral pneumonia and acute respiratory distress syndrome, and often patients who have contracted these infections die from respiratory failure (100, 101). Furthermore, much like in birds, dissemination of the virus away from the site of infection leads to other complications such as organ failure, encephalitis, and internal bleeding due to tissue destruction (22, 38, 102), all of which contribute to the lethal nature of these viruses. A summary of the varying degrees of clinical manifestations between the different species is depicted in **Figure 1.2**.

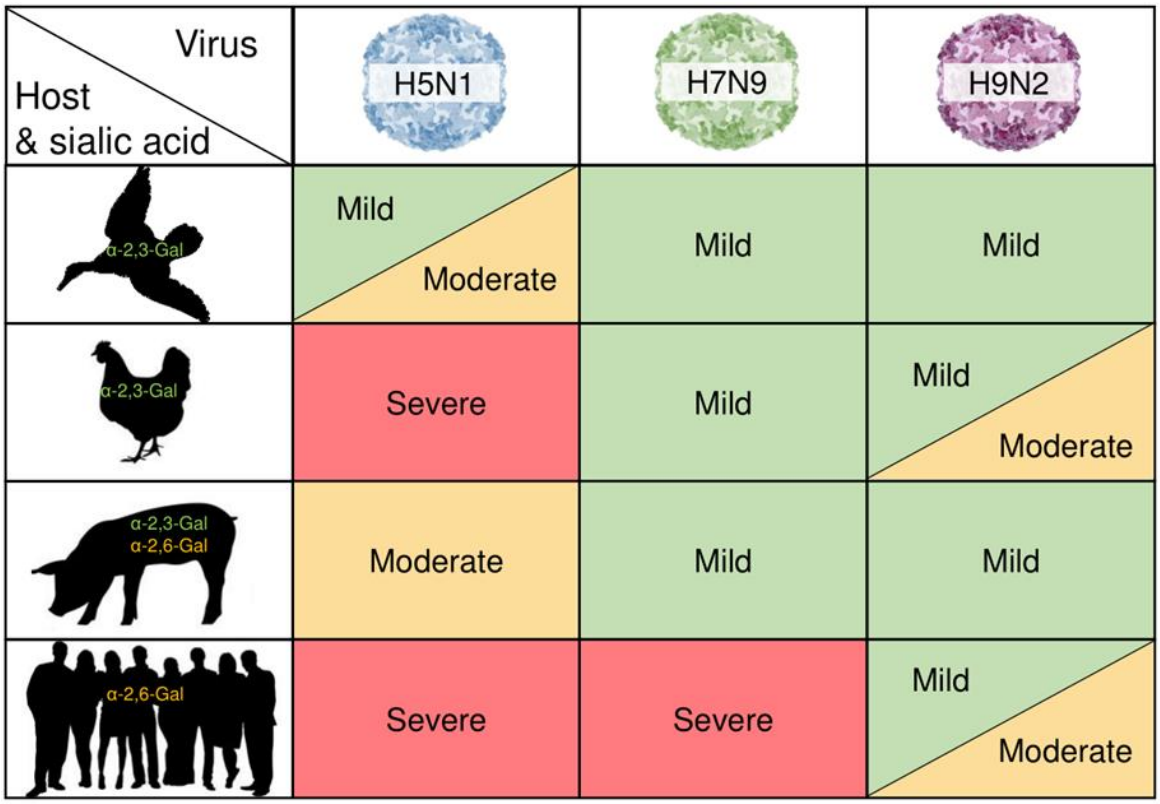

Figure 1.2. Zoonotic influenza pathology is linked to host biology
H5N1, H7N9, and H9N2 avian influenza (AI) viruses causing varying degrees of clinical manifestations across different species is shown against different host and their sialic acid properties. AI viral haemagglutinin proteins selectively and preferentially bind to sialic residues with either an α-2,3-Gal or α-2,6-Gal terminating sequence on the host cell surface to allow for viral fusion and entry. This represents viral fitness and is a potential mechanism underlying the degree of disease severity and susceptibility in the different hosts.

Additionally, in humans, AI subtypes have been associated with mortalities in very distinct age demographics when compared to seasonal influenza (**Figure 1.3**). Fatal cases in children (0-9 years) and younger adults (10-19 years) were predominantly caused by HPAI H5N1 infection, with 80.3% of H5N1 fatal cases seen in people aged 35 or under (51). A similar trend was observed with the 2009 pandemic strain, A(H1N1)pdm09, which led to increased mortalities in younger age groups compared to other seasonal strains circulating at the same time (103). Conversely, older patients (>60 years of age) were most susceptible to seasonal influenza strains (80% of mortality cases), except for the A(H1N1)pdm09 pandemic strain during which older patients were less susceptible to A(H1N1)pdm09-related mortality compared to those under 40 years of age, with one theory suggesting that the repeated

exposure to seasonal influenza viruses, mixed with repeated vaccinations, may allow older patients to retain greater immunity to epitopes of the 2009 pandemic strain, which was more similar to the 1918 H1N1 pandemic strain, compared to younger people who have had less repeated exposures (104, 105). For H7N9 LPAI infections, the highest mortality was also skewed towards older people, which is likely due to the propensity for H7N9 cases to be found in live poultry farmers, typically older men (106, 107). This emphasises the dynamic relationship between the pathogen and the human host, and how different strains of influenza viruses can lead to differential fatal outcomes across different ages (the pathogenesis of AI viral infections will be discussed in more detail in section **1.7**). Whilst influenza viruses remain of critical importance in terms of global health, other emerging zoonotic viruses can cause similar if not greater levels of disease across multiple age groups, such that influenza may become a secondary concern in a pandemic world. This is particularly the case for coronaviruses, which will be explored in more detail in the following section.

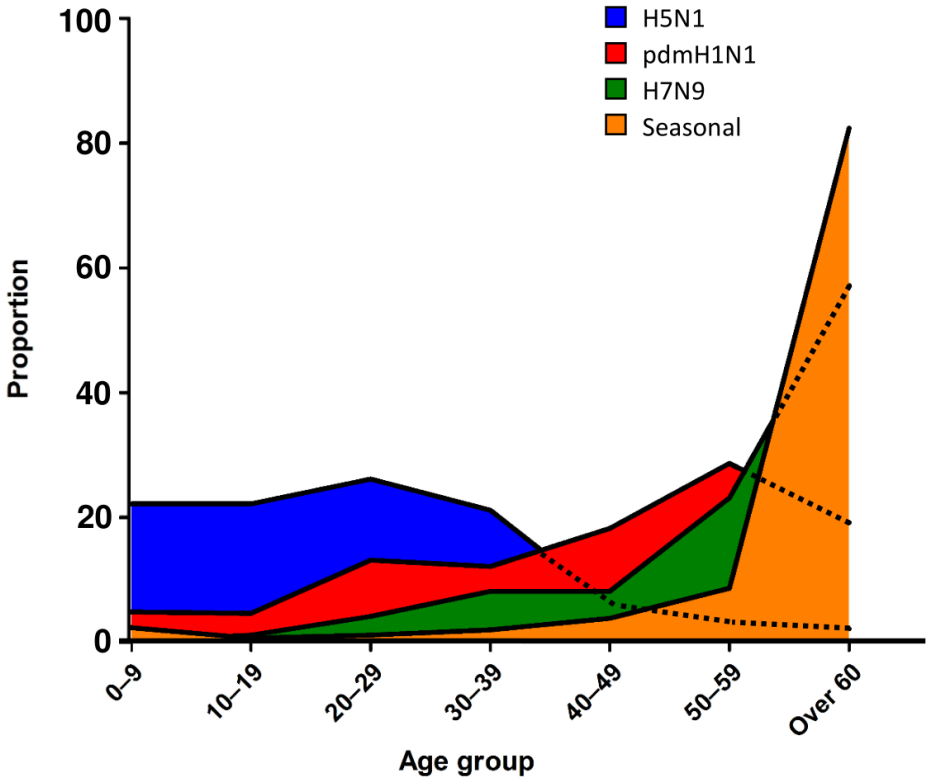

Figure 1.3. Age-related mortality trends highlight impact of host–pathogen relationships
Frequency of age groups of patients who succumb to different strains of influenza is graphed as a proportion of total fatalities for a given strain. When we assessed the age of patients who succumb to different strains of influenza, as a proportion of the total mortalities for a given strain, trends emerge as to the host susceptibilities. For seasonal influenza, older patients (>60 years old) were the most susceptible, however, for a variation on seasonal influenza, pdmH1N1 2009, the age of patients who succumbed was reduced and included significant mortalities between 20 and 59 years old. Interestingly, the highly pathogenic AI H5N1 was predominantly fatal in those under 40 years old, whereas H7N9, a low pathogenicity AI strain, followed a similar trend to seasonal influenza.

1.3 Emergence of novel SARS-CoV-2 virus

1.3.1 COVID-19 pandemic and epidemiology

While influenza viruses are considered the most well-studied respiratory virus with pandemic potential, novel zoonotic viruses of other classes also have potential to cause widespread infection, which is particularly the case for coronaviruses (CoV). Strains of Severe Acute Respiratory Syndrome (SARS) viruses have been responsible for two major outbreaks, the SARS outbreak of 2003 and the Coronavirus Infectious disease of 2019 (COVID-19) pandemic

(108). The SARS epidemic in southeast Asia caused roughly 8000 cases between 2002 and 2004, resulting in 774 deaths at an almost 10% mortality rate. However, the outbreak was short-lived and was mostly isolated to China following strict quarantine measures (109). The SARS-CoV virus studied in SARS patients was found to induce severe pulmonary lesions and alveolar damage, results which were also observed when the virus isolated from these patients was inoculated into macaques by Kuiken and colleagues (110). The COVID-19 pandemic, on the other hand, was first identified in Wuhan, China in late 2019 (111) before rapidly spreading across the world to cause the severe pandemic. By January 2021 nearly 88 million cases of COVID-19 have been reported worldwide, with 1.9 million confirmed deaths due to the virus (10), with a failure to adequately control and contain the virus on a global scale contributing to its wide reaching spread compared to the 2003 outbreak despite both viruses having similar basic reproductive rates (R_0) of between 2 and 3 (112). The mortality rate of SARS-CoV-2 is approximately 2%, lower than that seen compared to the SARS outbreak of 2003, however the far greater spread of the virus due to a lack of or ineffective quarantining methods worldwide has allowed the SARS-CoV-2 virus to reach a pandemic scale far greater than previously seen for a coronaviruses outbreak. Like many pandemic viruses, this virus is believed to be zoonotic in origin, with studies showing high conservation between the human infecting SARS-CoV-2 and several bat-infecting coronaviruses (113-115).

1.3.2 Virus structure and lifecycle

The SARS-CoV-2 virus is from the *Coronaviridae* virus family, which have single stranded, positive sense RNA genomes, and cause respiratory illness in their host through infection of the respiratory tract (113, 116). Coronaviruses bind to the host respiratory epithelium through association of the viral spike (S) protein with the angiotensin-converting enzyme 2 (ACE2) receptor on the cell surface, which was first identified by Li and colleagues for SARS-CoV infections in 2003 (117) and confirmed for SARS-CoV-2 in two studies by Ou and colleagues (118) and Hoffmann and colleagues (119). The transmembrane protease, serine 2 (TMPRSS2) enzyme was also identified as critical for the priming of S protein following ACE2

recognition for other coronaviruses (120). Ou and colleagues further showed how the virus was then internalized through receptor-mediated membrane fusion in an endocytic process through the use of pseudoviruses expressing SARS-CoV-2 S protein, with the use of inhibitors against endocytic mediators such as phosphatidylinositol 3-phosphate 5-kinase (PIKFYVE) and cathepsin-L decreasing the infectivity of these pseudoviruses (118). Once viral entry has occurred to begin the virus replication cycle (121, 122), the SARS-CoV-2 genome escapes to the cytoplasm, and the open reading frames (ORF) 1a and 1ab immediately produce polyprotein 1a/1ab, which is cleaved to produce the non-structural proteins required for the viral replication-transcription complex (123, 124). This complex is used to produce and replicate a nested set of RNAs encoding for the coronavirus' structural proteins: S, envelope (E), membrane (M), and nucleocapsid (N) (125). Viral particles are then assembled and released from the cell to infect other respiratory epithelial cells (Figure 1.4).

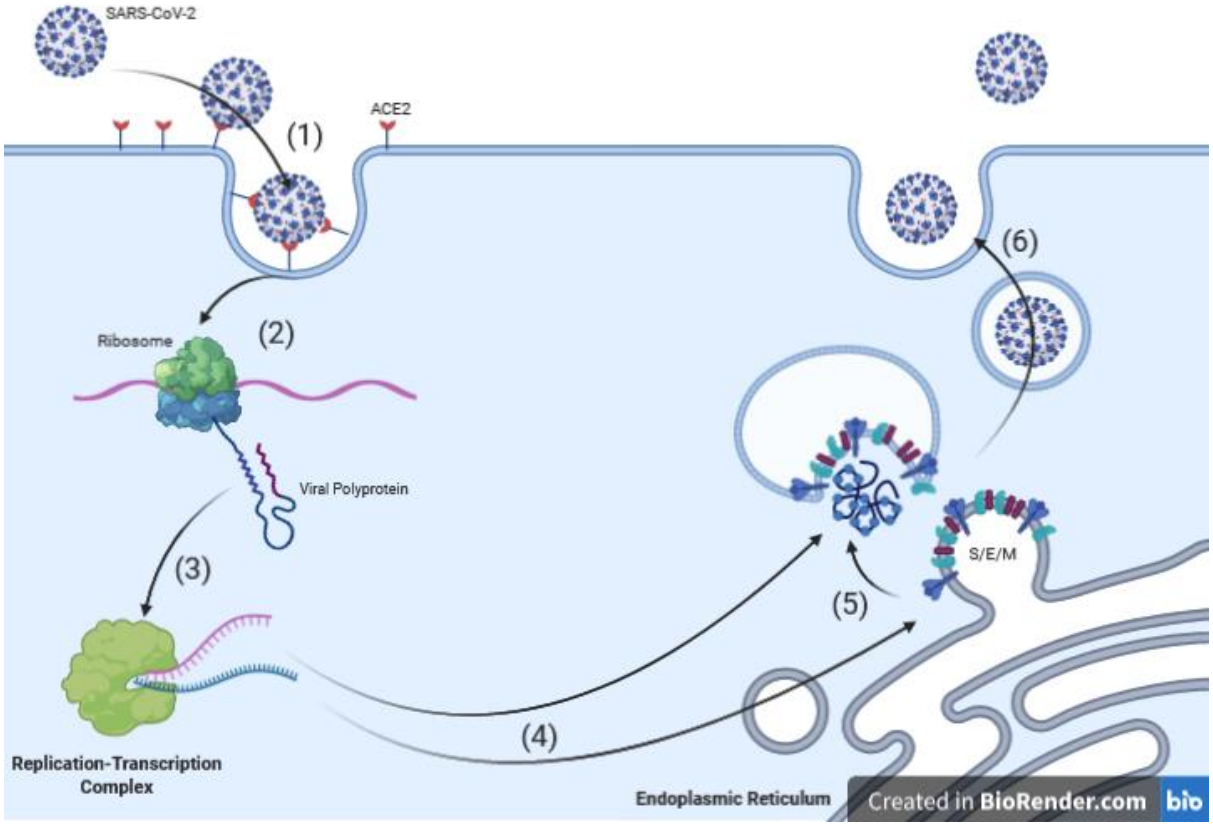

Figure 1.4. Schematic of the SARS-CoV-2 lifecycle
(1) SARS-CoV-2 attaches to the host cell via the ACE2 receptor and is internalised. (2) The viral genome escapes the endosome and is translated by ribosomes into the viral polyprotein. (3) The viral polyprotein is cleaved and folds to form the replication-transcription complex. (4) The replication-transcription complex transcribes RNAs for viral protein assembly. (5) Viral proteins are assembled on the endoplasmic reticulum membrane and bud off, encasing the genome containing nucleocapsid. (6) Virion assembly is completed, and new virus exits the cells to continue infection. Created in BioRender.com.

1.3.3 COVID-19 pathology and transmission

COVID-19 presents as a respiratory disease, with mild infections often being asymptomatic whilst severe cases lead to considerable morbidity and mortality. Severe cases are marked by respiratory distress and breathing difficulties, as well as coughing, headache and fatigue (126, 127). Other side effects of COVID-19 include anosmia and dysgeusia (a loss of smell and taste), with the first case reports of these effects recorded early after the onset of the pandemic (128-130). While disease symptoms of COVID-19 tend to be similar to those seen for other respiratory viruses, long-term effects of the infection are still being discovered, with a study by Huang and colleagues finding patients discharged six months prior continued to

have ongoing health issues, most commonly muscle weakness and fatigue, whilst patients who had severe cases of COVID-19 had sustained respiratory distress due to impaired pulmonary diffusion and lung lesions (131). Data obtained in retrospective studies from the 2003 SARS outbreak showed similar long-term pulmonary distress combined with neurological signs such as fatigue and depression (132, 133), as expected from the two related viruses, suggesting that as the pandemic continues to develop, long-term complications will require attention beyond the immediate infection symptoms. While neurological symptoms for influenza have been reported, especially in children, these cases are generally typified by encephalitis (134, 135). This contrasts COVID-19 disease where, despite encephalitis being among the more severe outcomes in case studies (136, 137), many of the neurological disorders associated with COVID-19 do not come with overt neurological disease such as viral encephalitis, a phenomenon observed in a human ACE2 mouse model for SARS-CoV (138).

Early infection with SARS-CoV-2 is confined to the upper respiratory tract following inhalation of virus-infected aerosols, and is generally asymptomatic (139). Patients who exhibit strong neutralising antibody responses and adequate immune cell control of infection generally clear the virus without complications (140, 141), however impaired immune responses may lead to severe respiratory distress seen in ~20% of cases (139). These severe cases are often marked by a large scale increase in pro-inflammatory cytokines such as IL-6, leading to inflammation and damage to the lung epithelium (142, 143). This respiratory distress allows the virus to enter the circulation as respiratory droplets, which are exhaled or coughed from the host to disseminate the virus through respiratory droplet transmission between close-contacts (144, 145). There is also evidence, however, to suggest that asymptomatic carriers can also transmit the virus, suggesting that the reservoir for the spread of this virus in the human population may be larger than just those displaying overt symptoms (146). As such, given there are currently no effective anti-viral treatments for SARS-CoV-2, there is an urgent and ongoing need for vaccine candidates to assist in controlling the spread of this virus.

1.3.4 Vaccine candidates against SARS-CoV-2

Due to its ability to spread rapidly and efficiently, vaccination efforts against SARS-CoV-2 were quickly launched following the onset of the pandemic. This was of particular importance as, due to the viruses' zoonotic origins, human hosts showed little to no natural immunity, further allowing the rapid spread of the disease. Developing vaccine candidates against SARS-CoV-2 is an essential step required to control the pandemic.

One of the leading vaccine candidates against this virus is the adenovirus vaccine candidate ChAdOx1-nCoV-2019 developed with The Jenner Institute's adenovirus vaccine platform, using a replication-deficient simian adenovirus vector for vaccine delivery. Like many of these vaccines, ChAdOx1-nCoV-2019 utilizes the SARS-CoV-2 spike protein to elicit an immune response against the virus, with this vaccine using a replication-deficient simian adenovirus vector for delivery of the antigen in a similar adenovirus-vector system previously used for other novel viruses such as Middle East Respiratory syndrome (MERS) coronavirus (147). Several studies have assessed the safety and immunogenicity of this vaccine, with phase 1/2 clinical trials in human subjects suggesting the vaccine has acceptable safety and ability to produce neutralising antibody responses, with a clinical study by Folgetti and colleagues showing increased serum titres of anti-S antibodies at day 28 post infection in a prime-boost vaccination regime (148). ChAdOx1-nCoV-2019 has also been put into several animal models, with vaccination of mice and pigs demonstrating that boosting the vaccination produces greater neutralising antibody responses against SARS-CoV-2 when compared to a single dose of the vaccine (149). Trials in non-human primates have also shown this vaccine can prevent the onset of viral pneumonia and generate enhanced antibody responses, again through a prime-boost strategy, with a study by van Doremalen and colleagues showing significantly lower viral loads in the respiratory tract of rhesus macaques vaccinated in this way. (150).

Whilst the adenoviral vector vaccine model has shown considerable promise, other vaccine strategies to emerge out of the pandemic have utilized novel mRNA vaccine technologies.

The two leading candidates, the Moderna mRNA-1273 vaccine and the Pfizer BNT162b2 mRNA vaccine, use a modified mRNA for the SARS-CoV-2 S protein delivered in a lipid-nanoparticle to cause the host to produce the S protein and thus an immune response against it, without the need for a viral vector or an attenuated form of the SARS-CoV-2 virus. The mRNA-1273 vaccine has shown a 94.1% efficacy in clinical trials, with Baden and colleagues reporting the vaccine significantly reduced severe onset of COVID-19 in the vaccinated group compared to the placebo group (151). The BNT162b2 vaccine showed similarly strong results, with a 95% efficacy shown in clinical trials, with Polack and colleagues noting that the safety and efficacy of this novel technology was comparable to other viral vectored methods used in other studies (152). Much like the ChAdOx1-nCoV-2019 vaccine studies, these two mRNA vaccines were given in a prime-boost regime, suggesting that most future vaccines against this virus will use this strategy.

While these results remain promising, it is still of critical importance to understand the immune responses to SARS-CoV-2, and indeed all respiratory viruses, in order to best understand these pathogens and how to overcome their disease. The following sections will discuss the immune system in greater detail, with reference to the immune cell subsets that drive immunity to pathogens, and with particular focus on how these cells fight against respiratory viruses such as influenza viruses and SARS-coronaviruses.

1.4 Innate immunity to respiratory viruses

The body's first line of defence against respiratory pathogens is the innate immune system, which acts as a physical barrier against infection while also employing immune cells with non-specific immune capabilities to fight against viruses. The mucus lining of the respiratory tract provides the first physical barrier to infection, with viral particles being trapped in the mucosal secretions preventing entry to the epithelia and removing the virus from the respiratory tract via ciliated cell flagellation (153, 154). While this provides an effective first barrier for many pathogens, influenza viruses have been shown to escape these mucosal secretions using

their NA protein, which cleaves 'decoy' receptors in the mucus that bind to the HA to prevent cell access to the host epithelium (155). Once at the cell surface, these viruses are also targeted by anti-viral factors on the cell surface; one notable example of these proteins, IFITMs, is explored in more detail in section **1.11**. Once these cells become infected, innate leukocytes form the next important role in preventing the spread of the viral infection.

1.4.1 Antigen presentation pathways

There are several types of innate leukocytes which are important in controlling respiratory viral infection. These cells broadly fall into the category of antigen presenting cells (APCs) that express major histocompatibility complex (MHC) class I and class II molecules to present antigens to lymphocytes for pathogen recognition, with MHC-II generally only found on 'professional' APCs while MHC-I is found on all nucleated cells. The MHC complex is comprised of a heterodimer of two peptide chains, a heavy α-chain and β_2-microglobulin chain for MHC-I, and homologous α- and β-chains for MHC-II (156). The conformation of these peptide helices forms a binding pocket, where peptides can be loaded and in the case of viral infection, these peptides are derived from viral protein components (157, 158). The MHC locus in humans, known as the Human Leukocyte Antigen (HLA) locus, is highly variable, allowing for a broad spectrum of peptides to be presented. HLAs are divided into three subfamilies, HLA-A, HLA-B and HLA-C, allowing for a wide array of peptide recognition and presentation (159).

Peptides for MHC presentation are processed in the target cell via the proteasome, a protein complex which captures larger proteins from the cytoplasm and degrades them into smaller fragments of 8-10 amino acids for MHC-I (160), and 13-25 amino acids for MHC-II (161), which can fit into the MHC binding pocket in order to be presented to other cells (162). In order to present viral peptides to mount an immune response against a viral threat, following interferon release a second complex known as the immunoproteasome is produced to specifically target viral proteins being synthesised, to create short peptides specific to the invading pathogen for presentation as a way to both degrade viral proteins as they are made while allowing an

immune response against these peptides to occur (163, 164). This pathway is utilised by both professional APCs, which present antigens that are either internalised or produced through actual infection of the cell, and by other cells such as the respiratory epithelium which become infected by the virus. Mutations in both the viral peptides, and also the MHC molecules themselves, may hinder these processes, which will be discussed in greater detail in Section **1.9.2**. Regardless, the presentation of peptide antigen loaded into these MHC molecules is critical in eliciting a targeted immune response specific to the pathogen at hand, and there are several innate cell types which play important roles in this process as discussed in the following sections (165, 166).

1.4.2 Innate leukocyte control of infection

One of the first APC types recruited to the site of infection are neutrophils, which are drawn to the area by the release of chemokines such as CCL3 and IL-8, and act as rapid responders to protect against viral infection (167, 168). This is done through the use of granulocyte factors such as defensins to directly inactivate virus (169), and through the release of pro-inflammatory cytokines which both halt viral infection and draw other leukocytes to the site of infection (170).

Following neutrophil infiltration to the site of infection, peripheral blood leukocytes known as monocytes are drawn to the area. This occurs through chemotaxis recruitment by alveolar macrophages and epithelial cells of the respiratory tract, which secret chemokines such as CCL2, and CCL5 (171). Monocytes, commonly classified by CD14 and CD11b expression in humans (172-174) and mice (175) respectively, use phagocytosis to ingest viral particles and apoptotic cells for antigen presentation through the MHC pathway. Human monocytes are split into three subsets based on function and surface expression: non-classical monocytes ($CD14^{-}CD16^{+}$), which along with antigen presentation and pro-inflammatory responses are associated with wound healing (176); intermediate monocytes ($CD14^{+}CD16^{+}$), which highly express MHC-II; and classical monocytes ($CD14^{+}CD16^{-}$), which are important in the IL-10 response and phagocytosis (177, 178). These cells also produce pro-inflammatory cytokines

such as IFNs and TNFα to further hinder viral replication and recruit adaptive immune cells to the site, and it is these factors that contribute to the immunopathology of respiratory virus infections, despite them being critical for controlling the ongoing infection (179, 180). Nevertheless, monocyte-derived cells such as alveolar macrophages have been shown to greatly ameliorate the outcomes of influenza infection in multiple animal species (181-183), and also provide protection against other pathogens such as bacterial infections (184).

Dendritic cells (DCs) are a key type of APC that help fight respiratory virus infection, and like all APCs use MHC molecules to present viral peptides to T cells to elicit a specific immune response against the viral pathogen. DCs are present in and around epithelial surfaces, including in the respiratory tract, where they are often characterised by CD11c expression coupled by expression of CD11b (185). DCs are characterized into two broader subsets based on their localisation, with resident DCs present in a number of tissues such as the skin and lung to act as initial responders at these sites (186), and migratory DCs which traffic through the blood either to become resident cells or as antigen "ferries" which carry antigen to the lymph node for lymphocyte activation (187). These can be further distinguished into conventional or myeloid DCs (cDCs), which are functionally similar to monocytes, and plasmacytoid or lymphoid DCs (pDCs), which are more similar to phenotypically to B cells though mostly function as IFN-producers (188). cDCs are mostly present as Type 1 DCs, which act as major stimulators of T cells through releasing cytokines such as IL-12 (189). One study by Ng and colleagues has confirmed that $CD103^+$ Type 1 cDCs are critical in modulating the cytotoxic T cell response following infection with influenza virus, as mice ablated in the cDCs were unable to mount an effective $CD8^+$ T cell response and thus succumbed to influenza virus infection (190). Type 2 DCs are far rarer in the blood and are associated with wound recovery, though a recent study by Shin and colleagues suggests a subset of these Type 2 cDCs may be important mediators of inflammation (191).

DCs induce influenza virus uptake by expressing DC-SIGN, which binds to influenza virus surface glycoproteins, leading to an induced infection in the DC and thus production of a

chemokine response and antigen presentation of viral peptides (192, 193). These APCs form a vital bridge in linking the innate immune response to the adaptive immune response by migrating to the draining lymph node to activate T cells.

Despite their importance in preventing the spread of initial viral infection, innate cells generally are unable to prevent and clear infections on their own, in part due to their quick but broad functionality. Thus, their role in activating the adaptive immune system is critical for specific immune responses targeting the virus, with activation of $CD4^+$ T helper cells a critical component in fighting the infection.

1.5 T cell immunity to respiratory viruses

1.5.1 T cell origins and maturation

Like all lymphocytes, T cells originate as bone marrow progenitor cells which migrate to the thymus to mature. T cells are generally classified by the expression of T cell receptor (TCR) which are highly variable molecules, with each T cell having a unique receptor specificity to recognize different antigens loaded onto MHC molecules. Most T cells express an αβ heterodimer, though a small subset of T cells express a γδ heterodimer which gives them different functionality to more conventional αβ T cells (194). The β-chain of the TCR is formed from the variable (V), diversity (D) and joining (J) gene segments of the variable region alongside the constant (C) region, whilst the α-chain is sequentially formed from the V and J segments (195). These reassortment events, combined with the imprecise joining of these chains, creates non-germline encoded sequence variations, allowing for a diverse array of TCRs to be generated (196). The now functional variant β-chain is expressed with the invariant pre-α-chain along with CD3 to form a pre-TCR complex, which acts as a critical checkpoint to bypass programmed cell death and continue the maturation of the T cell (197). Pre-TCR signalling initiates proliferation of the cell and initiates rearrangement of the α-chain, which

can then associate with the β-chain to form the TCR heterodimer expressed on the cell surface along with CD4 and CD8 (198).

The T cell's lineage is then finalised through the TCR's ability to engage with MHC class I (for $CD8^+$) or MHC class II (for $CD4^+$), with these interactions forming another important selection process whereby the cell's autoimmune tolerance is tested. Cells with low affinity to self-peptides are able to leave the thymus as mature T lymphocytes, while cells with high affinity for self-peptide undergo apoptosis (199). This thymic selection affects the total repertoire of TCRs, as despite a theoretical $10^{10} – 10^{20}$ possibly TCR variants, only around 10^7 have been reported in longitudinal studies, possibly due to those unselected variants being self-recognising (200). Regardless, this broad array of possible TCRs allows for the body to specifically encounter pathogens invading the body, with the cytotoxic T cell response the key immune response against viral infection.

1.5.2 $CD8^+$ T cell function and memory

Peripheral $CD8^+$ T cells are activated in the lymph node following recognition of antigen presented on MHC-I molecules by dendritic cells in the lymph node. This activation initiates proliferation, and these cells then traffic to the site of infection to combat the infection. One major function of $CD8^+$ T cells is its cytotoxic ability to directly kill virus-infected cells. This is achieved when cytotoxic T cells recognise infected cells expressing MHC-I loaded with viral peptides recognised by the TCR. This interaction between the cells induces the T lymphocytes to inject apoptotic molecules such as granzymes into the infected cells through pores formed at the immune synapse between the cells due to the release of perforin, with these granzymes causing programmed cell-death (201-203). $CD8^+$ T cells also secret a number of pro-inflammatory cytokines such as IFNs and TNFα (204), as well as IL-10 as a protective mediator against virus infection particularly observed in coronavirus models, with Trandem and colleagues showing that IL-10 expression by $CD8^+$ T cells is protective not only in the lungs but also is critical in protecting mice from tissue damage from viral encephalitis (205). $CD8^+$ T cells have also been shown to specifically target conserved epitopes of influenza

viruses from the less variable internal proteins, allowing them to effectively combat a broad array of influenza viruses (206).

Following the clearance of infection, these cytotoxic effector cells either undergo apoptosis, or form effector memory cells. This process of forming memory cells is driven by IL-12, with long-lived memory cells also showing increased expression of IL-7Rα (207, 208). Memory $CD8^+$ T cells are generally divided into two subsets, from which further classifications are generally made: effector memory cells (T_{EM}) and central memory cells (T_{CM}), which are differentiated by their expression of CD62L and CCR7, with T_{EM} having low expression of these molecules and T_{CM} having high expression (209). In more recent years, however, two further subsets, stem cell memory (T_{SCM}) and terminally differentiated memory (T_{EMRA}) have been identified as CD45RA-expressing variants of T_{CM} and T_{EM}, respectively (210, 211). T_{EM} cells generally are found in the circulation and are specialized at migrating to peripheral tissues to encounter infections using their cytotoxic properties. T_{CM} cells are localised to secondary lymphoid tissues and are used to encounter systemic infections (210). However, one set of T_{EM} cells can be found in the tissues themselves. These cells, known at tissue-resident memory (T_{RM}) cells, express CD69 and CD103 which enhance entry and retention in tissues, allowing these cells to act as cytotoxic sentinels within peripheral sites (212, 213). T_{RM} cells in the lung have been shown to be important responders against influenza virus infection, as they act as potent specific early-responders against the virus infection, with studies showing that these cells express high levels of CXCR3 to localise in the airways where they are able to readily act in response to viral stimulation (214, 215). These cells are also importantly guided towards development by $CD4^+$ helper T cells (216), which are required for $CD8^+$ T cell formation (217), showing the interconnectedness of these adaptive responses.

1.5.3 $CD4^+$ T cell function

Much like their $CD8^+$ counterparts, $CD4^+$ T cells recognise antigen presented by APCs such as dendritic cells in the lymph node and are then activated by costimulatory ligands and IL-2 to proliferate and elicit an immune response specifically against the pathogen at hand. These

cells make up the majority of circulating T cells, and recognise viral peptides presented to them by MHC-II (218). Commonly referred to as 'helper' cells, $CD4^+$ T cells have different effector functions to $CD8^+$ T cells, which are split into three differing types of responders: T helper type 1 (Th1), type 2 (Th2) and type 17 (Th17), which the latter is more involved in autoimmune diseases. Th1 cells produce IFN-γ and lymphotoxin as their primary cytokines, and modulate the pro-inflammatory response by recruiting other cellular factors to the site of infection (219). These pro-inflammatory cytokines act as a positive feedback loop to further activate other Th1 cells while also providing an anti-viral state to control infection. Th1 cells can also selectively enter inflamed tissues through their ability to bind P- and E-selectins (220). Th2 cells, on the other hand, are generally anti-inflammatory, and produce interleukins such as IL-4, IL-6 and IL-10 which guide the immune response towards an antibody-producing response (221). Interestingly, IAVs have been shown to dampen the Th2 response by gearing the immune response towards a Th1 response, preventing the recruitment of eosinophils and further Th2 cells (222).

Another lineage of $CD4^+$ T cells are T follicular helper (T_{FH}) cells, which specifically have important interactions with B cells (discussed more in **1.6**). T_{FH} cells can also be delineated by type 1, 2 and 17 responses and express the unique transcription factor Bcl6, which when upregulated by IL-6 and IL-21 lead to suppression of the regular T helper differentiation pathways in germinal centres (223). T_{FH} cells then interact with developing B cells by providing activating signals such as CD40L and IL-21 (224, 225), allowing for clonal selection of B cells required to fight a specific pathogen. Interestingly, these now activated antigen presenting B cells are also important in facilitating T helper cell-mediated responses to allow for greater long term memory, creating a feedback loop of T cell-B cell interactions (226).

1.6 Humoral immunity to respiratory viruses

1.6.1 B cell classification

B cells are lymphocytes which assist in the immune response by providing humoral immunity, with their main effector function being the secretion of immunoglobulin (Ig) molecules. These Igs, called antibodies, act by binding a specific antigen, either directly inactivating it or allowing phagocytic cells to recognise and ingest the Ig-bound antigen (227). Much like T cells, B cell progenitors begin in the bone marrow, where they undergo functional rearrangement of their Ig gene segments (228, 229) in a process similar to TCR rearrangement. The heavy chain of the Ig reassorts V, D, and J genes, whilst the light chain reassorts the V and J genes, allowing for a diverse array of Igs which can recognise upwards of 5×10^{13} different antigens (228). Two heavy chains and two light chains come together to form the Ig heterodimer (or heterodimers for some Ig subclasses), which have a V region for antigen recognition, and a C region which gives the Ig effector function (230). Igs are split into five isotypes, IgA, IgD, IgE, IgG, and IgM, each with different effector functions due to their differing C regions (231). Isotype class switching occurs in a sequential manner through a class switch recombination event in the C region of the heavy chain, with breaks in the switch region allowing removal of isotype exons to change isotype. The Ig begins as an IgM, and then this class switching can cycle through IgD, IgG, IgE, and then IgA selectively as required, allowing for single parent cells to generate various isotypes towards a single antigen (232).

As the first isotype produced sequentially, IgM acts as a primary responder against pathogens. These antibodies are unique in that they form a pentamer, rather than the monomer structure seen in other isotypes (230, 233). IgM expressed on the B cell surface associates with CD79a and CD79b (234), allowing for IgM signalling and eventually secretion. These IgMs have been shown to be important in the activation of the complement system, a system involving small immune factors that enhance the antibody response and phagocytosis of innate cells, through binding complement factors such as C1 and C4b (235, 236). Skountzou and colleagues have found that not only are IgMs important in controlling influenza

virus infections, but their responses are also long-lived, with IgM^+ plasma cells detectable in patients nine months post-influenza exposure in mice at significantly higher levels than IgG^+ cells which disappeared from the circulation at far earlier time points, and were still detectable by ELISpot assay 2 years post-infection (237). Moreover, a study by Shen and colleagues found IgM antibodies can have stronger neutralising capacity against influenza B viruses compared to IgG antibodies when administered pre-infection, highlighting their importance in combatting these viruses while also suggesting their potential use as a prophylactic treatment option (238). Interestingly, circulating IgMs known as "natural" Igs which are produced constantly in low levels by circulating B cells have also been shown to inhibit influenza infections prior to the onset of the major B cell response, further highlighting the importance of these factors in the early neutralisation of viral infections (239).

IgG is the most abundant isotype in the serum, encompassing approximately 75% of all circulating antibodies (230). These antibodies are also the longest lasting compared to other isotypes, with a half-life of between 10 and 21 days compared to IgM and IgA which only last 5 to 6 days (240). These responses, however, can be recalled by long-lasting memory B cells where specificity against the 1918 H1N1 pandemic stain of influenza virus were able to reactivate and produce IgG responses against the 2009 H1N1 pandemic influenza virus (241, 242). IgG antibodies also exhibit a phenomenon known as affinity maturation, whereby the IgG antibodies produced later in the immune response are better able to neutralise virus directly compared to those formed early in the response (243, 244). These antibodies often bind to the external proteins of the virus, such as the HA or NA of influenza viruses, preventing viral entry and allowing phagocytic cells to internalise and lyse viral particles (245, 246). Despite evidence suggesting IgG responses play a key role in SARS-CoV-2 immunity, a study by Markland and colleagues found that even though many COVID-19 patients had IgG titres against the virus, particularly in more severe disease cases, not all patients who recovered had detectable IgG against SARS-CoV-2, yet had other isotypes that were SARS-CoV-2-specific, suggesting that IgG antibodies are not essential for COVID-19 recovery (247-250).

The B cell response to respiratory viruses such as influenza viruses are stimulated in the mediastinal lymph node, where follicular B cells interact with $CD11b^+$ DCs carrying influenza antigens and begin to proliferate following stimulation of the B cell receptor and by IL-4, IL-5, and IL-6 (251). This proliferation is also driven by type I IFN signalling, which upregulates TLR3 and TLR7, and CD69 and CD86, allowing these cells to be more receptive to both innate cell signalling and T cell stimulation (252). $CD4^+$ T cells activate the B cells though cell-to-cell contact, with factors including T cell inducible co-stimulator (ICOS) which are critical in directing the humoral response towards the specific pathogen following recognition of antigen presented on MHC-II expressed on the B cell surface. Activated B cells are then able to secrete Igs to neutralise the viral threat, and following viral clearance, form long-lasting memory cells to combat any future viral infections (253).

Taken together, the adaptive and innate immune response form a protective system against respiratory pathogens. However, despite the best efforts of the immune system, viruses are still able to overcome many of these mechanisms to cause disease.

1.7 Pathogenesis of AI viruses

The immune system's defences against invading pathogens are complex, with many variable pathways that can be taken in order to control viral infection. However, viruses can often use these systems to their advantage. Additionally, overactivity of the immune system can contribute heavily to the pathology as a result of infection. *The following sections **1.7**-**1.9** are taken from a first-author paper already published (Horman et al., Front. Immunol., 2020, **Appendix**), and describe how these host-pathogen interactions contribute to disease pathology in the context of avian influenza viruses.*

1.7.1 Cytokine responses to HPAI infections

Several factors appear to contribute to the worsened pathology observed in HPAI infections when compared with LPAI infections. One hallmark of HPAI pathogenesis is a rapid and robust cytokine response, often referred to as a 'cytokine storm' or hypercytokinemia. This build-up

of cytokines causes an inflammatory environment at the site of infection, leading to immune cell infiltration. In addition to the hypercytokinemia, there is a well-established loss of leukocytes, leading to the severe pathogenesis seen in these infections (21). Recently, the main factors associated with pathology were further described by Kuchipudi and colleagues (2014). Following infection with H5N1 *in vitro,* chicken lung cells had increased expression of specific pro-inflammatory cytokines, particularly interleukins (IL)-6 and IL-8 when compared to cells infected with LPAI H2N3, suggesting that IL-6 and IL-8 may be key regulators leading to worsened pathology of HPAI compared to LPAI (254). IL-6 and IL-8 were also found to be significantly upregulated in the lungs of H5N1 infected ferrets, as well as in peripheral tissues, including the spleen, heart and liver (255). Interestingly, this study also found that IL-6 and IL-8 were downregulated in the nasal turbinates following infection with pandemic H1N1 virus, which produced a less severe clinical infection compared to the H5N1 in ferrets (255). These findings were consistent with studies completed in rhesus macaques, which similarly showed upregulation of TNFα, IL-6 and IL-8 in response to experimentally induced H5N1 infection, along with an increase in the antiviral interferons, findings which correlate to the severe fever symptoms observed in the macaques at the peak of the fever response at day six post infection (256). Moreover, infections with the recently emerged HPAI H5N6 in chickens, which caused human fatalities, was shown to have a very distinct immune response compared to other H5N6 strains by producing much higher levels of IL-6, IL-8 and other pro-inflammatory mediators such as tumour necrosis factor α (TNFα) compared to previously identified strains (257). While chickens and ferrets show similar pathogenesis, conversely, duck lung cells infected with the same viruses showed a decrease in IL-6 expression compared to the LPAI viruses, whilst IL-8 remained unchanged. It suggests that IL-6 may play a pivotal role in the regulation of AI pathology in birds and, as previously discussed, ducks typically show lessened disease severity following H5N1 infection compared to chickens (**Figure 1.2**)**.** Moreover in humans, H5N1 elicits a similarly robust cytokine response, with the upregulation of IL-6, IL-10 and TNFα in response to H5N1 (258).

1.7.2 Cytokine responses to H7N9 infections

As the H7N9 virus is usually classified as a LPAI in chickens, it is interesting to note that a similar trend was observed when H7N9 of human origin were shown to induce increased production of pro-inflammatory IL-6 and IL-8 cytokines when compared to H7N9 of chicken origin (259). In the same study, it was demonstrated that IFNλ1 production was reduced for the human isolate, suggesting a possible modulation of the immune response. In addition, Wu and colleagues (2016) also found that H7N9 patients had higher levels of C-reactive protein expression in their plasma compared to H1N1 patients, and as C-reactive protein is associated with broader inflammatory responses, it suggests that this may be yet another factor alongside these regulatory cytokines contributing to disease severity (260). A similar pro-inflammatory response was observed when alveolar macrophages were infected with H7N9, however when compared to H5N1, this cytokine response was demonstrated to be milder (261). Downregulation of these inflammatory responses to infection confers a level of immunity to these viruses in pigs, which hints at how pigs can act as mixing vessel species for AI without succumbing to severe disease. Human lung epithelial cells can express 100-fold higher levels of TNFα compared to pig lung epithelia, with suppressor of cytokine signalling 3 (SOCS3) identified as a key factor in reducing levels of TNFα in pig cells (262).

1.7.3 Leukopenia in HPAI infections

The mediators of cytokine production are resident and infiltrating immune cells, which release these cytokines in response to the infection to recruit other immune cells and hinder viral replication. This occurs following cellular activation and results in further activation of leukocytes recruited to the area in a positive feedback loop (263). As pro-inflammatory molecules are associated with apoptotic pathways in humans, increased cytokine production is likely to be a contributing factor in the loss of immune cells, or leukopenia, observed in severe cases of HPAI infection (84). These pro-inflammatory regulators lead to upregulation of the death signalling molecule Fas-ligand on the infected host cell to initiate the caspase-mediated Fas-associated pathway, in which Fas receptors on the immune cell (part of the

TNF-receptor family) bind to Fas-ligand and subsequently recruit the Fas-associated death domain (FADD) molecule (264). FADD interacts with caspase-8, which initiates a signalling cascade within the immune cell, resulting in the destruction of cellular components and thus cell death, which may be causative of the pathology seen in influenza patients (265). Indeed, both H5N1 and H7N9 have been observed to cause leukopenia in hospitalised patients (266-268). According to Boonnak and colleagues (2014), $CD8^+$ T cells can be particularly affected by the Fas-ligand mediated pathway, where Fas-ligand was upregulated on plasmocytoid dendritic cells during lethal H5N1 infection in mice, which then lead to apoptosis of influenza-specific $CD8^+$ T cells in the lung draining lymph nodes (264). Furthermore, in hospitalized H7N9-infected patients during the emergence of H7N9 in 2013, the persistence of immune cell subsets within the blood contributed to disease severity and fatal outcomes, with the continuation of $CD38^+HLA\text{-}DR^+$ $CD8^+$ T cell responses shown to be predictive of fatal outcomes, possibly due to longer-lasting inflammatory responses in the peripheral blood and lung (269). Loss of peripheral blood lymphocytes was also observed in human seasonal influenza A infections, with these cell subsets succumbing to apoptosis by the same apoptotic pathways described for AI viruses (270). In summary, LPAI versus HPAI viral strains differentially promote the induction of pro-inflammatory cytokines, which then alter disease outcomes in different species. The potential mechanisms by which certain HPAI AI viruses cause more severe disease will be further discussed in following sections.

1.8 Viral fitness across species

1.8.1 Sialic acid receptor binding preference

In order for AI viruses to be capable of infecting multiple host species they require viral adaptations allowing replication in different host cells, which ultimately increase their genetic fitness and create a sustainably replicating and transmitting virus (271). It is well established that for zoonotic transmission of AI viruses, the virus needs to present the appropriate HA binding specificity to allow viral fusion and entry. AI virus HA proteins typically have a binding

preference for sialic acid residues with an α-2,3-Gal terminating sequence found on the surface of avian cells (**Figure 1.2**), resulting in restriction to avian cells (92, 272). Therefore, for AI viruses to gain entry into human cells displaying an α-2,6-Gal terminating sequence, modifications to the HA binding site may be required to allow this new interaction.

One of the commonly associated amino acid substitutions for LPAI strains converting from avian to mammalian receptor-specificity is a HA Q226L substitution (87, 273-275). For example, LPAI H9N2 isolates from birds can adopt a Q226L substitution, which increases its mammalian receptor binding affinity and potentially infect mammalian hosts (276, 277). However, with regards to H7N9 human isolates, Belser and colleagues (2013) described the Q226 bearing Shanghai/1 and the L226 bearing Anhui/1 as binding to largely avian α-2,3-Gal receptor analogues and mixed α-2,3/α-2,6-Gal receptors, respectively (93). Despite these differences, infections with each isolate produced effective replication in the lower respiratory tract of ferrets, suggesting additional factors are involved in mammalian adaptation. Similarly, this Q226L mutation has not been commonly observed in the HA of H5N1 HPAI viruses (278, 279). However, alternative substitutions, HA Q192H and HA I151T, can confer increased ability for replication in human hosts. Moreover, Herfst and colleagues (2012) demonstrated a closely related change to the HA of H5N1, HA Q222L, conferring more efficient replication and transmission in the ferret model (95). Additional to this HA mutation, an E627K change in the polymerase basic 2 (PB2) protein in H5N1 HPAI was also shown to be critical for transmission in ferrets (93, 280-283).

1.8.2 Multi-basic cleavage sites

In addition to HA-sialic acid binding, key to viral fitness is the presence of a multi-basic cleavage site (MBCS), which has been shown extensively with H5N1, that the presence of a MBCS often dictates the use of the term HPAI (284, 285). The presence of a MBCS in the HA of influenza A viruses allows HA cleavage by additional enzymes such as furin-like proteases, whereas without a MBCS, the virus relies on only trypsin-like proteases (286). This flexible range of enzyme activity results in the virus being able to infect a greater range of cells and

can lead to systemic infection (284, 285, 287). Though commonly associated with H5N1, this motif is seen in other avian-infecting HPAI viruses such as H7N3, however these strains are less frequently transmitted to humans (55, 288). Interestingly, LPAI can also acquire MBCS motifs, changing the pathogenicity of the virus from low to high, such as in the case of an H7N8 outbreak in Turkey in 2016, where a LPAI virus caused a severe outbreak in the poultry due to the spontaneous addition of a MBCS, leading to over 800 bird deaths (289). However, the addition of a MBCS does not guarantee a LPAI virus to increase its pathogenicity, as recombinant H5 and H7 viruses do not exhibit HPAI pathology in chickens specifically due to the addition of a MBCS (290), which suggests that these motifs are one of many factors contributing to HPAI pathogenesis. H7N9 has also been shown to be able to obtain a MBCS to become highly pathogenic in chickens (291). Imai and colleagues (2017) showed increased disease severity of a MBCS-containing H7N9 virus in the ferret model compared to a LPAI H7N9 virus (54). However, H7N9 will still cause severe disease without a MBCS in most human cases, highlighting how unique this virus is in the AI landscape for its ability to show HPAI-like symptoms in mammals, while maintaining low pathogenicity in birds. Similarly for H5Nx viruses, several additional changes in the H5 HA protein, such as an N158D mutation, also allow greater replication of the virus in ferrets without the need for a MBCS, which combined with reassortment with human-adapted H1N1 gene segments shows the potential for these viruses to not only cross into humans but cause severe, sustained human infection without systemic spread (292). This, coupled with H7N9's ability to cause severe disease without the requirement of a MBCS, suggests that while the MBCS still acts as a key virulence factor for AI viruses, it is not a sole-determining factor for HPAI in humans.

1.8.3 Non-structural protein 1 (NS1)

Another key virulence factor elucidated in recent years is the ability of the non-structural protein 1 (NS1) to aid viral escape in the host immune system. In avian hosts, NS1 has been associated with worsened pathology through increases in iNOS and oxygen-reactive species for both LPAI H9N2 (293) and HPAI H5N1 (294). However, in contrast in mammals, the NS1

protein has been more closely associated with inhibition of host interferon (IFN) responses. Jia and colleagues (2010) showed that the H5N1 NS1 protein inhibits IFN production through interference with the JAK/STAT pathway. They found that expression of NS1 in HeLa cells prevented STAT phosphorylation and upregulated inhibitors of this pathway to prevent expression of IFNAR and SOCS3 proteins, which generally upregulate IFN expression (295). Furthermore, a naturally occurring deletion in the H5N1 NS1 effector domain can attenuate the virulence of the virus in both chickens and mice, suggesting that this protein is critical in the ability of H5N1 to suppress host immune antiviral responses across hosts (296). The pathogenicity of H5N1 in mice is also affected by the NS1 protein, as a single mutation (P42S) conferred greater pathogenicity to the virus by preventing nuclear factor-κB (NF-κB) and interferon-regulatory factor 3 (IRF3) signalling, and thus inhibiting IFN responses (297). Interestingly, in cats the NS1 protein can be associated with blocking NF-κB and IRF3 signalling in response to the emerging HPAI H5N6 virus, with inhibition of the IFN-β promoter blunting the feline IFN response (298), suggesting that NS1 may have different ways of interacting with influenza hosts across species to produce similar immune suppression. On the other hand, Thube and colleagues (2018) investigated the IFN responses of HPAI H5N1 compared to LPAI H11N1 and suggested that decreased interferon signalling occurred independently of NS1, suggesting other viral elements can also induce a reduced antiviral state in cells (299). It is worth noting that while the NS1 of LPAI H7N9 is inefficient at binding to CPSF30 (involved in pre-mRNA processing), a single I106M mutation restores CPSF30 binding to NS1 thereby blocking the expression of host antiviral genes. This renders the virus more virulent than other LPAI infections (300), which may explain why H7N9 causes more severe disease in humans compared to other LPAIs. These results also highlight inhibition of IFN-activation pathways as an important viral factor in preventing host-immune responses to infection, allowing for more productive infection and potentially more severe clinical outcomes.

1.9 Host factors contributing to worsened disease progression

1.9.1 Immunodeficiency

Broad immunodeficiency can lead to worsened pathology and disease outcomes in humans and animals. For example, immunocompromised patients who contract LPAI viruses such as H9N2 suffer severe respiratory distress, and though many of these LPAI remain mild even in immunocompromised patients, H9N2 induces stronger cytokine responses than seasonal influenza viruses (301, 302). These trends are also observed in avian hosts, in which Nili and Asasi found that chickens co-infected with other pathogens such as *M. gallisepticum* showed worsened clinical signs such as severe necrotizing tracheitis, leading to a 19% mortality in the flock (303, 304). Therefore, it is apparent that both the host and pathogen can contribute to perturbed inflammation and severe disease outcomes.

1.9.2 MHC interactions with influenza virus

The interaction between influenza virus peptides and major histocompatibility complex (MHC) molecules is a key host-pathogen interaction affecting the outcome of disease following initial infection. Different HLA subtypes confer different levels of susceptibility to influenza A viruses, as not all HLA subtypes respond to influenza peptides in the same way. For example, human populations expressing HLA-A*02:01 can elicit strong, cross-protective $CD8^+$ T cell responses following presentation of the internally conserved $M1_{58-66}$ epitope (305-308); this epitope is one of the most immunogenic influenza peptides observed in humans with HLA-A*02:01 being the most common HLA alleles expressed worldwide (305). Moreover, individuals lacking common HLA alleles may be at greater risk of influenza A infections, such as those carrying the HLA-A*24:02 allele, associated with increased mortality in individuals infected with pandemic H1N1 virus (309). Indigenous populations in particular are susceptible to influenza A due to a lowered prevalence of protective HLA variants towards these viruses (308). Wang and colleagues (2015) suggest that for AI viruses such as H7N9, MHC-interactions with internally conserved epitopes from other influenza A strains, such as pandemic H1N1, may explain why some populations show greater immunity through cross-

reactive $CD8^+$ T cell responses than others (100). However, some H7N9 peptides may have cross-conservation with human host proteins that the immune system recognises as "self", leading to an attenuated immune response to the virus and thus worsened disease progression due to T cell-mediated tolerance (310).

Interestingly, chickens show a restricted repertoire of MHC alleles compared to other species, and these haplotypes themselves are poorly characterised. As such, a few studies have been conducted into characterising T cell epitopes in response to H5N1 infections, one such study predicting 25 potential T cell epitopes in the nucleoprotein (NP) of H5N1 in four haplotypes (311). More recently, experiments into epitopes of a specific haplotype, BF2*15, further characterized NP epitopes that may lead to protective immunity against H5N1 (312). This limited repertoire may explain why chickens show more severe clinical outcomes due to HPAI such as H5N1 compared to waterfowl, as ducks show extensive diversity in their MHC Class I alleles which allows the immune system greater coverage for viral variation (313). A recent investigation into duck MHC class I molecules found that the duck *Anpl*-UAA*01 complex showed similar peptide binding properties to HLA-A*02:01 in humans and as such appears to cover a greater array of influenza A virus epitopes compared to similar chicken MHC molecules such as BF2*2101 (314). Furthermore, migratory shorebirds which act as reservoirs for AI viruses (in particular LPAI H9N2) show increased diversity in their MHC alleles, likely as a mechanism for protecting against foreign pathogens that may be encountered during migration. A study in red knots found high MHC diversity with 36 alleles detected across 8 birds, which when correlated to their low prevalence of shed AI virus and high antibody titres to AI viruses, they could mount effective immune responses towards these viruses, possibly via cytotoxic T lymphocyte responses recognising novel peptide/MHC complexes (315). Based on a culmination of human and animal evidence, the interactions between the various pathogen and host factors contributing to human influenza severity are summarised in **Figure 1.5**. The next section will discuss one of these host factors in more detail, the interferon-induced transmembrane (IFITM) protein family.

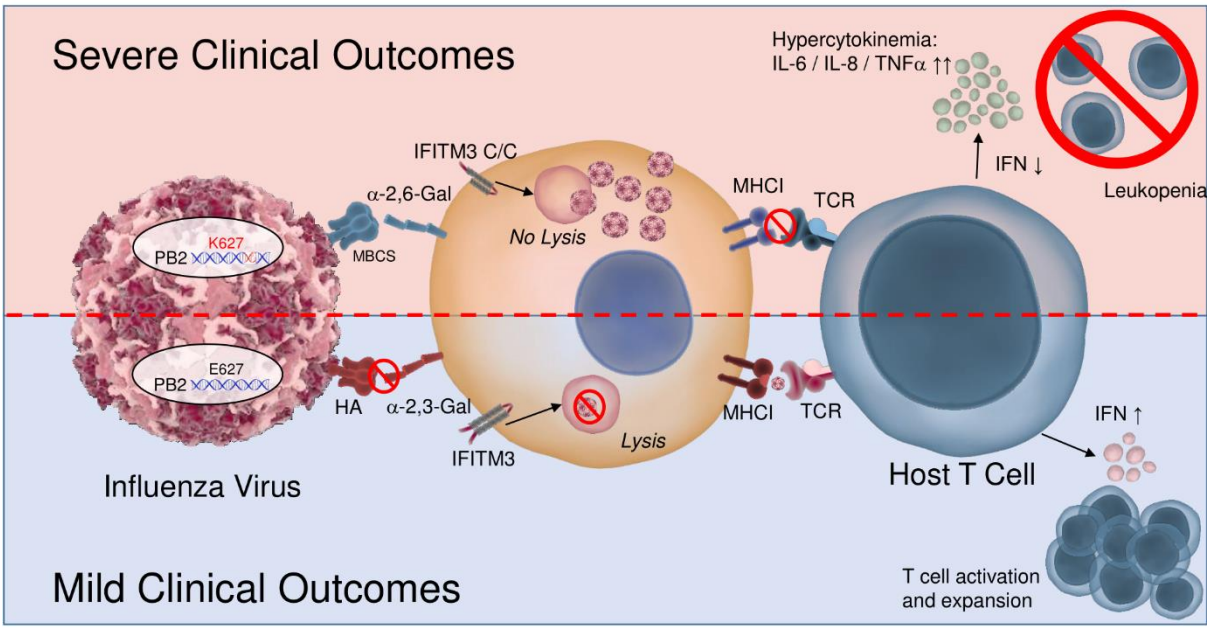

Figure 1.5. Mechanisms leading to severe clinical outcomes involve both host and pathogen elements
A number of factors have been elucidated to contribute to the severity of influenza disease outcomes. This includes viral fitness elements, such as the presence of a multi-basic cleavage site (MBCS), mutations to the polymerase basic 2 (PB2) genes, as well as the presentation of the HA protein capable of binding to human sialic acids. These viral fitness elements work in-concert with host factors such as modified IFITM proteins, with reduced ability to combat the virus and MHCI diversity which can or cannot present the antigen appropriately and efficiently to host T cells. Ultimately, these and other elements lead to changes in production of key cytokines as well as cellular activation that drives inflammation, cell death, and clinical manifestation of disease.

1.10 Interferon-Induced Transmembrane Proteins

1.10.1 IFITM protein family

IFITM proteins, which are key antiviral factors, are a family of transmembrane proteins that are stimulated by the presence of elevated interferon levels, which they themselves are regulated by interferon stimulated genes (ISGs) (**Figure 1.6a**). Thus, many respiratory viruses attempt to dampen the IFN response to evade these anti-viral factors (316, 317). IFITM proteins, mainly IFITM1, IFITM2 and IFITM3, are small transmembrane proteins, with a conserved structure of two transmembrane regions and a conserved intracellular loop (**Figure 1.6b**), with all mammalian IFITMs having the same AYSVK and ASTAKCLN motifs at the transmembrane boundaries, suggesting that these residues are critical for IFITM localization in the membrane (318, 319). While the transmembrane and intracellular regions are

conserved, the exact topology of the N- and C-terminus regions is unclear, as despite protein prediction models suggesting the regions are extracellular, topology models for IFITMs in both humans and mice have indicated that IFITM3 may possess an intracellular N-terminus domain (320), yet mouse IFITM1 may have two intracellular domains at its N- and C-terminals (321). The three proposed models of IFITM topology are displayed in **Figure 1.6c**. Furthermore, IFITM1 has been shown to localise to the cell surface, whilst IFITM2 and IFITM3 are more commonly localised in endosomal membranes, allowing IFITMs to potentially affect viral entry at multiple entry sites (322).

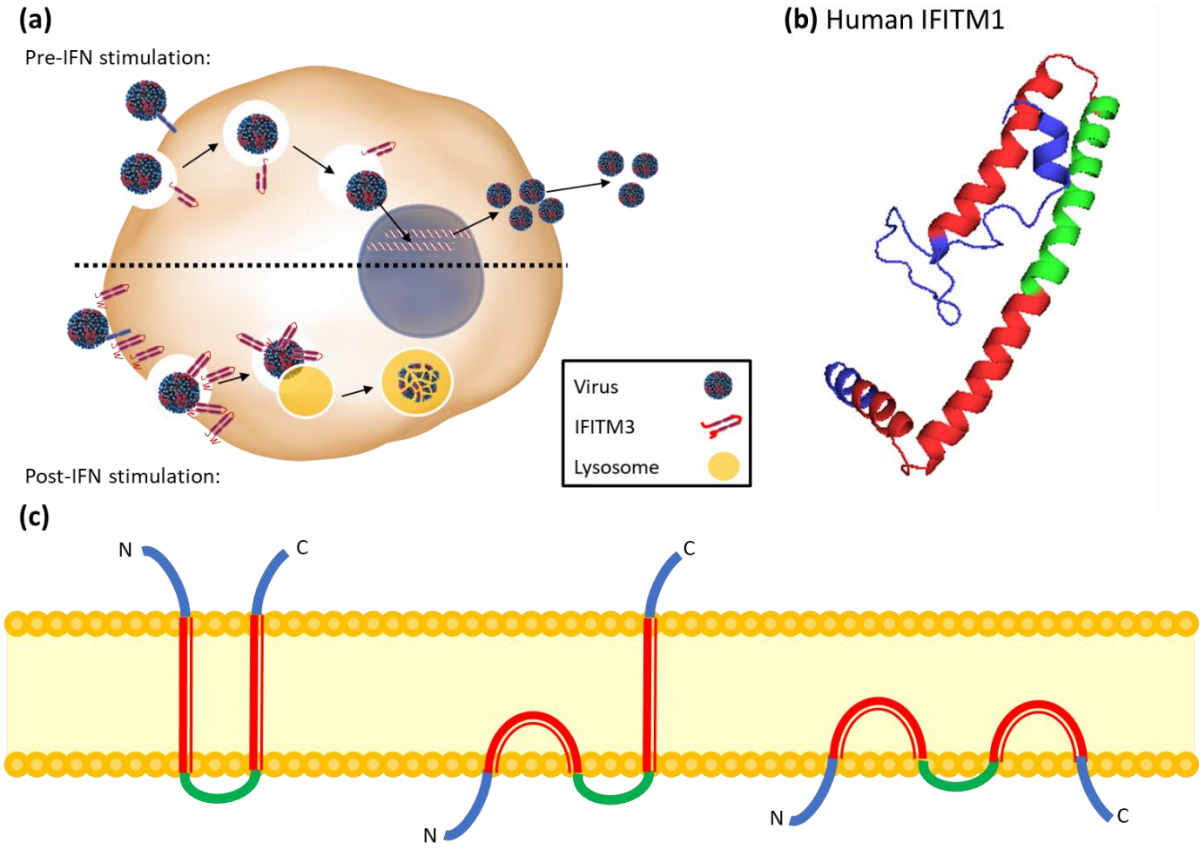

Figure 1.6. IFITM function and structural overview
(a) IFITM proteins (in this example, IFITM3), though present at low levels prior to IFN stimulation, initially are unable to completely block viral infection. However, following IFN stimulation, higher levels of expressed protein are able to successfully prevent viral endosomal escape, allowing for lysosomal destruction of the viral particle. **(b)** All mammalian IFITMs, such as human IFITM1 seen above, have conserved domains in their protein structure. Each protein has two transmembrane domains (red) surrounding a conserved intracellular loop (green), as well as an N- and C-terminal domain (blue). **(c)** There are three suggested topology models for IFITMs: the first is extracellular N- and C-terminal domains as often predicted by hydrophobicity plotting; the second is an external C-domain and internal N-domain; and the third is two intracellular domains.

1.10.2 IFITM function

The IFITM proteins can interfere with viral entry to the cytosol via cell membranes (323), with Brass and colleagues (2009) showing that over-expression of human IFITMs 1, 2, and 3 effectively blocked infection with several influenza A pseudoviruses (retroviruses expressing influenza surface proteins), including those enveloped with H5 and H7 proteins (324). Moreover, IFITM3 specifically localises to the endosomes due to phosphorylation of the Y20 tyrosine residue, enabling it to intrinsically target pH-dependent viral pathways such as that seen with influenza A viruses (325).

The IFITM3 molecule can play a significant role in mice and human influenza virus infections. T cells purified from mice inoculated with influenza antigen showed higher proportions of IFITM3 expression in the lungs due depletion of IFITM3-deficient cells, leading to the development of a more robust lung tissue-resident memory $CD8^+$ T cell response as well as a longer duration of response even following abatement of the IFN-α response due to the continued expression of IFITM3 (326). Furthermore, a study by Shi and colleagues found that SARS-CoV-2 is restricted by all of IFITM1, IFITM2, and IFITM3 in a similar way to other coronaviruses (327, 328), though there is evidence to suggest that some coronaviruses, including SARS-CoV-2, may have their entry enhanced by these proteins early in infection due to interactions between CoV-S protein and the IFITMs enabling viral entry (329), with a study by Bozzo and colleagues finding knockdown of these genes enhanced viral infection despite over-expression showing increased restriction (330). These results show the multi-faceted interactions between respiratory viruses and IFITMs, and how these proteins can be risk factors for disease. Whilst much of the research into IFITMs has primarily focussed on influenza viruses, recent studies have also investigated how these proteins interact with SARS-CoV-2 virus in a human setting.

1.10.3 IFITM mutations

A single nucleotide polymorphism (SNP) in the IFITM3 gene, *rs12252-C*, has been shown to strongly correlate to worsened disease progression, as this SNP leads to a truncated splice-

variant that affects the protein's ability to localise to the membrane (331, 332). This IFITM3 *rs12252-C* SNP was associated with severe hypercytokinemia and worsened disease progression in H7N9-infected hospitalised patients (333). In support, Zhang and colleagues (2013) showed that the *rs12252-C* mutation correlated to severe seasonal H1N1 influenza cases in Chinese populations where the mutation appeared in higher frequencies (332, 333). This trend was also seen in cases of SARS-CoV-2, where a study found the risk allele to correlate with worsened disease outcome in an age-dependent manner (334). However, studies have shown that while this SNP does affect IFITM3's ability to localise, restriction of the virus may continue with the variant protein or with a Y20A mutation to affect the localisation of the full protein (335). Furthermore, a recent study by Makvandi-Nejad and colleagues (2018) found that primary cell lines homozygous for the *rs12252-C* SNP expressed the non-truncated mRNA transcript and thus expressed the wild-type IFITM3 protein at levels greater than 99% when compared to the truncated versions (336), which may provide insights into why the *rs12252-C* mutation appears not to act as a significant risk factor in Caucasian populations, but perhaps in the Chinese patients.

Moreover, an additional SNP has recently been identified, *rs34481144-A,* which affects the promoter for the *IFITM3* gene, resulting in lower IFITM3 expression compared to hosts without the mutation. Interestingly, both the *rs12252-C* and *rs34481144-A* mutation were found to be non-overlapping in one study, as the risk allele for one was inherited with the protective allele of the other, suggesting a multifaceted IFITM response to influenza A viruses (337). Regardless, this risk allele has been identified as a potential factor in increased susceptibility to severe COVID-19 of some ethnic groups in the UK (338), whilst another mutation *rs6598045* was identified by Kim and Jeong as being correlative with worsened disease progression on a global population scale through metagenomic analysis (339). As such, it is clear that these genes are of critical importance in determining the disease outcome of many respiratory viruses, so understanding how they work in both humans and their animal models is highly important in understanding how to combat these pathogens.

1.10.4 IFITM function across species

IFITMs have been studied in a number of species, with IFITMs classified in mice and pigs, as well as in gallinaceous birds (340). IFITM1 and IFITM3 distribution in mice has been investigated in the context of H9N2 infection, with increased restriction of virus entry into host tissues due to upregulation in the lungs and peripheral tissues of BALB/c mice following inoculation. Interestingly, when infected with a H9N2 strain with higher pathogenicity and ability for systemic spread due to a K627E mutation (rV_{K627E}) in the viral PB2 protein, compared to the wild-type strain, IFITM3 was upregulated accordingly in the brain of rV_{K627E}-infected mice to combat this virus' ability to cause viral encephalitis (341). IFITM3 responses to H5 and H7 proteins have also been assessed in pigs and bats, with both these HA subtypes showing restricted entry due to the action of these IFITM3 proteins (342), suggestive of the broad action of IFITM molecules across species known to contract and potentially disseminate AI viruses. How IFITMs restrict AI viruses in "mixing vessel" species (i.e. pigs and bats) suggests that these proteins may have a key role in preventing the spread of human-infecting AI viruses through these routes, as well as contributing to these species showing lessened pathology compared to other mammalian species.

The role of IFITMs against AI viruses in avian species has not been clearly defined, though a study by Smith and colleagues (2013) has shown that chicken IFITM3 (which is "human IFITM1-like") similarly restricts H5 and H7 expressing viruses (343). However, when chickens were infected with H5N1, expression of IFITM molecules was not highly upregulated compared to other human-infecting seasonal strains such as H1N1, with IFITMs showing the weakest inhibiting effect against H7N9 (344). Hence, IFITM expression in chickens appears to be limited and does not vary greatly whether the virus is of low or high pathogenicity. Conversely, the IFITM expression profile observed in ducks is far more robust and variable between viral strains, whereby infection with LPAI H5N2 virus was reported to consistently cause a three-fold increase in IFITM1, 2, and 3 expression levels in the lungs and ileum on day one post-inoculation, whilst infection with the HPAI H5N1 virus caused up to a 93-fold

increase in IFITM3 expression in the lungs in a similar time frame (345). Therefore, understanding the differences in variable IFITM expression, and the reasons why chickens mount a lesser IFITM response to influenza viruses, may prove pivotal in understanding why some hosts succumb to HPAI infection whilst others survive. As such, understanding how these immune genes work within their disease models is of critical importance to having as high quality a model as possible.

1.11 The ferret model of human respiratory disease

1.11.1 Ferret suitability as a model of human disease

In order to gain a greater understanding of the multifaceted disease caused by respiratory viruses, animal models are used to replicate human infection. The ferret model of respiratory viruses, particularly influenza viruses, has become a gold standard animal model since its first use in the 1930s (346). Despite being more difficult to manipulate and house compared to mice due to their size and temperament, the ferret has distinct physiological advantages over the mouse model (**Table 1.1**), as ferrets show much more similar clinical signs from influenza virus infection to humans compared to mice (346, 347). Ferrets exhibit human-like clinical signs such as fever, sneezing and nasal discharge (348, 349). Moreover, ferrets can be infected with human-infecting influenza strains, as opposed to mice which require adapted viruses, and can also readily transmit virus between animals (346, 350). This is due to the ferret respiratory tract having very similar distribution of α-2,6-Gal terminating sialic acid receptors to humans, allowing for a similar pattern of infection in the respiratory epithelium (351). As such, the ferret model is commonly used for pathogenesis and transmission studies for novel and zoonotic respiratory viruses, such as AIV and novel coronaviruses (93, 145, 348, 352).

Table 1.1. Clinical advantages of the ferret model of influenza infection compared to the mouse model

Clinical Feature	Ferrets	Mice	Reference(s)
Fever	✓	✗	(348)
Nasal discharge	✓	✗	(348, 349)
Coughing/sneezing	✓	✗	(349, 350)
Malaise/lethargy	✓	✓	(350)
Weight loss	✓	✓	(353)
Hypercytokinemia	✓	✓	(354-356)
Airborne viral transmission	✓	✗	(350, 357)
Sialic acid distribution	✓	✗	(351, 358)

1.11.2 Ferret cellular immunology

While the ferret model has provided ample results for transmission studies, knowledge of the ferret cellular immune response is still relatively unstudied. Husbandry requirements and a general lack of reagents for ferrets limits the scope of experimental research using these animals to date. These issues are exacerbated by Biosafety Level 3 or 4 (BSL3/4) requirements for pathogens such as novel viruses, which make immunological experiments in ferrets difficult to undertake. As a result, ferret cellular immunology is still a developing field of research even in the context of influenza viruses, with only a handful of studies investigating changes in leukocyte populations following influenza virus infection (359-361). Music and

colleagues (2016) assessed the changes in leukocyte subsets following infection with a H3N2 virus strain in the blood across a 5 day infection trial, with this study identifying transient lymphopenia of $CD4^+$ and $CD8^+$ cells, and relative increases of $CD11b^+$ cells in the blood of infected ferrets at day 2 post-infection (361). However, while B cell subsets have rudimentarily been assessed either through cross-reactive antibodies or, in rarer cases, through the generation of ferret-specific antibodies (362), the classification of antigen presenting cells in the ferret has not yet been conducted. While these studies often speculate at what certain populations may be, such as $CD11b^+$MHC-II^{lo} populations being likely dendritic cells or granulocytes (359), further analysis and development of ferret-specific, or even yet to be determined cross-reactive, antibody panels are required to elucidate the immune cell subsets of the ferret in more detail.

1.11.3 Ferrets as a vaccine model

Outbred ferret populations give a more accurate representation of the genetic variability seen in human populations compared to clonally inbred mouse colonies. However, the ferret genome is poorly annotated with many common anti-viral genes, such as IFITMs and Mx (363, 364), have not been classified in the ferret model. While studies have worked to elucidate the sequences and functions of pro-inflammatory factors in the ferret (365, 366), cell-associated mediators of immunity require further investigation to extend our knowledge of this animal model.

Despite these shortcomings from an immunological perspective, the ferret model remains a valuable model for testing vaccine candidates against both seasonal and emerging respiratory viruses (367-369). The ferret model was used to assess vaccine candidates to the A(H1N1)pdm09 outbreak (370), and has also been used to assess vaccine options against emerging avian influenza strains such as H5N1 (369, 371, 372). In these studies, vaccine efficacy was typically assessed via reductions in clinical signs and morbidity, viral shedding and transmission, as well as seroconversion to produce a protective antibody response against the viral antigen tested. Given the high impact that these respiratory viruses have on

a global scale, it is therefore important to gain critical information on how these viruses interact with their host in the best available model, as increasing our understanding of the ferret model will not only benefit future studies, but may assist in deciphering the immune responses that are important for future pandemic viruses.

1.12 Study rationale & research aims

Building an understanding of how respiratory viruses interact with their hosts is critical to planning for future pandemic outbreaks. The ferret model is used as an animal model of human respiratory viruses, allowing for research into how these potentially deadly viruses interact with the mammalian immune system and cause disease. This PhD thesis used this model to gain insight into how severe respiratory pathogens such as avian influenza viruses and SARS-coronaviruses impact the cellular immune responses in mammals, as well as how vaccination may change these immune dynamics. Furthermore, classification of innate cellular factors adds to our knowledge of this model, to improve the model for use in future studies for disease preparedness.

Specifically, the aims of my PhD thesis were to:

1. Investigate the cellular immune response to H7N9 AIV in the ferret model.
2. Investigate the cellular immune response to SARS-CoV-2 in the ferret model, and the impact that a novel vaccine candidate has on the immune system.
3. Identify and characterise the IFITM gene family in the ferret model.

Chapter 2: Materials & Methods

2.1 Materials

2.1.1 Media & Buffers

Ferret Lung Epithelial (FRL) Media: Dulbecco's Modified Eagle Medium (DMEM) supplemented with 2mM L-Glutamine, 10 U/mL penicillin/streptomycin, Non-Essential Amino Acids (1x), 0.5mM β-mercaptoethanol, 4-(2-hydroxyethyl)-1-piperazineethanesulfonic acid (HEPES) and 10% Heat-Inactivated Foetal Calf Serum (HI-FCS) (all Gibco, Thermo Fisher Scientific, Waltham, MA, USA).

2x Freezing Media: For freezing of FRL cell lines, HI-FCS was supplemented with 10% dimethyl sulfoxide (DMSO) (Sigma-Aldrich, MO, USA). For freezing of samples at PC3, DMEM was supplemented with 40% HI-FCS and 20% DMSO.

FACS Buffer: Phosphate Buffered Saline (PBS) with 2% HI-FCS and 0.02% sodium azide (Sigma-Aldrich).

2X Leibovitz L-15 Media: 27.4g of Leibovitz L-15 medium powder (Gibco), 8ml/L of 7% $NaHCO_3$ (buffered in Hanks Buffered Salt Solution (HBSS), Melbourne Diagnostics Unit), 800μM HEPES (pH 6.8), 200U/ml penicillin and 200μg/ml streptomycin (all Gibco) in 1L Baxter water (Baxter Healthcare, Old Toongabbie, NSW, Australia).

Plaque Assay Overlay Media: Equal volumes of 2xL15 media and 1.8% (w/v) Type I agarose (Sigma-Aldrich) in Baxter water, supplemented with 2μg/ml Trypsin Worthington (Worthington Biochemical Corporation, Lakewood, NJ, USA).

SARS-CoV-2 Propagation Media: DMEM supplemented with 2% foetal bovine serum (FBS), 10 mM HEPES, 100 U/mL penicillin, 100 μg/mL streptomycin and 250 ng/mL amphotericin.

2.1.2 Cell lines

The cell line used in Chapter 5 were ferret lung epithelial cells (FRL), which were explanted and transformed by infection with Adenovirus 5 (ATCC, Manassas, VA, USA). The transformed FRL epithelial cells were propagated and cloned by limiting dilution. The FRL cells were given by Assoc. Professor Tuck-Weng Kok (University of Adelaide) for this study. FRL cells were cultured in FRL media in T75 flasks and were passaged every 3-4 days as required using trypsin (Gibco).

Madin-Darby Canine Kidney (MDCK) cells were used for plaque assays performed in Chapter 5. The cells were from laboratory stocks at The University of Melbourne and were originally sourced from the American Type Culture Collection (ATCC).

Vero E6 cells (BEI Resources, Manassas, VA, USA) were used for the growth of SARS-CoV-2 virus in Chapter 4. The cells were from laboratory stocks at the Australian Centre for Disease Preparedness (ACDP) and were originally sourced from the AT.

2.1.3 Virus strains

All viruses used in Chapters 3-5 are listed below in **Table 2.1.**

Table 2.1 Virus strains

VIRUS	VIRUS SPECIES	CHAPTER USED	SOURCE
A/Anhui/1/2013(H7N9)	Influenza virus	3	WHO CC[1]
SARS-CoV-2 hCoV-19/Australia/VIC01/2020	Coronavirus	4	VIDRL[2]
A/*WSN*/1933(H1N1)	Influenza virus	5	WHO CC
A/Puerto Rico/8/1934(H1N1) (PR8)	Influenza virus	5	Laboratory stock[3]
A/Hong Kong/1/1968(H3N2) (X31)	Influenza virus	5	Laboratory stock[3]

[1] World Health Organisation Collaborating Centre, Melbourne, VIC, Australia

[2] Victorian Infectious Diseases Reference Laboratory, Melbourne, VIC, Australia

[3] Originally from Department of Immunology, St Jude Children's Research Hospital, Memphis, TN, USA.

Influenza viruses were propagated by allantoic cavity inoculation of specific-pathogen-free (SPF) embryonated chicken eggs between days 9-11 of embryogenesis, as carried out by members of the Health & Biosecurity team at ACDP or Kedzierska laboratory members at the University of Melbourne. Propagation of virus occurred over 10-11 days before virus stocks were titrated in chicken eggs and the 50% egg infectious dose (EID_{50})/mL calculated according to Reed and Muench (373).

SARS-CoV-2 propagation was performed in Vero E6 cells (BEI Resources, Manassas, VA, USA) in SARS-CoV-2 Propagation Media. This was done under PC4 conditions by members of the Dangerous Pathogens team at ACDP.

2.1.4 Antibodies

Antibodies used in Chapters 3 and 4 are listed below in **Table 2.2.**

Table 2.2 Antibodies for flow cytometry

ANTIBODY	CATALOG #	MANUFACTURER	CLONE	FLUOROCHROME
CXCR5	Made in-house	Kent Laboratory, The University of Melbourne	C05	Unconjugated
MHC-II	WS0525F-100	Kingfisher, St.Paul, MN, USA	CAT82a	Unconjugated
CD4	Made in-house	CSIRO	TIA1	PE
PD-1	Made in-house	Kent Laboratory, The University of Melbourne	CL1	AF647
CD8	56-0086-42	ThermoFisher	OKT1	AF700
T/B ACTIVATION	561529	Becton-Dickinson, Franklin Lakes, NJ, USA	GL7	AF647
IG	618-102-130	Rockland,	-	FITC
CD14	555398	Becton-Dickinson	M5E2	PE
CD11B	557686	Becton-Dickinson	M1/70	APC
IFNΓ	3112-71-100T	Mabtech, Stockholm, Sweden	MTF14	AF488
CD79A	333508	BioLegend, San Diego, CA, USA	HM47	PerCP-Cy5.5
A/NP	ab20921	Abcam, Cambridge, UK	431	FITC
SECONDARY ANTIBODIES:				
GOAT ANTI-MOUSE IGG (H+L) CROSS-ADSORBED SECONDARY ANTIBODY	A11001	Invitrogen	-	AF488

SAV-BRILLIANT VIOLET 421	405225	BioLegend	-	BV421

2.1.5 Primers and probes

Sequences for the primer/probe sets used for cytokine analysis in Chapter 3 were taken from Carolan *et al.* (365), and were synthesized by Integrated Design Technologies (IDT, Integrated Design Technologies, Inc., Coralville, IA, USA). The sequences of these primer/probe sets are listed below in **Table 2.3**.

Table 2.3 qPCR primers and probes for ferret cytokines

Sequence 5' → 3'

GENE	FORWARD (FWD)	PROBE	REVERSE (RVS)
GAPDH	TGCGGCCAAGGCAGTAG	CTGAGCTGAATGGGAAG	AGGCCATGCCAGTGAGCTT
IFNα	TCCATCCTGAGGAACTACTTCCAG	GAATCTCCCTCTATCTGC	AGGCACAAGGGCTGTATTGC
IFNβ	ATATTTCTCCACCACGGTTCTTG	AACTATAACTTACTTCGATTCCA	ACTCCACACTGCTGCTGCTTAG
IFNγ	AACTGGAGAGAGGAGAGTGACAAAA	TCTCCTTCTACTTGAAACTGT	GTCTTCCTTGATGGTATCCATGC
IL-1β	CCTGGTGCTGTATAACTCGTATGAG	TCGGGCGCTCCAC	TTGGTTCACACTAGTTCCGTTGA
IL-6	GCAGAGAACAACCTAAATCTTCCAA	CTGGCAGAAGAGGAC	TGATTGAATTGAGACTGGAAGCA
IL-8	GGCACCTTGCATCAACATGA	TTCCAAGCTGGCTGTTG	AAGCAGGAAAACTGCCAAGAGA
IL-10	GCTGCGGCGCTGTCA	CTCCACCGCCTTGCTCTTAT	CGATTTCTGCCCTGTGAG
MCP1	GCAGCAAGTGTCCCAAAGAAG	ATCCTCAAGACATTCCT	GACTGGGGTCAGCGCAGAT
TNFα	TGCCATCAGACGGGCTGTA	CTTATCTACTCGCAGGTCC	ACATCCTCGGCCCTTGAAG

Primers designed from IFITM sequences in Chapter 5 are listed below in **Table 2.4.** These primers were synthesized by IDT and reconstituted in DNAse-free water (Promega, Madison, WI, USA).

Table 2.4 PCR primers for IFITM sequences

	Sequence 5' → 3'	
GENE	**FORWARD**	**REVERSE**
IFITM1	ATGGTCAAGGAGAACACGGTGG	TTAATGGTAGCCACCACTCTCC
IFITM2	ATGAGCCACAACGCCCAG	TCAGTCACACGCACACATAC
IFITM3	ATGGAGACCCCCCAGACCTTG	CTAGTAGCCTCCATGCTGTCTG

Primer/probe sets for detection of ferret IFITM transcripts in Chapter 5 were designed and synthesised by ThermoFisher Scientific (Thermo Fisher Scientific, Waltham, MA, USA), with the sequences of these primers and probes listed below in **Table 2.5.**

Table 2.5 qPCR primers and probes for IFITM sequences

	Sequence 5' → 3'		
GENE	**FORWARD**	**PROBE**	**REVERSE**
IFITM1	GCCAAGTGCCTGAACATCTGT	CTGACCACTGTATCTGTTGT	GCCACCACTCTCCTTCATAACC
IFITM2	CAACGCCCAGCCCTTCT	CCCTGATACCCACGCCG	TCCTCCTTGAGCATCTCGTAGGT
IFITM3	GGGCCTCCTGCTGACCAT	CGTTCATCATCCTTTTTGTCA	CGGAATCATCAGCGATCCA

2.2 Methods for ferret studies

Ferret animal studies were carried out in PC3 or PC4 biocontainment conditions for both the H7N9 and SARS-CoV-2 experiments in Chapters 3 and 4, with PC4 work carried out by trained staff members at ACDP. Once samples had either been fixed in a 4% paraformaldehyde (PFA) or lysed in a lysis buffer compliant with the correct bio-risk management strategy for viral inactivation (such as RLT buffer in the RNA extraction kits), experiments could then be undertaken safely in PC2 conditions.

Sections 2.2.1, 2.2.2, 2.2.6 and 2.2.7 are described in the Methods section in Chapter 3 as a published article in Frontiers in Immunology.

2.2.1 Ferret viral challenge study (H7N9)

Fitch ferrets that were approximately 6 months of age (CSIRO Werribee Animal Facility) and serologically negative by hemagglutination inhibition (HI) assay for H7N9 were used in this study. Prior to initiation of the study, all ferrets were free from signs of clinical disease. Body temperatures were measured using an implantable subcutaneous microchip (Destron Fearing, Delray Beach, FL, USA). Baseline body weights and temperatures were obtained for three consecutive days before challenge (i.e. day -3, -2 and -1) and on the day just prior to the challenge (day 0).

Six ferrets were infected intranasally with 1 x 10^6 EID_{50} of virus diluted in 0.5 mL of sterile PBS, and four ferrets were mock-infected with an equivalent dilution of allantoic fluid collected from SPF chicken eggs in sterile PBS as non-infected controls. Following viral challenge, ferrets were monitored daily for body weight, temperature, and clinical signs of illness (including sneezing, lethargy, nasal discharge, diarrhea and neurological dysfunction) for the duration of the study. Blood samples were collected every second day. Animals were anesthetized with ketamine/xylazine, and blood samples of 200–250 µL were taken from the jugular or axillary vein on days 1, 3, 5, and from the heart at the time of euthanasia for the terminal bleed. For virus titration, nasal washes were collected on days 1, 3, 5 and upon euthanasia, as described previously (374, 375).

All ferrets were euthanised on day 7 (study endpoint) or earlier due to ethical endpoints (≥10% weight loss or escalation of clinical signs). All procedures described here were reviewed and approved by the Commonwealth Scientific and Industrial Research Organisation (CSIRO), Australian Animal Health Laboratories (AAHL) Animal Ethics Committee (AEC#1861) and were performed in accordance with the *Australian Code for the Care and Use of Animals for Scientific Research (8th Edition 2013)*.

2.2.2 Histopathology of tissues from H7N9-infected ferrets

Histological analysis of ferret tissues following infection was performed by John Bingham and Jean Payne (CSIRO ACDP) as previously described (376). Tissues were fixed in 10% neutral-buffered formalin for at least 24 hours, processed into paraffin wax, cut and stained using haematoxylin and eosin for examination for histopathological lesions. Consecutive tissue sections were stained in an immunohistochemistry (IHC) test for influenza A virus nucleoprotein (376).

2.2.3 RNA extraction

RNA was extracted from ferret tissue samples using a RNeasyPlus kit (Qiagen, Hilden, Germany) as per manufacturer's instructions for the H7N9 trial. Briefly, cells were pelleted and lysed using RLT lysis buffer, and then 70% ethanol was added. RNA was bound to a column and washed using RW1 and RPE buffers, before elution in 30 µL RNase-free water. RNA extraction for the SARS-CoV-2 ferret trial was performed using the MagMAX™-96 Viral RNA Isolation Kit lysing/binding solution, then RNA was extracted as per the manufacturer's instructions using the KingfisherFlex magnetic particle processor (ThermoFisher Scientific). Briefly, RNA from the lysed cells is bound to the magnetic beads in the kit, washed in Wash Solutions 1 and 2, and then eluted in the kit elution buffer.

2.2.4 cDNA synthesis from ferret RNA

RNA from the H7N9 ferret trial was converted into cDNA using SuperScript™ III First-Strand Synthesis SuperMix (Invitrogen, Thermo Fisher Scientific, Waltham, MA, USA) as per kit instructions by setting up the 2-step cDNA synthesis mastermixes for incubations on the Biorad T100 Thermal Cycler (Biorad, Hercules, CA, USA) (**Table 2.6** and **2.7**).

Table 2.6 cDNA synthesis step one

REAGENT	VOLUME x1 REACTION (µL)
RNA	1
Random Hexamers	1
Annealing Buffer	1
RNase-free water	5

Incubate on thermocycler for 5 min at 65°C.

Table 2.7 cDNA synthesis step two

REAGENT	VOLUME x1 REACTION (µL)
2X First-Strand Reaction Mix	10
Enzyme Mix	2
TOTAL	20

Run on thermocycler with the following protocol for 10 min at 25°C, 50 min at 50°C, and then 10 min at 85°C. The reaction was then held at 4°C.

2.2.5 Quantitative real-time PCR (qRT-PCR)

Relative expression of ferret immune genes was assessed using a StepOne Plus™ Real-Time PCR System and the comparative threshold cycle (Ct) method according to manufacturer's instructions (Applied Biosystems, Foster City, CA, USA), using the primer/probe sets described in **Table 2.3**. If the assay used cDNA, Applied Biosystems TaqMan Universal PCR MasterMix (Applied Biosystems) was used in a reaction as described in **Table 2.8**, using a StepOne Plus™ Real-Time PCR System (Applied Biosystems) and the comparative threshold cycle (Ct) method according to manufacturer's instructions. If RNA was to be used for transcript analysis, qPCRs were set up using an AgPath-ID™ One-Step RT-PCR Kit (ThermoFisher Scientific), with the protocol in **Table 2.9**. Samples were plated and centrifuged, then loaded onto the StepOne or QuantStudio 6 Flex Real-Time PCR machine (both ThermoFisher), with Fluorescein amidite (FAM) dye used as the reporter and carboxyrhodamine (ROX) used as a passive reference dye.

Table 2.8 Quantitative Real-Time PCR protocol for transcript assessment using cDNA

REAGENT	VOLUME x1 REACTION (µL)
2X TaqMan Universal MasterMix	12.5
Nuclease-free water	7.5
10X FWD Primer	1
10X RVS Primer	1
10X Probe	1
cDNA	2
TOTAL	25

Run with the above protocol for 50°C for 2min, 95°C for 10min, and then for 45 cycles of 95°C for 15sec and 60°C for 1min.

Table 2.9 One-Step Real-Time PCR protocol for transcript assessment using RNA

REAGENT	VOLUME x1 REACTION (µL)
2X RT-PCR Buffer	12.5
Nuclease-free water	10.2
100X FWD Primer	0.1
100X RVS Primer	0.1
100X Probe	0.1
25X Enzyme Mix	1
RNA	1
TOTAL	25

Run with the above protocol for 50°C for 2min, 95°C for 10min, followed by 45 cycles of 95°C for 15sec and 60°C for 1min.

Relative gene expression was calculated using mean values obtained from ΔΔCt. These Ct values were fitted to a theoretical standard curve equation $n = 10^{(Ct-Cn)/-3.32}$, where n is the copy number, Ct is the Ct value obtained from the qPCR run, and Cn is the cycle number in the run procedure. For relative gene expression, copy numbers were expressed as Copies/10^6 copies of GAPDH (i.e. $n_{(cytokine)}/n_{(GAPDH)}$ x 1,000,000). For fold change, ΔΔCt values for control samples were standardized to 1, and changes in cytokine levels were assessed as $\Delta\Delta Ct_{(test\ sample)}/\Delta\Delta Ct_{(control)}$.

2.2.6 Ferret IFN-γ ELISA assay

Ferret lung and spleen cells were pelleted by centrifugation at 1500× g_{max} for 5 minutes and washed in PBS. Cells (1.25×10^4/96-well) were cultured with or without live H7N9 virus for 48 hours at 37°C/5% CO_2. The Ferret IFN-γ ELISA Development Kit (ALP) (Mabtech) was used to determine the quantity of IFN-γ secreted by cells *ex vivo* at endpoint and after restimulation with live H7N9 virus (MOI 0.1). Briefly, the plate was blocked with PBS containing 0.05% Tween20 and 0.1% bovine serum albumin (BSA), then washed in PBS containing 0.05% Tween20. Cells were then added and incubated for 2 hours at room temperature. The plate was washed, and detection antibody was added for 1 hour at room temperature. The plate was then washed again, and a 1:1000 dilution of Streptavidin-HRP was added for 1 hour at room temperature. The plate was washed and TMB substrate added to develop the assay for

15 minutes. Stop solution was then added, and the ELISA plates were measured using a Multiskan Ascent Plate Reader with Ascent Software Version 2.6 (ThermoFisher Scientific).

2.2.7 Serology of H7N9 infected ferrets

To assess antibody responses, serum was collected prior to infection and at the point of euthanasia. Haemagglutinin Inhibition assays were performed on RDE treated sera by using homologous antigen (Influenza A/Anhui/1/2013) as per the standard method. HI titers were expressed as the reciprocal of the highest serum dilution causing complete inhibition of hemagglutination.

2.2.8 Ferret viral challenge and vaccine assessment study for SARS-CoV-2

This study (Chapter 4) was a randomized, placebo-controlled study assessing ChAdOx1-nCoV-2019 (The Jenner Institute, Oxford, UK) as a vaccine candidate against a control (PBS). ChAdOx1-nCoV-19-2019 was assessed by two different routes of administration, intranasal (IN) and intramuscular (IM). The study was carried out as a block design with two cohorts of 20 outbred ferrets of approximately 4 months of age (total of 40 animals, 20 males and 20 females). On vaccination days, ChAdOx1-nCoV-2019 stocks were diluted with sterile PBS to $2.5x10^{10}$ virus particles in 100 µL. ChAdOx1-nCoV-2019 was then administered as either an IM injection into the rear thigh muscle or dropwise to alternating nares for the IN inoculation. Ferrets were then monitored daily for 3 days post administration for any reaction from the ChAdOx1-nCoV-2019. At challenge (Cohort 1 - day 28; Cohort 2 – day 56), all ferrets were intranasally exposed to a 50% Tissue Culture Infectious Dose ($TCID_{50}$) target of $3x10^4$ of SARS-CoV-2. Following challenge, animals were assessed at least once per day (twice-daily for days 2-12 post-challenge) for the presence of clinical signs such as reduced interaction score, fever (via microchip temperature), and respiratory disease. On day 42 (Cohort 1) or day 70 (Cohort 2) ferrets had blood samples collected, representative of day 14 post challenge, and then between days 43-45 (Cohort 1) or days 71-73 (Cohort 2) ferrets were humanely killed and tissue samples were collected at necropsy for analysis. All procedures described here were reviewed and approved by the Commonwealth Scientific and Industrial Research Organisation (CSIRO), Australian Animal Health Laboratories (AAHL) Animal Ethics Committee (AEC#2002) and were performed in accordance with the *Australian Code for the Care and Use of Animals for Scientific Research (8th Edition 2013)*.

2.2.9 Tissue sample collection and processing

Lung, spleen, and mediastinal lymph nodes were harvested from trial ferrets by ADCP animal house staff and placed in PBS. Lung samples were manually minced using a scalpel followed

by enzymatic digestion (150 U/mL Collagenase I and 100 U/mL DNase I (both ThermoFisher Scientific) in DMEM) while single-cell suspensions of spleen and lymph node samples were prepared by passing the tissue though a 70 µm strainer. Peripheral blood mononuclear cells were isolated by hypotonic lysis of red blood cells using erythrocyte lysing solution (0.15 M NH_4Cl, 10 mM $KHCO_3$, and 1mM EDTA pH 7.3). Cell suspensions were washed and resuspended in PBS for counting using a Scepter 2.0 handheld automated cell counter (Merck, Kenilworth, NJ, USA).

2.2.10 Flow cytometry

Cells processed from ferret tissues were stained with the antibodies listed in Table 2.2. Cell numbers between 0.05 and $2x10^6$ as allowed by cell counts were stained for 1 hour at 4°C, washed in FACS buffer. Required secondary antibodies were added for 1 hour at 4°C, and again washed in FACS buffer. Cells were then fixed with either 4% PFA or BD Fix/Perm Buffer (BD Biosciences Becton-Dickinson, San Jose, CA, USA)) if intracellular staining was required, for 1 hour on ice. Intracellular stains were then added for 1 hour at 4°C in BD Perm Wash buffer, and then again washed in BD Perm Wash buffer (BD Biosciences). Cells were finally resuspended in FACS buffer and analyzed using the LSR II (Becton-Dickinson). Flow cytometry data were analyzed using FlowLogic software (Version 7.2.1, Inivai Technologies, Mentone, VIC, Australia).

2.2.11 ELISpot assay

IFN-γ–producing cells were detected using a ferret IFN-γ ELISpot assay, as per the manufacturer's instructions (Mabtech). Briefly, plates were pre-treated with DMEM with 10% HI-FCS added, then cells were diluted to $1.25x10^4$ cells per well and plated for overnight culture in the ELISpot plate. Cells were removed and the plate washed 5 times with 200 µL PBS with care taken to remove the wash buffer without touching the membrane with pipette tips. 100 µL of IFN antibody was added to each well, and the plate was incubated at room temperature for 2 hours. Antibody was then removed and washed with PBS five times. 100 µL of streptavidin-ALP was then added to each well and the plate was incubated for 1 hour at room temperature. Finally, after removing the streptavidin-ALP and washing the plate, 100 µL of TMB substrate was added to each well to develop the assay for approximately 15 minutes. After clear spots had emerged, the plate was washed with copious deionized water and left to dry for 30 minutes. The plate was then read under a microscope or by AID vSPOT Spectrum ELISpot reader (Advanced Imaging Devices GmbH, Strasburg, Germany).

2.2.12 Statistical analysis

GraphPad Prism (Version 8.1.1, GraphPad Software, San Diego, CA, USA) was used for graphical and statistical analysis of data. For analyzing the H7N9 infected ferrets compared to the non-infected controls, all six ferrets were grouped regardless of timepoint to give an overall view of the infection time course. For these analyses, student t tests were conducted between the two groups. Time course data was analyzed by 2-way ANOVA.

For SARS-CoV-2 infected ferrets, timepoint changes within vaccination groups was assessed by one-way ANOVA, using a Tukey's multiple comparisons test.

2.2.13 Correlation analysis

Analyses of immune variables were made into correlation and principle component analysis (PCA) plots by Peter Durr, using custom R scripts in the bioinformatics software.

2.3 Methods for ferret IFITMs

2.3.1 Ferret IFITM gene identification

The ferret IFITM gene region was identified between the conserved flanking genes for Protein-Glucosylgalactosylhydroxylysine Glucosidase (*PGGHG*) and β-1,4-N-Acetyl-Galactosaminyltransferase 4 (*B4GALNT4*, Scaffold GL897275.1: 99,108-236,675) in the Ensembl genome browser (version 101) (377), and run through the GENSCAN server (http://argonaute.mit.edu/GENSCAN.html) to identify potential coding regions (378). These regions were put through BLAST to identify the gene locations, and these genome regions were exported and aligned to Ensembl coding regions (if available).

2.3.2 Nucleic acid isolation for IFITM identification

Both genomic DNA and RNA was extracted from ferret splenocytes, bone marrow cells, and FRL cells using DNeasy and RNeasyPlus kits respectively (Qiagen) as per manufacturer's instructions. RNA was then converted into cDNA using SuperScript™ III First-Strand Synthesis SuperMix (Invitrogen) as per kit instructions (Section **2.2.4**, Tables **2.6** and **2.7**).

2.3.3 PCR for IFITM sequencing

PCR assays were performed from nucleic acids produced in Section **2.3.3** using a GoTaq Green PCR master mix (Promega) using the following reaction conditions (**Table 2.10**), and primers as described in **Table 2.4**.

Table 2.10 GoTaq Green PCR for ferret IFITM amplification

REAGENT	VOLUME x1 REACTION (µL)
2X GoTaq Green MasterMix	12.5
Nuclease-free water	6.5
FWD primer	2.5
RVS primer	2.5
(c)DNA	1
TOTAL	25

This reaction was run on thermocycler wat 95°C for 2min, then for 35 cycles of 95°C for 30sec, 55°C for 30sec, 72°C for 1min, and then finally the at 72°C for 5min.

PCR products then underwent gel electrophoresis on a 2% agarose gel, with gel bands excised and purified using the Wizard® SV Gel and PCR Clean-Up System (Promega), as per manufacturer's instructions using the centrifugation method. Briefly, gel segments were placed in membrane binding solution at 65° until the gel had completely dissolved, and then the mixture was placed on a column. The PCR product was then washed twice in Membrane Wash solution, then eluted in 30µL nuclease-free water This purified product was then sent to Micromon (Monash University, Clayton, VIC, Australia) for Sanger sequencing.

2.3.4 Rapid Amplification of cDNA Ends (RACE) PCR

Partial coding sequence for IFITM2 was amplified using the 3' RACE System for Rapid Amplification of cDNA Ends kit (ThermoFisher Scientific Scientific), as per manufacturer's instructions. Briefly, cDNA was generated from ferret RNA with a dC-tail, and this cDNA was amplified using IFITM2 forward primer (**Table 2.4**) and the adaptor primer provided in the kit. These products were separated by gel electrophoresis and sequenced as in **2.3.2** to obtain the full-length transcript.

2.3.5 Phylogenetic analysis of IFITMs

IFITM protein sequences from multiple species were aligned using MEGA7 (version 7.0.26), with heatmap data generated from calculated synteny between the different proteins. Phylogenetic trees were generated by Maximal Likelihood method in MEGA7 (379).

2.3.6 Stimulation of FRL cells with IFN and influenza virus

For stimulation time course assays, 0.5 x 10^6 cells/mL of FRL cells were seeded into 24-well plates and grown to confluence overnight. Either 0.5 µg/mL of ferret IFNα (generated in-house, CSIRO) or influenza virus (A/WSN/1933(H1N1), MOI 1) was added to the stimulation wells. Cells were harvested and RNA was extracted at 2, 4, 8, 24, 48, and 72 hours post-stimulation using a RNeasyPlus kit (Qiagen) as per manufacturer's instructions (Section **2.2.3**).

2.3.7 Real-Time PCR for ferret IFITMs

Levels of ferret IFITM transcript in tissues and cell culture following stimulation were assessed by qPCR, using the newly designed primer/probe sets described in **Table 2.5**. If the assay used cDNA, Applied Biosystems TaqMan Universal PCR MasterMix (Applied Biosystems, Foster City, CA, USA) was used in a reaction as described in **Table 2.11**, using a StepOne Plus™ Real-Time PCR System (Applied Biosystems) and the comparative threshold cycle (Ct) method according to manufacturer's instructions.

Table 2.11 Quantitative Real-Time PCR protocol for transcript assessment using cDNA

REAGENT	VOLUME x1 REACTION (µL)
2X TaqMan Universal MasterMix	10
Nuclease-free water	7
20X IFITM qPCR assay	1
cDNA	2
TOTAL	20

Run for 50°C for 2min, 95°C for 10min, then for 45 cycles of 95°C for 15sec and 60°C for 1min.

If RNA was to be used for transcript analysis, qPCRs were set up using an AgPath-ID™ One-Step RT-PCR Kit (ThermoFisher Scientific), with the following protocol (**Table 2.12**).

Table 2.12 One-Step Real-Time PCR protocol for transcript assessment using RNA

REAGENT	**VOLUME x1 REACTION (µL)**
2X RT-PCR Buffer	12.5
Nuclease-free water	10.4
20X IFITM qPCR assay	0.1
25X Enzyme Mix	1
RNA	1
TOTAL	25

Run for 50°C for 2min, 95°C for 10min, then for 45 cycles of 95°C for 15sec and 60°C for 1min.

Relative gene expression of IFITMs was assessed as described in Section **2.2.5**.

Chapter 3: The dynamics of the ferret immune response during H7N9 influenza virus infection

frontiers in Immunology

ORIGINAL RESEARCH
published: 24 September 2020
doi: 10.3389/fimmu.2020.559113

The Dynamics of the Ferret Immune Response During H7N9 Influenza Virus Infection

*William S. J. Horman[1,2], Thi H. O. Nguyen[1], Katherine Kedzierska[1], Jeffrey Butler[3], Songhua Shan[3], Rachel Layton[3], John Bingham[3], Jean Payne[3], Andrew G. D. Bean[2] and Daniel S. Layton[2]**

[1] Department of Microbiology and Immunology, The Peter Doherty Institute for Infection and Immunity, University of Melbourne, Parkville, VIC, Australia, [2] Commonwealth Scientific and Industrial Research Organisation Health and Biosecurity, Australian Centre for Disease Prevention, East Geelong, VIC, Australia, [3] Commonwealth Scientific and Industrial Research Organisation, Australian Centre for Disease Prevention, East Geelong, VIC, Australia

As the recent outbreak of SARS-CoV-2 has highlighted, the threat of a pandemic event from zoonotic viruses, such as the deadly influenza A/H7N9 virus subtype, continues to be a major global health concern. H7N9 virus strains appear to exhibit greater disease severity in mammalian hosts compared to natural avian hosts, though the exact mechanisms underlying this are somewhat unclear. Knowledge of the H7N9 host-pathogen interactions have mainly been constrained to natural sporadic human infections. To elucidate the cellular immune mechanisms associated with disease severity and progression, we used a ferret model to closely resemble disease outcomes in humans following influenza virus infection. Intriguingly, we observed variable disease outcomes when ferrets were inoculated with the A/Anhui/1/2013 (H7N9) strain. We observed relatively reduced antigen-presenting cell activation in lymphoid tissues which may be correlative with increased disease severity. Additionally, depletions in $CD8^+$ T cells were not apparent in sick animals. This study provides further insight into the ways that lymphocytes maturate and traffic in response to H7N9 infection in the ferret model.

Keywords: influenza, H7N9, ferrets, antigen presenting cells, animal model, zoonoses

OPEN ACCESS

Edited by:
Xulin Chen,
Jinan University, China

Reviewed by:
Davide Angeletti,
University of Gothenburg, Sweden
Randy A. Albrecht,
Icahn School of Medicine at Mount Sinai, United States
Shinji Watanabe,
National Institute of Infectious Diseases (NIID), Japan

***Correspondence:**
Daniel S. Layton
daniel.layton@csiro.au

Specialty section:
This article was submitted to Viral Immunology, a section of the journal Frontiers in Immunology

Received: *05 May 2020*
Accepted: *12 August 2020*
Published: *24 September 2020*

Citation:
Horman WSJ, Nguyen THO, Kedzierska K, Butler J, Shan S, Layton R, Bingham J, Payne J, Bean AGD and Layton DS (2020) The Dynamics of the Ferret Immune Response During H7N9 Influenza Virus Infection. Front. Immunol. 11:559113. doi: 10.3389/fimmu.2020.559113

INTRODUCTION

In recent years cases of zoonotic strains of avian influenza (AI) causing severe disease in humans have caused significant global concern, with fears that these viruses may lead to devastating pandemic events in future (1, 2). One such group of viruses are strains of H7N9 influenza virus, which have caused over 1,500 cases of infection (with a ∼40% mortality rate) in humans since their first detection in 2013 (3, 4). Of most concern with the H7N9 viruses has been the ability for this virus to present as a low pathogenicity virus in its native avian hosts and yet present with severe clinical symptoms and death in humans, without obtaining virulence factors such as multi-basic cleavage sites usually required for high pathogenicity infections. Deciphering the immune cellular mechanisms associated with disease severity progression will provide a better understanding as to why H7N9 infections can produce severe disease in humans.

Changes in leukocyte subsets have previously been shown to correlate with more severe outcomes during AI infection, with decreases in T cell populations commonly reported in both human (H7N9 virus) and avian (H5N6 virus) hosts (5, 6). Decreases in T lymphocytes are often accompanied by upregulation of several pro-inflammatory cytokines such as interferons

(IFN), most notably IFN-γ, as well as interleukins (IL) such as IL-6 (7). Overproduction of cytokines or hypercytokinemia has also been identified as a key contributing factor in severe AI pathogenesis in both chickens and macaques, where induction of pro-inflammatory cytokines is associated with cellular apoptosis and tissue damage (8, 9). Furthermore, macrophages have been shown to be predominantly pro-inflammatory responders to H7N9 strains in a mouse model (10), though highly pathogenic strains such as H5N1 and H7N9 display attenuated macrophage inflammation responses compared to seasonal strains such as H1N1 and H3N2 (11, 12). While hypercytokinemia is common amongst many AI virus infections, H7N9 strains such as the human infecting A/Anhui/1/2013 virus have been associated with dampened IFN responses in humans (13, 14). Furthermore, they have previously been associated with an attenuated humoral immune response in the mouse model (15). These studies demonstrate the unpredictable nature and wide spectrum of pathogenicity of AI viruses.

Investigations into the pathogenesis and transmission of many human-infecting influenza viruses have been conducted in ferrets, as the clinical presentation in these animals is considered a more robust representation of human illness when compared to mice (16). However, only a limited number of studies exist looking at influenza-specific immunity in ferrets, which have primarily focused on seasonal influenza strains (17–19). In this study, we aimed to examine the ferret immune response to H7N9 influenza virus infection by analyzing leukocyte population variation associated with disease pathogenesis. This study found the ferret model may allow for increased knowledge of the outcomes of H7N9 infections and help in boosting our understanding of both this model and of these viruses in readiness for potential future outbreaks.

METHODS

Ethics

All procedures described here were reviewed and approved by the Commonwealth Scientific and Industrial Research Organization (CSIRO), Australian Center for Disease Prevention (ACDP) Animal Ethics Committee (AEC#1861) and were performed in accordance with the Australian Code for the Care and Use of Animals for Scientific Research (8th Edition 2013).

Virus

Influenza virus A/Anhui/1/2013(H7N9) used in this study was propagated by allantoic cavity inoculation of 9–11-days of embryogenesis specific-pathogen-free (SPF) embryonated chicken eggs. The virus stock was titrated in chicken eggs and the 50% egg infectious dose (EID_{50}) /mL was calculated according to Reed and Muench (20). All *in vitro* and *in vivo* work involving live virus was conducted within biosafety level three facilities at ACDP. Animal work was performed using personal protective equipment and powered air purifying respirators.

Ferret Viral Challenge Studies

Fitch ferrets that were ∼6 months of age (CSIRO Werribee Animal Facility) and serologically negative by hemagglutination inhibition (HI) assay for H7N9 were used in this study. Prior to initiation of the study, all ferrets were free from signs of clinical disease. Body temperatures were measured using an implantable subcutaneous microchip (Destron Fearing, Delray Beach, FL, USA). Baseline body weights and temperatures were obtained for 3 consecutive days before challenge (i.e., day −3, −2, and −1) and on the day just prior to the challenge (day 0).

Six ferrets were infected intranasally with 1×10^6 EID_{50} of virus diluted in 0.5 mL of sterile PBS, and four ferrets were mock-infected with an equivalent dilution of allantoic fluid collected from SPF chicken eggs in sterile PBS as non-infected controls. Following viral challenge, ferrets were monitored daily for body weight, temperature, and clinical signs of illness (including sneezing, lethargy, nasal discharge, diarrhea, and neurological dysfunction) for the duration of the study. Blood samples were collected every second day. Animals were anesthetized with ketamine/xylazine, and blood samples of 200–250 μL were taken from the jugular or axillary vein on days 1, 3, 5, and from the heart at the time of euthanasia for the terminal bleed. For virus titration, nasal washes were collected on days 1, 3, 5, and upon euthanasia, as described previously (6, 21).

All ferrets were euthanised on day 7 (study endpoint) or earlier due to ethical endpoints (≥10% weight loss or escalation of clinical signs).

Histopathology

Histological analysis of ferret tissues following infection was performed as previously described (22). Tissues were fixed in 10% neutral-buffered formalin for at least 24 h, processed into paraffin wax, cut and stained using haematoxylin and eosin for examination for histopathological lesions. Consecutive tissue sections were stained in an immunohistochemistry (IHC) test for influenza A virus nucleoprotein (22).

Sample Collection and Processing

Lung, spleen, and mediastinal lymph nodes were harvested and processed, as previously described (17). Briefly, lung samples were manually minced using a scalpel followed by enzymatic digestion (150 U/mL Collagenase I and 100 U/mL DNase I) while single-cell suspensions of spleen and lymph node samples were prepared by passing the tissue though a 70 μm strainer. Peripheral blood mononuclear cells were isolated by hypotonic lysis of red blood cells using erythrocyte lysing solution (0.15 M NH_4Cl, 10 mM $KHCO_3$, and 1mM EDTA pH 7.3). Viral titers in tissues were measured on MDCK cells by standard $TCID_{50}$ assay.

Quantitative Real-Time PCR (Qrt-Pcr)

Relative expression of ferret immune genes was assessed using a StepOnePlus™ Real-Time PCR System and the comparative threshold cycle (Ct) method according to manufacturer's instructions (Applied Biosystems, Foster City, CA, USA). Relative gene expression was calculated using mean values obtained from ΔΔCt relative to the housekeeper gene (GAPDH), with each ferret compared to the average of the control ferrets for each gene. Primers for ferret cytokines, as well as relative gene expression calculations, were obtained from Carolan et al. (23).

Flow Cytometry

Cells processed from ferret tissues were stained with anti-CD4 (AlexaFluor 488, CSIRO ACDP sourced from WEHI (24), Geelong, VIC, Australia), anti-CD8 (PE, clone OKT8, eBioscience, CA, USA), anti-GL7 (AlexaFluor 647, clone GL7, BD Phamingen, San Diego, CA, USA), anti-MHC-II (biotin, clone CAT82A, Kingfisher, Saint Paul, MN, USA), and anti-CD11b (AlexaFluor 647, clone M1/70, BD Pharmingen, San Diego, CA, USA). Cells were stained for 1 h at 4°C, washed in FACS buffer (PBS, 4% FCS, 0.01% Sodium Azide) and analyzed using the LSR II (Becton-Dickinson, Franklin Lakes, NJ, USA). Flow cytometry data were analyzed using FlowLogic software (Version 7.2.1, Inivai Technologies, Mentone, VIC, Australia).

Serology

To assess antibody responses, serum was collected prior to infection and at the point of euthanasia. Haemagglutinin Inhibition assays were performed on RDE treated sera by using homologous antigen (Influenza A/Anhui/1/2013) as per the standard method. HI titers were expressed as the reciprocal of the highest serum dilution causing complete inhibition of hemagglutination.

Functional IFN-γ Assays

Ferret lung and spleen cells were pelleted by centrifugation at 1,500 × g_{max} for 5 min and washed in PBS. Cells (1.25×10^4/96-well) were cultured with or without live H7N9 virus for 48 h at 37°C/5% CO_2. The Ferret IFN-γ ELISA Development Kit (ALP) (Mabtech, Stockholm, Sweden) was used to determine the quantity of IFN- γ secreted by cells *ex vivo* at endpoint and after restimulation with live H7N9 virus (MOI 0.1). ELISA plates were measured using a Multiskan Ascent Plate Reader with Ascent Software Version 2.6 (ThermoFisher, Waltham, MA, USA). IFN-γ-producing cells were detected using a ferret IFN-γ ELISpot assay, as per the manufacturer's instructions (Mabtech, Stockholm, Sweden).

Statistical Analysis

For analyzing the infected ferrets compared to the non-infected controls, all six ferrets were grouped regardless of timepoint to give an overall view of the infection time course. For these analyses, student *t*-tests were conducted between the two groups. Time course data was analyzed by 2-way ANOVA.

RESULTS

Ferrets Can Exhibit Moderate to Severe Clinical Signs Following H7N9 Virus Infection

To assess the impact of H7N9 virus in ferrets, viral pathogenicity was firstly assessed based on observation of clinical signs of infected ferrets throughout the 7-day study (**Figure 1**). From the six H7N9-infected ferrets, three ferrets showed little to no clinical signs and survived until the study endpoint (Day 7). Of the remaining ferrets, two showed mild clinical signs but severe weight loss, leading to euthanasia at day 5 post-infection. One ferret, however, showed moderate to severe clinical signs consistent with those seen in highly pathogenic avian influenza infections (25), and was euthanised at day 6 due to escalation of these clinical signs (**Figure 1A**). This ferret's increase in clinical signs was identified by a play score of two, with play scores >1 signifying moderate-to-severe clinical signs (**Figure 1B**). Significant weight losses (>5% compared to baseline, $p < 0.0001$) were observed in all the infected ferrets when compared to the control ferrets from day 3 until the study endpoint (**Figure 1C**). Similarly, infected ferrets also showed a significant increase ($p < 0.05$) in body temperature at day 2 post-infection, with an average temperature of 40.1 ± 0.6°C compared to the controls at 38.4 ± 0.4°C (**Figure 1D**). Consequently, H7N9 infection in ferrets resulted in variable clinical symptoms, but overall body weight losses and heightened body temperatures at 48 h post-infection, which are within the typical timeframe for onset of influenza illness in humans.

Lack of Viral Clearance and Lower Antibody Responses Were Associated With Worsened Disease Progression

To further examine the clinical progression between the infected ferrets, viral titres from the nasal washes were determined to assess whether differences in viral replication or clearance were correlative with worsened disease progression. Titres >4.0 $\log_{10}$ $TCID_{50}$/mL were obtained for all infected ferrets at day 1 post-infection and virus was still detected in all ferrets at day 3 post-infection (>3.0 $\log_{10}$ $TCID_{50}$/mL, **Figure 2A**). One ferret had cleared the virus by day 5 post-infection, while the other two ferrets that survived until the end of the study showed viral clearance at day 7 (**Figure 2A**). Neither the day 5 nor the day 6 ferrets showed viral clearance by the point of euthanasia. Only one ferret euthanised on day 5 showed live virus in the lung (>4.0 $\log_{10}$/mL, **Figure 2B**). Additionally, antibody titres were measured in the ferret sera, with animals euthanized on day 7 showing the highest HI titres (all >64) and the ferret euthanized on day 6 showed a HI titer >8. The two ferrets euthanised at day 5 had no detectable HI titer (**Figure 2C**).

Infected Ferrets Showed Variability in Pathological Outcomes in Respiratory Tissues

Infected ferrets showed a variety of pathological outcomes following viral challenge. Challenged ferrets exhibited epithelial metaplasia in the nasal turbinates (**Figure 3a**), with ferrets euthanised at the earlier day 5 time point exhibiting viral infection of the nasal epithelium (**Figure 3b**). The day 6 ferret showed the most severe lung pathology, with the lungs of this ferret showing diffuse interstitial pneumonia, with severe alveolar oedema and inflammatory cell infiltration in the alveolar spaces and around the blood vessels (**Figure 3c**). Other infected ferrets showed broncho-interstitial pneumonia and interstitial inflammation (**Figure 3d**) and bronchitis, with infected epithelial cells and early stage lesions observed in one of the day 5 ferrets (**Figure 3e**). Bronchial adenitis was also present in some of the infected ferrets, with necrosis of the bronchial glands observed along with viral antigen (**Figure 3f**).

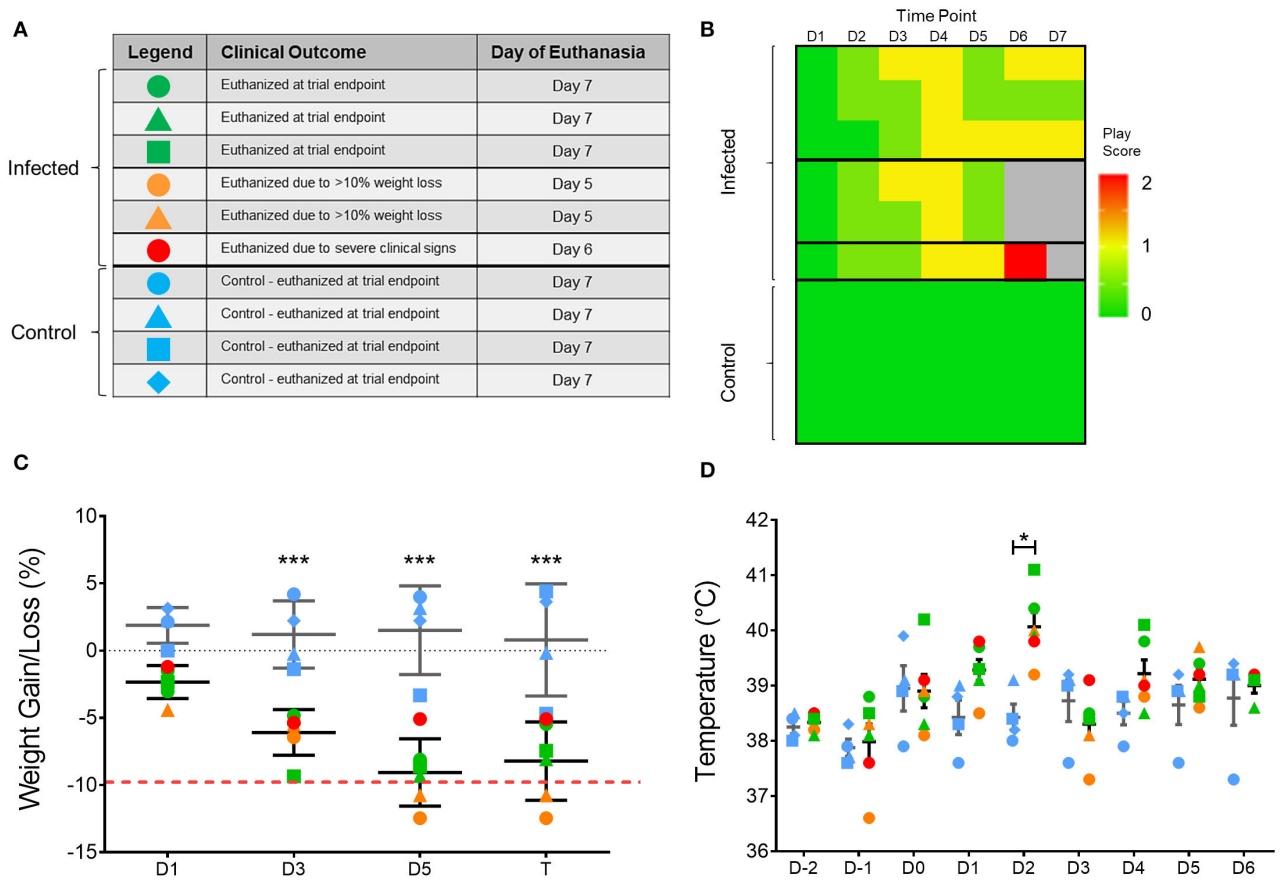

FIGURE 1 | Variation in clinical outcome amongst study ferrets. **(A)** Summary of ferret characteristics and classification of ferrets according to clinical signs and time of euthanasia. Blue represents the uninfected controls; green represents ferrets which survived until trial endpoint (day 7); yellow represents ferrets with few clinical signs but reached ethical weight loss point (day 5); and red represents the ferret which showed severe clinical signs and was euthanised at (day 6). **(B)** Individual play scores measured for ferrets daily, with 0 signifying no signs, 1 minor clinical signs, and 2 moderate-to-severe clinical signs. Ferrets reaching a score of 2 were euthanised for ethical reasons. **(C)** Body weight and **(D)** temperature of each ferret throughout the study according to the legend shown in **(A)**. Mean and SD are shown, $n = 6$ for H7N9-infected ferrets, $n = 4$ for control ferrets. Weight data are plotted as a percentage change from the initial D-3 weight recording on days post-infection. Time points marked with (*) indicate significant differences between infected and controls where $p < 0.05$, and (***) indicates $p < 0.001$.

These changes in pathology contrast to what is seen in the healthy nasal turbinates (**Figure 3g**), and lung (**Figure 3h**) of uninfected ferrets where no lesions were present. The number of localized lesions and qualitative assessment of epithelial metaplasia was also recorded to support the histopathological findings (**Supplementary Figure 1**). Here, we observed epithelial metaplasia in the turbinates of all ferrets sampled, as well as several occurrences of bronchio-interstitial pneumonia and bronchio-adenitis. We also observed viral antigen in a number of tissues sampled (**Supplementary Figure 1**), though interestingly, viral antigen was not observed in the diffuse interstitial pneumonia of lung lesions associated with the ferret euthanized due to clinical disease.

Disease Severity Is Associated With Different Expression Profiles of Pro-inflammatory Cytokines

Changes in certain pro-inflammatory cytokines (including IL-6, TNFα, and IFNγ) have been associated with H7N9 disease severity in humans and animal models (7). We measured levels of mRNA transcripts of several pro-inflammatory cytokines commonly associated with influenza infections. In the blood there were few differences between the groups, with MCP1 the only tested cytokine showing an average fold increase >5-fold compared to the controls at day 1 post-infection (data not shown). However, intriguingly the ferret euthanised on day 6 showed a large decrease in IL-6 (**Figure 4A**, 34-fold) and IFN-γ (**Figure 4B**, 25-fold) transcript levels on day 5. This also coincided with a lack of detectible IFN-γ in terminal serum by ELISA, though this trend was consistent across all tested ferrets (data not shown). In the spleen at endpoint, there appeared to be variable outcomes for the day 7 ferrets, with somewhat increased pro-inflammatory cytokine levels such as type I IFNs (IFN-α and IFN-β) in the day 5 ferrets, and decreased levels in the day 6 ferret compared to the controls (**Figure 4C**). In the lung, TNFα was significantly reduced (**Figure 4D**, $p < 0.05$) in the infected animals, though no other consistent trends were seen. The ability to produce IFN-γ *ex vivo* or after restimulation

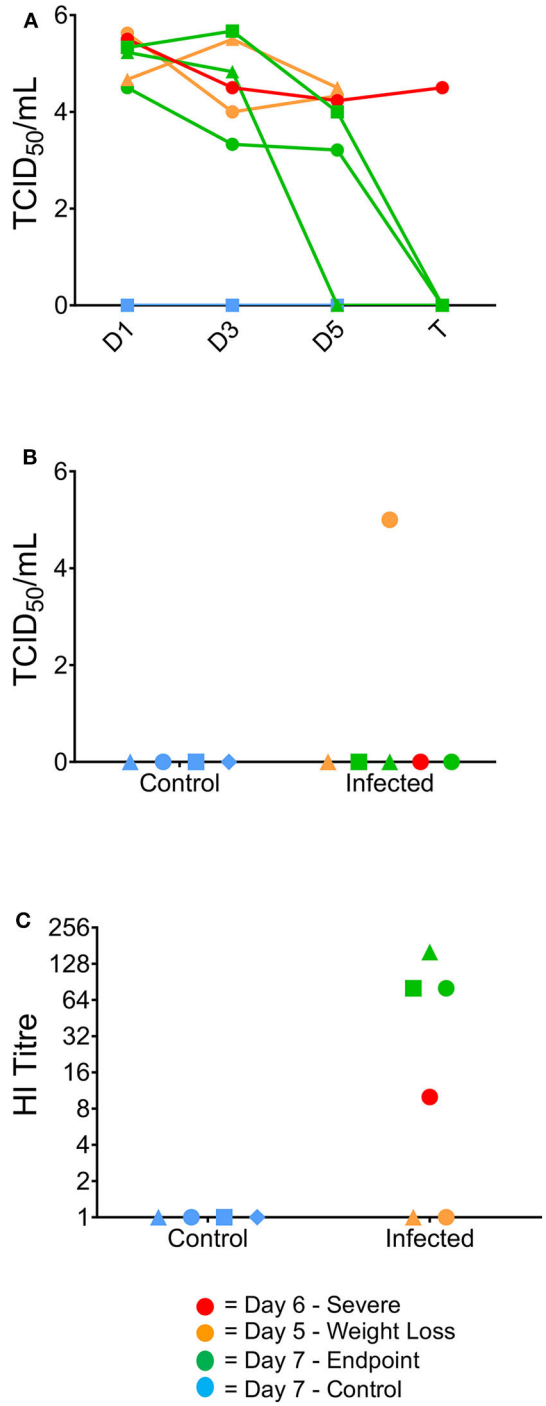

FIGURE 2 | Virological and serological data correlating to clinical outcome. Virus titres ($TCID_{50}$/ml) in nasal washes collected from the ferrets on days 1, 3, 5, and 7 post-infection **(A)**, and in the lung at the time of humane euthanasia **(B)**. Day 7 ferrets showed viral clearance by study endpoint, whilst earlier timepoint ferrets did not clear the virus by euthanasia. **(B)** One of the 2 day five ferrets was the only ferret to show live virus in the lungs post-study. **(C)** Haemagglutination inhibition assay titres in ferret serum samples collected from terminal bleeds. Day 7 ferrets also exhibited elevated serum titres by HI assay from terminally collected samples, whereas the 1 day six ferret was the only culled ferret to have a positive serum sample.

with live H7N9 virus was also assessed in spleen (**Figure 4E**) and lung cells (**Figure 4F**). There were no significant differences except for in the infected lungs, where IFN-γ-producing cells were significantly higher compared to the control ferrets *ex vivo* ($p = 0.0389$). Based on these findings, our ferret infection model showed observable changes in the cytokine profiles at a key site of infection in the lung compared to non-infected controls.

T Cell Populations Increase in the Infected Lungs, but No Apparent Change Is Present in the Peripheral Blood

Depletions in T cell numbers in the spleen and lungs have previously been reported for highly pathogenic avian strains H5N1 and H5N6 in both chickens and mice (6, 26). Similarly, patients that died from H7N9 infection were found to have lower T cell numbers in the blood compared to those that survived (5). Therefore, in order to assess lymphocyte involvement in disease progression we investigated the cellular responses associated with H7N9-infection both in the blood at several timepoints, and in the tissues at endpoint. Here, we found that in the blood the numbers of $CD4^+$ and $CD8^+$ T cells in infected ferrets were generally lower than the control ferrets, particularly for the $CD8^+$ T cell population at day 1 ($p < 0.001$). Nevertheless, these T cell populations remained low but relatively stable over the 7 days of infection (**Figure 5A**). The GL7 monoclonal antibody can be used as a marker activated T lymphocytes. However, GL7 expression was absent on the T cell subsets examined. Interestingly we observed significantly higher numbers of $CD4^+$ T cells in the spleen ($p = 0.0272$) and in the lungs ($p = 0.0048$) of infected ferrets, and a trend toward higher numbers of $CD8^+$ T cells in the lungs (**Figures 5B,C**), indicating a T cell response to H7N9 infection at a key site of infection.

Antigen Presenting Cell-Like Activation During H7N9 Infection in Tissues

Antigen presenting cells (APCs), such as macrophages residing in the lungs, have previously been recognized as key pro-inflammatory responders during H5N1, H7N7, and H7N9 infections in mice (10). Cells expressing higher levels of $CD11b^+$ have been shown to directly kill virally-infected cells in humans, and act as important antigen-presenting cells by upregulating MHC class II expression in the ferret model correlating to reduced pathology associated with influenza infection (17, 27). In general, H7N9-infected ferrets showed higher levels of CD11b/MHC-II dual-expressing cells ($CD11b^+MHC\text{-}II^+$) in the spleen, lung and lymph nodes compared to the control ferrets (**Figures 6A–C**). At the site of infection in the lungs, infected ferrets showed significantly higher levels of MHC-II single-positive cells ($MHC\text{-}II^+$, $p = 0.0286$). Conversely, CD11b single-positive cells ($CD11b^+$) from infected ferrets were found at elevated levels in the spleen and lymph nodes. Individually, we did observe that the ferrets euthanised on days 5 and 6 had higher $CD11b^+$ cells in the spleen, suggesting a less activated and immature phenotype, and a trend toward lower $CD11b^+MHC\text{-}II^+$ cells in the lymph nodes when compared to the other ferrets. When analyzed

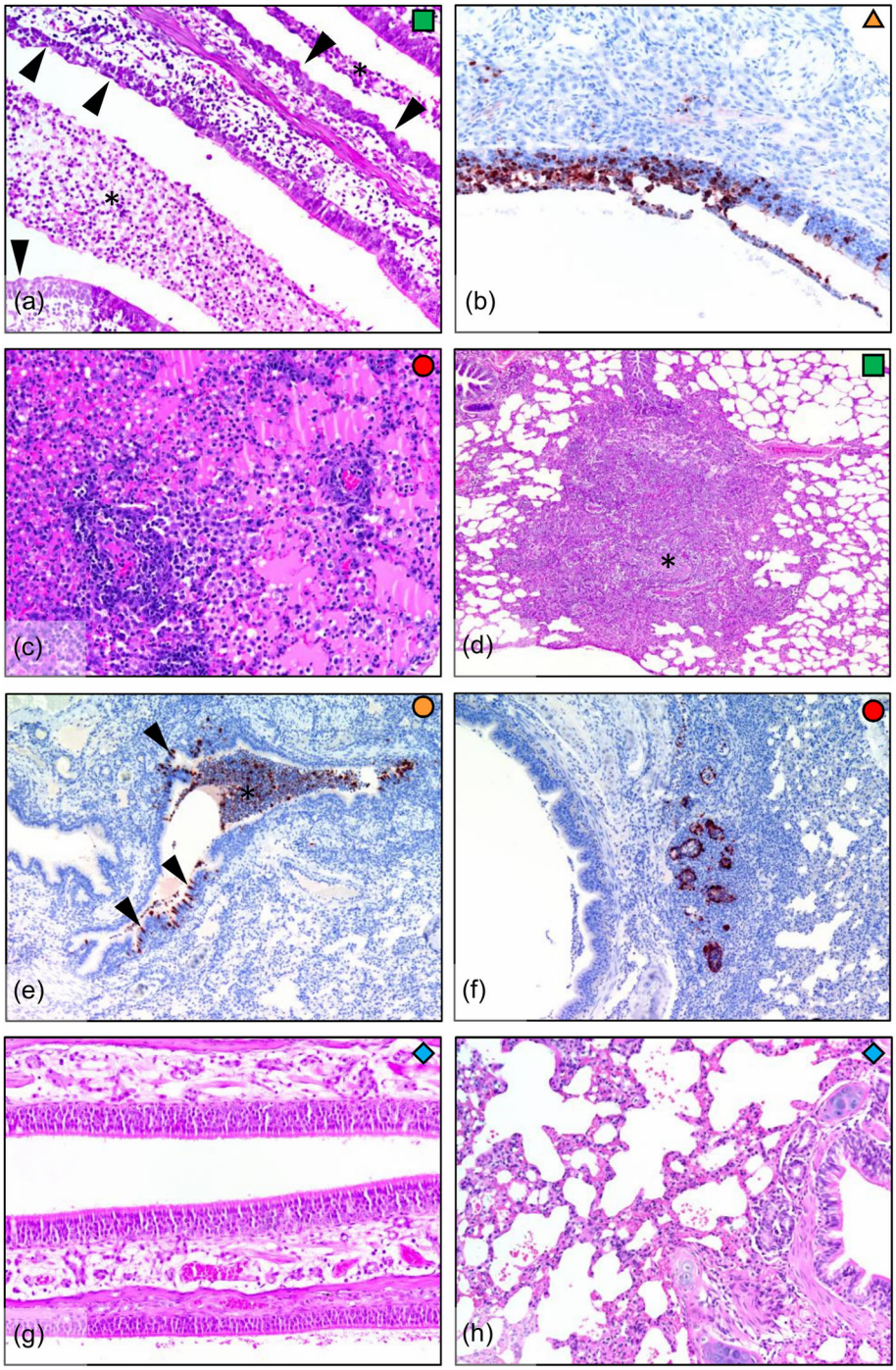

FIGURE 3 | Histopathology in ferrets infected with H7N9 virus. **(a)** Infected nasal turbinate, showing epithelial metaplasia (arrowheads) and suppurative inflammatory exudate (*) in airways (day 7, HE stain). **(b)** Nasal turbinate during early infection (day 5) showing viral infection of turbinate epithelium (IHC stain). **(c)** Diffuse interstitial pneumonia, showing severe alveolar oedema and inflammatory cell infiltration around blood vessels and into the alveolar spaces (lung, day 6). **(d)** Broncho-interstitial pneumonia, showing a large focal lesion involving an obliterated airway and surrounding inflammation into the interstitium (lung, day 7). **(e)** Bronchitis, showing infection of bronchial epithelium (arrowheads) and filling of the airway with infected sloughed cells and inflammatory cells (*). In this example, the bronchial inflammatory response is minimal, indicating that the lesion is in the early stages (lung, day 5). **(f)** Bronchial adenitis, showing viral antigen and necrosis of bronchial glands (lung, day 6). **(g)** No pathology was observed in the nasal turbinates, or **(h)** in the lungs of the uninfected controls (day 7).

by time point, there are statistically greater proportions of these cells in the ferrets that survived until trial endpoint compared to the controls ($p = 0.0009$) and the earlier timepoint ferrets ($p = 0.0039$, **Figure 6D**). As such, as these markers are often attributed to antigen-presenting cell maturation in the mouse model (28), APC activation in response to H7N9

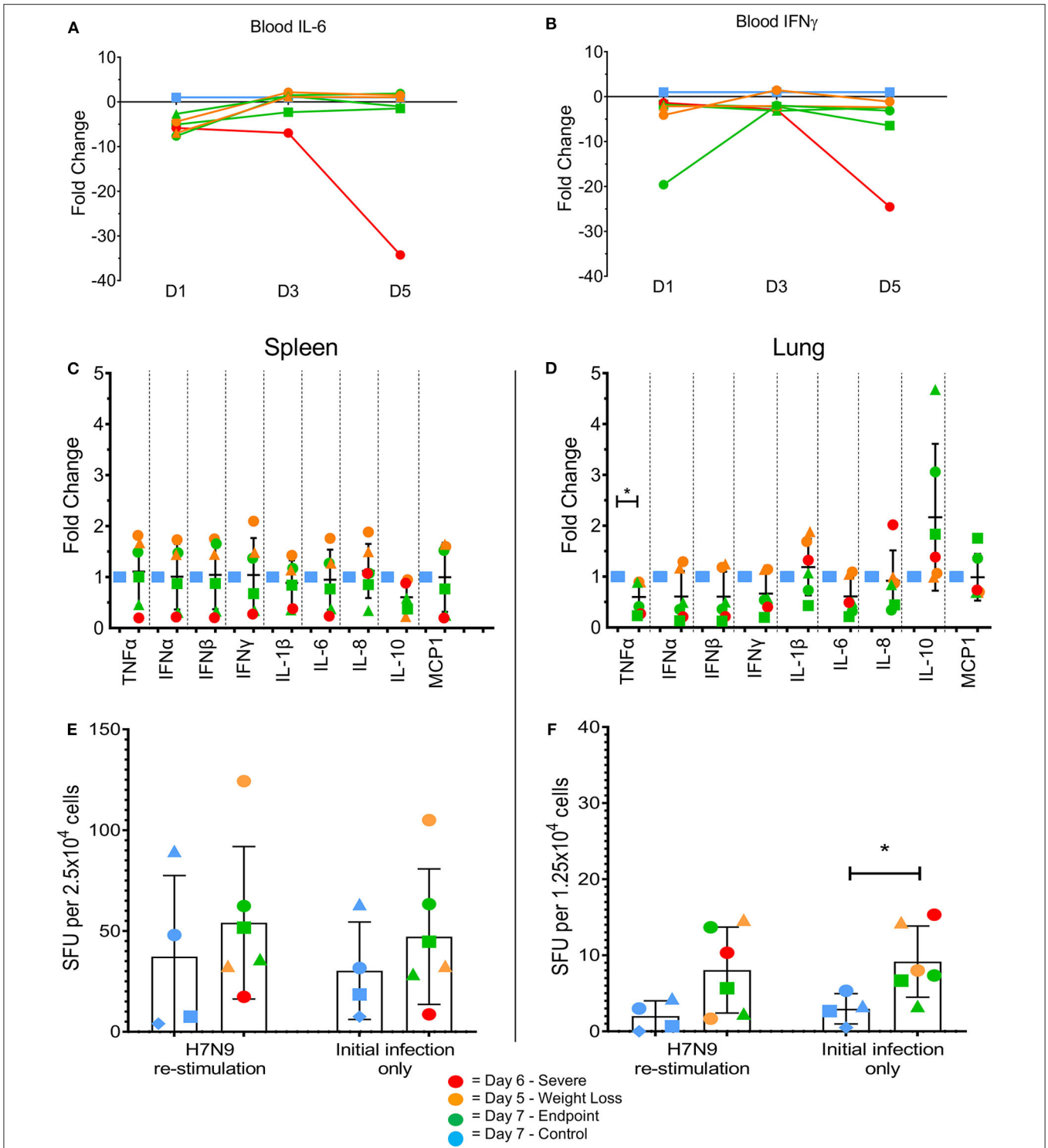

FIGURE 4 | Changes in pro-inflammatory cytokine levels in multiple tissues by qPCR and ELISpot assay. Immune cytokine levels were determined using TaqMan qPCR assays on cDNA prepared from the RNA of lysed tissues. In the blood samples the day 5 ferret showed large decreases in **(A)** IL-6 and **(B)** IFN-γ at day 5 post-infection. **(C)** In the spleen, little variation was seen between control and infected samples. Levels of IFN-γ producing cells were determined by ELISpot assay. **(D)** In the lung, H7N9-infected ferrets showed a significant fold change in TNFα. **(E)** In the lung, H7N9-infected ferrets showed significantly greater levels ($p = 0.0389$) of spots compared to non-infected controls without re-stimulation with H7N9. **(F)** In the spleen, little variation was seen between control and infected samples regardless of re-stimulation. Data marked with (*) indicate $p < 0.05$.

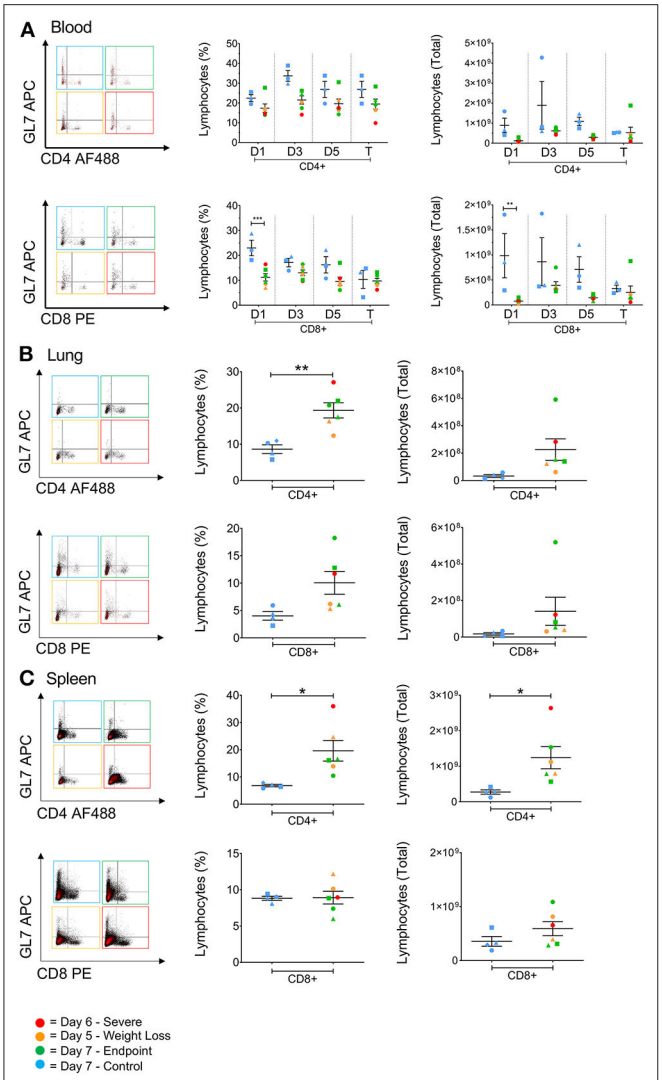

FIGURE 5 | The effect of H7N9 on T lymphocyte subsets. Representative FACS plots of $CD4^+$ and $CD8^+$ T cell subsets plotted against GL7 activation marker, with percentage of positive cells and total cell numbers **(A)** in the blood over time, **(B)** in the lung, and **(C)** in the spleen. Time points marked with (*) indicate $p < 0.05$, (**) indicates $p < 0.01$, and (***) indicates $p < 0.001$. For blood samples, $n = 3$ for control, rather than $n = 4$, due to insufficient cell numbers recovered for one ferret.

infection may be associated with disease severity seen in the ferret model.

DISCUSSION

The recent SARS-CoV-2 outbreak has brought a sharp focus onto zoonotic viruses causing severe global pandemics. While sustained human-to-human transmission of avian-origin H7N9 viruses has yet to occur, if a zoonotic outbreak of these high-consequence viruses were to occur, the results could be a pandemic much like the SARS-CoV-2 outbreak but with a virus which has potential for much higher mortality rate. As such, avian influenza viruses continue to present as a major global health concern, with one of the key concerns being what makes these viruses cause such severe consequences in mammalian hosts.

Influenza-related symptoms of ferrets more closely resemble human clinical symptoms than that of mice (16, 29), with outbred ferret populations giving a more accurate representation of the genetic variability seen in human populations compared to clonally inbred mouse colonies. However, husbandry requirements and a general lack of reagents for ferrets limits the scope of experimental research using these animals to date. These issues are exacerbated by Biosafety Level 3 (BSL3) requirements for pathogens such as H7N9, which make immunological experiments in ferrets difficult to undertake. As a result, ferret cellular immunology is still a developing field of research in the context of influenza viruses, with only a handful of studies investigating changes in leukocyte populations following influenza virus infection (17–19). For avian-origin influenza viruses such as H7N9, little work has been done to investigate how cellular subsets are affected by viral infection, with the bulk of experiments using AI in the ferret model focusing on classifying viruses through clinical outcome-based pathogenesis and transmission studies (30–32). Thus, our study aimed to give new insight into how H7N9 affects mammalian hosts in the ferret model with a focus on cellular subsets.

The ferrets in our viral challenge presented clinical outcomes with different severities. Five of the six ferrets showed little to no clinical signs, nevertheless only three survived until study endpoint without complications. Two ferrets reached the ethical weight loss cut-off of ≥10% by day 5 post-infection, giving us two different time points to assess the immune response. Furthermore, one ferret showed a quite different disease outcome, in which the ferret presented an escalation of clinical signs and was euthanised for ethical reasons at day 6 post-infection. Other studies have previously shown clinical variation between strains of H7N9 (15), however most studies with A /Anhui/1/2013 (H7N9) show ferrets presenting only mild clinical signs (1, 4, 33). To our knowledge, this is the first reported result showing variable disease outcome in an animal study using a single low pathogenicity H7N9 strain, in which one ferret showed severe clinical outcomes. While the findings of this study are novel for this model, we were limited by the number of animals that could be used in this study and thus limited by our statistical power. Furthermore, there are limitations in directly comparing ferrets euthanised on different days as, particularly for our serological data, it is difficult to discern whether the results are a function of observed severity or differences in the sampling time. As such, we believe the results from our observational study can provide a rationale for developing future ferret studies with greater numbers. It is also worth noting that ferrets used for these experiments are outbred animals, which may suggest that other combinations of host factors may be contributing to the variability seen in clinical presentation.

The airway pathology in these infected ferrets was variable, with different degrees of severity observed in the six animals. These findings were generally consistent with pathology observed

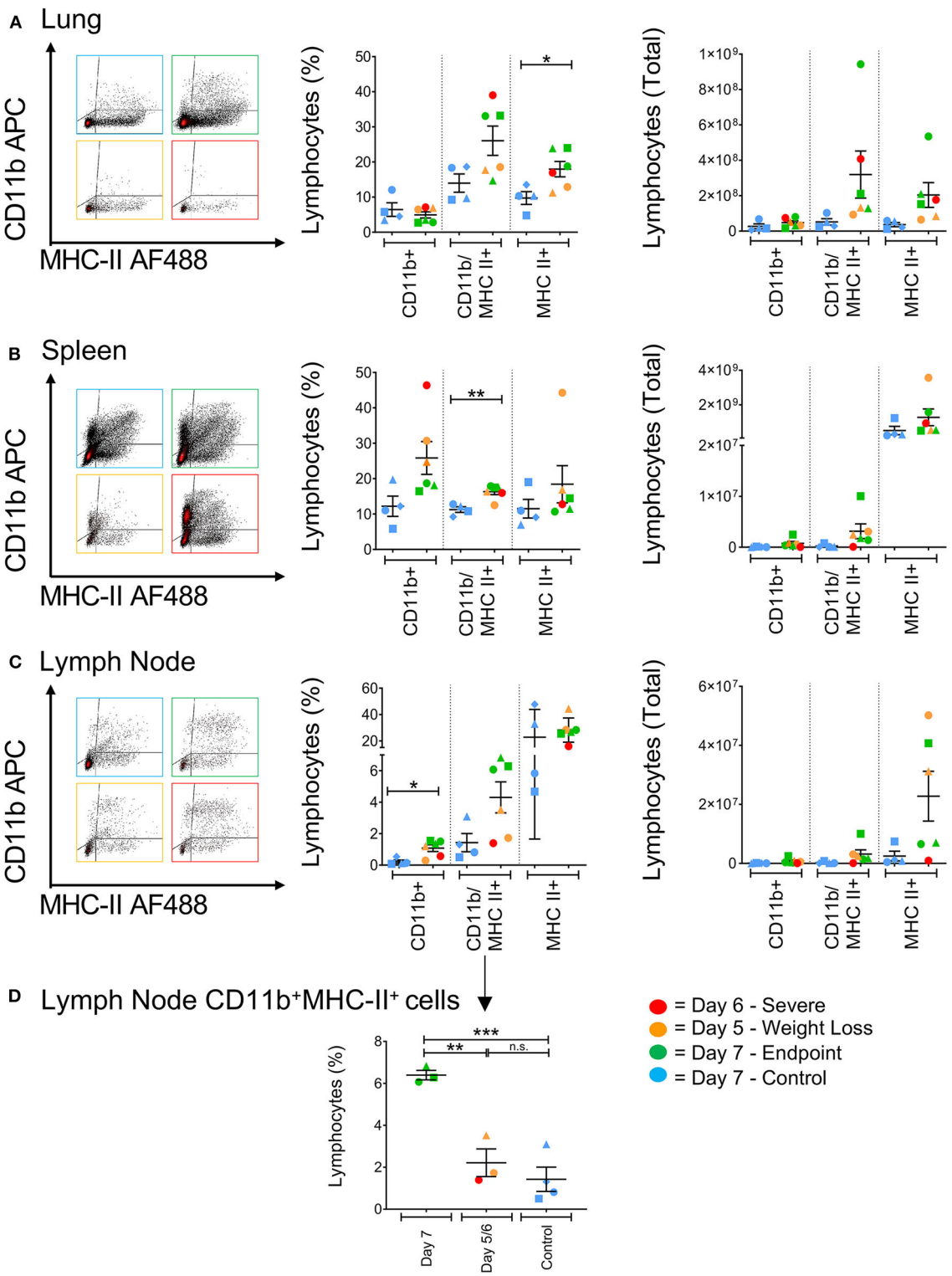

FIGURE 6 | The effect of H7N9 infection on antigen presenting cell subsets. Representative FACS plots of CD11b$^+$ and MHC-II$^+$ antigen-presenting cell subsets, with percentage of positive cells and total cell numbers **(A)** in the lung, **(B)** in the spleen, and **(C)** in the mediastinal lymph node. **(D)** Ferrets had significantly greater levels of CD11b$^+$MHC-II$^+$ cells in the lymph node at Day 7 compared to earlier time points and the control animals. Data marked with (*) indicate $p < 0.05$, (**) indicates $p < 0.01$, and (***) indicates $p < 0.001$.

in other studies in which ferrets were infected with LPAI H7N9 or pdm09 (H1N1) viruses (4, 31, 32, 34–36). While the day 6 ferret which showed worsened disease progression did exhibit the most severe lung pathology, the lack of viral antigen in and around these lesions (**Supplementary Figure 1**) means they cannot conclusively be classified as being caused by the influenza infection, and thus we are hesitant to classify disease presentation in this ferret as like a high pathogenicity infection based on the histopathology findings regardless of the increase in clinical signs.

Hypercytokinemia has frequently been associated with worsened disease progression in cases of severe AI infections, therefore we aimed to assess the induction of pro-inflammatory cytokines in this ferret model of infection. Upregulation of pro-inflammatory cytokines such as TNF-α and IL-6 commonly observed following H7N9 infection in both cell culture (14, 37) and in severe human cases, which follow similar patterns of pathogenesis to infections with HPAI H5N1 viruses (5, 38, 39). Whilst the localized pro-inflammatory cytokine response to influenza infection has been characterized for circulating influenza strains in ferrets (40), examination into these responses for avian influenza viruses remains limited. Our study found limited induction of cytokine responses at the site of infection in the lungs and in lymphoid tissues, and while attenuated IFN responses have been previously reported in human bronchial epithelial cells infected with H7N9 (14), and in ferrets severely infected with seasonal influenza strains (41), the overall lack of cytokine induction was an unexpected finding. A limitation of this study was that these tissues could only be sampled at study endpoint, which may suggest the pro-inflammatory response had abated at the site of infection by the time of sampling given that these responses typically occur in short timeframes of 24–48 h post-infection (42), though a lack of an evident cytokine response in the day 6 ferret still presenting clinical signs and shedding live virus was surprising. Furthermore, levels of IFN-γ were below the threshold of detection by ELISA in the serum of infected ferrets, and a previous study has shown IFN-γ detectable in the lungs of seasonal influenza-infected ferrets from day 5 post-infection at low levels, with greater detection observed from days 8–11 (19). These results suggest both timing and sampling may be critical for future studies to best capture the overall IFN-γ response to H7N9, if there is such a response occurring. Sampling in the blood of infected ferrets over the course of the study also found no large-scale upregulation of the cytokines tested, with only the early innate cytokine MCP1 showing an average fold increase >5-fold compared to the controls at day 1 post-infection. However, in the day 6 ferret, decreases in both IFN-γ (25-fold) and IL-6 (24-fold) where observed at day 5 post-infection, coinciding with an escalation in clinical signs in this animal. The decrease in IL-6 in particular was unexpected, as previous studies have implicated higher levels of IL-6 correlating to worsened disease progression (41). Our findings here suggest an immune dysregulation, rather than an over-activation, for worsened disease progression, and may be attributed to other factors in the cellular response.

Immunological work to determine the innate and adaptive responses to these viruses has mostly been conducted from infected patients or in the mouse model. Human cases are often marked by leukopenia, though these measurements are routinely made via hematology rather than flow cytometric analysis (43, 44). In other species however, we have previously described the lymphopenia for highly pathogenic strains of avian influenza, measuring splenic $CD8^+$ T cells following infection with highly pathogenic H5N6 in chickens via FACS analysis (6). In this study, $CD8^+$ T cells levels were relatively stable. A loss of lymphocytes detected via hematological analysis at day 1 (data not shown) was reconciled with our FACS data showing a significant difference between $CD8^+$ T cells in the blood, in which control animals had much higher levels compared to the infected animals. However, this loss was short-lived, as no further significant differences were observed across the study time points in the blood. This data is suggestive of a potential early "transient lymphopenia" of circulating leukocytes, which has previously been identified in one study during influenza infection in ferrets, and is also a phenomenon seen in humans following influenza A infection (17, 45). Our data appears to show $CD8^+$ T cells levels in the blood of infected animals remaining relatively and consistently low across time points, whilst greater variation was observed in the uninfected control levels.

Furthermore, reagents for FACS analysis in the ferret are still relatively novel, often not well-characterized, and heavily reliant on cross-reactivity from other species. While $CD4^+$ and $CD8^+$ T cells have previously been examined in influenza-infected ferrets (18), little work has been conducted for innate cell subsets. Myeloid-derived and antigen-presenting cells (APCs) have only been identified and analyzed in a handful of ferret studies, with one such study speculating that $CD11b^+$ cells are likely granulocytes such as neutrophils (17, 18). As such, we have used these studies, together with mouse and human studies (46–49), as a basis for possible classification of APCs, with $CD11b^+$MHC-II^+ cells suggested as likely "mature" or "activated" APCs. However, further work is needed to classify these innate cell subsets in the ferret model.

APCs such as alveolar macrophages have been recognized as key early responders against influenza virus infection, as they mount robust pro-inflammatory cytokine responses within 24 h of infection (27). While our study found no significant differences in APC numbers in infected lungs compared to control numbers, there was a trend toward much greater levels of MHC-II^+ APCs in the lung, especially in our cell counts. Rather, it was in the peripheral tissues that we found variability in the APC subsets. $CD11b^+$MHC-II^+ "mature" cells were found in the spleens of infected ferrets at significantly higher levels ($p = 0.0029$), however the trend toward higher $CD11b^+$ cells in the earlier time point ferrets suggests a higher level of immature myeloid cells, or the presence of pro-inflammatory granulocytes; however, the latter is less likely due given the lack of pro-inflammatory cytokines detected in the spleen. Moreover, in the draining lymph node a significant increase in $CD11b^+$ cells ($p = 0.0153$) was observed. Interestingly, in the lymph node the 3 day seven ferrets showed noticeably higher levels of $CD11b^+$MHC-II^+ "activated" cells, with statistically greater proportions of these cells compared to the controls ($p = 0.0009$) and the earlier timepoint ferrets ($p = 0.0039$), which may suggest that these APC responses do not occur as early as day 5.

This study found increased pathology in the ferret model diverges from the commonly observed pathogenesis markers such as lymphopenia and hypercytokinemia, suggesting another varied pathway that H7N9 viruses can cause severe disease in mammalian hosts. Further investigation into the ferret model may allow for better characterization of these outcomes and assist in increasing our knowledge of these viruses in preparation for any potential pandemic events.

DATA AVAILABILITY STATEMENT

All datasets generated for this study are included in the article/**Supplementary Material**.

ETHICS STATEMENT

The animal study was reviewed and approved by Australian Animal Health Laboratories (AAHL) Animal Ethics Committee, CSIRO.

AUTHOR CONTRIBUTIONS

All authors agreed on the final draft of the manuscript prior to submission. WH wrote the first draft and revised the manuscript. TN, KK, JBu, SS, JBi, JP, AB, and DL reviewed and edited the manuscript.

FUNDING

WH was supported by a joint CSIRO/University of Melbourne OneHealth Scholarship. This project was supported by CSIRO strategic funding.

SUPPLEMENTARY MATERIAL

The Supplementary Material for this article can be found online at: https://www.frontiersin.org/articles/10.3389/fimmu.2020.559113/full#supplementary-material

REFERENCES

1. Watanabe T, Kiso M, Fukuyama S, Nakajima N, Imai M, Yamada S, et al. Characterization of H7N9 influenza A viruses isolated from humans. *Nature*. (2013) 501:551. doi: 10.1038/nature12392
2. Horman WSJ, Nguyen THO, Kedzierska K, Bean AGD, Layton DS. The drivers of pathology in zoonotic avian influenza: the interplay between host and pathogen. *Front Immunol*. (2018) 9:1812. doi: 10.3389/fimmu.2018.01812
3. World Health Organization. *Influenza at the Human-Animal Interface: Summary and Assessment, 13 February to 9 April 2019*. (2019) Available online at: https://www.who.int/influenza/human_animal_interface/Influenza_Summary_IRA_HA_interface_09_04_2019.pdf (accessed May 20, 2020).
4. Imai M, Watanabe T, Kiso M, Nakajima N, Yamayoshi S, Iwatsuki-Horimoto K, et al. A highly pathogenic avian H7N9 influenza virus isolated from a human is lethal in some ferrets infected via respiratory droplets. *Cell Host Microbe*. (2017) 22:615–26.e8. doi: 10.1016/j.chom.2017.09.008
5. Wang Z, Wan Y, Qiu C, Quiñones-Parra S, Zhu Z, Loh L, et al. Recovery from severe H7N9 disease is associated with diverse response mechanisms dominated by CD8? T cells. *Nat Commun*. (2015) 6:6833. doi: 10.1038/ncomms7833
6. Butler J, Stewart CR, Layton DS, Phommachanh P, Harper J, Payne J, et al. Novel reassortant H5N6 influenza A virus from the Lao people's democratic republic is highly pathogenic in chickens. *PLoS ONE*. (2016) 11:e0162375. doi: 10.1371/journal.pone.0162375
7. Wang Z, Zhang A, Wan Y, Liu X, Qiu C, Xi X, et al. Early hypercytokinemia is associated with interferon-induced transmembrane protein-3 dysfunction and predictive of fatal H7N9 infection. *Proc Natl Acad Sci USA*. (2014) 111:769–74. doi: 10.1073/pnas.1321748111
8. Kuchipudi SV, Tellabati M, Sebastian S, Londt BZ, Jansen C, Vervelde L, et al. Highly pathogenic avian influenza virus infection in chickens but not ducks is associated with elevated host immune and pro-inflammatory responses. *Vet Res*. (2014) 45:118. doi: 10.1186/s13567-014-0118-3
9. Shinya K, Gao Y, Cilloniz C, Suzuki Y, Fujie M, Deng G, et al. Integrated clinical, pathologic, virologic, and transcriptomic analysis of H5N1 influenza virus-induced Viral pneumonia in the rhesus macaque. *J Virol*. (2012) 86:6055–66. doi: 10.1128/JVI.00365-12
10. Morrison J, Josset L, Tchitchek N, Chang J, Belser JA, Swayne DE, et al. H7N9 and other pathogenic avian influenza viruses elicit a three-pronged transcriptomic signature that is reminiscent of 1918 influenza virus and is associated with lethal outcome in mice. *J Virol*. (2014) 88:10556–68. doi: 10.1128/JVI.00570-14
11. Friesenhagen J, Boergeling Y, Hrincius E, Ludwig S, Roth J, Viemann D. Highly pathogenic avian influenza viruses inhibit effective immune responses of human blood-derived macrophages. *J Leukoc Biol*. (2012) 92:11–20. doi: 10.1189/jlb.0911479
12. Belser JA, Zeng H, Katz JM, Tumpey TM. Infection with highly pathogenic H7 influenza viruses results in an attenuated proinflammatory cytokine and chemokine response early after infection. *J Infect Dis*. (2011) 203:40–8. doi: 10.1093/infdis/jiq018
13. Arilahti V, Mäkelä SM, Tynell J, Julkunen I, Österlund P. Novel avian influenza A (H7N9) virus induces impaired interferon responses in human dendritic cells. *PLoS ONE*. (2014) 9:e96350. doi: 10.1371/journal.pone.0096350
14. To KKW, Lau CCY, Woo PCY, Lau SKP, Chan JFW, Chan K-H, et al. Human H7N9 virus induces a more pronounced pro-inflammatory cytokine but an attenuated interferon response in human bronchial epithelial cells when compared with an epidemiologically-linked chicken H7N9 virus. *Virol J*. (2016) 13:42. doi: 10.1186/s12985-016-0498-2
15. Lee ACY, Zhu H, Zhang AJX, Li C, Wang P, Li C, et al. Suboptimal humoral immune response against influenza A(H7N9) virus is related to its internal genes. *Clin Vaccine Immunol*. (2015) 22:1235–43. doi: 10.1128/CVI.00443-15
16. Belser JA, Katz JM, Tumpey TM. The ferret as a model organism to study influenza A virus infection. *Dis Model Mech*. (2011) 4:575–9. doi: 10.1242/dmm.007823
17. Music N, Reber AJ, Kim JH, York IA. Peripheral leukocyte migration in ferrets in response to infection with seasonal influenza virus. *PLoS ONE*. (2016) 11:e0157903. doi: 10.1371/journal.pone.0157903
18. DiPiazza A, Richards K, Batarse F, Lockard L, Zeng H, García-Sastre A, et al. Flow cytometric and cytokine elispot approaches to characterize the cell-mediated immune response in ferrets following influenza virus infection. *J Virol*. (2016) 90:7991–8004. doi: 10.1128/JVI.01001-16
19. Ryan KA, Slack GS, Marriott AC, Kane JA, Whittaker CJ, Silman NJ, et al. Cellular immune response to human influenza viruses differs between H1N1 and H3N2 subtypes in the ferret lung. *PLoS ONE*. (2018) 13:e0202675. doi: 10.1371/journal.pone.0202675
20. Reed LJ, Muench H. A simple method of estimating fifty per cent endpoints. *Am J Epidemiol*. (1938) 27:493–7. doi: 10.1093/oxfordjournals.aje.a118408
21. Laurie KL, Horman W, Carolan LA, Chan KF, Layton D, Bean A, et al. Evidence for viral interference and cross-reactive protective immunity between influenza B virus lineages. *J Infect Dis*. (2018) 217:548–59. doi: 10.1093/infdis/jix509
22. Wibawa H, Bingham J, Nuradji H, Lowther S, Payne J, Harper J, et al. The pathobiology of two Indonesian H5N1 avian influenza viruses representing

different clade 2.1 sublineages in chickens and ducks. *Comp Immunol Microbiol Infect Dis*. (2013) 36:175–91. doi: 10.1016/j.cimid.2012.12.001
23. Carolan LA, Butler J, Rockman S, Guarnaccia T, Hurt AC, Reading P, et al. TaqMan real time RT-PCR assays for detecting ferret innate and adaptive immune responses. *J Virol Methods*. (2014) 205:38–52. doi: 10.1016/j.jviromet.2014.04.014
24. Layton DS, Xiao X, Bentley JD, Lu L, Stewart CR, Bean AGD, et al. Development of an anti-ferret CD4 monoclonal antibody for the characterisation of ferret T lymphocytes. *J Immunol Methods*. (2017) 444:29–35. doi: 10.1016/j.jim.2017.02.009
25. Edenborough KM, Lowther S, Laurie K, Yamada M, Long F, Bingham J, et al. Predicting disease severity and viral spread of H5N1 influenza virus in ferrets in the context of natural exposure routes. *J Virol*. (2016) 90:1888–97. doi: 10.1128/JVI.01878-15
26. Boonnak K, Vogel L, Feldmann F, Feldmann H, Legge KL, Subbarao K. Lymphopenia associated with highly virulent H5N1 virus infection due to plasmacytoid dendritic cell-mediated apoptosis of T cells. *J Immunol*. (2014) 192:5906–12. doi: 10.4049/jimmunol.1302992
27. Wang J, Nikrad MP, Travanty EA, Zhou B, Phang T, Gao B, et al. Innate immune response of human alveolar macrophages during influenza A infection. *PLoS ONE*. (2012) 7:e29879. doi: 10.1371/journal.pone.0029879
28. Hao X, Kim TS, Braciale TJ. Differential response of respiratory dendritic cell subsets to influenza virus infection. *J Virol*. (2008) 82:4908–19. doi: 10.1128/JVI.02367-07
29. Sweet C, Price GE, Fenton RJ. Chapter 119-The ferret as an animal model of influenza virus infection. In: Zak O, Sande MA, editors. *Handbook of Animal Models of Infection*. London: Academic Press (1999). p. 989–98. doi: 10.1016/B978-012775390-4/50258-X
30. Zitzow LA, Rowe T, Morken T, Shieh W-J, Zaki S, Katz JM. Pathogenesis of avian influenza A (H5N1) viruses in ferrets. *J Virol*. (2002) 76:4420–9. doi: 10.1128/JVI.76.9.4420-4429.2002
31. Xu L, Bao L, Deng W, Dong L, Zhu H, Chen T, et al. Novel avian-origin human influenza A (H7N9) can be transmitted between ferrets via respiratory droplets. *J Infect Dis*. (2013) 209:551–6. doi: 10.1093/infdis/jit474
32. Zhu H, Wang D, Kelvin DJ, Li L, Zheng Z, Yoon SW, et al. Infectivity, transmission, and pathology of human-isolated H7N9 influenza virus in ferrets and pigs. *Science*. (2013) 341:183–6. doi: 10.1126/science.1239844
33. Belser JA, Gustin KM, Pearce MB, Maines TR, Zeng H, Pappas C, et al. Pathogenesis and transmission of avian influenza A (H7N9) virus in ferrets and mice. *Nature*. (2013) 501:556–9. doi: 10.1038/nature12391
34. Barman S, Krylov PS, Fabrizio TP, Franks J, Turner JC, Seiler P, et al. Pathogenicity and transmissibility of North American triple reassortant swine influenza A viruses in ferrets. *PLoS Pathog*. (2012) 8:e1002791. doi: 10.1371/journal.ppat.1002791
35. Moore IN, Lamirande EW, Paskel M, Donahue D, Kenney H, Qin J, et al. Severity of clinical disease and pathology in ferrets experimentally infected with influenza viruses is influenced by inoculum volume. *J Virol*. (2014) 88:13879–91. doi: 10.1128/JVI.02341-14
36. Smith JH, Nagy T, Driskell E, Brooks P, Tompkins SM, Tripp RA. Comparative pathology in ferrets infected with H1N1 influenza A viruses isolated from different hosts. *J Virol*. (2011) 85:7572–81. doi: 10.1128/JVI.00512-11
37. Zhao C, Qi X, Ding M, Sun X, Zhou Z, Zhang S, et al. Pro-inflammatory cytokine dysregulation is associated with novel avian influenza A (H7N9) virus in primary human macrophages. *J Gen Virol*. (2016) 97:299–305. doi: 10.1099/jgv.0.000357
38. Chi Y, Zhu Y, Wen T, Cui L, Ge Y, Jiao Y, et al. Cytokine and chemokine levels in patients infected with the novel avian influenza A (H7N9) virus in China. *J Infect Dis*. (2013) 208:1962–7. doi: 10.1093/infdis/jit440
39. de Jong MD, Simmons CP, Thanh TT, Hien VM, Smith GJD, Chau TNB, et al. Fatal outcome of human influenza A (H5N1) is associated with high viral load and hypercytokinemia. *Nat Med*. (2006) 12:1203–7. doi: 10.1038/nm1477
40. Carolan LA, Rockman S, Borg K, Guarnaccia T, Reading P, Mosse J, et al. Characterization of the localized immune response in the respiratory tract of ferrets following infection with influenza A and B viruses. *J Virol*. (2016) 90:2838–48. doi: 10.1128/JVI.02797-15
41. Svitek N, Rudd PA, Obojes K, Pillet S, von Messling V. Severe seasonal influenza in ferrets correlates with reduced interferon and increased IL-6 induction. *Virology*. (2008) 376:53–9. doi: 10.1016/j.virol.2008.02.035
42. Wang Y, Swiecki M, Cella M, Alber G, Schreiber RD, Gilfillan S, et al. Timing and magnitude of type I interferon responses by distinct sensors impact CD8 T cell exhaustion and chronic viral infection. *Cell Host Microbe*. (2012) 11:631–42. doi: 10.1016/j.chom.2012.05.003
43. Chen Y, Liang W, Yang S, Wu N, Gao H, Sheng J, et al. Human infections with the emerging avian influenza A H7N9 virus from wet market poultry: clinical analysis and characterisation of viral genome. *Lancet*. (2013) 381:1916–25. doi: 10.1016/S0140-6736(13)60903-4
44. Wang C, Yu H, Horby PW, Cao B, Wu P, Yang S, et al. Comparison of patients hospitalized with influenza A subtypes H7N9, H5N1, and 2009 pandemic H1N1. *Clin Infect Dis*. (2014) 58:1095–103. doi: 10.1093/cid/ciu053
45. Nichols JE, Niles JA, Roberts NJ. Human lymphocyte apoptosis after exposure to influenza A virus. *J Virol*. (2001) 75:5921. doi: 10.1128/JVI.73.13.5921-5929.2001
46. Lee ACY, To KKW, Zhu H, Chu H, Li C, Mak WWN, et al. Avian influenza virus A H7N9 infects multiple mononuclear cell types in peripheral blood and induces dysregulated cytokine responses and apoptosis in infected monocytes. *J Gen Virol*. (2017) 98:922–34. doi: 10.1099/jgv.0.000751
47. Misharin AV, Morales-Nebreda L, Mutlu GM, Budinger GRS, Perlman H. Flow cytometric analysis of macrophages and dendritic cell subsets in the mouse lung. *Am J Respir Cell Mol Biol*. (2013) 49:503–10. doi: 10.1165/rcmb.2013-0086MA
48. Zaynagetdinov R, Sherrill TP, Kendall PL, Segal BH, Weller KP, Tighe RM, et al. Identification of myeloid cell subsets in murine lungs using flow cytometry. *Am J Respir Cell Mol Biol*. (2013) 49:180–9. doi: 10.1165/rcmb.2012-0366MA
49. Duan M, Li WC, Vlahos R, Maxwell MJ, Anderson GP, Hibbs ML. Distinct macrophage subpopulations characterize acute infection and chronic inflammatory lung disease. *J Immunol*. (2012) 189:946. doi: 10.4049/jimmunol.1200660

Conflict of Interest: The authors declare that the research was conducted in the absence of any commercial or financial relationships that could be construed as a potential conflict of interest.

Chapter 4: Immunogenicity of prime/boost vaccination with the SARS-CoV-2 vaccine candidate ChAdOx1-nCoV-2019 in the ferret model

The work presented in this chapter forms the basis of a co-first author manuscript in preparation for *npj Vaccine*, and ELISpot and serology data is taken from Marsh *et al.* (2021) published in *npj Vaccines (*reference number: NPJVACCINES-01140, **Appendix**).

Glenn A. Marsh, Alexander J. McAuley, Gough G. Au, … William S.J.Horman, … Sarah C. Gilbert, & S.S. Vasan – May 2021

ChAdOx1 nCoV-19 (AZD1222) Vaccine Candidate Significantly Reduces SARS-CoV-2 Shedding in Ferrets

I performed the majority of the work presented in this chapter, with assistance from Daniel Layton in performing the assays and data analysis, and from Peter Durr in completing the bioinformatic analysis. The serology data experiment was performed by Glenn Marsh. Several antibodies were kindly given for this study by Stephen Kent, Jennifer Juno, and Adam Wheatley.

Chapter 4

The immunogenicity of prime/boost vaccination with the SARS-CoV-2 vaccine candidate ChAdOx1-nCoV-2019 in the ferret model

Abstract

The SARS-CoV-2 pandemic at the beginning of 2020 called for rapid development of vaccine candidates against the novel virus. One such vaccine candidate, the ChAdOx1-nCoV-2019 vaccine, uses a replication-deficient simian adenovirus vector to express SARS-CoV-2 spike (S) antigen, in order to elicit an immune response against the virus. This study assessed the immunogenicity of a prime/boost vaccination regime in the ferret model, using flow cytometric analysis to investigate changes in immune cell subsets. Ferrets given two doses of the vaccination exhibited increases in B cell proportions in the circulation at day 5 post-challenge, as well as increases in $CD8^+$ and $CD4^+PD\text{-}1^+$ T cells. These ferrets also showed greater proportions of $CD14^+CD11b^+$ antigen presenting cells, suggesting the prime/boost animals had launched more robust adaptive and innate immune responses in response to SARS-CoV-2 infection. These results further strengthen our rationale for a two-dose vaccination course, which is currently being used in humans all over the world.

4.1 Introduction

In December 2019, an outbreak of a novel coronavirus was identified in Wuhan, China (111). This virus, now known as SARS-CoV-2, causes the severe respiratory disease COVID-19, which has rapidly spread across the world to cause a severe pandemic. By February 2021, over 110 million cases of COVID-19 have been reported worldwide, with 2.4 million confirmed deaths due to the virus (380).

Developing vaccine candidates against SARS-CoV-2 is an essential step required to control the pandemic. The adenovirus vaccine candidate ChAdOx1-nCoV-2019 has been developed using The Jenner Institute's adenovirus vaccine platform, using a replication-deficient simian adenovirus vector for vaccine delivery (381). This vaccine candidate utilises the full-length structural surface glycoprotein (spike or 'S' protein) of the virus to elicit an immune response. Vaccination of rhesus macaques with ChAdOx1-nCoV-2019 provided animals with protection from viral pneumonia following SARS-CoV-2 challenge (150), whilst Phase 1/2 human clinical trials have shown acceptable safety levels, as well as humoral and cellular immune responses befitting its clinical use (148). Furthermore, the ferret model for human respiratory virus infection has been used as an infection model of mild human SARS-CoV-2 infection, with viral shedding from the upper respiratory tract for up to 11 days post-infection with little to no clinical signs (145, 382-384). Therefore, using the ferret model is considered an effective method to test vaccine efficacy through assessment of reductions in viral shedding.

Extensive research has gone into assessing the cellular immune response to SARS-CoV-2, as deciphering how this virus interacts with the host immune system may provide valuable insights for guiding vaccine development. Several studies have shown that both $CD4^+$ and $CD8^+$ T cells play a pivotal role in protecting individuals against SARS-CoV-2 in cases of acute and chronic disease, with $CD4^+$ T follicular helper cells in particular associated with patient recovery (141, 385-387). Moreover, suboptimal $CD8^+$ T cell responses or T cell exhaustion and depletion are associated with worsened disease outcomes (388, 389), making memory T cell responses a key area of investigation for vaccine candidates. While work to elucidate the

dynamics of the immune response to SARS-CoV-2 in humans continues to evolve, studies into the cellular immune responses in ferrets are limited, with those few previous studies in this model focussing on the cellular dynamics of influenza infections (361, 390). Thus, our ferret study aimed to classify the cellular immune responses following SARS-CoV-2 virus challenge in unvaccinated control ferrets and those previously inoculated with one or two doses of ChAdOx1-nCoV-2019 vaccine, both intranasally and intramuscularly. Immune cell subsets were assessed in the blood and relevant tissues to determine the cellular immune dynamics in this system.

4.2 Results

4.2.1 Study overview

This study was a randomized, placebo-controlled study assessing the ChAdOx1-nCoV-2019 vaccine candidate. Gender balanced groups of 8 ferrets were administered ChAdOx1-nCoV-2019 by either intranasal (IN) or intramuscular (IM), and as either a single dose (prime only) for 28 days or a two dose (prime/boost) regime with the second dose occurring 28 days after the first dose (see Section 2.2.8, Chapter 2). Blood samples were taken 4 days prior to SARS-CoV-2 challenge, as well as 5 and 14 days post challenge. Control ferrets were inoculation with sterile PBS before virus challenge. Ferrets were humanely killed, and tissue samples were collected between 15-17 days post challenge (**Figure 4.1**).

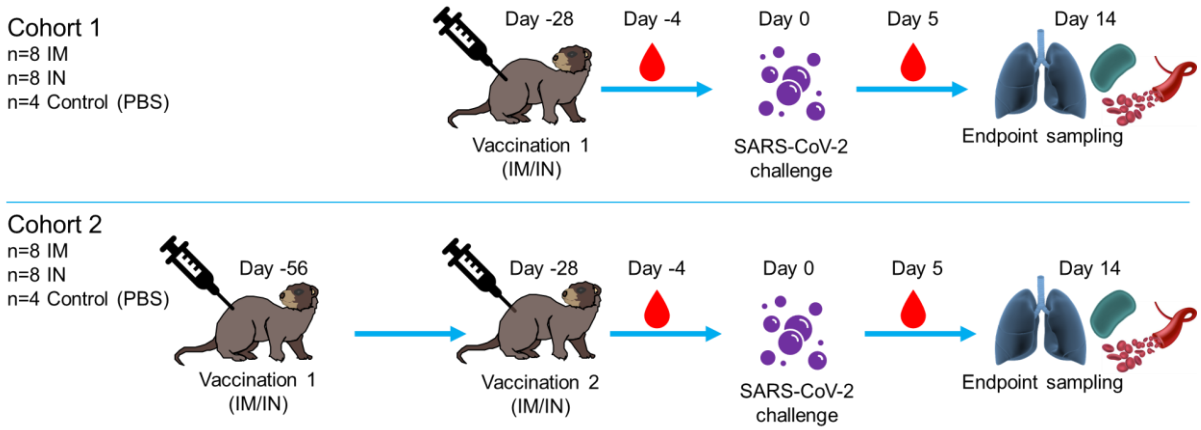

Figure 4.1. Schematic outline of the vaccination study

Ferrets were administered ChAdOx1-nCoV-2019 vaccine or sterile PBS for control ferrets at 56 days ('cohort 2', prime/boost) and 28 days ('cohort 1', prime and 'cohort 2', prime/boost, n=20 for both cohorts). SARS-CoV-2 viral challenge occurred at day 0. At both timepoints, vaccination was given either by intranasal (IN) or intramuscular (IM) administration, with n=8 for each administration method, and n=4 for each control timepoint. Blood samples were taken at day -4 pre challenge and day 5 and day 14 post challenge, and endpoint sampling of tissues days 15-17.

Tissues samples were processed into single cell suspensions, and then used for flow cytometric analysis using three antibody panels which were labelled as 'B cell', 'T cell', and 'Antigen Presenting Cell (APC)' due to their target antigens (**Table 4.1**). The intracellular

marker CD79a was used as a negative selector of B cells in the T cell panel and was thus also used as an alternative measure of B cells external to the B cell panel. The MHC-II antibody in the APC panel was also used as alternate B cells measurement, when examined as an MHC-II^{+}CD11b^{-} population, giving three separate measures of B cell populations. Due to suboptimal staining and a lack of reagent for all samples, further analysis of IFNγ and CXCR5 populations was not completed.

Table 4.1. Antibody panels for immune cell staining

Antibody	Antibody Panel		
	T Cell	**B Cell**	**APC**
CD4	X		
CD8	X		
IFNγ	X		
CXCR5	X		
CD79a*	X		
PD-1	X		
IgG/M/A		X	
GL7		X	
MHC-II*			X
CD11b			X
CD14			X

* Used for B cell analysis external to the B cell panel.

4.2.2 IM-boosted ferrets had increased $CD14^{+}CD11b^{+}$ cells in the blood with multiple populations

For antigen presenting cells, cells were gated as total live cells to include monocytes and granulocytes and were analyzed using an antibody panel to distinguish cells by their expression of the monocyte CD14, the myeloid CD11b and the activating MHC-II markers (**Figure 4.2**). Interestingly, $CD14^{+}CD11b^{+}$ cells separated into low to intermediate ($CD14^{lo}CD11b^{lo}$) and high populations ($CD14^{hi}CD11b^{hi}$), which also expressed low and moderate levels of $MHC\text{-}II^{+}$, respectively. The $CD14^{hi}CD11b^{hi}$ population likely represents a more mature or activated phenotype.

IM prime/boost ferrets saw a significant increase in $CD14^{+}CD11b^{+}$ cells at day 5, though a trend towards increased proportions of these cells was observed in all groups (**Figure 4.3a**). When comparing the ratios of $CD14^{hi}CD11b^{hi}$ over $CD14^{lo}CD11b^{lo}$ expressing populations, the IM prime group showed a significant increase in the ratio of $CD14^{hi}CD11b^{hi}/CD14^{lo}CD11b^{lo}$ cells from day -4 to day 5, suggestive of an increase in monocyte activation in response to the SARS-CoV-2 challenge (**Figure 4.3b**).

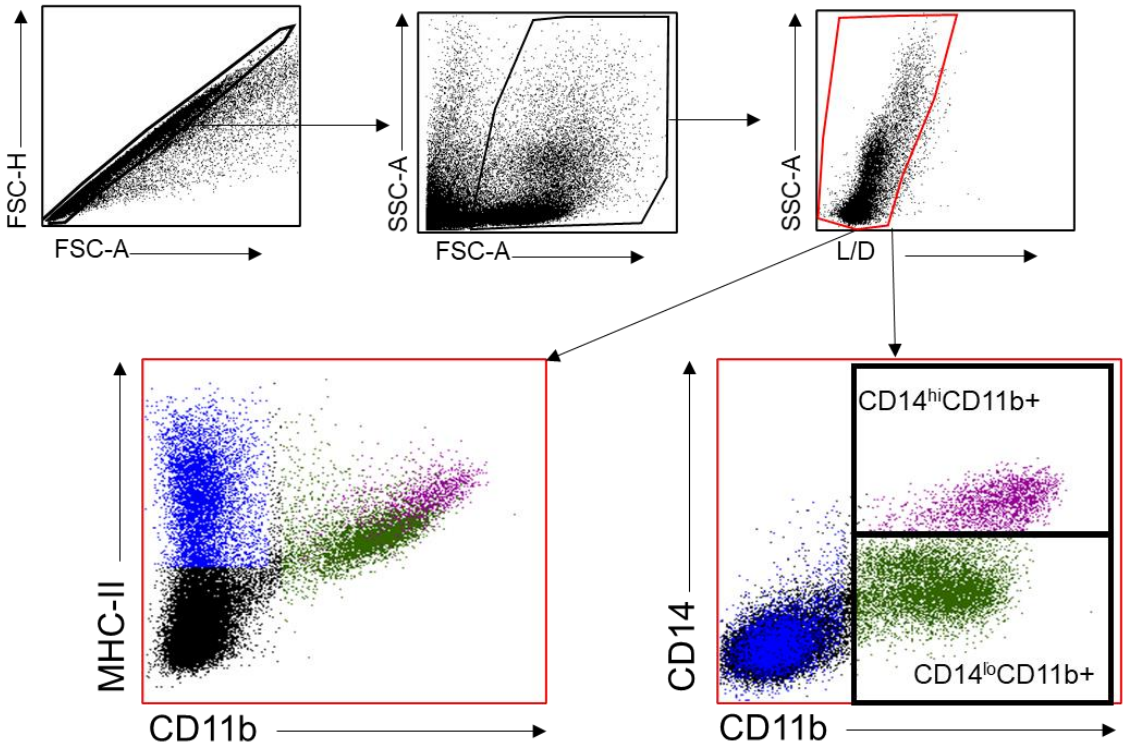

Figure 4.2. Gating strategies for antigen presenting cells

Stained cells from the flow cytometry analysis were gated for single cells, total leukocytes, and then live leukocytes (red). From this gate, $CD14^+$ and $CD11b^+$ cells were analyzed as antigen presenting cells, with two populations observed gated as $CD14^+$ or $CD11b^+$ high (purple) and low to intermediate (green) cells. These cells were also back-gated against MHC-II.

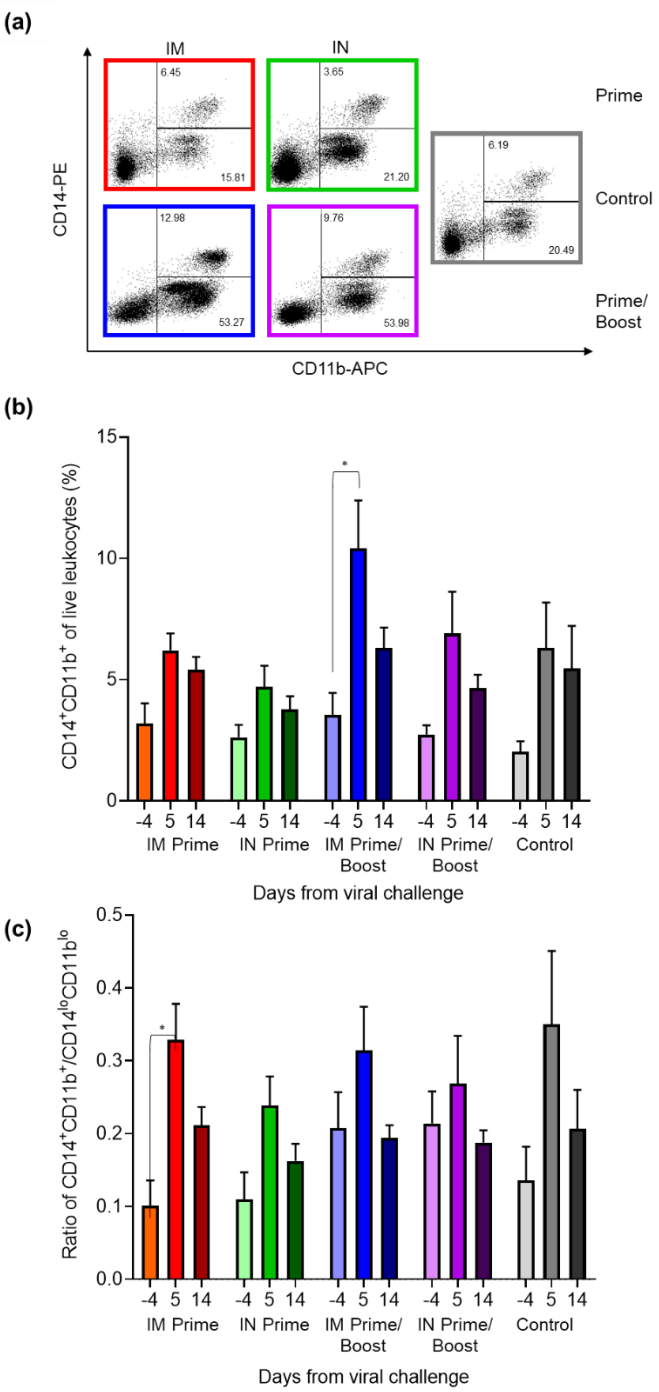

Figure 4.3. Two populations of $CD14^+CD11b^+$ cells were present in the blood

(a) Representative FACS plots and **(b)** relative proportions of $CD14^+CD11b^+$ cells in the blood over time. **(c)** Analysis showing the ratio of $CD14^{hi}CD11b^{hi}/CD14^{lo}CD11b^{lo}$ expression of APC markers. For all day-4 groups, n=8. For IM prime at days 5 and 14, n=7, and for control at days 5 and 14, n=6. FACS plot border colour represents the group at timepoint observed in the bar graphs. Error bars represent SEM, and data marked with (*) indicate $p<0.05$.

4.2.3 Boosted ferrets have greater CD11b expression in spleen

In the spleen, two different phenotypes were observed for $CD14^+$ and $CD11b^+$ cells, with distinct populations of $CD14^{hi}CD11b^{lo}$ and $CD14^{lo}CD11b^{hi}$ cells possibly representing monocytes and dendritic cells respectively (**Figure 4.4a**). The boosted ferrets showed significantly higher proportions of $CD14^{lo}CD11b^{hi}$ cells in the spleen compared to prime only ferrets (**Figure 4.4b**), though no significant differences were observed for the $CD14^{hi}CD11b^{lo}$ populations (**Figure 4.4c**). Intriguingly, the boosted ferrets had consistently lower ratios of $CD14^{hi}CD11b^{lo}$/$CD14^{lo}CD11b^{hi}$ in both the spleen and lymph node (**Figure 4.4d**), suggesting greater uptake of these activated antigen presenting cells from the circulation following SARS-CoV-2 challenge.

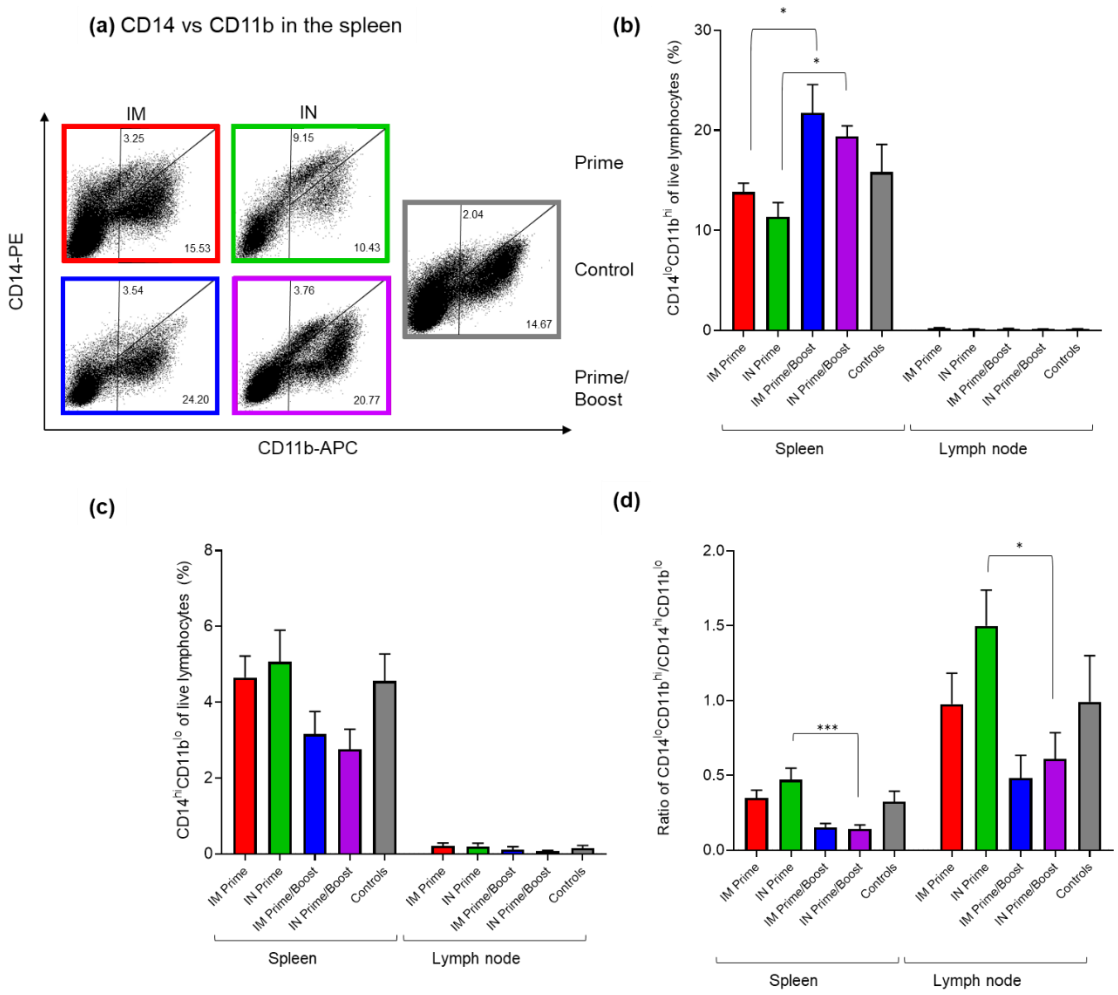

Figure 4.4. Prime/boost ferrets showed greater CD11b expression in spleen, and had consistently lower ratios of $CD14^{hi}CD11b^{lo}$/$CD14^{lo}CD11b^{hi}$

Representative FACS plots of **(a)** $CD14^{+}CD11b^{+}$ cells in the spleen showing variable expression of these two markers. **(b)** Relative proportions of $CD14^{lo}CD11b^{hi}$ and **(c)** $CD14^{hi}CD11^{lo}$ populations in the spleen and lymph node. **(d)** Ratio of the proportions of high:low expressing populations. For all day-4 groups, n=8. For IM prime at days 5 and 14, n=7, and for control at days 5 and 14, n=6. FACS plot border colour represents the group at timepoint observed in the bar graphs. Error bars represent SEM, and data marked with (*) indicate $p<0.05$, and (**) indicates $p<0.01$.

4.2.4 Boosting ChAdOx1-nCoV-2019 induces surface immunoglobulin and MHC-II^{+}CD11b^{-} cells in the blood

Anti-IgG/M/A was used to assess immunoglobulin-expressing B cells in the blood as a measure of humoral immunity induction. Both prime-only groups showed no significant increases in IgG/M/A^{+} cell populations in the blood (**Figure 4.5a**). However, both inoculation routes in the prime/boost group showed significant increases in IgG/M/A^{+} cells in blood at day 5 post infection before a significant decrease at day 14, suggestive of a B cell antibody response in these ferrets towards the SARS-CoV-2 challenge (**Figure 4.5a**). Interestingly, the control ferrets showed a similar trend towards increases in IgG/M/A^{+} cells at day 5, and though this increase in proportions was not significant, it is suggestive of the prime/boost vaccine regime more closely mimicking the natural immune response to viral challenge, but to a greater extent. A significant increase in MHC-II^{+}CD11b^{-} cells, likely B cells due to the lack of other antigen presenting cell-specific markers, was also present in the IM boost group (**Figure 4.5b**), which is indicative of the IM boost giving the greatest increase in Ig-producing B cells in response to SARS-CoV-2 challenge.

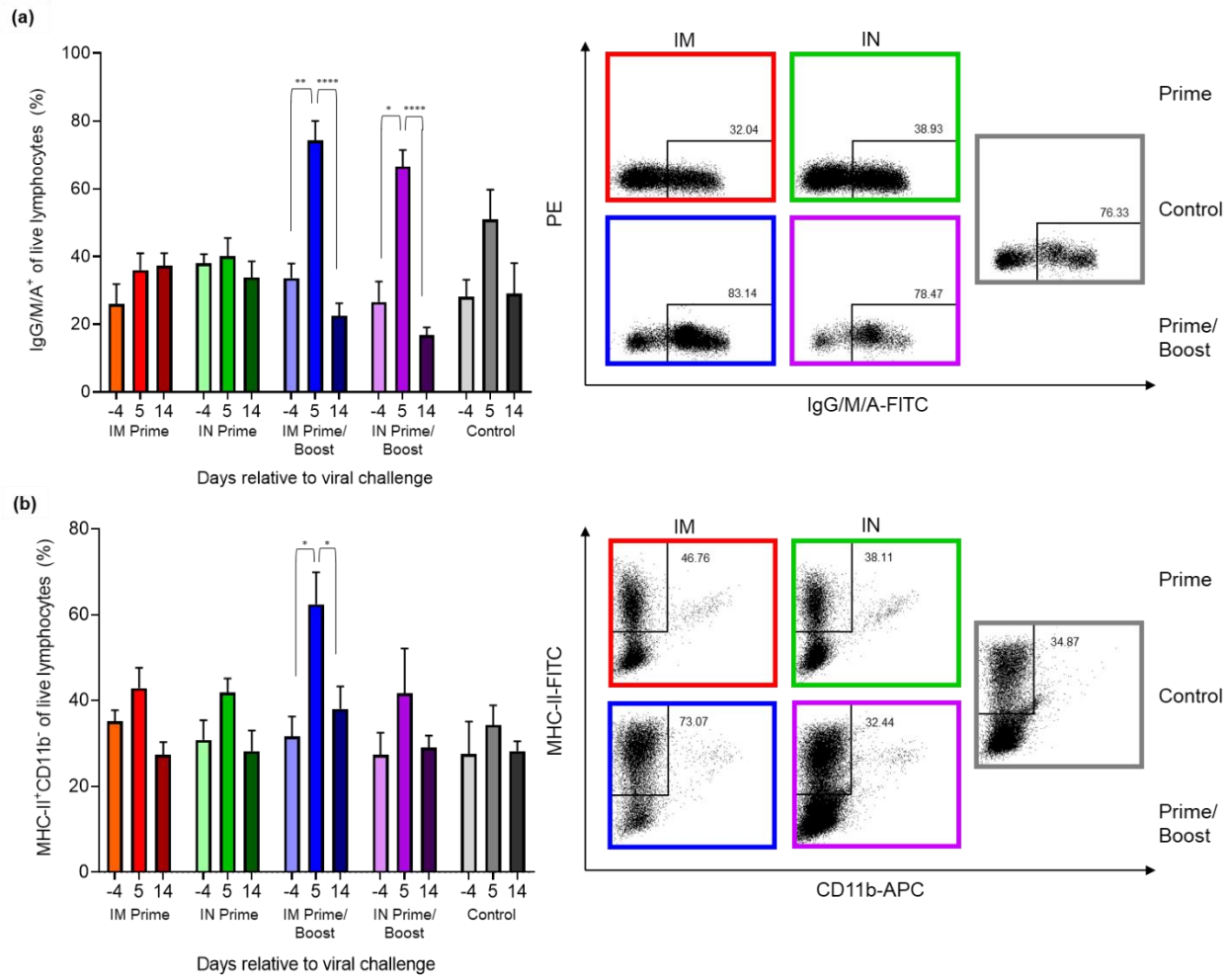

Figure 4.5. Prime/boost vaccination induces greater surface immunoglobulin expression and MHC-II single positive cells in the blood

Representative FACS plots and relative proportions of **(a)** IgG/M/A$^+$ and **(b)** MHC-II$^+$CD11b$^-$ cell subsets in the blood across time. For all day-4 groups, n=8. For IM prime at days 5 and 14, n=7, and for control at days 5 and 14, n=6. FACS plot border colour represents the group and timepoint (day 5) observed in the bar graphs. Error bars represent SEM, and data marked with (*) indicate $p<0.05$, (**) indicates $p<0.01$, and (****) indicates $p<0.0001$.

4.2.5 Boosting ChAdOx1-nCov-2019 induces greater antibody titres by microneutralization assay

Antibody levels induced by the vaccine candidate were assessed in serum samples collected on a weekly basis using a standard virus microneutralisation assay. This assay assessed the ability of the samples to neutralise 100 $TCID_{50}$ of SARS-CoV-2 virus. No virus-neutralising antibodies were detected in control animals which did not receive any vaccine regimen (**Figure 4.6a, b**).

IM prime ferrets reliably showed detectable neutralising antibodies prior to challenge, which were subsequently boosted by viral challenge. Prime-only intranasal administration did not reliably induce detectable neutralising antibodies in the serum prior to challenge and, following challenge, only 75% of animals had measurable neutralising antibodies (**Figure 4.6b**). Both IM and IN administration of the vaccine in a prime/boost regimen led to a sharp increase in neutralising antibody levels in all ferrets 7 days after the second vaccination, which then declined prior to challenge, but were still at detectable levels, and remained detectable 14 days after virus challenge. Integrated analysis of the neutralisation data demonstrated that the administration of a boost dose of ChAdOx1 nCoV-19 increased the overall neutralisation levels in a similar manner regardless of administration route (**Figure 4.6c**).

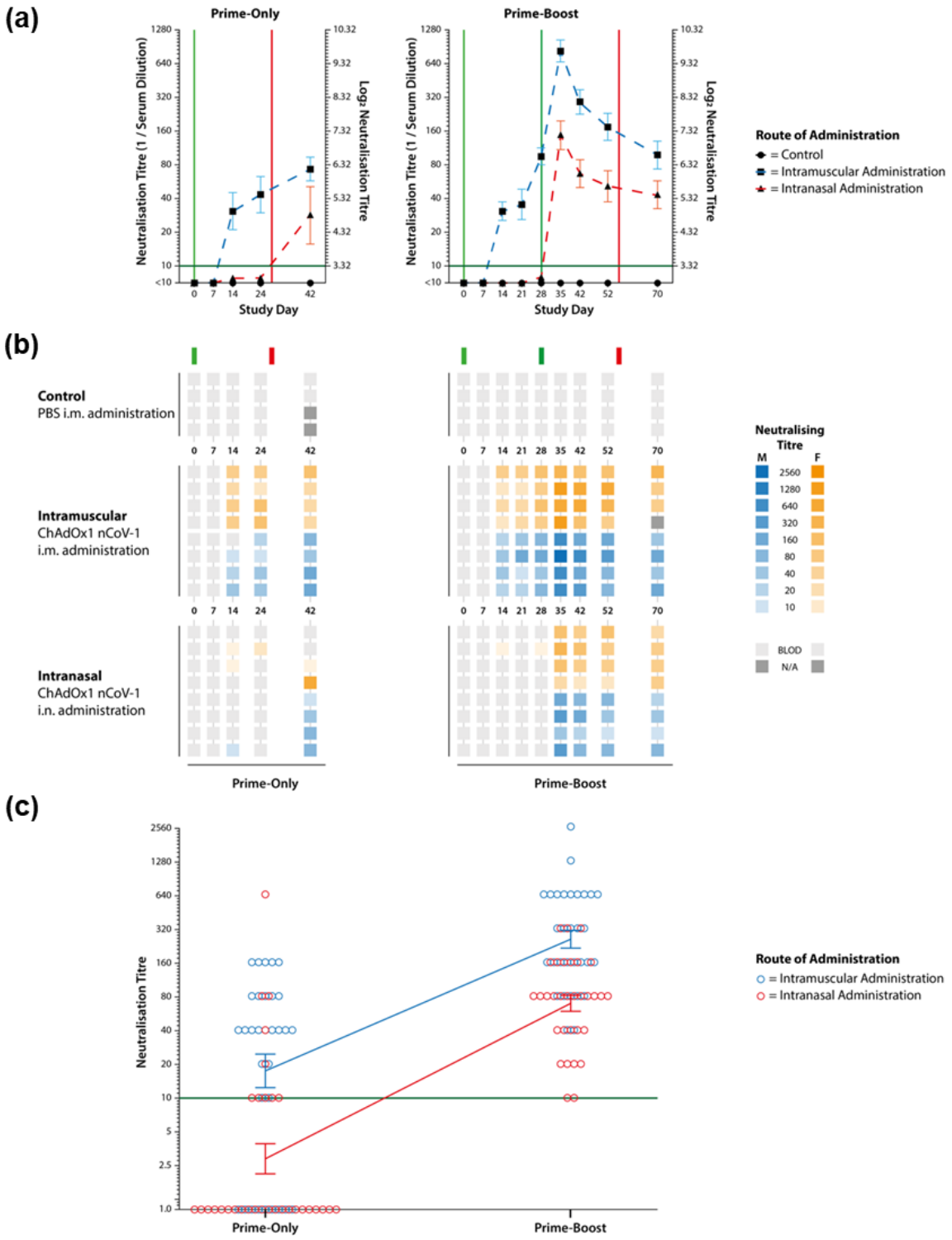

Figure 4.6. Serum Virus Neutralisation Titres Against SARS-CoV-2

Individual ferret serum samples were tested using a virus microneutralisation assay with a 2-fold dilution series starting at 1:10, with the neutralisation titre stated as the highest dilution of serum leading to 100% virus neutralisation. **(a)** Mean titres were calculated for each study group from log_2-transformed data and plotted with SEM. Green vertical lines represent dates of ChAdOx1 nCoV-19 administration, whilst red vertical lines represent

virus challenge at study day 28 or 56 for the two cohorts, respectively. The dark green horizontal line represents the limit of detection of the assay. **(b)** Neutralising titres for individual ferrets were presented in a heatmap with vaccine administration and challenge dates represented with green and red lines, respectively. **(c)** Integrated analysis of neutralisation titres from prime only and prime/boost administrations. Neutralisation titres from prime only animals were combined from study days 7, 14, 24, and 40, whilst neutralisation titres from prime/boost animals were combined from study days 35, 42, 52, and 70. These represent the same timeframe relative to challenge date. For both IM and IN administration of ChAdOx1 nCoV-19, the increase in neutralisation titre in the prime/boost ferrets is similar, as indicated by the almost-parallel linking lines. The vertical lines with error bars represent mean and standard error of the mean (SEM) from $\log_2$-transformed data.

4.2.6 Higher proportions of B cells were present in the tissues of the prime/boost group compared to the prime-only group

B and T cells were gated from total lymphocytes (**Figure 4.7**). B cells were analyzed as IgG/M/A$^+$, MHC-II$^+$CD11b$^-$, and CD79a$^+$ populations, representing both activated and naïve B cell populations, respectively. T cells were analyzed as CD4$^+$ and CD8$^+$ populations. CD4$^+$ helper T cells were further analyzed by the activating PD-1 and the inflammatory chemokine CXCR5 markers to identify subsets of T follicular helper cells, though due to a lack of CXCR5 antibody across the trial, the CXCR5 data was not included in further analyses.

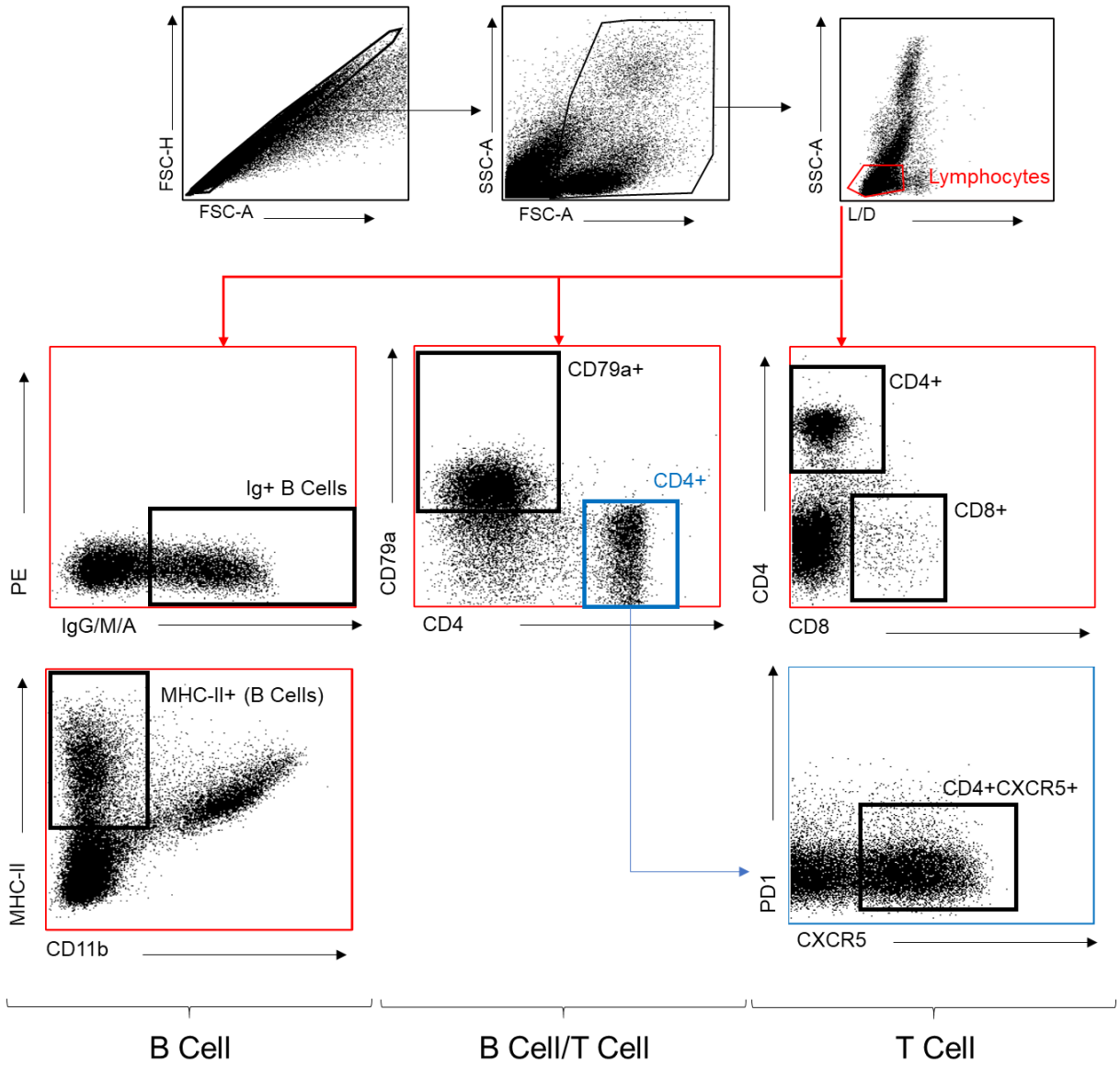

Figure 4.7. Gating strategies for B and T lymphocytes

Stained cells from the flow cytometry analysis were gated for single cells, total leukocytes (excluding debris), and then live lymphocytes (red). From this lymphocyte gate, B cell analysis was performed by gating on IgG/MA^{+}, MHC-II^{+}CD11b^{-}, and CD79a^{+} cells. T lymphocytes were analyzed through gating on CD8^{+} and CD4^{+} positive cells, with further analysis on CD4^{+} gated cells identifying CXCR^{+} or PD-1^{+} cells.

Along with Ig^+ cells, we also examined the GL7 marker as an indication of B cell activation. The induction of a greater B cell response to SARS-CoV-2 challenge in the boost group was also evident in the lymph nodes of infected animals, with boosted ferrets showing higher proportions of B cells, and significantly higher levels of "activated" $GL7^{hi}IgG/M/A^+$ B cells present in the IN prime/boost group compared to IN prime only (**Figure 4.8a**). Interestingly, the spleen of the IN prime group also had significantly higher levels of $IgG/M/A^+$ B cells than both the control and IN prime/boost groups (**Figure 4.8b**). $MHC\text{-}II^+CD11b^-$-containing B cells were also found in higher proportions in the spleen of the IN prime/boost group (**Figure 4.8c**). These findings suggest greater proliferation, activation and dissemination of B cells in this group compared to its prime only corresponding group.

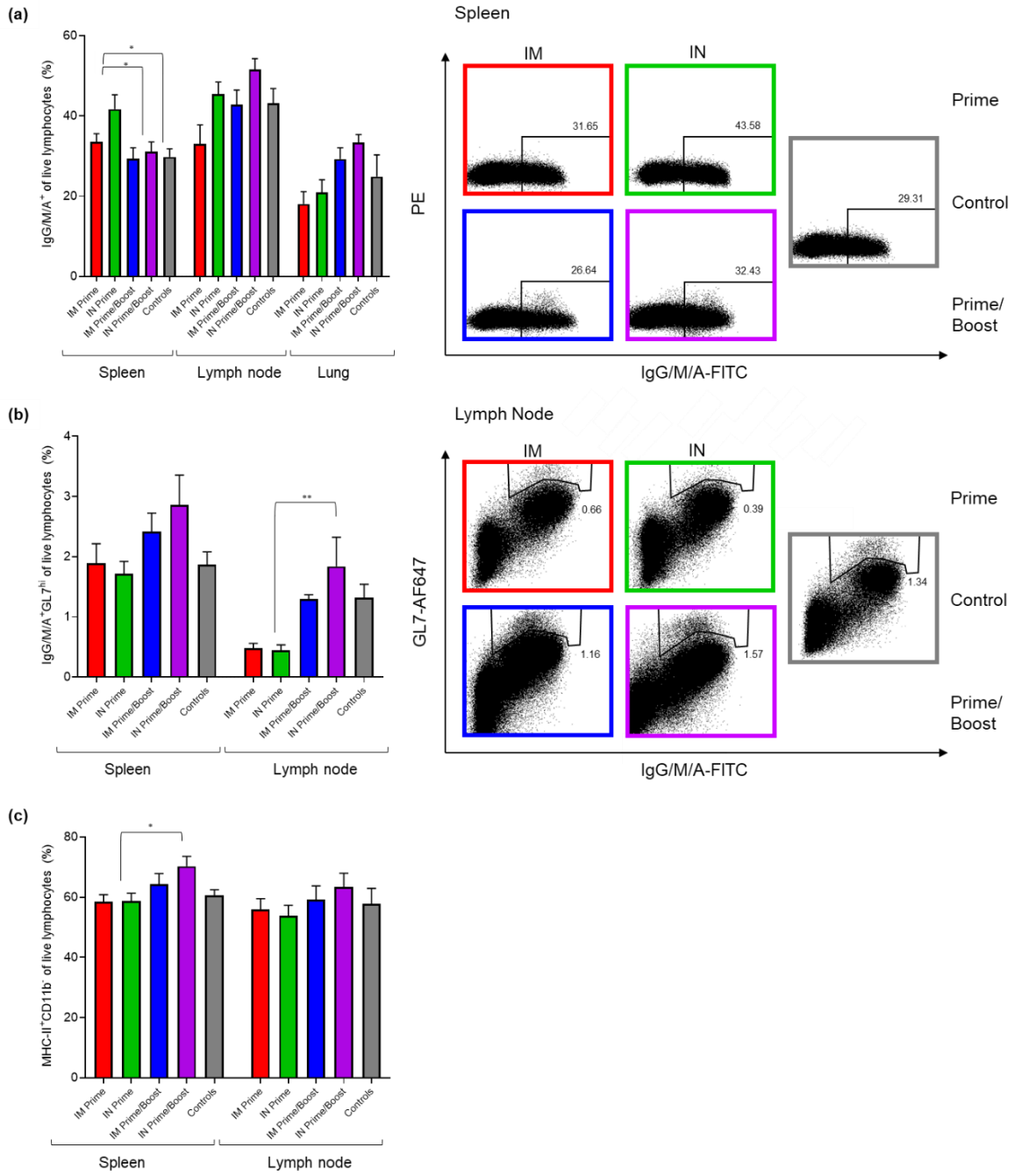

Figure 4.8. Higher proportions of GL7^{+} B cells were present in the tissues of boosted ferrets

Representative FACS plots from the spleen, and relative proportions of **(a)** IgG/M/A^{+}GL7^{hi} cells in the spleen, lung and lymph node. **(b)** Total IgG/M/A^{+} was also assessed in the spleen and lymph node, with representative FACS plots showing populations present in the spleen. Relative proportions of **(c)** MHC-II^{+}CD11b^{-} single positive cells were also assessed in the spleen. For all day-4 groups, n=8. For IM prime at days 5 and 14, n=7, and for control at days 5 and 14, n=6. FACS plot border colour represents the group and observed in the bar graphs. Error bars represent SEM, and data marked with (*) indicate $p<0.05$, and (**) indicates $p<0.01$.

4.2.7 Boosting ChAdOx1-nCoV-2019 elicits higher levels of CD8$^+$ T cells in the blood.

We next wanted to assess the proportions of CD8$^+$ T cells in the blood, as cytotoxic T lymphocytes are important mediators in controlling infection. At day 5 post-infection, both the IM and IN prime/boost groups showed a significant increase in circulating CD8$^+$ T cells comparable to the controls, which was not observed in the prime only group (**Figure 4.9a**), though these levels decreased by day 14. The prime only group saw no significant changes across the sampling timepoints (**Figure 4.9a**), and no significant increases or decreases were observed for CD8$^+$ T cells in any of the assessed tissues.

In the circulation, CD4$^+$ T cell proportions significantly dropped from day -4 to day 5 in both the prime only groups, whilst a significant increase was observed in the IN boost group from day 5 to day 14 (**Figure 4.9b**). Interestingly, levels of CD4$^+$PD-1$^+$ T cells had a trend towards being higher in the prime only group, yet both the control and boost groups saw significant increases in CD4$^+$PD-1$^+$ T cells at day 5 to proportions comparable to the prime group before decreasing again at day 14 (**Figure 4.9c**). Moreover, CD4$^+$PD-1$^+$ T cells were found in significantly higher proportions in the lungs of IN prime ferrets compared to the IN boosted ferrets, while having a trend towards higher proportions overall (**Figure 4.9c**). These results suggest T cell down-regulation is occurring at day 5 post-infection in the lungs of boosted ferrets.

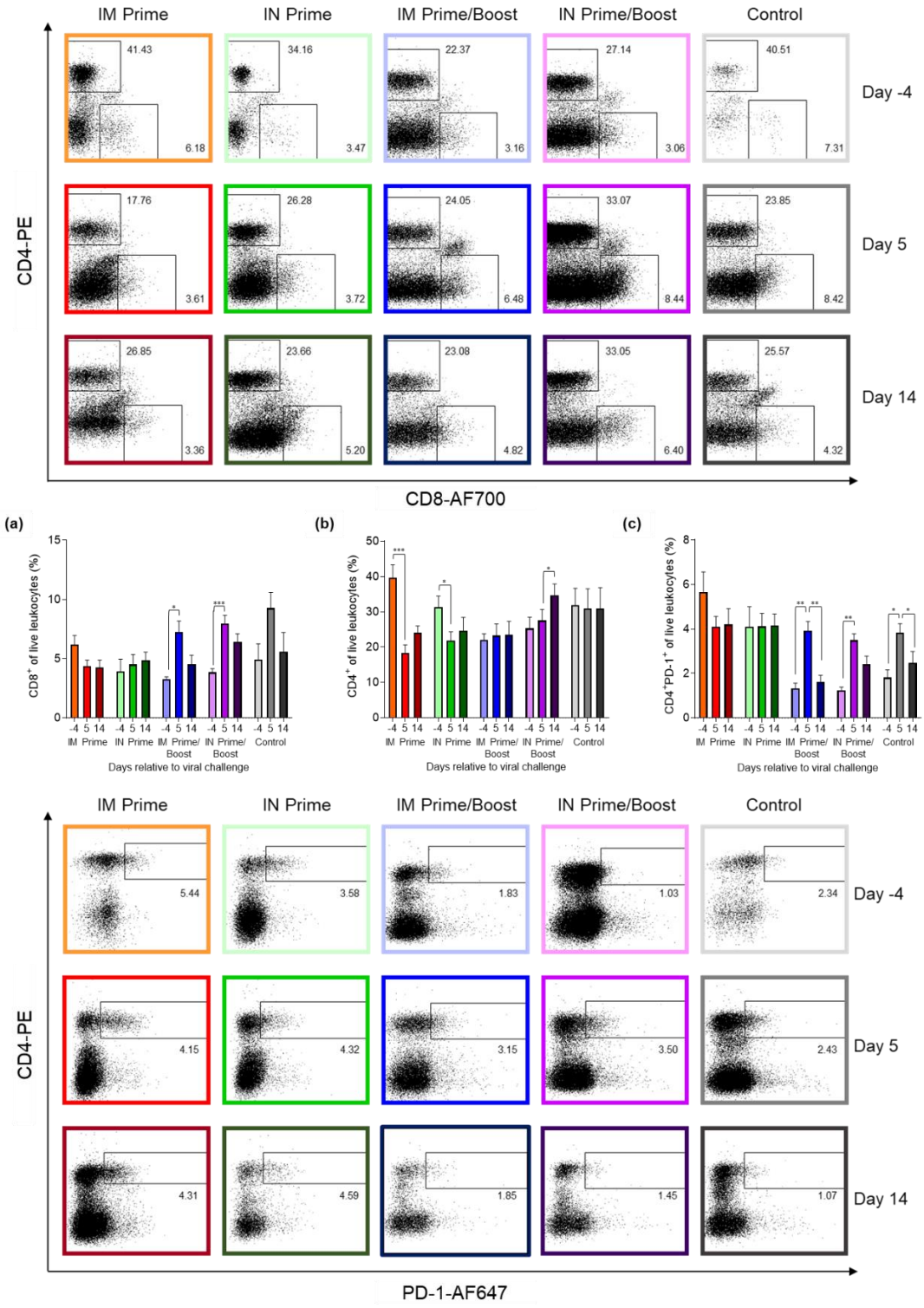

Figure 4.9. Distinct changes in T cells proportions were present in the blood of vaccinated ferrets

Representative FACS plots and relative proportions of **(a)** $CD8^+$, **(b)** $CD4^+$, and **(c)** $CD4^+PD\text{-}1^+$ cell subsets in the blood across time. For all day-4 groups, n=8. For IM prime at days 5 and 14, n=7, and for control at days 5 and 14, n=6. FACS plot border colour represents the group at timepoint observed in the bar graphs. Error bars represent SEM, and data marked with (*) indicate $p<0.05$, (**) indicates $p<0.01$, and (***) indicates $p<0.001$.

4.2.8 Intramuscular prime/boost ferrets showed higher numbers of IFNγ-producing cells in the blood after viral challenge

To measure T cell functionality, interferon-gamma (IFNγ)-producing leukocytes (containing T cells) were measured by IFNγ enzyme-linked immunospot (ELISpot) in the blood (**Figure 4.10, section 2.2.11**), with infected samples tested without further stimulation. The prime only group showed very minimal IFNγ production prior to (day -4) and post virus challenge (day 5). At day 5 post-challenge, the prime/boost groups elicited variably higher levels of IFNγ production compared to the prime only groups, with significantly higher numbers of IFNγ-producing cells observed in the IM prime/boost group compared to the IM prime only animals ($p<0.01$). IFNγ responses observed in the intranasal prime/boost group also trended higher than the prime only group following virus challenge, albeit not significant. There was also a trend towards higher IFNγ responses on day 5 compared to day -4 in the IM and IN prime/boost groups, however these were not significant given the small ferret numbers. Overall, our data suggests that the prime/boost ferrets showed higher levels of T cell function post virus challenge compared to prime only ferrets.

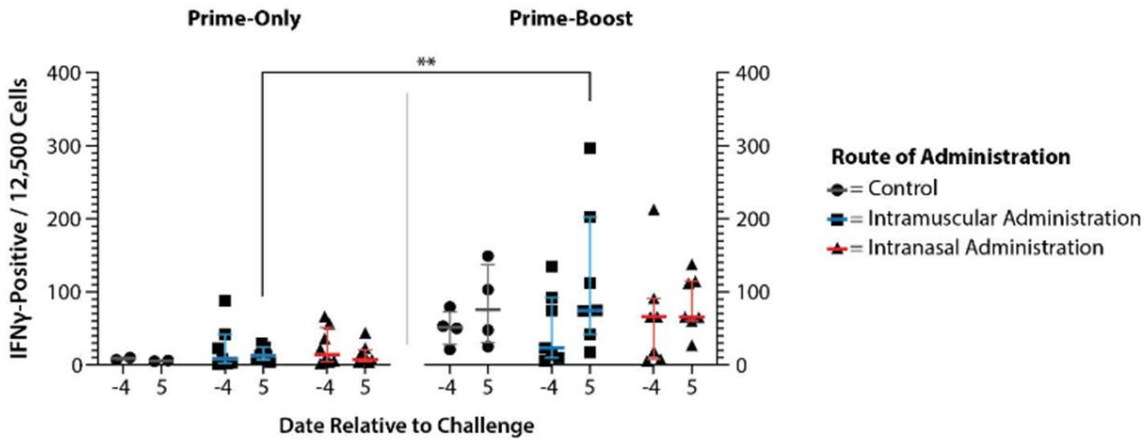

Figure 4.10. IM prime/boost ferrets showed greater levels of circulating IFNγ-producing cells than prime only ferrets

PBMCs were isolated from blood samples taken on Days -4 and 5, relative to challenge, for quantification of circulating IFNγ-producing cells by ELISpot assay. Prime-only animals had few IFNγ-producing cells, whilst prime-boost animals had greater numbers. Comparison of intramuscular prime-boost with intramuscular and intranasal prime-only post-challenge results demonstrated statistical significance (**, $p<0.01$).

4.2.9 Principal component analysis suggests the number of doses, not the delivery method, affect the delineation of the immune response at day five post infection.

Using the available flow cytometry parameters, principal component analysis (PCA) was performed to assess whether the trial ferrets cluster by similarity in their immune responses. No clear clusters were observed at day -4, other than a minor cluster in the IM prime group in the $CD4^+$ parameter, with most groups showing similar scattering to the overall average positioning (**Figure 4.11a**). The groups separated out at day 5, however, with the prime only ferrets clustering based on the $CD79a^+$ variable whilst the prime/boost ferrets clustered based on their Ig^+ expression (**Figure 4.11b**). Interestingly, the control ferrets do not closely cluster, but rather show similarities to both groups, which is reconciled in the FACS data as the control ferrets did show variable phenotypes. Lastly, by day 14 the ferrets were again all randomly clustered, suggesting the abatement of any specific immune responses as a result of the vaccination regimes (**Figure 4.11c**).

(a) Day -4

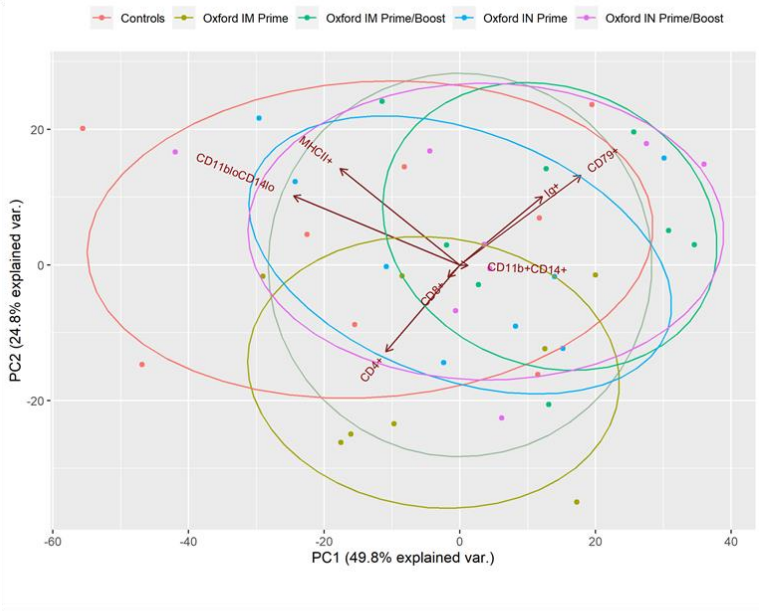

(b) Day 5

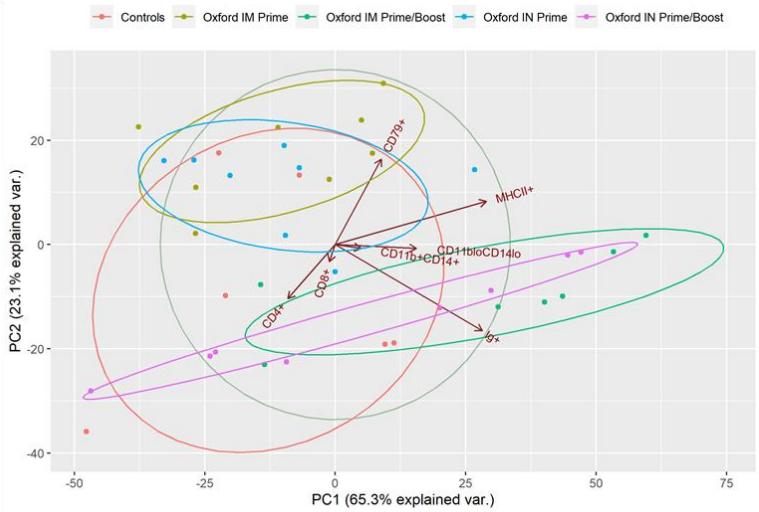

(c) Day 14

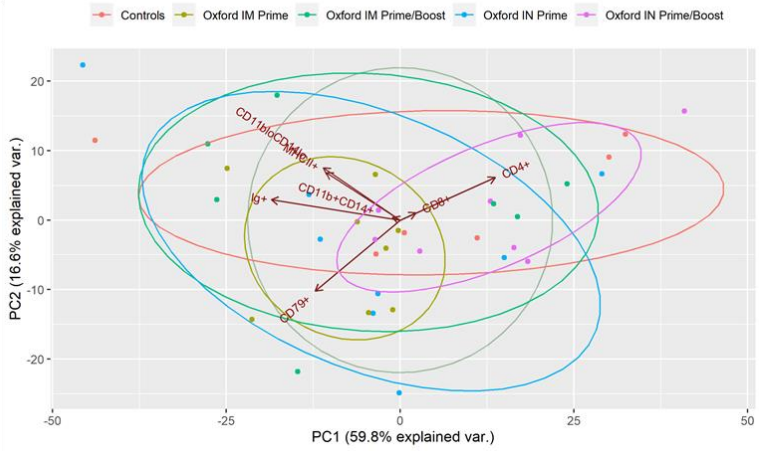

Figure 4.11. PCA analysis shows that prime only and prime/boost ferrets diverge in their immune responses at day 5 post infection, regardless of the route of inoculation

PCA analysis was performed using the flow cytometry data to assess whether ferret populations are differentiated expression of certain markers at **(a)** day -4, **(b)** day 5 and **(c)** day 14 post infection. Each ferret is represented by a single point, with the colours identifying the group and inoculation route (the average grouping of all points is marked in grey). Populations are separately along the axes of the flow cytometry parameters (dark red).

As the number of vaccination doses appeared to be a greater influence on the immune responses elicited compared to the route of inoculation, further correlations were made between the FACS variable for each to assess whether increases in one parameter were associated with increases or decreases in others. Correlation plots for the prime only ferrets showed that there was a negative correlation between $CD4^+$ and $CD79a^+$ cells at day -4 for both the prime only (**Figure 4.12a**) and for the prime/boost groups (**Figure 4.12b**). At day 5 post infection, there were again strong negative correlations between $CD4^+$ increases, though in this instance with decreases in $CD8^+$, MHC-II^+, and $CD14^+CD11b^+$ cells, and MHC-II increases were positively correlated with $CD79a^+$ and Ig^+ responses (**Figure 4.12c**). The starkest observations however were seen in the prime/boost ferrets at day 5, with strong correlations in every variable except between $CD14^+CD11b^+$ and both $CD8^+$ and $CD79a^+$ (**Figure 4.12d**). Interestingly, in these ferrets Ig^+ responses strongly correlated to an increase in APC and B cell markers such as CD79a and MHC-II, and to decreases in both $CD4^+$ and $CD8^+$ T cells, with the matching increases in these T cell markers also strongly correlated to decrease in the APC and B cell marker proportions. These further suggest that the Ig response is stronger following prime/boost vaccination, whilst also hinting at the role of APCs in providing some form of anti-viral immunity in this model.

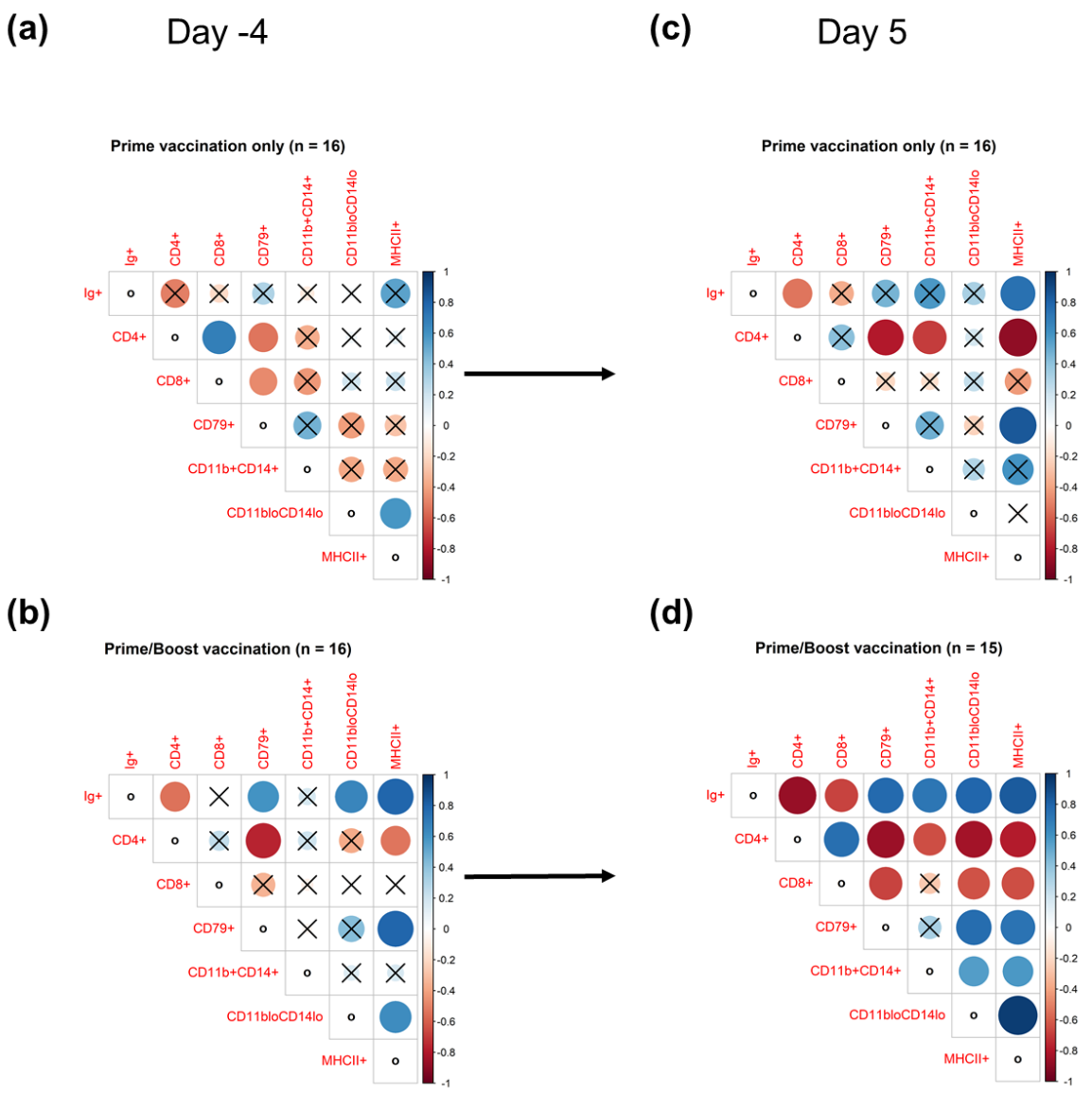

Figure 4.12. Correlation analysis shows that prime only and prime/boost ferrets diverge in their immune responses at day 5 post infection, regardless of the route of inoculation

Correlation analysis was performed using the flow cytometry data to assess whether changes in the proportions of immune cells correlated to increases or decreases in other cell subsets. Based on the PCA analysis, both inoculation methods were merged and assessed as single groups at day -4 for **(a)** prime only and **(b)** prime/boost ferrets, and then at day 5 to assess the effect of viral challenge both groups in **(c)** and **(d)** respectively. A positive correlation is indicated by a blue circle and a negative correlation by a red circle, with the size of the circle indicating the strength of the correlation. Circles marked with an **x** indicate a non-significant correlation.

4.3 Discussion

The ChAdOx1-nCoV-2019 vaccine candidate was one of several promising vaccine candidates to emerge in early 2020 to fight the rapid spread of SARS-CoV-2 across the world. Like many of these vaccines, ChAdOx1-nCoV-2019 utilizes the SARS-CoV-2 spike protein to elicit an immune response against the virus, with this vaccine using a replication-deficient simian adenovirus vector for delivery of the antigen in a similar adenovirus-vector system previously used for other novel viruses such as Middle East Respiratory syndrome (MERS) coronavirus (147). Several studies have assessed the safety and immunogenicity of this vaccine, with phase 1/2 clinical trials in human subjects suggesting the vaccine has acceptable safety and ability to produce neutralizing antibody responses (148). ChAdOx1-nCoV-2019 has also been put into several animal models, with vaccination of mice and pigs suggesting that two doses of the vaccination produces greater neutralizing antibody responses against SARS-CoV-2 (149). Trials in non-human primates have also shown this vaccine can prevent the onset of viral pneumonia and generate enhanced antibody responses, again through a prime/boost strategy (150).

This chapter aimed to classify the cellular immune responses occurring in the ferret model of human SARS-CoV-2 infection, following inoculation with either one or two doses of the ChAdOx1-nCoV-2019 vaccine. Ferrets were chosen as a model due to their effectiveness as a model of human respiratory infection, with several studies showing this model successfully models replicative infection of SARS-CoV-2 (145, 382-384). Despite this, a paucity of knowledge and reagents for the ferret model has thus far prevented more extensive investigation into the dynamics of the cellular immune response to this virus or the vaccine candidates, making this an important study to further give insight into the immunology of this model in a SARS-CoV-2 context. Due to the constraints of the study design and working at PC4 for sample harvesting, it is however important to note that absolute cell counts were not able to be obtained, and thus changes in cell change proportions provide a less concrete indication of immune cell dynamics. Regardless, these data still provide valuable insight into

how the immune cell populations are interacting with the virus, allowing for speculation about the immune mechanisms taking place in this system.

There were distinct differences between the immune responses of ferrets given one vaccination (the 'prime only' group) compared to those that received a second inoculation (the 'prime/boost' group) from an immunological viewpoint. When assessing antigen presenting cell subsets, the prime/boost ferret group showed increased proportions of $CD14^{+}CD11b^{+}$ cells in the blood at day 5 compared to the prime only group, though this result was only significant in the IM-injected ferrets. The identity of these cells has only been speculated in ferrets, with one study suggesting that $CD11b^{+}$ cells identified in the blood are predominantly neutrophils (361), whilst another suggests them to be other myeloid-derived cells such as monocytes (359). However, $CD14^{+}$ cells in humans are often identified as dendritic cells (DCs), with studies showing murine $CD11b^{+}$ DCs and human $CD14^{+}$ resident DCs are functionally similar and are monocyte-derived (172, 173), suggesting that these cells identified in the blood of ferrets are possibly DCs or monocyte-derived DC-precursor cells. Monocytes and dendritic cells have previously been shown to be pro-inflammatory modulators of Th1 immunity in a CpG adjuvanted protein vaccine model in the murine system (391), and thus could plausibly be initiating a similar type of response in our prime/boost ferret system for the ChAdOx1-nCoV-2019 vaccine.

Given the importance of directing antibody responses to vaccination, the differences in B cell proportions as assessed by $MHC^{+}CD11b^{-}$ and overall $IgG/M/A^{+}$ cells were notable. The prime/boost group showed higher proportions of $IgG/M/A^{+}$ cells in the circulation at day 5 post infection regardless of the route of inoculation, whilst the prime only group showed lower levels of these cells. This increase is suggestive of an increased memory B cell response occurring against the SARS-CoV-2 challenge following a second vaccination boost, a phenomenon observed for this vaccine candidate in other animal models (149). Moreover, these increases in immunoglobulin positive cells were reconciled in the serological data, where neutralizing antibody responses were recorded post-challenge. However, and increase in $MHC\text{-}II^{+}CD11b^{-}$

cells was also observed in the circulation of IM-inoculated ferrets at day 5 post-challenge in the boost group, further suggesting an increase in B cell activity in the blood post-challenge. Conversely, at day five the prime only ferrets for both inoculation methods showed an increase in CD79a$^+$ cells, which are likely immature B cells which have not yet differentiated into activated effector B cells (392, 393). Studies in mice with mRNA vaccines have shown greater protection against SARS-CoV-2 is correlative with significant increases in both germinal centre B cells and, more importantly, SARS-CoV-2 specific B cells which produced antibodies against the virus (394), with the upregulation of markers such as MHC-II and expression of surface Ig seen in this study suggesting that these cells are better activated by a prime/boost. These responses are often driven by CD4$^+$ T cell interactions in the germinal centre where CD79a$^+$ cells reside, with studies with simian immunodeficiency virus in rhesus macaques showing a critical role in driving the B cell response towards a more mature phenotype in the germinal centre following vaccination (395). Therefore, we next aimed to identify the CD4$^+$ T cell responses that may or may not be occurring to drive the immune response towards a greater neutralizing antibody response.

Proportions of CD4$^+$ T cells were significantly higher in the blood of prime only ferrets compared to prime/boost ferrets before viral challenge, though levels of these cells significantly dropped following viral challenge, which may suggest either recruitment of CD4$^+$ T cells into the periphery, or some level of leukopenia as seen in SARS-CoV-2 infected humans (389). Furthermore, circulating CD4$^+$ T cells significantly increased in the circulation of IN prime/boost ferrets, whilst the IM and control groups retained stable proportions. Of note however is a significant increase in CD4$^+$PD-1$^+$ T cells in the blood of both boost groups following viral challenge at day 5. The PD-1 marker has been used in other studies to identify T follicular helper cells, with PD-1$^+$ T cells shown to contribute to high-avidity antibody production following influenza virus vaccination (396), although use of this marker in ferrets is still very novel (397). Given the significant increases in both IgG/M/A$^+$ and MHC-II$^+$CD11b$^-$ populations in the blood of prime/boost ferrets at day 5 post-infection, it is likely that these

$CD4^+PD\text{-}1^+$ T cells are T follicular helper cells driving the B cell response towards antibody production.

There were noticeably greater levels of $CD8^+$ T cells in the circulation at day 5 in the prime/boost group, suggestive of a greater effector T cell response to viral challenge following the two doses of the vaccine as opposed to one. Despite their importance in directly killing virus-infected cells and producing pro-inflammatory cytokines, $CD8^+$ T cell responses have generally been limited in scale in other vaccination studies, with preliminary data of one mRNA vaccine candidate showing low levels of $CD8^+$ activation by intracellular cytokine-staining assays (398). This is despite $CD8^+$ T cells having a critical role in protection against SARS-CoV-2, as studies have shown depletion or exhaustion of $CD8^+$ T cells are corelative with worsened disease outcomes (388, 389, 399). These results suggest that two vaccination doses elicit memory of these cytotoxic cells to a greater extent than one dosage, which may allow for greater clearance of virus. Furthermore, despite no significant increases in $CD8^+$ cells in the spleen by FACS analysis, assessment of IFNγ-producing cells by ELISpot assay showed significant increases in these cells in the circulation of the prime/boost ferrets at day 5 when compared to the prime only group. Interestingly, however, assessment of T cell activation by ELISpot in human ChAdOx1-nCov-2019 trials found no such difference in IFN-γ producing cell numbers between prime/boost groups, with both groups showing similar peaks of IFN-γ producing activity at day 14 post-challenge (148). Nonetheless, increases in IFN-γ production and $CD8^+$ T cell proportions suggest that the ChAdOx1-nCoV-2019 vaccine is eliciting a Th1 response, similar to what has previously been seen for this vaccine in the porcine and murine models as well as other SARS-CoV-2 vaccines tested in humans (149, 400). Thus, the ChAdOx1-nCoV-2019 vaccine best elicits protective immunity from both the humoral and adaptive T cell responses when use in a prime/boost regime.

The work presented in this chapter suggests that a prime/boost vaccination regime elicits a more robust immunogenic profile against SARS-CoV-2 compared to one vaccination alone, and that the immune response produced through the prime/boost vaccination is a Th1 immune

response. The PCA analysis further supports this claim, as on day 5 post infection the prime/boost ferrets cluster into a group showing greater Ig^+ and APC marker expression compared to the prime only ferrets regardless of inoculation route, as the prime only ferrets are more associated with a less mature $CD79a^+$ immune phenotype. Correlation analysis also suggests a greater immune activation in the prime/boost ferrets, as increases in Ig^+ where strongly correlated to increases in the APC and B cell markers, though interestingly also with decreases in T cell markers.

This study provides evidence for a prime/boost vaccination regime being the ideal method to elicit a strong antibody response against SARS-CoV-2, and thus may guide the decision-making process for the ultimate distribution and vaccination of the human populace with the ChAdOx1-nCoV-2019 vaccine in the near future. Furthermore, the large-scale implementation of immunological methodologies used in this trial can act as a framework for future vaccination efforts using the ferret model, to give greater insights into not only the neutralizing antibody response but the broader cellular immune responses occurring on the whole.

Chapter 5: Upregulated expression of ferret Interferon-Inducible Transmembrane genes by IFN-α and influenza virus infection

AMERICAN SOCIETY FOR MICROBIOLOGY | Journal of Virology®

VIRUS-CELL INTERACTIONS

Ferret Interferon (IFN)-Inducible Transmembrane Proteins Are Upregulated by both IFN-α and Influenza Virus Infection

William S. J. Horman,[a,b] Katherine Kedzierska,[a] Christina L. Rootes,[b] Andrew G. D. Bean,[b] Thi H. O. Nguyen,[a] Daniel S. Layton[b]

[a]Department of Microbiology and Immunology, University of Melbourne at the Peter Doherty Institute for Infection and Immunity, Parkville, Victoria, Australia
[b]Commonwealth Science and Industrial Research Organisation, Health & Biosecurity, Australian Centre for Disease Preparedness, East Geelong, Victoria, Australia

Thi H. O. Nguyen and Daniel S. Layton contributed equally to this study.

ABSTRACT The current fears of a future influenza pandemic have resulted in an increased emphasis on the development and testing of novel therapeutic strategies against the virus. Fundamental to this is the ferret model of influenza infection, which is critical in examining pathogenesis and treatment. Nevertheless, a precise evaluation of the efficacy of any treatment strategy in ferrets is reliant on understanding the immune response in this model. Interferon-inducible transmembrane proteins (IFITMs) are interferon-stimulated proteins shown to be critically important in the host immune response against viral infections. These proteins confer intrinsic innate immunity to pH-dependent viruses such as influenza viruses and can inhibit cytosolic entry of such viruses to limit the severity of infection following interferon upregulation. Mutations in IFITM genes in humans have been identified as key risk factors for worsened disease progression, particularly in the case of avian influenza viruses such as H7N9. While the IFITM genes of humans and mice have been well characterized, no studies have been conducted to classify the IFITM locus and interferon-driven upregulation of IFITMs in ferrets. Here, we show the architecture of the ferret IFITM locus and its synteny to the IFITM locus of other mammalian and avian species. Furthermore, we show that ferret *IFITM1*, *-2*, and *-3* are functionally responsive to both interferon-α (IFN-α) and influenza virus stimulation. Thus, we show that ferret IFITMs exhibit interferon-stimulated properties similar to those shown in other species, furthering our knowledge of the innate immune response in the ferret model of human influenza virus infections.

IMPORTANCE IFITM proteins can prevent the entry of several pH-dependent viruses, including high-consequence viruses such as HIV, influenza viruses, and SARS-coronaviruses. Mutations in these genes have been associated with worsened disease outcomes with mutations in their IFITM genes, highlighting these genes as potential disease risk factors. Ferrets provide a valuable tool to model infectious diseases; however, there is a critical shortage of information regarding their interferon-stimulated genes. We identified the putative ferret IFITM genes and mapped their complete gene locus. Thus, our study fills a critical gap in knowledge and supports the further use of the ferret model to explore the importance of IFITMs in these important diseases.

KEYWORDS influenza, IFITM, ferrets, interferon

The identification of immune pathways that protect against viruses such as influenza may lead to novel antiviral approaches. The interferon (IFN) pathway is an important immune response produced to induce an antiviral state in the body, through stimulating multiple IFN-stimulated genes that block further viral production and infection. One group of IFN-stimulated genes is the interferon-inducible transmembrane

Citation Horman WSJ, Kedzierska K, Rootes CL, Bean AGD, Nguyen THO, Layton DS. 2021. Ferret interferon (IFN)-inducible transmembrane proteins are upregulated by both IFN-α and influenza virus infection. J Virol 95:e00111-21. https://doi.org/10.1128/JVI.00111-21.

Editor Stacey Schultz-Cherry, St. Jude Children's Research Hospital

Address correspondence to Thi H. O. Nguyen, thonguyen@unimelb.edu.au, or Daniel S. Layton, daniel.layton@csiro.au.

Received 22 January 2021
Accepted 25 April 2021
Accepted manuscript posted online 5 May 2021
Published 24 June 2021

(IFITM) gene family, which has been shown to restrict the entry of multiple viruses as part of this IFN response (1, 2). These proteins are small transmembrane proteins commonly expressed in endosomes and have a conserved topology of two transmembrane regions and an intracellular domain (3).

As their name suggests, IFITM genes are upregulated in response to IFN stimulation. Nevertheless, *IFITM1*, *IFITM2*, and *IFITM3* have been shown to be expressed constitutively across multiple tissues in the human body (4–6), while *IFITM5* expression is mostly confined to osteoblasts due to its suspected role in osteogenesis (7). This constitutive expression serves as an important first line of innate defense against influenza viruses by restricting viral entry and limiting the spread of infection early in the immune response. IFITM proteins act through inhibition of viral envelope hemifusion with the endosome, preventing viral pore formation and the escape of viral elements into the cytoplasm (8–10). While the exact mechanism used to inhibit pore formation is still being investigated, studies have shown that multiple interactions between IFITM proteins and the endosomal membrane alter the membrane's fluidity (10) and cholesterol homeostasis of the endosome (11), which combine to block viral entry.

IFITM proteins have been shown to inhibit the viral entry and replication of several pH-dependent enveloped viruses, including cytomegalovirus, dengue virus, and importantly, influenza virus (1, 5, 12). IFITM3, in particular, has been well characterized as an anti-influenza protein, with several studies showing increased influenza A titers and influenza-related pathology in *IFITM3* knockout mice (13–15), while overexpression of IFITMs in human lung cell lines has been shown to decrease influenza A virus titers (1). However, mutations in these genes have been shown to increase susceptibility to influenza A viruses, with *IFITM3* mutations such as *rs12252* and *rs34481144* conferring greater susceptibility to severe influenza virus infections in some populations (16–18).

Orthologues to IFITM genes have been characterized in mice (6, 15, 19), pigs (19–21), and avian species such as chickens (22), ducks, and geese (23, 24). While mice have often been used for influenza virus studies, the ferret model of human influenza is regarded as the most suitable small animal model to human infection, as their disease pathology is more similar to that of humans than that seen in mice, and their husbandry and practical usage are better than that offered in a nonhuman primate model (25). Unfortunately, due to the limited characterization of the ferret genome, there is little detail regarding many antiviral and interferon-stimulated genes, and how they may act as part of the ferret immune response to viral challenge, making our knowledge incomplete. In terms of ferret IFITMs, only *IFITM5* (GenBank accession no. XM_004781053.2) has been reported at the transcript level (26).

Here, we describe the ferret IFITM gene locus, identifying and annotating ferret *IFITM1*, *-2* and *-3*, as well as validating *IFITM5*. We demonstrate the upregulatory function of these newly identified ferret IFITMs genes which increased in mRNA levels in response to IFN-α and influenza virus stimulation, thereby providing important tools to better understand the ferret model of human influenza viruses.

RESULTS

Identification of the ferret IFITM locus. The ferret IFITM gene region was identified between the conserved flanking genes for protein-glucosyl galactosyl hydroxylysine glucosidase (*PGGHG*) and β-1,4-*N*-acetyl-galactosaminyltransferase 4 (*B4GALNT4*, scaffold GL897275.1:99108–236675) in the Ensembl genome browser (version 101) (27) and run through the GENSCAN server (http://argonaute.mit.edu/GENSCAN.html) to identify potential coding regions (28). These regions were put through BLAST to identify the gene locations, and these genome regions were exported and aligned to Ensembl coding regions (if available) (Fig. 1a). Once the coding genes were identified, the four putative genes were assigned nomenclature based on the IFITM regions found for other species. *IFITM5* existed in Ensembl as a putative gene (ENSMPUG00000008479; Ensembl scaffold GL897275.1:115472–119139), which was followed by two predicted coding regions. These predicted coding regions, ENSMPUT00000008557 (Ensembl scaffold

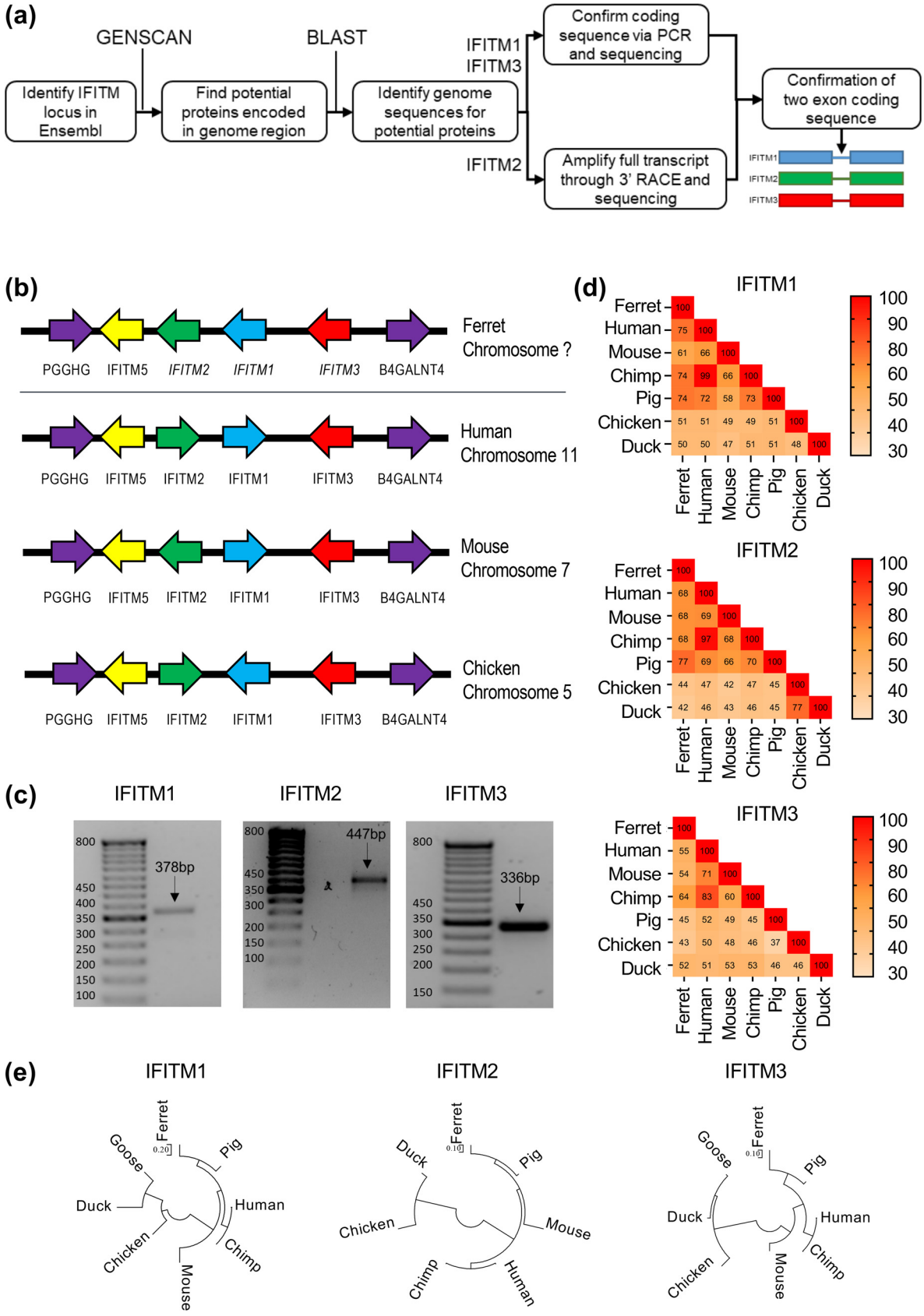

FIG 1 The ferret IFITM locus shows similar architecture to that seen in other species, with high levels of protein homology. (a) Flowchart showing the *in silico* pathway used to identify *IFITM*-coding sequences in the ferret genome, followed by PCR analysis to confirm the

(Continued on next page)

GL897275.1:124417–125501) and ENSMPUT00000008570 (Ensembl scaffold GL897275.1: 145266–146548), showed IFITM-like sequences for *IFITM1* and *IFITM3*, respectively. Interrogation of the locus using GENSCAN and TBLASTN analysis subsequently found another partial IFITM-like sequence which was not listed as a predicted coding region in Ensembl, with this full product amplified and confirmed by 3′ rapid amplification of cDNA ends (RACE) PCR as an IFITM-like coding sequence also. Thus, the ferret genome shows an IFITM locus with four putative IFITM genes, flanked by *B4GALNT4* and *PGGHG* as seen in other species, with a suggested order of *IFITM2*, *IFITM1*, and *IFITM3* as per the locus architecture of other species (Fig. 1b). As no ferret karyotyping has taken place, this locus could not be assigned to a chromosome as has been done for other species. These gene sequences were then confirmed by PCR and sequencing (Fig. 1c), and all three of the novel ferret IFITM genes were found to have two exons like other mammalian IFITMs and had conserved intron-exon boundaries (Fig. 2a). The sequence of *IFITM5* was also amplified by PCR and sequenced for preliminary analysis (Fig. 2b and c).

Ferret IFITMs show distinct homology to the IFITMs of other species at an amino acid level. Translated protein sequences for these IFITM-like coding sequences were aligned by multiway pairwise alignment with sequences from human, mouse, chimpanzee, pig, chicken, and duck IFITMs (Fig. 1d). Based on genomic and protein-level synteny between other mammalian IFITM genes, we annotated ENSMPUT00000008557 as ferret *IFITM1* and orthologous to human *IFITM1*, our newly found transcript as ferret *IFITM2* and orthologous to human *IFITM2*, and ENSMPUT00000008570 as ferret *IFITM3* and orthologous to human *IFITM3*. Ferret IFITM proteins showed the greatest sequence homology to pig IFITMs, which was reflected in the phylogenetic analysis of these protein sequences (Fig. 1e) using the maximal likelihood method in MEGA7 version 7.0.26 (29, 30).

Ferret IFITM proteins show similar topological features to other mammalian IFITMs and conserved transmembrane regions. At the protein level, all IFITMs analyzed showed the same predicted topology, with two transmembrane regions and an intracellular domain observed in the protein sequence alignments (Fig. 3). These proteins were modeled using the Phyre2 webserver, to show possible protein structures of these IFITMs (Fig. 4a). All mammalian IFITMs show conserved motifs (AYSVK at the N-terminal end and ASTAKCLN at the C-terminal end) at the boundary of the transmembrane (highlighted in red) and conserved intracellular loop (highlighted in green), with protein modeling for ferret IFITM1 also exhibiting these motifs (Fig. 4b, highlighted in purple) as predicted by topology prediction (31, 32). These predicted proteins also show distinct homology to the predicted protein structure of the known human IFITMs, with the regions of ferret and human IFITM1 shown in Fig. 4c. These protein predictions suggest that the putative proteins encoded by these newly identified IFITM genes show the same conserved structure observed across IFITMs in multiple species.

Ferret IFITMs are differentially expressed at a basal level in a range of tissues. IFITMs are widely expressed in humans in various tissues, with high levels of mRNA in the lung, liver, and heart (4, 33, 34). In order to determine the tissue distribution of ferret IFITMs, we assessed the basal gene expression levels by quantitative PCR (qPCR) in multiple tissues harvested from female fitch ferrets ($n = 3$). Interestingly, we demonstrated *IFITM1* basal expression to be highest in copy number in the thymus and bone marrow compared to other tissues (Fig. 5a), whereas *IFITM2* and *IFITM3* expression were both most abundant in the liver (Fig. 5b and c). All three IFITMs were also highly expressed in the lung and showed the lowest levels of expression in the skin. *IFITM2* was more highly expressed than *-1* and *-3* in all tissues assessed. Given that these basal levels of expression were present without stimulation, we then wanted to assess how these genes responded to IFN stimulation.

FIG 1 Legend (Continued)
sequences. (b) Schematic of the ferret IFITM gene locus compared to humans, mice, and chickens, with IFITM genes flanked by the *PGGHG* and *B4GALNT4* genes (purple). Arrow direction indicates the orientation of the gene. (c) Ferret IFITM sequences were amplified by PCR and visualized by gel electrophoresis. (d) Heatmap of percentage homology between IFITM proteins from multiple species. (e) Phylogenic trees generated with the maximum likelihood method show the relative evolutionary history among species for IFITM1, IFITM2, and IFITM3 proteins.

(a)

>Ferret IFITM1 coding sequence
ATGGTCAAGGAGAACACGGTGGACATCCTGGGCCCCCCCCAGAGCTCGGCTCCCGTGACCACCA
CCGTGATCGACATCCGTGGTGAGACAGCCGTGCCCGACCACATCGTCTGGTCCCTGTTCAACACC
ATCTTCTTGAACTGGTGCTGCCTGGGCTTCATGGCCTTTGCCTACTCTGTGAAGTCCAGGGACCG
GAAGATGGTGGGTGATGTGATTGGGGCCCAGACTTATGCCTCCACCGCCAAGTGCCTGAACATCT
GTGCCCTGGTCCTGGGCCTCCTGCTGACCACTGTATCTGTTGTTTTTCTGGTGATTGCCTATACTA
CAGCCTACAGTATGATTTTAAAGGTTATGAAGGAGAGTGGTGGCTACCATTAA

>Ferret IFITM2 coding sequence
ATGAGCCACAACGCCCAGCCCTTCTTCCCTGATACCCACGCCGGCGTCCCCCCGACCTACGAGAT
GCTCAAGGAGGAGCACAGGTGGCTGTGCTCGGGCCCCCCCAGAGCTCGGCTCCCGTGACCACCA
CCGTGATCAATATCCGTGGTGAGACAGCCGTGCCCGACCACATCGTCTGGTCCCTGTTCAACACC
ATCTTCTTGAACTGGTGCTGCCTGGGTTTCGTGGCCTTTGCCTACTCTGTGAAGTCCAGGGACCG
GAAGATGGTGGGTGATGTGATTGGGGCCCAGACTTATGCCTCCACCGCCAAGTGCCTGAACATCT
GTTCCCTGGTCCTGGGCCTCCTGCTGACCATTGCATTCGTTGTTTTTTTGGTGATTGGATATATTAT
GATTCCCCATATGATTTTACAGGTTGTGAGCTACAATGAGGTGTCCCAGGCCTAG

>Ferret IFITM3 coding sequence
ATGGAGAACCCCCAGAGCTTGGCTCCCAAGACCACCACCGTGATCGACATCCCGACGGAGACGC
CTGTGCGGGACCACATCGTCTGGTCCCTGTTCAACACCATCTTCTTGAACTGGTGCTGCCTGGGTT
TCGTGGCCTTTGCCTACTCTGTGAAGTCCAGGGACCGGAAGATGGTGGGTGATGTGATTGGGGCC
CAGACTTATGCCTCCACCGCCAAGTGCCTGAACGTCTGTTCCCTGGTCCTGGGCCTCCTGCTGAC
CATCACGTTCATCATCCTTTTTGTCACTGGATCGCTGATGATTCCGCAGATGGTCAGACAGCATGG
AGGCTACTAG

(b)

>Ferret IFITM5 coding sequence
ATGGACACGTCGTACCCCCGCGAGGACCCCCGGGCCCCGACGGCCCACAAGG
CAGACGGCGCCGCCCACACGGCCCTCACCCTGGGGGCGCCCAGACCCCCAC
CTCGAGACCACTTGATCTGGTCGGTGTTCAGCACGCTCTACCTGAACCTGTGCT
GCCTCGGCTTCCTGGCGCTGGCCTACTCCATCAAGGCCCGGGACCAGAAAGTG
GCTGGAGACCTGGAGGCAGCCCGGCGTCTGGGGTCCAAAGCCAAGTGCTACA
ACATCCTGGCCATGATGTGGGCGCTGGTGCCACCGCTGCTGCTGCTGGCGCTG
GTGGTGACAGGCGCGCTACACCTGTCGCGGCTGGCCAAGGACTCCGCTGCCT
TCTTTAGCACCAAGTTCGATGACTCGGACTATGACTGA

(c)

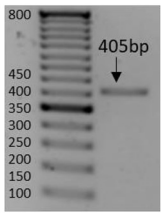

FIG 2 Nucleotide sequences for ferret IFITMs. (a) Coding sequences for both exons of ferret *IFITM1*, *IFITM2*, and *IFITM3* obtained from sequencing, with exon 1 in black and exon 2 in red. (b) Coding sequence of ferret *IFITM5* from sequencing data based on the putative transcript found in Ensembl. (c) The sequence of *IFITM5* was confirmed by PCR of cDNA obtained from ferret bone marrow.

Ferret IFITMs are highly upregulated by IFN-α. To validate their expected function as IFN-stimulated genes (ISG), ferret lung epithelial cells were stimulated with ferret IFN-α to assess gene upregulation. All three ferret IFITMs were upregulated in a time-dependent manner by qPCR following stimulation with ferret IFN-α (Fig. 6a). Each IFITM continued to increase in transcript number over the 72 h of stimulation, with *IFITM1* observed to be the most highly upregulated (55-fold compared to the unstimulated control), while *IFITM2* and *IFITM3* were both upregulated 10-fold ($P < 0.0001$, Fig. 6a). Despite the much higher fold change, raw transcript numbers of *IFITM1* were lower than those seen for *IFITM2* and *IFITM3* (Fig. 6b), with *IFITM2* showing the greatest overall transcript levels at the basal expression level and following IFN-α stimulation.

Influenza virus infection induces IFITM gene upregulation. As IFITMs have been associated with protection from viral infection, we next assessed whether these genes were upregulated as part of the cellular immune response to influenza virus infection in the ferret. IFITM transcript levels were measured in ferret lung epithelial cells with A/WSN/33 (H1N1) influenza virus. The transcriptional peak in terms of fold change was at 24 h for all three IFITMs following a significant increase at the 24-h time point, with *IFITM1* showing a greater 124-fold increase and *IFITM2* and *IFITM3* showing 9-fold and 6-fold increases, respectively ($P < 0.0005$, Fig. 6c). However, *IFITM1* showed lower transcript levels despite the larger fold change (Fig. 6d), with the overall transcript levels being lower than those observed in the IFN-α stimulation. Moreover, the level of transcript appeared to peak and then decrease following

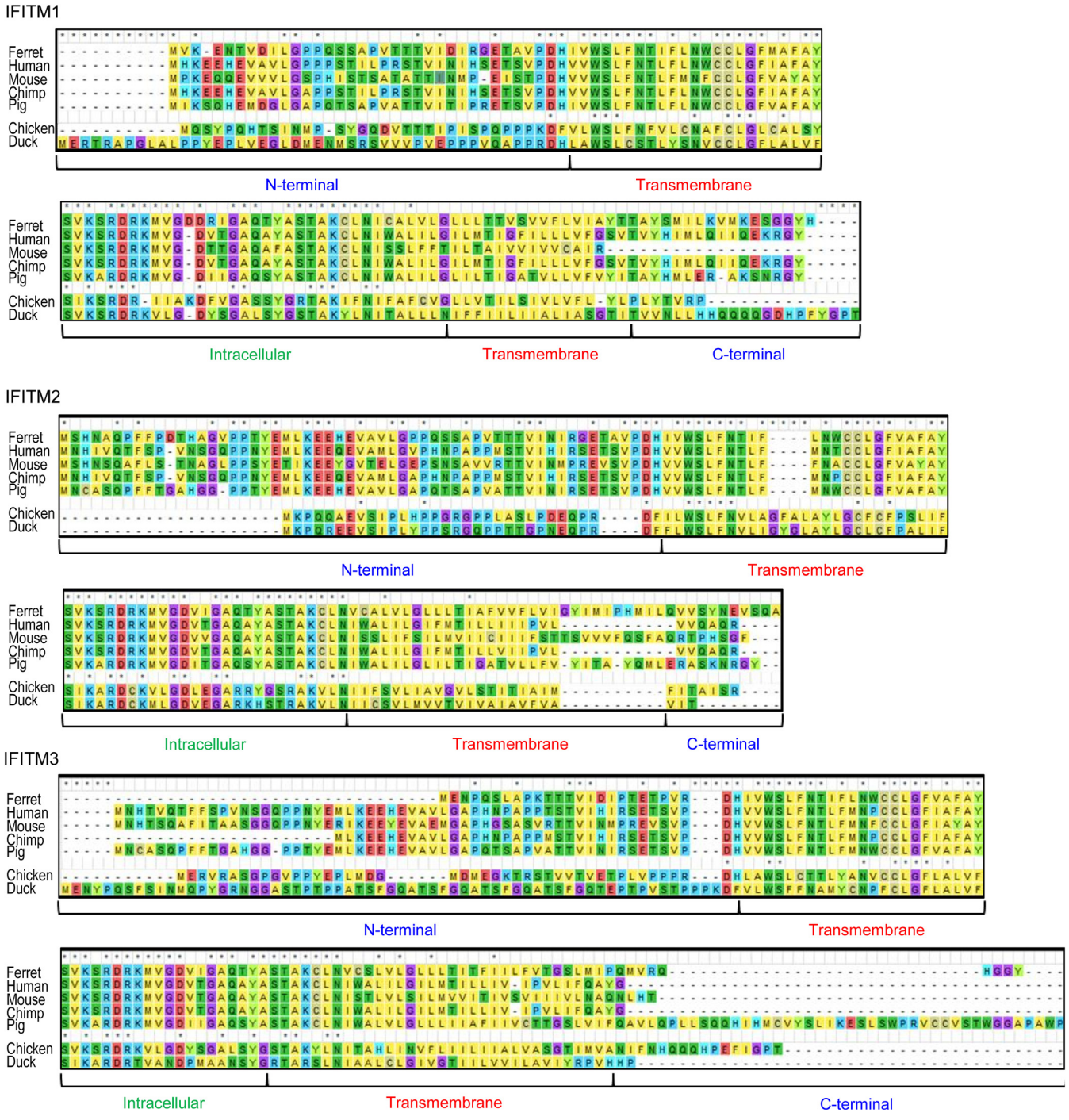

FIG 3 Ferret IFITMs show conserved topology and motifs seen in other mammalian IFITMs. Protein sequence alignments for IFITM1, IFITM2, and IFITM3 of multiple species. Conserved residues are indicated by an asterisk (*), and predicted protein topology is indicated below the alignment.

the 24-h time point, in contrast to what was observed in the IFN-α stimulation, where transcript levels steadily increased across the time points. Therefore, these data support the idea that these newly identified putative ferret IFITM genes function as IFITM genes following IFN-α stimulation and influenza virus infection.

DISCUSSION

The identification and understanding of immune genes which contribute to the effective control of respiratory viruses, such as influenza viruses, is important in maintaining human

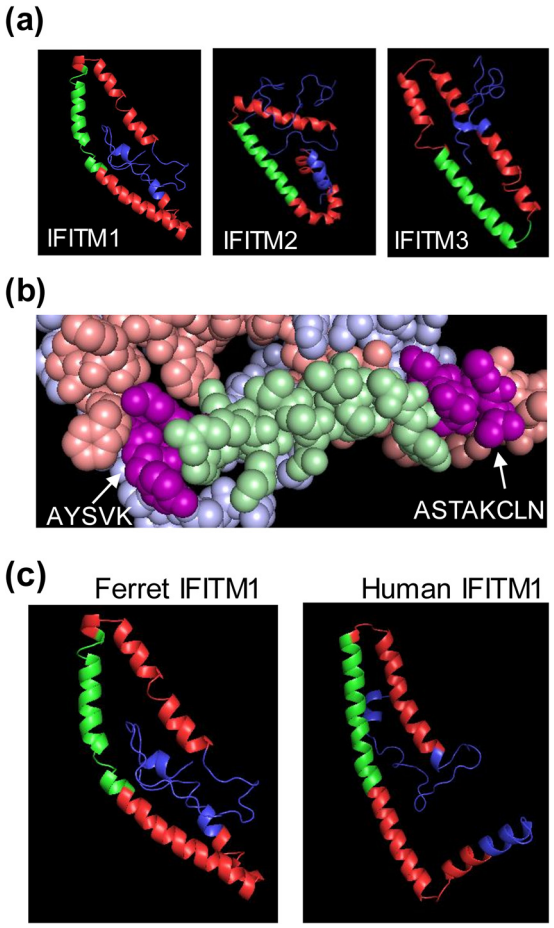

FIG 4 Ferret IFITM1 protein modeling shows conserved structure compared to human IFITM1 models. (a) Protein sequences for ferret IFITMs were modeled using the Phyre2 webserver to create predicted protein structures with predicted features colored as follows: transmembrane regions (red), conserved intracellular loops (green), N- and C-terminal regions (blue). (b) Protein prediction modeling of ferret IFITM1 shows the conserved AYSVK and ASTAKCLN motifs (purple) observed in the transmembrane regions (red) surrounding the conserved intracellular loop (green). N- and C-terminal regions are marked in blue. (c) Protein modeling of both ferret IFITM1 and human IFITM1 shows conserved structures across species. Both models show conserved transmembrane (red) and intracellular (green) regions, as well as N- and C-terminal regions (blue).

health toward the potentially fatal zoonotic infections often modeled in ferrets. The ferret model is commonly used for human influenza, due to the similarities in the ferret respiratory tract receptor distribution and clinical signs to those of humans (25, 35, 36). Despite these advantages, overall knowledge of the immune response in ferrets is still limited, with only a few studies looking into immune cell subtypes (37–39), and even fewer studies investigating innate immune antiviral factors of the proinflammatory response (40, 41). This lack of in-depth understanding of the ferret immune response means that understudied factors such as these interferon-stimulated genes may be having an unknown effect on transmission or immunological studies in the ferret model. This is the case in humans, where IFITM mutations have strongly correlated with worsened disease outcome for patients infected with avian influenza viruses (16, 18, 42). This issue is compounded by a poorly annotated genome, which makes identifying and classifying ferret immune genes a difficult endeavor. Here, we identified and validated ferret IFITM genes and designed tools for measuring these genes via qPCR. Our findings are essential for future research of IFITMs in ferret disease models.

The IFITM locus has been identified and studied across many vertebrate species, with more detailed analysis observed in humans and mice (13, 15) and limited knowledge of IFITMs in species such as pigs and gallinaceous birds (20, 22, 24). In the ferret

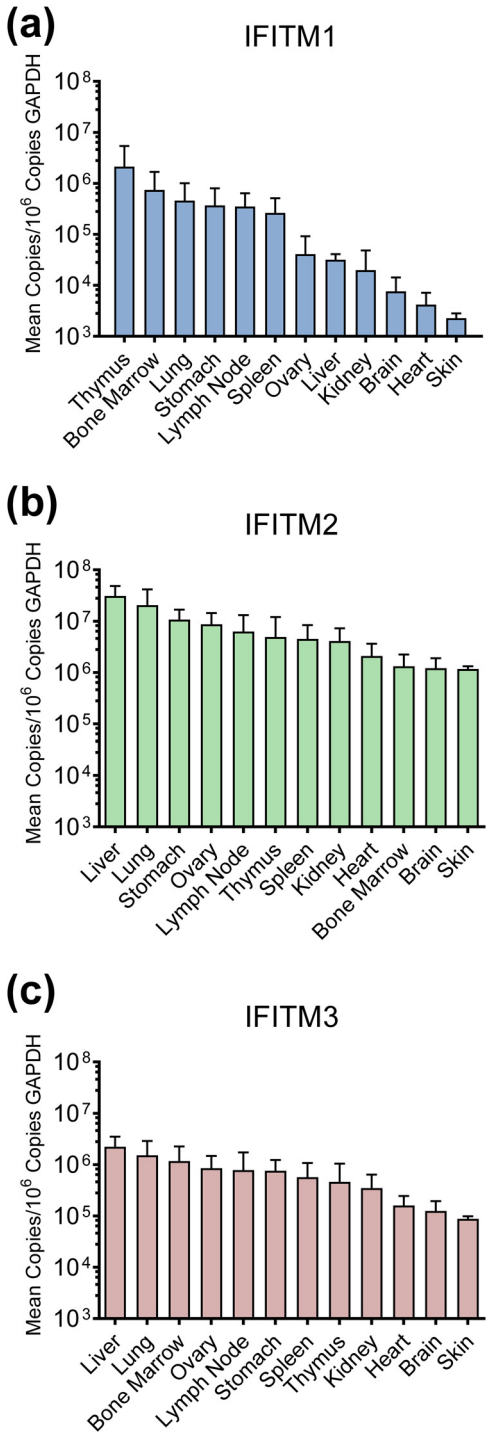

FIG 5 Ferret IFITMs are found in multiple tissues by qPCR. (a to c) Transcript levels of ferret IFITMs assessed in multiple tissues using qPCR ($n = 3$ for each tissue, with each point being an average of duplicate tests). Basal expression of IFITMs was assessed in unstimulated ferret tissues, with expression plotted as the mean copy number per 10^6 copies of GAPDH, with error bars representing the standard deviation (SD).

genome, *in silico* analysis showed a predicted *IFITM5* gene sequence between the common flanking genes *PGGHG* and *B4GALNT4*, suggestive of the conserved nature of these gene loci across mammals and other vertebrates. This has also been suggested in more extensive analytical studies assessing how these genes have evolved in

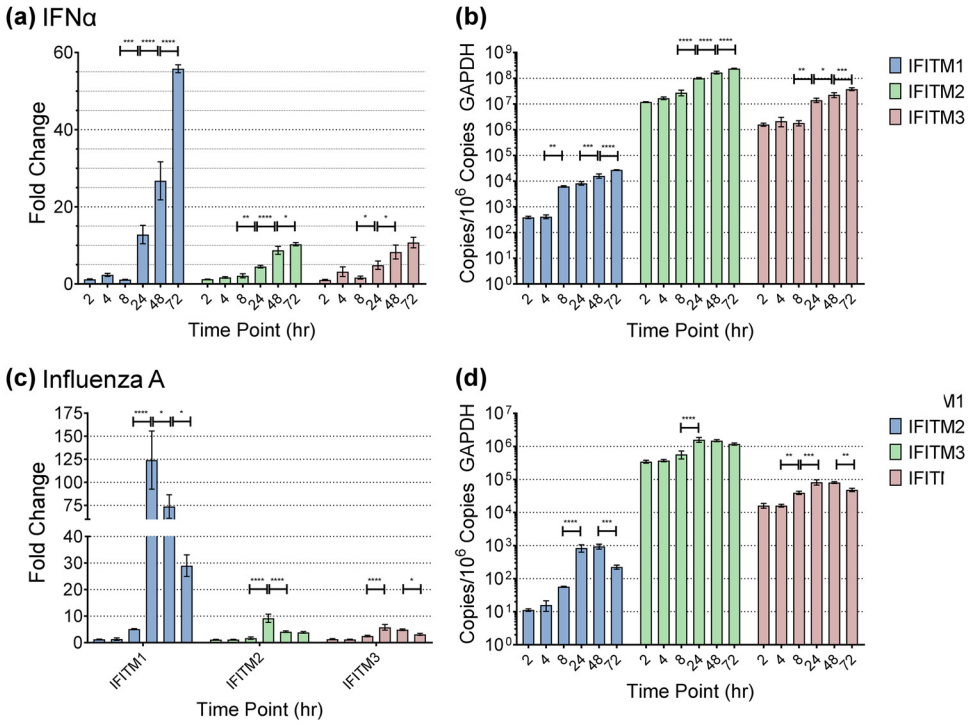

FIG 6 IFITM transcript levels increase following stimulation with ferret IFN-α and influenza A virus. (a and b) IFITM transcript levels were measured in FRL cells following IFN-α stimulation for 2, 4, 8, 24, 48, and 72 h and are shown as (a) fold change compared to an unstimulated control and (b) copy number per 10^6 copies of GAPDH. (c and d) IFITM transcript levels were also assessed following stimulation with influenza A/WSN/33 (H1N1) virus as fold change (c) and copy number (d) for all three ferret IFITMs (repeated in triplicate for each). *, $P < 0.05$; **, $P < 0.01$; ***, $P < 0.001$; ****, $P < 0.0001$ (Tukey's multiple-comparison test, compared to adjacent time points), with error bars representing SD.

chordate species (21). While further genome interrogation was able to identify three putative IFITM gene sequences, their exact identities required a more comprehensive investigation, as the nomenclature around IFITM genes is variable and complicated by similarities shown across *IFITM1* and *-3*. For example, chicken *IFITM1* was originally identified as *IFITM3*-like, and vice versa for *IFITM3*, causing a switch in how these proteins were named (22). This nomenclature is shared by duck IFITMs but not the putative goose IFITMs (23), making comparative analyses difficult, highlighting the importance of developing appropriate functional analysis to determine nomenclature.

Protein-coding sequences in this ferret genomic region were identified by GENSCAN, and IFITM-like sequences were pulled from the analysis for further investigation (28). Based on the locus architecture of other mammalian species, we discovered three putative IFITM genes correlating to *IFITM1*, *-2*, and *-3* in the genome scaffold following the *IFITM5* gene. These three sequences were identified, and following alignment with the sequences of other species, it was confirmed that the ferret IFITM locus follows the same basic organization as that seen in other species, with the order of IFITMs being *IFITM5-2-1-3*. This conserved gene order supports the idea that the IFITM locus is highly conserved across mammalian species.

The proteins encoding these nucleotide sequences showed clear "IFITM"-like structures based on conserved regions observed in other species. All mammalian IFITMs have conserved transmembrane regions, with the putative ferret IFITM proteins displaying the same AYSVK and ASTAKCLN motifs seen in other species at the transmembrane boundaries (22, 43). While the transmembrane and intracellular regions are conserved, the exact topology of the N- and C-terminal regions in the ferret requires further work to elucidate. Despite the protein prediction models used suggesting that the regions are extracellular, topology models for IFITMs in both humans and mice

have indicated that *IFITM3* may possess an intracellular N-terminal domain (3), yet mouse *IFITM1* may have two intracellular domains at its N terminus and C terminus (44).

Despite most commonly being associated with respiratory pathogen defense in the lungs of humans, IFITMs have been associated with antiviral protection in a range of tissues in the murine model. For example, *IFITM3* has been show to protect the heart from H1N1 infection in the mouse model during systemic infection (45), while infection with H9N2 elicited upregulation of murine *IFITM1* and *IFITM3* in tissues such as the kidney, brain, and liver (6). Through assessing basal IFITM expression in multiple tissues of the ferret body, we were able to show that IFITMs are expressed at various, but detectable, levels in different tissues, highlighting these genes' function as important initial protection against a broad array of viral threats due to their basal expression in virus-susceptible tissues. Furthermore, the high basal expression of these genes in the lung tissues was a good rationale to use ferret lung epithelial cells in the stimulation studies to validate the function of these genes, which were already highly expressed prior to stimulation.

Our experiments show that ferret IFITM genes are stimulated during interferon-driven responses as shown in other mammalian species (15). Interestingly, these genes appear to continue to be activated for prolonged periods after IFN stimulation, with continued upregulation of these genes still evident after 72 h. This is despite initial induction of ISGs often occurring as early as the 2 h time point (46), suggesting that these proteins can act as sustained responders, provided IFN is present in the system. Our studies also show that these genes are also upregulated in the presence of H1N1 influenza virus, though in both experiments it was intriguing to note that, at a transcript level, *IFITM1* was the most greatly upregulated by fold change but had the lowest transcript level. While less highly upregulated, *IFITM2* and *IFITM3* showed greater transcript levels, even at a basal level with no stimulation, than what was seen after 24 h of influenza virus infection for *IFITM1*. This may be suggestive of *IFITM1* having a different role or mechanism of action in the antiviral response to influenza, which has also been shown in the case of other viruses which enter via endosomes such as Zika viruses (47, 48), or that it may need lower levels of expression to enact antiviral function. Moreover, most influenza-related studies tend to focus on *IFITM3*, which is commonly shown to exhibit the greatest anti-influenza properties and may affect the antibody response to influenza viruses (13, 15, 49, 50). As such, the differences in these two proteins gives an idea of how IFITMs provide broader antiviral protection, as IFITM1 is more effective against viruses that enter via the cell membrane, such as filoviruses, due to its localization on the cell surface compared to IFITM3 in the endosome, which is more effective against enveloped viruses (1, 8, 11, 48). Further research is required to confirm the membrane localization of these novel proteins to confirm these functional differences.

Identification and classification of the IFITM gene family in ferrets contributes to our understanding of the ferret model of human influenza and gives insight into an important ISG which may play a role in how this model is used. This study fills that knowledge gap while also providing a framework for future investigations into other antiviral genes not yet investigated in the ferret genome.

MATERIALS AND METHODS

Ethics and processing of ferret tissues. All procedures involving ferret tissues were reviewed and approved by the Commonwealth Scientific and Industrial Research Organisation (CSIRO), Australian Animal Health Laboratories (AAHL) Animal Ethics Committee (AEC no. 1926) and were performed in accordance with the Australian Code for the Care and Use of Animals for Scientific Research (7th edition 2004).

Ferret tissues were aseptically collected and homogenized using a FastPrep-48 grinder and lysis system (MP Biomedicals, Irvine, CA, USA). Briefly, homogenized tissues were lysed using the MagMAX-96 viral RNA isolation kit lysing/binding solution, and then RNA was extracted as per the manufacturer's instructions using the KingfisherFlex magnetic particle processor (Thermo Fisher Scientific, Missouri, USA).

Cell culture. Ferret lung epithelial cells (FRL) were explanted and transformed by infection with adenovirus 5 (ATCC, Manassas, VA, USA). The transformed FRL epithelial cells were propagated and cloned

TABLE 1 Quantitative real-time PCR primer sequences (5′ to 3′)

Gene	Forward	Probe	Reverse
IFITM1	GCCAAGTGCCTGAACATCTGT	CTGACCACTGTATCTGTTGT	GCCACCACTCTCCTTCATAACC
IFITM2	CAACGCCCAGCCCTTCT	CCCTGATACCCACGCCG	TCCTCCTTGAGCATCTCGTAGGT
IFITM3	GGGCCTCCTGCTGACCAT	CGTTCATCATCCTTTTTGTCA	CGGAATCATCAGCGATCCA

by limiting dilution. The FRL cells were given for this study by Tuck-Weng Kok, University of Adelaide (tuckweng.kok@adelaide.edu.au). FRL cells were cultured in Dulbecco's modified Eagle medium supplemented with 2 mM L-glutamine, 10 U/ml penicillin/streptomycin, nonessential amino acids (1×), 0.5 mM β-mercaptoethanol, HEPES, and 10% fetal calf serum (HI-FCS) (Gibco, Thermo Fisher Scientific, Missouri, USA).

Viruses. The influenza virus A/WSN/1933 (H1N1) used in this study was propagated by allantoic cavity inoculation of specific-pathogen-free (SPF) embryonated chicken eggs aged between embryonic days 9 and 11. The virus stock was titrated in chicken eggs, and the 50% egg infectious dose (EID_{50})/ml was calculated according to Reed and Muench (51).

Stimulation of FRL cells with IFN and virus. For stimulation assays, 0.5×10^6 cells/ml of FRL cells were plated into 24-well plates, and either 0.5 μg/ml of ferret IFN-α (generated in-house, CSIRO) or influenza virus (multiplicity of infection [MOI], 1) was added to the stimulation wells. Cells were harvested, and RNA was extracted at 2, 4, 8, 24, 48, and 72 h poststimulation using a RNeasyPlus kit (Qiagen, Hilden, Germany) as per the manufacturer's instructions.

3′ RACE PCR. Partial coding sequence for *IFITM2* was amplified using the 3′ RACE system for rapid amplification of cDNA ends kit (Thermo Fisher Scientific) as per the manufacturer's instructions. Briefly, cDNA was generated from ferret RNA with a dC-tail, and this cDNA was amplified using IFITM2 forward primer (5′-ATGAGCCACAACGCCCAG-3′) and the adaptor primer provided in the kit. These products were separated by gel electrophoresis and sequenced to obtain the full-length transcript.

Quantitative real-time PCR (qRT-PCR). PCR was performed using a StepOnePlus real-time PCR system and the comparative threshold cycle (C_T) method according to manufacturer's instructions (Applied Biosystems, Foster City, CA, USA). Relative gene expression was calculated using mean values obtained from $\Delta\Delta CT$. These C_T values were fitted to a theoretical standard curve equation, $n = 10^{(Ct-Cn)/-3.32}$, where n is the copy number, Ct is the C_T value obtained from the qPCR run, and Cn is the cycle number in the run procedure. For relative gene expression, copy numbers were expressed as copies/10^6 copies of GAPDH (i.e., $n_{(cytokine)}/n_{(GAPDH)} \times 1{,}000{,}000$). For fold change, $\Delta\Delta CT$ values for control samples were standardized to 1, and changes in cytokine levels were assessed as $\Delta\Delta CT_{(test\ sample)}/\Delta\Delta CT_{(control)}$. Primers for ferret GAPDH were obtained from sequences developed by Carolan et al. (52), and primers for ferret IFITMs were designed from sequences obtained in this study (Table 1).

Statistics. Time course data were analyzed by one-way analysis of variance (ANOVA), using a Tukey's multiple-comparison test to assess differences between each time point.

REFERENCES

1. Brass AL, Huang I-C, Benita Y, John SP, Krishnan MN, Feeley EM, Ryan BJ, Weyer JL, van der Weyden L, Fikrig E, Adams DJ, Xavier RJ, Farzan M, Elledge SJ. 2009. The IFITM proteins mediate cellular resistance to influenza A H1N1 virus, West Nile virus, and dengue virus. Cell 139:1243–1254. https://doi.org/10.1016/j.cell.2009.12.017.
2. Zhao X, Li J, Winkler CA, An P, Guo J-T. 2019. IFITM genes, variants, and their roles in the control and pathogenesis of viral infections. Front Microbiol 9:3228. https://doi.org/10.3389/fmicb.2018.03228.
3. Weston S, Czieso S, White IJ, Smith SE, Kellam P, Marsh M. 2014. A membrane topology model for human interferon inducible transmembrane protein 1. PLoS One 9:e104341. https://doi.org/10.1371/journal.pone.0104341.
4. Uhlen M, Fagerberg L, Hallstrom BM, Lindskog C, Oksvold P, Mardinoglu A, Sivertsson A, Kampf C, Sjostedt E, Asplund A, Olsson I, Edlund K, Lundberg E, Navani S, Szigyarto CA-K, Odeberg J, Djureinovic D, Takanen JO, Hober S, Alm T, Edqvist P-H, Berling H, Tegel H, Mulder J, Rockberg J, Nilsson P, Schwenk JM, Hamsten M, von Feilitzen K, Forsberg M, Persson L, Johansson F, Zwahlen M, von Heijne G, Nielsen J, Ponten F. 2015. Tissue-based map of the human proteome. Science 347:1260419. https://doi.org/10.1126/science.1260419.
5. Chan YK, Huang IC, Farzan M. 2012. IFITM proteins restrict antibody-dependent enhancement of dengue virus infection. PLoS One 7:e34508. https://doi.org/10.1371/journal.pone.0034508.
6. Yu M, Qi W, Huang Z, Zhang K, Ye J, Liu R, Wang H, Ma Y, Liao M, Ning Z. 2015. Expression profile and histological distribution of IFITM1 and IFITM3 during H9N2 avian influenza virus infection in BALB/c mice. Med Microbiol Immunol 204:505–514. https://doi.org/10.1007/s00430-014-0361-2.
7. Hanagata N, Li X. 2011. Osteoblast-enriched membrane protein IFITM5 regulates the association of CD9 with an FKBP11–CD81–FPRP complex and stimulates expression of interferon-induced genes. Biochem Biophys Res Commun 409:378–384. https://doi.org/10.1016/j.bbrc.2011.04.136.
8. Desai TM, Marin M, Chin CR, Savidis G, Brass AL, Melikyan GB. 2014. IFITM3 restricts influenza A virus entry by blocking the formation of fusion pores following virus-endosome hemifusion. PLoS Pathog 10:e1004048. https://doi.org/10.1371/journal.ppat.1004048.
9. Feeley EM, Sims JS, John SP, Chin CR, Pertel T, Chen L-M, Gaiha GD, Ryan BJ, Donis RO, Elledge SJ, Brass AL. 2011. IFITM3 inhibits influenza A virus infection by preventing cytosolic entry. PLoS Pathog 7:e1002337. https://doi.org/10.1371/journal.ppat.1002337.
10. Li K, Markosyan RM, Zheng Y-M, Golfetto O, Bungart B, Li M, Ding S, He Y, Liang C, Lee JC, Gratton E, Cohen FS, Liu S-L. 2013. IFITM proteins restrict viral membrane hemifusion. PLoS Pathog 9:e1003124. https://doi.org/10.1371/journal.ppat.1003124.
11. Amini-Bavil-Olyaee S, Choi YJ, Lee JH, Shi M, Huang I-C, Farzan M, Jung JU. 2013. The antiviral effector IFITM3 disrupts intracellular cholesterol homeostasis to block viral entry. Cell Host Microbe 13:452–464. https://doi.org/10.1016/j.chom.2013.03.006.
12. `Stacey MA, Clare S, Clement M, Marsden M, Abdul-Karim J, Kane L, Harcourt K, Brandt C, Fielding CA, Smith SE, Wash RS, Brias SG, Stack G, Notley G, Cambridge EL, Isherwood C, Speak AO, Johnson Z, Ferlin W, Jones SA, Kellam P, Humphreys IR. 2017. The antiviral restriction factor IFN-induced transmembrane protein 3 prevents cytokine-driven CMV pathogenesis. J Clin Invest 127:1463–1474. https://doi.org/10.1172/JCI84889.

13. Everitt AR, Clare S, Pertel T, John SP, Wash RS, Smith SE, Chin CR, Feeley EM, Sims JS, Adams DJ, Wise HM, Kane L, Goulding D, Digard P, Anttila V, Baillie JK, Walsh TS, Hume DA, Palotie A, Xue Y, Colonna V, Tyler-Smith C, Dunning J, Gordon SB, Smyth RL, Openshaw PJ, Dougan G, Brass AL, Kellam P, The GenISIS Investigators. 2012. IFITM3 restricts the morbidity and mortality associated with influenza. Nature 484:519–523. https://doi.org/10.1038/nature10921.
14. Londrigan SL, Wakim LM, Smith J, Haverkate AJ, Brooks AG, Reading PC. 2020. IFITM3 and type I interferons are important for the control of influenza A virus replication in murine macrophages. Virology 540:17–22. https://doi.org/10.1016/j.virol.2019.11.003.
15. Bailey CC, Huang IC, Kam C, Farzan M. 2012. Ifitm3 limits the severity of acute influenza in mice. PLoS Pathog 8:e1002909. https://doi.org/10.1371/journal.ppat.1002909.
16. Allen EK, Randolph AG, Bhangale T, Dogra P, Ohlson M, Oshansky CM, Zamora AE, Shannon JP, Finkelstein D, Dressen A, DeVincenzo J, Caniza M, Youngblood B, Rosenberger CM, Thomas PG. 2017. SNP-mediated disruption of CTCF binding at the IFITM3 promoter is associated with risk of severe influenza in humans. Nat Med 23:975–983. https://doi.org/10.1038/nm.4370.
17. Pan Y, Yang P, Dong T, Zhang Y, Shi W, Peng X, Cui S, Zhang D, Lu G, Liu Y, Wu S, Wang Q. 2017. IFITM3 Rs12252-C variant increases potential risk for severe influenza virus infection in Chinese population. Front Cell Infect Microbiol 7 https://doi.org/10.3389/fcimb.2017.00294.
18. Zhang Y-H, Zhao Y, Li N, Peng Y-C, Giannoulatou E, Jin R-H, Yan H-P, Wu H, Liu J-H, Liu N, Wang D-Y, Shu Y-L, Ho L-P, Kellam P, McMichael A, Dong T. 2013. Interferon-induced transmembrane protein-3 genetic variant rs12252-C is associated with severe influenza in Chinese individuals. Nat Commun 4:1418. https://doi.org/10.1038/ncomms2433.
19. Hornick AL, Li N, Oakland M, McCray PB Jr, Sinn PL. 2016. Human, pig, and mouse interferon-induced transmembrane proteins partially restrict pseudotyped lentiviral vectors. Hum Gene Ther 27:354–362. https://doi.org/10.1089/hum.2015.156.
20. Benfield CTO, Smith SE, Wright E, Wash RS, Ferrara F, Temperton NJ, Kellam P. 2015. Bat and pig IFN-induced transmembrane protein 3 restrict cell entry by influenza virus and lyssaviruses. J Gen Virol 96:991–1005. https://doi.org/10.1099/vir.0.000058.
21. Hickford D, Frankenberg S, Shaw G, Renfree MB. 2012. Evolution of vertebrate interferon inducible transmembrane proteins. BMC Genomics 13:155. https://doi.org/10.1186/1471-2164-13-155.
22. Smith SE, Gibson MS, Wash RS, Ferrara F, Wright E, Temperton N, Kellam P, Fife M. 2013. Chicken interferon-inducible transmembrane protein 3 restricts influenza viruses and lyssaviruses in vitro. J Virol 87:12957–-12966. https://doi.org/10.1128/JVI.01443-13.
23. Wang A, Sun L, Wang M, Jia R, Zhu D, Liu M, Sun K, Yang Q, Wu Y, Chen X, Cheng A, Chen S. 2017. Identification of IFITM1 and IFITM3 in goose: gene structure, expression patterns, and immune reponses against Tembusu virus infection. J BioMed Res International 2017:1–13. https://doi.org/10.1155/2017/5149062.
24. Blyth GAD, Chan WF, Webster RG, Magor KE. 2016. Duck interferon-inducible transmembrane protein 3 mediates restriction of influenza viruses. J Virol 90:103–116. https://doi.org/10.1128/JVI.01593-15.
25. Belser JA, Katz JM, Tumpey TM. 2011. The ferret as a model organism to study influenza A virus infection. Dis Model Mech 4:575–579. https://doi.org/10.1242/dmm.007823.
26. Leon AJ, Banner D, Xu L, Ran L, Peng Z, Yi K, Chen C, Xu F, Huang J, Zhao Z, Lin Z, Huang SHS, Fang Y, Kelvin AA, Ross TM, Farooqui A, Kelvin DJ. 2013. Sequencing, annotation, and characterization of the influenza ferret infectome. J Virol 87:1957–1966. https://doi.org/10.1128/JVI.02476-12.
27. Yates AD, Achuthan P, Akanni W, Allen J, Allen J, Alvarez-Jarreta J, Amode MR, Armean IM, Azov AG, Bennett R, Bhai J, Billis K, Boddu S, Marugán JC, Cummins C, Davidson C, Dodiya K, Fatima R, Gall A, Giron CG, Gil L, Grego T, Haggerty L, Haskell E, Hourlier T, Izuogu OG, Janacek SH, Juettemann T, Kay M, Lavidas I, Le T, Lemos D, Martinez JG, Maurel T, McDowall M, McMahon A, Mohanan S, Moore B, Nuhn M, Oheh DN, Parker A, Parton A, Patricio M, Sakthivel MP, Abdul Salam AI, Schmitt BM, Schuilenburg H, Sheppard D, Sycheva M, et al. 2020. Ensembl 2020. Nucleic Acids Res 48:D682–D688. https://doi.org/10.1093/nar/gkz966.
28. Burge C, Karlin S. 1997. Prediction of complete gene structures in human genomic DNA. J Mol Biol 268:78–94. https://doi.org/10.1006/jmbi.1997.0951.
29. Kumar S, Stecher G, Tamura K. 2016. MEGA7: Molecular Evolutionary Genetics Analysis Version 7.0 for bigger datasets. Mol Biol Evol 33:1870–1874. https://doi.org/10.1093/molbev/msw054.
30. Jones DT, Taylor WR, Thornton JM. 1992. The rapid generation of mutation data matrices from protein sequences. Comput Appl Biosci 8:275–282. https://doi.org/10.1093/bioinformatics/8.3.275.
31. Käll L, Krogh A, Sonnhammer ELL. 2004. A combined transmembrane topology and signal peptide prediction method. J Mol Biol 338:1027–1036. https://doi.org/10.1016/j.jmb.2004.03.016.
32. Kelley LA, Mezulis S, Yates CM, Wass MN, Sternberg MJE. 2015. The Phyre2 Web portal for protein modeling, prediction and analysis. Nat Protoc 10:845–858. https://doi.org/10.1038/nprot.2015.053.
33. Thul PJ, Åkesson L, Wiking M, Mahdessian D, Geladaki A, Ait Blal H, Alm T, Asplund A, Björk L, Breckels LM, Bäckström A, Danielsson F, Fagerberg L, Fall J, Gatto L, Gnann C, Hober S, Hjelmare M, Johansson F, Lee S, Lindskog C, Mulder J, Mulvey CM, Nilsson P, Oksvold P, Rockberg J, Schutten R, Schwenk JM, Sivertsson Å, Sjöstedt E, Skogs M, Stadler C, Sullivan DP, Tegel H, Winsnes C, Zhang C, Zwahlen M, Mardinoglu A, Pontén F, von Feilitzen K, Lilley KS, Uhlén M, Lundberg E. 2017. A subcellular map of the human proteome. Science 356:eaal3321. https://doi.org/10.1126/science.aal3321.
34. Pontén F, Jirström K, Uhlen M. 2008. The Human Protein Atlas: a tool for pathology. J Pathol 216:387–393. https://doi.org/10.1002/path.2440.
35. van Riel D, Munster VJ, de Wit E, Rimmelzwaan GF, Fouchier RAM, Osterhaus ADME, Kuiken T. 2007. Human and avian influenza viruses target different cells in the lower respiratory tract of humans and other mammals. Am J Path 171:1215–1223. https://doi.org/10.2353/ajpath.2007.070248.
36. Sweet C, Price GE, Fenton RJ. 1999. The ferret as an animal model of influenza virus infection, p 989–998. In Zak O, Sande MA (ed), Handbook of animal models of infection. Academic Press, London, UK.
37. Music N, Reber AJ, Kim JH, York IA. 2016. Peripheral leukocyte migration in ferrets in response to infection with seasonal influenza virus. PLoS One 11:e0157903. https://doi.org/10.1371/journal.pone.0157903.
38. DiPiazza A, Richards K, Batarse F, Lockard L, Zeng H, García-Sastre A, Albrecht RA, Sant AJ. 2016. Flow cytometric and cytokine ELISpot approaches to characterize the cell-mediated immune response in ferrets following influenza virus infection. J Virol 90:7991–8004. https://doi.org/10.1128/JVI.01001-16.
39. Ryan KA, Slack GS, Marriott AC, Kane JA, Whittaker CJ, Silman NJ, Carroll MW, Gooch KE. 2018. Cellular immune response to human influenza viruses differs between H1N1 and H3N2 subtypes in the ferret lung. PLoS One 13:e0202675. https://doi.org/10.1371/journal.pone.0202675.
40. Cameron CM, Cameron MJ, Bermejo-Martin JF, Ran L, Xu L, Turner PV, Ran R, Danesh A, Fang Y, Chan P-KM, Mytle N, Sullivan TJ, Collins TL, Johnson MG, Medina JC, Rowe T, Kelvin DJ. 2008. Gene expression analysis of host innate immune responses during lethal H5N1 infection in ferrets. J Virol 82:11308–11317. https://doi.org/10.1128/JVI.00691-08.
41. Carolan LA, Rockman S, Borg K, Guarnaccia T, Reading P, Mosse J, Kelso A, Barr I, Laurie KL. 2016. Characterization of the localized immune response in the respiratory tract of ferrets following infection with influenza A and B viruses. J Virol 90:2838–2848. https://doi.org/10.1128/JVI.02797-15.
42. Wang Z, Zhang A, Wan Y, Liu X, Qiu C, Xi X, Ren Y, Wang J, Dong Y, Bao M, Li L, Zhou M, Yuan S, Sun J, Zhu Z, Chen L, Li Q, Zhang Z, Zhang X, Lu S, Doherty PC, Kedzierska K, Xu J. 2014. Early hypercytokinemia is associated with interferon-induced transmembrane protein-3 dysfunction and predictive of fatal H7N9 infection. Proc Natl Acad Sci U S A 111:769–774. https://doi.org/10.1073/pnas.1321748111.
43. Siegrist F, Ebeling M, Certa U. 2011. The small interferon-induced transmembrane genes and proteins. J Interferon Cytokine Res 31:183–197. https://doi.org/10.1089/jir.2010.0112.
44. Hach JC, McMichael T, Chesarino NM, Yount JS. 2013. Palmitoylation on conserved and nonconserved cysteines of murine IFITM1 regulates its stability and anti-influenza A virus activity. J Virol 87:9923–9927. https://doi.org/10.1128/JVI.00621-13.
45. Kenney AD, McMichael TM, Imas A, Chesarino NM, Zhang L, Dorn LE, Wu Q, Alfaour O, Amari F, Chen M, Zani A, Chemudupati M, Accornero F, Coppola V, Rajaram MVS, Yount JS. 2019. IFITM3 protects the heart during influenza virus infection. Proc Natl Acad Sci U S A 116:18607–18612. https://doi.org/10.1073/pnas.1900784116.
46. Larner AC, Chaudhuri A, Darnell JE Jr. 1986. Transcriptional induction by interferon. New protein(s) determine the extent and length of the induction. J Biol Chem 261:453–459. https://doi.org/10.1016/S0021-9258(17)42492-6.
47. Savidis G, Perreira JM, Portmann JM, Meraner P, Guo Z, Green S, Brass AL. 2016. The IFITMs inhibit Zika virus replication. Cell Rep 15:2323–2330. https://doi.org/10.1016/j.celrep.2016.05.074.
48. Huang I-C, Bailey CC, Weyer JL, Radoshitzky SR, Becker MM, Chiang JJ, Brass AL, Ahmed AA, Chi X, Dong L, Longobardi LE, Boltz D, Kuhn JH,

Elledge SJ, Bavari S, Denison MR, Choe H, Farzan M. 2011. Distinct patterns of IFITM-mediated restriction of filoviruses, SARS coronavirus, and influenza A virus. PLoS Pathog 7:e1001258. https://doi.org/10.1371/journal.ppat.1001258.
49. Lei N, Li Y, Sun Q, Lu J, Zhou J, Li Z, Liu L, Guo J, Qin K, Wang H, Zhao J, Li C, Sun L, Wang D, Zhao Z, Shu Y. 2020. IFITM3 affects the level of antibody response after influenza vaccination. Emerg Microbes Infect 9:976–987. https://doi.org/10.1080/22221751.2020.1756696.
50. Gerlach T, Hensen L, Matrosovich T, Bergmann J, Winkler M, Peteranderl C, Klenk H-D, Weber F, Herold S, Pöhlmann S, Matrosovich M. 2017. pH optimum of hemagglutinin-mediated membrane fusion determines sensitivity of influenza A viruses to the interferon-induced antiviral state and IFITMs. J Virol 91:e00246-17. https://doi.org/10.1128/JVI.00246-17.
51. Reed LJ, Muench H. 1938. A simple method of estimating fifty per cent endpoints. Am J Epidemiol 27:493–497. https://doi.org/10.1093/oxfordjournals.aje.a118408.
52. Carolan LA, Butler J, Rockman S, Guarnaccia T, Hurt AC, Reading P, Kelso A, Barr I, Laurie KL. 2014. TaqMan real time RT-PCR assays for detecting ferret innate and adaptive immune responses. J Virological Methods 205:38–52. https://doi.org/10.1016/j.jviromet.2014.04.014.

Chapter 6: Concluding Remarks

The ferret has been used as an animal model for investigating human respiratory diseases since the 1930s, with several distinct advantages over other animal models (346). Despite being more difficult to manipulate and house compared to mice due to their size and temperament, ferrets display more comparable clinical signs to humans following influenza virus infection such as fever, sneezing and nasal discharge, whereas these symptoms are not observed in mice (346-349). Moreover, ferrets can be infected with naturally occurring viral isolates from humans whereas mice often require the viruses to be adapted, and ferrets can also readily transmit virus between animals (346, 350, 351). Thus, ferrets are an incredibly powerful tool for studying pathogenesis and transmission of novel and zoonotic respiratory viruses which threaten human health (93, 145, 348, 352). However, there is still a paucity of data surrounding the immune responses in ferrets, and thus to improve the model for future studies, more detailed analyses of how ferret immune cell subsets traffic and counteract viral infection is required. The work presented in this PhD thesis aims to further our understanding of the ferret model and how it can be used to assess the mammalian immune response to high consequence respiratory viruses, as well as guide vaccination development to assist in overcoming the pandemic threat that these viruses bring.

The work presented in Chapter 3 (published in *Frontiers in Immunology*, 2020) aimed to gain a greater understanding of the immune cell dynamics of the ferret in the context of an avian influenza virus infection, in this instance A/Anhui/1/2013(H7N9) virus. To achieve this, a cohort of ferrets was infected with the H7N9 virus and examined across a seven-day time period, and clinical data such as weight, temperature and blood data were taken every second day. Following humane euthanasia, tissues were harvested, and immune cell subsets were analysed by flow cytometric analysis to assess how ferret lymphocytes traffic in response to the infection. This study demonstrated that the LPAI H7N9 virus could cause variable disease outcome, as one ferret showed far worsened disease progression compared to the others in

the cohort. Variability in disease outcome has previously been reported for other H7N9 strains (401), but not for this human-infecting strain which typically only causes mild clinical signs in the ferret model (37, 54, 93), as well as in outbred mice (402). Despite this, the outbred nature of these animals may still be a factor, as several genetic factors such as IFITM and MHC mutations have been correlated with worsened disease outcomes in humans (310, 336). Indeed, A/Anhui/1/2013(H7N9) infected humans have shown a variety of outcomes such as those observed in this study, though little is known as to the true cause or causes for the worsened disease outcome seen in humans.

This worsened disease progression correlated with a lack of viral clearance and lower HI titres, which was evident in the histopathological findings where the ferrets euthanised at earlier timepoints had more severe lung pathology and virus evident in the nasal passage. A novel finding in this study was the time dependent decrease in two pro-inflammatory cytokines in the blood of the severely affected ferret, with IFNγ and IL-6 transcript levels showing stark decreases compared to the other ferrets at the day 5 timepoints, a surprising observation given worsened disease is usually correlated to increases in these cytokines (354). Thus, this study provides further insight into the complex nature of AIV pathology, showing a variable disease correlate to previous work which has often had a focus on drastic increases in cytokines through hypercytokinemia.

This study further aimed to classify immune cell subsets which may have influenced disease outcomes. For AI viruses, worsened disease progression is often associated with a loss in T cells populations, with marked declines in both mice and chickens following HPAI infections with H5 subtype viruses (375, 403). Whilst this trend is less commonly observed in LPAI, human cases of H7N9 with severe outcomes also see decreases in T cell numbers (404). However, the ferrets in this cohort did not exhibit any notable decline in T cells other than an initial drop at day 1 post infection for $CD8^+$ T cells, which is consistent with the transient lymphopenia observed in the ferret model for seasonal influenza strains (361), suggesting that our study has been able to show that low-pathogenicity AIV have similar cytotoxic T

lymphocyte kinetics to more commonly-used strains, giving us confidence in the model for immune cell analysis. $CD4^+$ T cells were also found to be significantly higher in the spleen and lungs of the infected ferrets, whilst a trend towards higher $CD8^+$ T cells in the lungs was suggestive of an active T cell immune response occurring at the site of infection.

While T cell subsets have previously been investigated in ferrets in a seasonal infection context (359), there has been very few studies that have looked into APCs in this model, despite APCs being recognized as highly important innate cells in the pro-inflammatory response against AI viruses in the mouse model (405). This study is the first to assess APC migration and dynamics in the ferret model, focussing on $CD11b^+$ and MHC-II^+ cells. Double-positive cells ($CD11b^+$MHC-II^+) were generally higher in the tissues of infected animals, and as such we termed these cells to be a more "mature" or "activated" phenotype based on studies in the ferret (361) and in the mouse (175), whilst suggesting the $CD11b^+$MHC-II^- cells to be more "immature" myeloid cells rather than granulocytes due to the lack of a pro-inflammatory response in these tissues (172). As such, it appeared that the timing of the innate immune response was also important, as the ferrets euthanised at earlier timepoints had a more "immature" phenotype compared to those ferrets which lasted the full seven days. Those ferrets which lasted the full trial without clinical signs showed less $CD11b^+$MHC-II^- cells in the spleen and more $CD11b^+$MHC-II^+ cells in the lymph node, suggesting of an active phenotype wherein activated cells migrate to the lymph node, and less activated cells remain in the spleen. The results of this analysis provide a novel interrogation of ferret APCs, giving an insight into their activation pathways and how they traffic following activation during viral infection. Given the limited antibodies available for use in the ferret model, these results give a framework for future work to assess APCs to emerging respiratory viruses, an area greatly lacking in the ferret context, and therefore more closely align our understanding of these cells to what occurs during human infections Thus, this study provided new insights into the way immune cells traffic in the ferret, in the first in-depth analysis of these cells in the context of an AIV infection, and build on the very limited knowledge we have of staining for and assessing

ferret immune cells. Furthermore, assessment of these cells under PC3 conditions will provide a guide to future studies looking to assess the ferret cellular immune response to emerging respiratory viruses of high human consequence.

Based on the establishment of investigating immune responses in an AIV ferret model (Chapter 3), Chapter 4 assessed the ferret immune response to the novel SARS-CoV-2 and one of its vaccine candidates, the ChAdOx1-nCoV-2019 vaccine developed by AstraZeneca on The Jenner Institute's adenovirus vaccine platform. This study involved ten times more ferrets than the H7N9 study, allowing for greater statistical power across multiple ferret cohorts. Furthermore, the trial had great implications in assessing the immune response generated by the ChAdOx1-nCoV-2019 vaccine, and whether a single dose or a prime-boost regime was more effective at protecting against SARS-CoV-2. The first major finding of this study was that a prime-boost vaccination regime produced greater protective immune responses against SARS-CoV-2 infection, as the two doses elicited a greater Ig response in the blood when assessed by FACS analysis, suggesting that a prime/boost regime would be the best way forward for vaccination rollouts to elicit a strong antibody response. Furthermore, an intramuscular injection produced a significant increase in MHC-II$^+$ cells, suggesting that two doses of ChAdOx1-nCoV-2019 vaccine injected into the muscle provides the greatest neutralising antibody response in the circulation. Activated B cells were also present in higher levels in the draining lymph node of prime-boost ferrets inoculated intranasally, suggesting that while both inoculation routes effectively induce a B cell response, the intranasal method may elicit a greater antigen-specific response in the draining lymph node as is commonly seen in other vaccine models (406), providing another challenge for rational vaccine design given the strong prevalence and preference for intramuscular vaccination.

While inducing a protective humoral response against viral infection is a critical function of vaccinations, in recent years there has been an increasing focus on how vaccines can also elicit a T cell response to combine both aspects of the adaptive immune response for greater overall protection (407, 408). This is particularly the case for SARS-CoV-2 vaccination

strategies, considering that T cells have been shown in multiple studies to be key mediators of protective immunity against coronaviruses (408-411). The work conducted in this Chapter showed that prime-boost vaccination induced a greater $CD8^+$ T cell response in the circulation, an important finding given dampened $CD8^+$ T cell responses have been linked to worsened disease outcomes in severe COVID-19 cases (388, 389, 412). Supported by the ELISpot data showing increases in IFNγ-producing cells, the prime-boost strategy appears to elicit a Th1 type immune response similar to that seen in other animal models assessing this vaccine (149), and is an important finding given $CD8^+$ T cell depletion and Th2 response skewing has been associated with severe disease outcome in SARS-CoV patients (413). APC data also supports the idea of a Th1 response being produced as $CD14^+CD11b^+$ cells were also found in higher proportions in the circulation of prime-boost ferrets, with these speculated to be monocytes or dendritic cells which have previously been shown to be pro-inflammatory modulators of Th1 immunity in a CpG adjuvanted protein vaccine model in the murine system (391). Given the increased focus on vaccines eliciting Th1 immunity (400, 414, 415), these data indicate that the prime/boost vaccination regime is providing not only a strong humoral response, but the desired T lymphocyte activation and action required for effective viral immunity.

This ferret study increased our knowledge of the ferret immune response to respiratory viruses and their vaccine candidates, providing a wealth of data surrounding immune cell trafficking on a scale not previously seen in this model. Furthermore, the study provided critical insight into how prime-boost vaccination regimes can be used to successfully induce a protective immune response against SARS-CoV-2. The data from this trial suggests that two intramuscular injections of the ChAdOx1-nCoV-2019 vaccine is sufficient to elicit both a strong neutralizing antibody response and a $CD8^+$ T cell response, and thus for the vaccine rollout of ChAdOx1-nCov-2019 giving two doses rather than one will be critical for inducing sufficient protection. While this vaccine shows sufficient immunogenicity and protection against SARS-CoV-2, incidences of thrombosis with thrombocytopenia syndrome (TSS) marked by blood clots

causing serious vaccine side effects and mortality have negatively swayed public perceptions about this vaccine, and lead to the vaccine to not be recommended to Australians under the age of 60 due to an increased risk of developing TSS despite the very low incidence rates (416, 417). Given the issues both medically and from a public perspective surrounding this technology, as well as the low incident rates making investigation into TTS in the ferret model almost impossible, future pandemic responses may opt against using this adenoviral vector technology, though a 'mix-and-match' strategy may be able to mitigate some of the risk. Indeed, one study suggests that using a heterologous vaccine strategy of ChAdOx1-nCOv-2 followed by a dose of the Pfizer BNT162b2 mRNA vaccine induced comparably strong immune responses to a homologous approach of either ChAdOx1-nCov-2019 or BNT162b2, suggesting that this may be a strategy to use in future to maximise the effectiveness of vaccine candidates (418). Regardless, this study may assist in guiding the vaccination rollout of one of the leading vaccine candidates to assist in curbing the influence of the ongoing COVID-19 pandemic. A manuscript draft is currently in preparation for this body of work.

To further delve into the ferret immunobiology, Chapter 5 (published in *Journal of Virology*, 2021) aimed to define the IFITM gene family in the ferret. Given the anti-viral properties of IFITMs in preventing respiratory virus infections (340, 419, 420) (Chapter 1 section 10, published as a review in *Frontiers in Immunology,* 2018*)*, the lack of information regarding IFITMs in the gold-standard ferret model for human respiratory virus disease was concerning. The fact that mutations in these genes can confer greater risk to respiratory viruses (330, 421) suggested that this was a key immune gene that required classification in this model. The IFITM locus was found in the ferret genome through the already identified common flanking genes *PGGHG* and *B4GALNT4*, as well as a proposed coding sequence for *IFITM5*. Within this genomic region, three novel coding regions were identified based on *in silico* analysis, with putative coding sequences representing *IFITM1* and *IFITM3*, and a newly identified sequence confirmed by 3' RACE PCR to be that of ferret *IFITM2*. Sequence analysis at both a nucleotide and amino acid level confirmed these genes as homologues to IFITMs seen in other species, whilst conserved transmembrane boundaries suggest a high level of

conservation amongst IFITM proteins. A set of novel qPCR assays were then developed to assess how these transcripts were expressed, and these assays were able to confirm that the *IFITM* transcripts identified were upregulated in the presence of both IFNα and influenza virus, confirming the identity of these genes as the suspected interferon-stimulated genes.

Further work will be undertaken to assess whether, in conjunction to their interferon-stimulated gene (ISG) properties, these novel *IFITM* genes exhibited anti-viral properties. Preliminary studies (beyond the scope of PhD thesis) have generated a CRISPR-Cas9 system to selectively disrupt the *IFITM* genes of ferret cells using sgRNAs designed specifically for each gene to generate knockout (KO) cell lines. Future directions will be to analyze these KO cell lines via PCR and Inference of CRISPR edits (422), as well as stimulating these KO cells with influenza virus to check for greater infectivity. These data provide a framework for not only future studies into ferret IFITMs, but ferret immune genes as a whole, with this investigation being one of the first in-depth analyses of a ferret anti-viral gene family conducted in the literature. The design of the sgRNAs is crucial to successfully producing a KO cell line, which needs to be verified at the protein level in future studies.

Overall, this PhD thesis provides novel insights into the ferret model of human respiratory disease and the immune responses occurring in the ferret against emerging respiratory pathogens. Investigations of the immune cell dynamics occurring in the ferret following H7N9 avian influenza virus infection resulted in an increased knowledge of the trafficking of lymphocytes, and particularly APCs, thereby providing the first in-depth study of the immunology of avian influenza viruses in ferrets. The work conducted in this initial study allowed for a transition into a larger-scale SARS-CoV-2 study, with these techniques used in a trial assessing the efficacy of the ChAdOx1-nCoV-2019 in the ferret model. This study used the antibody panel developed in the H7N9 study to show that a prime-boost vaccination regime elicits the strongest protective immune response against SARS-CoV-2 for both humoral and T cell mediated immunity, results which helped to guide the vaccination scheme for use at a population level to vaccinate against the pandemic virus. These studies provide new and

unique immunological insights into how the ferret model can be used in the future, whilst classification of ferret IFITM genes adds another piece of information to better understand this vitally important animal model. This PhD thesis gives critically needed new insights into this model and how it can be used for studying respiratory viruses, which is of huge importance given their ability to spread rapidly and cause severe human disease.

References

1. Shi T, Arnott A, Semogas I, Falsey AR, Openshaw P, Wedzicha JA, et al. The Etiological Role of Common Respiratory Viruses in Acute Respiratory Infections in Older Adults: A Systematic Review and Meta-analysis. J Infect Dis. 2020;222(Supplement_7):S563-s9.
2. Ruuskanen O, Lahti E, Jennings LC, Murdoch DR. Viral pneumonia. Lancet (London, England). 2011;377(9773):1264-75.
3. Australian Institute of Health & Welfare. Disease expenditure in Australia. Canberra: AIHW; 2019.
4. Trucchi C, Paganino C, Orsi A, Amicizia D, Tisa V, Piazza MF, et al. Hospital and economic burden of influenza-like illness and lower respiratory tract infection in adults ≥50 years-old. BMC Health Services Research. 2019;19(1):585.
5. Bouvier NM, Palese P. The biology of influenza viruses. Vaccine. 2008;26 Suppl 4(Suppl 4):D49-53.
6. World Health Organization. Influenza at the human-animal interface: Summary and assessment, 13 February to 9 April 2019: World Health Organisation; 2019 [Available from: https://www.who.int/influenza/human_animal_interface/Influenza_Summary_IRA_HA_interface_09_04_2019.pdf.
7. Troeger C, Blacker B, Khalil IA, Rao PC, Cao J, Zimsen SRM, et al. Estimates of the global, regional, and national morbidity, mortality, and aetiologies of lower respiratory infections in 195 countries, 1990–2016: a systematic analysis for the Global Burden of Disease Study 2016. The Lancet Infectious Diseases. 2018;18(11):1191-210.
8. Paget J, Spreeuwenberg P, Charu V, Taylor RJ, Iuliano AD, Bresee J, et al. Global mortality associated with seasonal influenza epidemics: New burden estimates and predictors from the GLaMOR Project. J Glob Health. 2019;9(2):020421-.
9. Troeger CE, Blacker BF, Khalil IA, Zimsen SRM, Albertson SB, Abate D, et al. Mortality, morbidity, and hospitalisations due to influenza lower respiratory tract infections, 2017: an analysis for the Global Burden of Disease Study 2017. The Lancet Respiratory Medicine. 2019;7(1):69-89.
10. World Health Organization. Weekly epidemiological update - 12 January 2021: World Health Organisation; 2021 [Available from: https://www.who.int/publications/m/item/weekly-epidemiological-update---12-january-2021.
11. Krammer F, Smith GJD, Fouchier RAM, Peiris M, Kedzierska K, Doherty PC, et al. Influenza. Nat Rev Dis Primers. 2018;4(1):3-.
12. Matsuzaki Y, Katsushima N, Nagai Y, Shoji M, Itagaki T, Sakamoto M, et al. Clinical Features of Influenza C Virus Infection in Children. J Infect Dis. 2006;193(9):1229-35.
13. Matsuzaki Y, Sugawara K, Mizuta K, Tsuchiya E, Muraki Y, Hongo S, et al. Antigenic and Genetic Characterization of Influenza C Viruses Which Caused Two Outbreaks in Yamagata City, Japan, in 1996 and 1998. Journal of Clinical Microbiology. 2002;40(2):422.
14. Su S, Fu X, Li G, Kerlin F, Veit M. Novel Influenza D virus: Epidemiology, pathology, evolution and biological characteristics. Virulence. 2017;8(8):1580-91.
15. Luo J, Ferguson L, Smith DR, Woolums AR, Epperson WB, Wan XF. Serological evidence for high prevalence of Influenza D Viruses in Cattle, Nebraska, United States, 2003-2004. Virology. 2017;501:88-91.
16. White SK, Ma W, McDaniel CJ, Gray GC, Lednicky JA. Serologic evidence of exposure to influenza D virus among persons with occupational contact with cattle. Journal of clinical virology : the official publication of the Pan American Society for Clinical Virology. 2016;81:31-3.
17. World Health Organization. A revision of the system of nomenclature for influenza viruses: a WHO memorandum. Bulletin of the World Health Organization. 1980;58(4):585-91.

18. Guo YJ, Xu XY, Cox NJ. Human influenza A (H1N2) viruses isolated from China. J Gen Virol. 1992;73 (Pt 2):383-7.
19. Kolosova NP, Ilyicheva TN, Danilenko AV, Svyatchenko SV, Goncharova NI, Bulanovich JA, et al. Severe cases of seasonal influenza and detection of seasonal A(H1N2) in Russia in 2018-2019. Archives of virology. 2020;165(9):2045-51.
20. Butt KM, Smith GJD, Chen H, Zhang LJ, Leung YHC, Xu KM, et al. Human Infection with an Avian H9N2 Influenza A Virus in Hong Kong in 2003. Journal of Clinical Microbiology. 2005;43(11):5760-7.
21. To K-F, Chan PKS, Chan K-F, Lee W-K, Lam W-Y, Wong K-F, et al. Pathology of Fatal Human Infection Associated With Avian Influenza A H5N1 Virus. Journal of Medical Virology. 2001;63:242-6.
22. Gao R, Cao B, Hu Y, Feng Z, Wang D, Hu W, et al. Human infection with a novel avian-origin influenza A (H7N9) virus. The New England Journal of Medicine. 2013;368(20):1888-97.
23. Rota PA, Wallis TR, Harmon MW, Rota JS, Kendal AP, Nerome K. Cocirculation of two distinct evolutionary lineages of influenza type B virus since 1983. Virology. 1990;175(1):59-68.
24. Kanegae Y, Sugita S, Endo A, Ishida M, Senya S, Osako K, et al. Evolutionary pattern of the hemagglutinin gene of influenza B viruses isolated in Japan: cocirculating lineages in the same epidemic season. J Virol. 1990;64(6):2860-5.
25. Cowling BJ, Ip DKM, Fang VJ, Suntarattiwong P, Olsen SJ, Levy J, et al. Aerosol transmission is an important mode of influenza A virus spread. Nature communications. 2013;4:1935-.
26. Altman MO, Angeletti D, Yewdell JW. Antibody Immunodominance: The Key to Understanding Influenza Virus Antigenic Drift. Viral immunology. 2018;31(2):142-9.
27. Houser K, Subbarao K. Influenza vaccines: challenges and solutions. Cell Host Microbe. 2015;17(3):295-300.
28. Grohskopf LA, Olsen SJ, Sokolow LZ, Bresee JS, Cox NJ, Broder KR, et al. Prevention and control of seasonal influenza with vaccines: recommendations of the Advisory Committee on Immunization Practices (ACIP) -- United States, 2014-15 influenza season. MMWR Morbidity and mortality weekly report. 2014;63(32):691-7.
29. Milne GJ, Halder N, Kelso JK, Barr IG, Moyes J, Kahn K, et al. Trivalent and quadrivalent influenza vaccination effectiveness in Australia and South Africa: results from a modelling study. Influenza and other respiratory viruses. 2016;10(4):324-32.
30. Qu Y, Zhang R, Cui P, Song G, Duan Z, Lei F. Evolutionary genomics of the pandemic 2009 H1N1 influenza viruses (pH1N 1v). Virol J. 2011;8:250.
31. Smith GJ, Vijaykrishna D, Bahl J, Lycett SJ, Worobey M, Pybus OG, et al. Origins and evolutionary genomics of the 2009 swine-origin H1N1 influenza A epidemic. Nature. 2009;459(7250):1122-5.
32. Mena I, Nelson MI, Quezada-Monroy F, Dutta J, Cortes-Fernández R, Lara-Puente JH, et al. Origins of the 2009 H1N1 influenza pandemic in swine in Mexico. eLife. 2016;5.
33. Simonsen L, Spreeuwenberg P, Lustig R, Taylor RJ, Fleming DM, Kroneman M, et al. Global mortality estimates for the 2009 Influenza Pandemic from the GLaMOR project: a modeling study. PLoS Med. 2013;10(11):e1001558-e.
34. Kilbourne ED. Influenza pandemics of the 20th century. Emerg Infect Dis. 2006;12(1):9-14.
35. Centers for Disease Control and Prevention (CDC). Isolation of avian influenza A(H5N1) viruses from humans--Hong Kong, May-December 1997. MMWR Morbidity and mortality weekly report. 1997;46(50):1204-7.
36. Lycett SJ, Duchatel F, Digard P. A brief history of bird flu. Philos Trans R Soc Lond B Biol Sci. 2019;374(1775):20180257-.
37. Watanabe T, Kiso M, Fukuyama S, Nakajima N, Imai M, Yamada S, et al. Characterization of H7N9 influenza A viruses isolated from humans. Nature. 2013;501:551.

38. Claas ECJ, Osterhaus ADME, van Beek R, De Jong JC, Rimmelzwaan GF, Senne DA, et al. Human influenza A H5N1 virus related to a highly pathogenic avian influenza virus. The Lancet. 1998;351(472-477).
39. Hutchinson EC, von Kirchbach JC, Gog JR, Digard P. Genome packaging in influenza A virus. 2010;91(2):313-28.
40. Dou D, Revol R, Östbye H, Wang H, Daniels R. Influenza A Virus Cell Entry, Replication, Virion Assembly and Movement. Front Immunol. 2018;9:1581-.
41. Ayllon J, García-Sastre A. The NS1 protein: a multitasking virulence factor. Current topics in microbiology and immunology. 2015;386:73-107.
42. Ehrhardt C, Seyer R, Hrincius ER, Eierhoff T, Wolff T, Ludwig S. Interplay between influenza A virus and the innate immune signalling. Microbes and Infection. 2010;12:81-7.
43. Puranik A, Slomka MJ, Warren CJ, Thomas SS, Mahmood S, Byrne AMP, et al. Transmission dynamics between infected waterfowl and terrestrial poultry: Differences between the transmission and tropism of H5N8 highly pathogenic avian influenza virus (clade 2.3.4.4a) among ducks, chickens and turkeys. Virology. 2020;541:113-23.
44. Tong S, Zhu X, Li Y, Shi M, Zhang J, Bourgeois M, et al. New World Bats Harbor Diverse Influenza A Viruses. PloS Pathogens. 2013;9(10).
45. Xing Z, Cardona CJ, Li J, Dao N, Tran T, Andrada J. Modulation of the immune response in chickens by low-pathogenicity avian influenza virus H9N2. Journal of General Virology. 2008;89(5):1288-99.
46. Daoust P-Y, Kibenge FSB, Fouchier RAM, van de Bildt MWG, van Riel D, Kuiken T. Replication of Low Pathogenic Avian Influenza Virus in Naturally Infected Mallard Ducks (Anas Platyrhynchos) Causes No Morphologic Lesions. Journal of Wildlife Diseases. 2011;42(2):401-9.
47. Alexander DJ. An overview of the epidemiology of avian influenza. Vaccine. 2007;25:5637-44.
48. Du Y, Chen M, Yang J, Jia Y, Han S, Holmes EC, et al. Molecular Evolution and Emergence of H5N6 Avian Influenza Virus in Central China. Journal of Virology. 2017.
49. Visperas E, Simeon LM. First bird flu outbreak: 400,00 to be culled. The Philippine Star. 2017.
50. World Health Organization. Cumulative number of confirmed human cases for avian influenza A(H5N1) reported to WHO, 2003-2017: World Health Organization; 2017 [Available from: http://www.who.int/influenza/human_animal_interface/2017_10_30_tableH5N1.pdf?ua=1.
51. Lai S, Qin Y, Cowling BJ, Ren X, Wardrop NA, Gilbert M, et al. Global epidemiology of avian influenza A H5N1 virus infection in humans, 1997-2015: a systematic review of individual case data. The Lancet Infectious Diseases. 2016;16:e108-18.
52. World Health Organization. Influenza at the human-animal interface: Summary and assessment, 28 September to 30 October 2017: World Health Organization; 2017 [2017]. Available from: http://www.who.int/influenza/human_animal_interface/Influenza_Summary_IRA_HA_interface_10_30_2017.pdf.
53. World Health Organization. Avian Influenza Weekly Update Number 774: World Health Organisation; 2021 [Available from: https://www.who.int/docs/default-source/wpro---documents/emergency/surveillance/avian-influenza/ai-20210108.pdf?sfvrsn=c0382d50_81.
54. Imai M, Watanabe T, Kiso M, Nakajima N, Yamayoshi S, Iwatsuki-Horimoto K, et al. A Highly Pathogenic Avian H7N9 Influenza Virus Isolated from A Human Is Lethal in Some Ferrets Infected via Respiratory Droplets. Cell Host & Microbe. 2017;22(5):615-26.e8.
55. Lopez-Martinez I, Balish A, Gisela B-B, Jones J, Nuñez-García TE, Jang Y, et al. Highly Pathogenic Avian Influenza A(H7N3) Virus in Poultry Workers, Mexico, 2012. Emerging Infectious Diseases. 2013;19(9):1531-4.
56. Huo X, Chen L, Qi X, Huang H, Dai Q, Yu H, et al. Significantly elevated number of human infections with H7N9 in Jiangsu in eastern China, October 2016 to January 2017. Eurosurveillance. 2017;22(13).

57. Su S, Gu M, Liu D, Cui J, Gao GF, Zhou J, et al. Epidemiology, Evolution, and Pathogenesis of H7N9 Influenza Viruses in Five Epidemic Waves since 2013 in China. Trends in Microbiology. 2017;25(9):713-28.
58. Zhou L, Ren R, Yang L, Bao C, Wu J, Wang D, et al. Sudden increase in human infection with avian influenza A(H7N9) virus in China, September-December 2016. Western Pacific Surveillance and Response Journal. 2017;8(1):6-14.
59. Pinsent A, Pepin KM, Zhu H, Guan Y, White MT, Riley S. The persistance of multiple strains of avian influenza in live bird markets. Proceedings of the Royal Society B. 2017;284.
60. Wan X-F, Dong L, Lan Y, Long L-P, Xu C, Zou S, et al. Indications that Live Poultry Markets Are a Major Source of Human H5N1 Influenza Virus Infection in China. Journal of Virology. 2011;85(24):13432-8.
61. Bano S, Naeem K, Malik SA. Evaluation of Pathogenic Potential of Avian Influenza Virus Serotype H9N2 in Chickens. Avian Diseases. 2003;47(817):817-22.
62. Kalaiyarasu S, Kumar M, Kumar DS, Bhatia S, Dash SK, Bhat S, et al. Highly pathogenic avian influenza H5N1 virus induces cytokine dysregulation with suppressed maturation of chicken monocyte-derived dendritic cells. Microbiology and Immunology. 2016;60:687-93.
63. Huang Y, Li X, Zhang H, Chen B, Jiang Y, Yang L, et al. Human Infection with an Avian Influenza A (H9N2) Virus in the Middle Region of China. Journal of Medical Virology. 2015;87:1641-8.
64. Naguib MA, Arafa A-SA, El-Kady MF, Selim AA, Gunalan V, Maurer-Stroh S, et al. Evolutionary trajectories and diagnostic challenges of potentially zoonotic avian influenza viruses H5N1 and H9N2 co-circulating in Egypt. Infection, Genetics and Evolution. 2015;34:278-91.
65. Yu X, Jin T, Cui Y, Pu X, Li J, Liu G, et al. Influenza H7N9 and H9N2 Viruses: Coexistence in Poultry Linked to Human H7N9 Infection and Genome Characteristics. Journal of Virology. 2014;88(6):3423-31.
66. Yuan J, Zhang L, Kan X, Jiang L, Yang J, Guo Z, et al. Origin and Molecular Characteristics of a Novel 2013 Avian Influenza A(H6N1) Virus Causing Human Infection in Taiwan. Clinical Infectious Disease. 2013;57.
67. Chen H, Yuan H, Gao R, Zhang J, Wang D, Xiong Y, et al. Clinical and epidemiological characteristics of a fatal case of avian influenza A H10N8 virus infection: a descriptive study. The Lancet. 2014;383:714-21.
68. Lu H, Castro AE, Pennick K, Liu J, Yang Q, Dunn P, et al. Survival of Avian Influenza Virus H7N2 in SPF Chickens and Their Environments. Avian Diseases. 2003;47(s3):1015-21.
69. Gharaibeh S. Pathogenicity of an Avian Influenza Serotype H9N2 in Chickens. Avian Diseases. 2008;52(1):106-10.
70. França M, Stallknecht DE, Poulson R, Brown J, Howerth EW. The Pathogenesis of Low Pathogenic Avian Influenza in Mallards. Avian Diseases. 2012;56:976-80.
71. Curran JM, Robertson ID, Ellis TM, Selleck PW, O'Dea MA. Variation in the Responses of Wild Species of Duck, Gull, and Wader to Inoculatiion with a Wild-Bird-Origin H6N2 Low Pathogenicity Avain Influenza Virus. Avian Diseases. 2013;57(3):581-6.
72. Wang J, Li CC, Diao YX, Sun XY, Hao DM, Liu X, et al. Different outcomes of infection of chickens and ducks with duck-origin H9N2 influenza A virus. Acta Virologica. 2014;58:223-30.
73. Aly MM, Arafa A-SA, Hassan MK. Epidemiological Findings of Outbreaks of Disease Caused by Highly Pathogenic H5N1 Avian Influenza Virus in Poultry in Egypt During 2006. Avian Diseases. 2008;52(2):269-77.
74. Perkins LEL, Swayne DE. Pathobiology of A/Chicken/Hong Kong/220/97 (H5N1) Avian Influenza Virus in Seven Gallinaceous Species. Veterinary Pathology. 2001;38(2):149-64.
75. Bingham J, Green DJ, Lowther S, Klippel J, Burggraaf S, Anderson DE, et al. Infection studies with two highly pathogenic avian influenza strains (Vietnamese and

Indonesian) in Pekin ducks (Anas platyrhynchos), withparticular reference to clinical disease, tissue tropism and viral shedding. Avian Pathology. 2009;38(4):267-78.
76. Acland HM, Silverman Bachin LA, Eckroade RJ. Lesions in Broiler and Layer Chickens in an Outbreak of Highly Pathogenic Avian Influenza Virus Infection. Veterinary Pathology. 1984;21:564-9.
77. Keawcharoen J, van Riel D, van Amerongen G, Bestebroer TM, Beyer WE, van Lavieren R, et al. Wild Ducks a Long-Distance Vectors of Highly Pathogenic Avian Influenza Virus (H5N1). Emerging Infectious Diseases. 2008;14(4):600-7.
78. Pantin-Jackwood MJ, Swayne DE. Pathobiology of Asian Highly Pathogenic Avian Influenza H5N1 Virus Infections in Ducks. Avian Diseases. 2007;51(s1):250-9.
79. Suzuki K, Okada H, Itoh T, Tada T, Mase M, Nakamura K, et al. Association of Increased Pathogenicity of Asian H5N1 Highly Pathogenic Avian Influenza Viruses in Chickens with Highly Efficient Viral replication Accompanied by Early Destruction of Innate Immune Responses. Journal of Virology. 2009;83(15):7475-86.
80. Jeong O-M, Kim M-C, Kim M-J, Kang H-M, Kim H-R, Kim Y-J, et al. Experimental infection of chickens, ducks and quails with highly pathogenic H5N1 avian influenza virus. Journal of Veterinary Science. 2009;10(1):53-60.
81. Yamamoto Y, Nakamura K, Yamada M, Mase M. Corneal Opacity in Domestic Ducks Experimentally Infected With H5N1 Highly Pathogenic Avian Influenza Virus. Veterinary Pathology. 2016;53(1):65-76.
82. Yamamoto Y, Nakamura K, Yamada M, Mase M. Comparative Pathology of Chickens and Domestic Ducks Experimentally Infected with Highly Pathogenic Avian Influenza Viruses (H5N1) Isolated in Japan in 2007 and 2008. Japanese Agricultural Research Quarterly. 2010;44(1):73-80.
83. Ito T, Couceiro JNSS, Kelm S, Baum LG, Krauss S, Castrucci MR, et al. Molecular Basis for the Generation in Pigs of Influenza A Viruses with Pandemic Potential. Journal of Virology. 1998;72(9):7367-73.
84. Lipatov AS, Kwon YK, Sarmento LV, Lager KM, Spackman E, Suarez DL, et al. Domestic Pigs Have Low Succeptibility to H5N1 Highly Pathogenic Avian Influenza Viruses. PloS Pathogens. 2008;4(7).
85. Zhu Q, Yang H, Chen W, Cao W, Zhong G, Jiao P, et al. A Naturally Occurring Deletion in Its NS Gene Contributes to the Attentuation of an H5N1 Swine Influenza Virus in Chickens. Journal of Virology. 2008;82(1):220-8.
86. Zhou P, Hong M, Merrill MM, He H, Sun L, Zhang G. Serological report of influenza a (H7N9) infections among pigs in Southern China. BMC Veterinary Research. 2014;10(203).
87. Liu Q, Zhou B, Ma W, Bawa B, Ma J, Wang W, et al. Analysis of Recombinant H7N9 Wild-Type and Mutant Viruses in Pigs Shows that the Q226L Mutation in HA Is Important for Transmission. Journal of Virology. 2014;88(14):8153-65.
88. Balzli C, Lager KM, Vincent A, Gauger P, Brockmeier S, Miller L, et al. Susceptibility of swine to H5 and H7 low pathogenici avian influenza viruses. Influenza and Other Respiratory Viruses. 2016;10(4):346-52.
89. Yum J, Park EH, Ku KB, Kim JA, Oh SK, Kim HS, et al. Low infectivity of novel avian-origin H7N9 influenza virus in pigs. Archives Of Virology. 2014;159:2745-9.
90. Jones JC, Baranovich T, Zaraket H, Guan Y, Shu Y, Webby RJ, et al. Human H7N9 Influenza A Viruses Replicate in Swine Respiratory Tissue Explants. Journal of Virology. 2013;87(22):12496-8.
91. Kwon TY, Lee SS, Kim CY, Shin JY, Sunwoo SY, Lyoo YS. Genetic characterization of H7N2 influenza viruses isolated from pigs. Veterinary Microbiology. 2011;153.
92. van Riel D, Munster VJ, de Wit E, Rimmelzwaan GF, Fouchier RAM, Osterhaus ADME, et al. H5N1 Virus Attachment to Lower Respiratory Tract. Science. 2006;312(5772):399.
93. Belser JA, Gustin KM, Pearce MB, Maines TR, Zeng H, Pappas C, et al. Pathogenesis and transmission of avian influenza A (H7N9) virus in ferrets and mice. Nature. 2013;501:556.

94. Zhang Q, Shi J, Deng G, Guo J, Zeng X, He X, et al. H7N9 Influenza Viruses Are Transmissible in Ferrets by Respiratory Droplet. Science. 2013;341(6144):410.
95. Herfst S, Schrauwen EJA, Linster M, Chutinimitkul S, De Wit E, Munster VJ, et al. Airborne Transmission of Influenza A/H5N1 Virus Between Ferrets. Science. 2012;336:1534-41.
96. Zaraket H, Baranovich T, Kaplan BS, Carter R, Song M-S, Paulson JC, et al. Mammalian adaptation of influenza A(H7N9) virus is limited by a narrow genetic bottleneck. Nature Communications. 2015;6(6553).
97. Edenborough KM, Lowther S, Laurie KL, Yamada M, Long F, Bingham J, et al. Predicting Disease Severity and Viral Spread of H5N1 Influenza Virus in Ferrets in the Context of Natural Exposure Routes. Journal of Virology. **2015**;90(4):1888-97.
98. Tundup S, Kandasamy M, Perez JT, Mena N, Steel J, Nagy T, et al. Endothelial cell tropism is a determinant of H5N1 pathogenesis in mammalian species. PloS Pathogens. 2017;13(3).
99. Zaman M, Gasimov V, Oner AF, Dogan N, Adisasmito W, Coker R, et al. Recognizing true H5N1 infections in humans during confirmed outbreaks. The Journal of Infection in Developing Countries. 2014;8(202-207).
100. Wang Z, Wan Y, Qiu C, Quiñones-Parra S, Zhu Z, Loh L, et al. Recovery from severe H7N9 disease is associated with diverese response mechanims dominated by CD8+ T cells. Nature Communications. 2015;6(6833).
101. Hu Y, Lu S, Song Z, Wang W, Hao P, Li J, et al. Association between adverse clinical outcome in human disease caused by novel influenza A H7N9 virus and sustained viral shedding and emergence of antiviral resistance. The Lancet. 2013;381(9885):2273-9.
102. Zhang Z, Zhang J, Huang K, Li K-S, Yuen K-Y, Guan Y, et al. Systemic infection of avian influenza A virus H5N1 subtype in humans. Human Pathology. 2009;40:735-9.
103. Simonsen L, Spreeuwenberg P, Lustig R, Taylor RJ, Fleming DM, Kroneman M, et al. Global Mortality Estimates for the 2009 Influenza Pandemic from the GLaMOR Project: A Modeling Study. PloS Medicine. 2013;10(11).
104. Xing Z, Cardona CJ. Preexisting immunity to pandemic (H1N1) 2009. Emerg Infect Dis. 2009;15(11):1847-9.
105. Fang Y, Banner D, Kelvin AA, Huang SSH, Paige CJ, Corfe SA, et al. Seasonal H1N1 Influenza Virus Infection Induces Cross-Protective Pandemic H1N1 Virus Immunity through a CD8-Independent, B Cell-Dependent Mechanism. Journal of Virology. 2012;86(4):2229.
106. Zhou L, Tan Y, Kang M, Liu F, Ren R, Wang Y, et al. Preliminary Epidemiology of Human Infections with Highly Pathogenic Avian Influenza A(H7N9) Virus, China, 2017. Emerging Infectious Diseases. 2017;23(8).
107. Mackay IM. VDU's blog [Internet]2014. [cited 2018]. Available from: https://virologydownunder.blogspot.com.au/2014/11/influenza-ah7n9-virus-detection-numbers.html.
108. Yang Y, Peng F, Wang R, Yange M, Guan K, Jiang T, et al. The deadly coronaviruses: The 2003 SARS pandemic and the 2020 novel coronavirus epidemic in China. J Autoimmun. 2020;109:102434-.
109. Chan-Yeung M, Xu R-H. SARS: epidemiology. Respirology. 2003;8 Suppl(Suppl 1):S9-S14.
110. Kuiken T, Fouchier RAM, Schutten M, Rimmelzwaan GF, van Amerongen G, van Riel D, et al. Newly discovered coronavirus as the primary cause of severe acute respiratory syndrome. Lancet (London, England). 2003;362(9380):263-70.
111. World Health Organization. Novel Coronavirus – China. Jan 12, 2020.: World Health Organisation; 2020 [Available from: https://www.who.int/csr/don/12-january-2020-novel-coronavirus-china/en/.
112. Petersen E, Koopmans M, Go U, Hamer DH, Petrosillo N, Castelli F, et al. Comparing SARS-CoV-2 with SARS-CoV and influenza pandemics. The Lancet Infectious Diseases. 2020;20(9):e238-e44.

113. Benvenuto D, Giovanetti M, Ciccozzi A, Spoto S, Angeletti S, Ciccozzi M. The 2019-new coronavirus epidemic: Evidence for virus evolution. Journal of medical virology. 2020;92(4):455-9.
114. Lu R, Zhao X, Li J, Niu P, Yang B, Wu H, et al. Genomic characterisation and epidemiology of 2019 novel coronavirus: implications for virus origins and receptor binding. Lancet (London, England). 2020;395(10224):565-74.
115. Zhou P, Yang X-L, Wang X-G, Hu B, Zhang L, Zhang W, et al. A pneumonia outbreak associated with a new coronavirus of probable bat origin. Nature. 2020;579(7798):270-3.
116. Chen Y, Li L. SARS-CoV-2: virus dynamics and host response. The Lancet Infectious Diseases. 2020;20(5):515-6.
117. Li W, Moore MJ, Vasilieva N, Sui J, Wong SK, Berne MA, et al. Angiotensin-converting enzyme 2 is a functional receptor for the SARS coronavirus. Nature. 2003;426(6965):450-4.
118. Ou X, Liu Y, Lei X, Li P, Mi D, Ren L, et al. Characterization of spike glycoprotein of SARS-CoV-2 on virus entry and its immune cross-reactivity with SARS-CoV. Nature Communications. 2020;11(1):1620.
119. Hoffmann M, Kleine-Weber H, Schroeder S, Krüger N, Herrler T, Erichsen S, et al. SARS-CoV-2 Cell Entry Depends on ACE2 and TMPRSS2 and Is Blocked by a Clinically Proven Protease Inhibitor. Cell. 2020;181(2):271-80.e8.
120. Matsuyama S, Nagata N, Shirato K, Kawase M, Takeda M, Taguchi F. Efficient activation of the severe acute respiratory syndrome coronavirus spike protein by the transmembrane protease TMPRSS2. J Virol. 2010;84(24):12658-64.
121. Ziegler CGK, Allon SJ, Nyquist SK, Mbano IM, Miao VN, Tzouanas CN, et al. SARS-CoV-2 Receptor ACE2 Is an Interferon-Stimulated Gene in Human Airway Epithelial Cells and Is Detected in Specific Cell Subsets across Tissues. Cell. 2020;181(5):1016-35.e19.
122. Kuba K, Imai Y, Rao S, Gao H, Guo F, Guan B, et al. A crucial role of angiotensin converting enzyme 2 (ACE2) in SARS coronavirus-induced lung injury. Nature medicine. 2005;11(8):875-9.
123. Snijder EJ, van der Meer Y, Zevenhoven-Dobbe J, Onderwater JJM, van der Meulen J, Koerten HK, et al. Ultrastructure and origin of membrane vesicles associated with the severe acute respiratory syndrome coronavirus replication complex. Journal of virology. 2006;80(12):5927-40.
124. V'kovski P, Kratzel A, Steiner S, Stalder H, Thiel V. Coronavirus biology and replication: implications for SARS-CoV-2. Nature Reviews Microbiology. 2020.
125. Hussain S, Pan Ja, Chen Y, Yang Y, Xu J, Peng Y, et al. Identification of novel subgenomic RNAs and noncanonical transcription initiation signals of severe acute respiratory syndrome coronavirus. Journal of virology. 2005;79(9):5288-95.
126. Dhama K, Khan S, Tiwari R, Sircar S, Bhat S, Malik YS, et al. Coronavirus Disease 2019-COVID-19. Clin Microbiol Rev. 2020;33(4):e00028-20.
127. Huang C, Wang Y, Li X, Ren L, Zhao J, Hu Y, et al. Clinical features of patients infected with 2019 novel coronavirus in Wuhan, China. Lancet (London, England). 2020;395(10223):497-506.
128. Eliezer M, Hautefort C, Hamel A-L, Verillaud B, Herman P, Houdart E, et al. Sudden and Complete Olfactory Loss of Function as a Possible Symptom of COVID-19. JAMA Otolaryngology–Head & Neck Surgery. 2020;146(7):674-5.
129. Mermelstein S. Acute anosmia from COVID-19 infection. Practical neurology. 2020;20(4):343-4.
130. Alamri A, Oriez C, Bouilloud F, Dupuy O, Ben Hamou A. Sudden onset anosmia and dysgeusia in two patients: An early sign of SARS-CoV-2 infection. Presse medicale (Paris, France : 1983). 2020;49(1):104027.
131. Huang C, Huang L, Wang Y, Li X, Ren L, Gu X, et al. 6-month consequences of COVID-19 in patients discharged from hospital: a cohort study. The Lancet. 2021.

132. Moldofsky H, Patcai J. Chronic widespread musculoskeletal pain, fatigue, depression and disordered sleep in chronic post-SARS syndrome; a case-controlled study. BMC Neurol. 2011;11:37-.
133. Zhang P, Li J, Liu H, Han N, Ju J, Kou Y, et al. Long-term bone and lung consequences associated with hospital-acquired severe acute respiratory syndrome: a 15-year follow-up from a prospective cohort study. Bone research. 2020;8:8.
134. Asadi-Pooya AA, Yaghoubi E, Nikseresht A, Moghadami M, Honarvar B. The Neurological Manifestations of H1N1 Influenza Infection; Diagnostic Challenges and Recommendations. Iran J Med Sci. 2011;36(1):36-9.
135. Khandaker G, Zurynski Y, Buttery J, Marshall H, Richmond PC, Dale RC, et al. Neurologic complications of influenza A(H1N1)pdm09: surveillance in 6 pediatric hospitals. Neurology. 2012;79(14):1474-81.
136. Ye M, Ren Y, Lv T. Encephalitis as a clinical manifestation of COVID-19. Brain Behav Immun. 2020;88:945-6.
137. Xiang P, Xu X, Gao L, Wang H, Xiong H, Li RJC. First case of 2019 novel coronavirus disease with encephalitis. 2020;202003:00015.
138. Netland J, Meyerholz DK, Moore S, Cassell M, Perlman S. Severe Acute Respiratory Syndrome Coronavirus Infection Causes Neuronal Death in the Absence of Encephalitis in Mice Transgenic for Human ACE2. Journal of Virology. 2008;82(15):7264.
139. Ahmad T, Chaudhuri R, Joshi MC, Almatroudi A, Rahmani AH, Ali SM. COVID-19: The Emerging Immunopathological Determinants for Recovery or Death. 2020;11(2815).
140. Cao Y, Su B, Guo X, Sun W, Deng Y, Bao L, et al. Potent Neutralizing Antibodies against SARS-CoV-2 Identified by High-Throughput Single-Cell Sequencing of Convalescent Patients' B Cells. Cell. 2020;182(1):73-84.e16.
141. Thevarajan I, Nguyen THO, Koutsakos M, Druce J, Caly L, van de Sandt CE, et al. Breadth of concomitant immune responses prior to patient recovery: a case report of non-severe COVID-19. Nature Medicine. 2020;26(4):453-5.
142. McGonagle D, Sharif K, O'Regan A, Bridgewood C. The Role of Cytokines including Interleukin-6 in COVID-19 induced Pneumonia and Macrophage Activation Syndrome-Like Disease. Autoimmunity Reviews. 2020;19(6):102537.
143. Han H, Ma Q, Li C, Liu R, Zhao L, Wang W, et al. Profiling serum cytokines in COVID-19 patients reveals IL-6 and IL-10 are disease severity predictors. Emerg Microbes Infect. 2020;9(1):1123-30.
144. Somsen GA, van Rijn C, Kooij S, Bem RA, Bonn D. Small droplet aerosols in poorly ventilated spaces and SARS-CoV-2 transmission. The Lancet Respiratory Medicine. 2020;8(7):658-9.
145. Richard M, Kok A, de Meulder D, Bestebroer TM, Lamers MM, Okba NMA, et al. SARS-CoV-2 is transmitted via contact and via the air between ferrets. Nature Communications. 2020;11(1):3496.
146. Rothe C, Schunk M, Sothmann P, Bretzel G, Froeschl G, Wallrauch C, et al. Transmission of 2019-nCoV Infection from an Asymptomatic Contact in Germany. New England Journal of Medicine. 2020;382(10):970-1.
147. Alharbi NK, Padron-Regalado E, Thompson CP, Kupke A, Wells D, Sloan MA, et al. ChAdOx1 and MVA based vaccine candidates against MERS-CoV elicit neutralising antibodies and cellular immune responses in mice. Vaccine. 2017;35(30):3780-8.
148. Folegatti PM, Ewer KJ, Aley PK, Angus B, Becker S, Belij-Rammerstorfer S, et al. Safety and immunogenicity of the ChAdOx1 nCoV-19 vaccine against SARS-CoV-2: a preliminary report of a phase 1/2, single-blind, randomised controlled trial. The Lancet. 2020;396(10249):467-78.
149. Graham SP, McLean RK, Spencer AJ, Belij-Rammerstorfer S, Wright D, Ulaszewska M, et al. Evaluation of the immunogenicity of prime-boost vaccination with the replication-deficient viral vectored COVID-19 vaccine candidate ChAdOx1 nCoV-19. npj Vaccines. 2020;5(1):69.

150. van Doremalen N, Lambe T, Spencer A, Belij-Rammerstorfer S, Purushotham JN, Port JR, et al. ChAdOx1 nCoV-19 vaccine prevents SARS-CoV-2 pneumonia in rhesus macaques. Nature. 2020;586(7830):578-82.
151. Baden LR, El Sahly HM, Essink B, Kotloff K, Frey S, Novak R, et al. Efficacy and Safety of the mRNA-1273 SARS-CoV-2 Vaccine. The New England journal of medicine. 2020.
152. Polack FP, Thomas SJ, Kitchin N, Absalon J, Gurtman A, Lockhart S, et al. Safety and Efficacy of the BNT162b2 mRNA Covid-19 Vaccine. New England Journal of Medicine. 2020;383(27):2603-15.
153. Chen X, Liu S, Goraya MU, Maarouf M, Huang S, Chen J-L. Host Immune Response to Influenza A Virus Infection. 2018;9(320).
154. Olofsson S, Kumlin U, Dimock K, Arnberg NJTLid. Avian influenza and sialic acid receptors: more than meets the eye? 2005;5(3):184-8.
155. Cohen M, Zhang X-Q, Senaati HP, Chen H-W, Varki NM, Schooley RT, et al. Influenza A penetrates host mucus by cleaving sialic acids with neuraminidase. Virol J. 2013;10:321-.
156. Wieczorek M, Abualrous ET, Sticht J, Álvaro-Benito M, Stolzenberg S, Noé F, et al. Major Histocompatibility Complex (MHC) Class I and MHC Class II Proteins: Conformational Plasticity in Antigen Presentation. Front Immunol. 2017;8:292-.
157. Falk K, Rötzschke O, Stevanović S, Jung G, Rammensee HG. Allele-specific motifs revealed by sequencing of self-peptides eluted from MHC molecules. Nature. 1991;351(6324):290-6.
158. Brown JH, Jardetzky TS, Gorga JC, Stern LJ, Urban RG, Strominger JL, et al. Three-dimensional structure of the human class II histocompatibility antigen HLA-DR1. Nature. 1993;364(6432):33-9.
159. Jin P, Wang E. Polymorphism in clinical immunology – From HLA typing to immunogenetic profiling. Journal of Translational Medicine. 2003;1(1):8.
160. Matsumura M, Fremont DH, Peterson PA, Wilson IA. Emerging principles for the recognition of peptide antigens by MHC class I molecules. Science. 1992;257(5072):927.
161. Chicz RM, Urban RG, Lane WS, Gorga JC, Stern LJ, Vignali DA, et al. Predominant naturally processed peptides bound to HLA-DR1 are derived from MHC-related molecules and are heterogeneous in size. 1992;358(6389):764-8.
162. Tanaka K. The proteasome: overview of structure and functions. Proc Jpn Acad Ser B Phys Biol Sci. 2009;85(1):12-36.
163. McCarthy MK, Weinberg JB. The immunoproteasome and viral infection: a complex regulator of inflammation. Frontiers in microbiology. 2015;6:21-.
164. Shin E-C, Seifert U, Kato T, Rice CM, Feinstone SM, Kloetzel P-M, et al. Virus-induced type I IFN stimulates generation of immunoproteasomes at the site of infection. J Clin Invest. 2006;116(11):3006-14.
165. DiPiazza A, Nogales A, Poulton N, Wilson PC, Martínez-Sobrido L, Sant AJ. Pandemic 2009 H1N1 Influenza Venus reporter virus reveals broad diversity of MHC class II-positive antigen-bearing cells following infection in vivo. Scientific reports. 2017;7(1):10857-.
166. Jongsma MLM, Guarda G, Spaapen RM. The regulatory network behind MHC class I expression. Molecular immunology. 2019;113:16-21.
167. Lamichhane PP, Samarasinghe AE. The Role of Innate Leukocytes during Influenza Virus Infection. Journal of immunology research. 2019;2019:8028725.
168. Tate MD, Ioannidis LJ, Croker B, Brown LE, Brooks AG, Reading PC. The role of neutrophils during mild and severe influenza virus infections of mice. PloS one. 2011;6(3):e17618-e.
169. Daher KA, Selsted ME, Lehrer RI. Direct inactivation of viruses by human granulocyte defensins. J Virol. 1986;60(3):1068-74.
170. Tate MD, Deng YM, Jones JE, Anderson GP, Brooks AG, Reading PC. Neutrophils ameliorate lung injury and the development of severe disease during influenza infection. J Immunol. 2009;183(11):7441-50.

171. Herold S, von Wulffen W, Steinmueller M, Pleschka S, Kuziel WA, Mack M, et al. Alveolar epithelial cells direct monocyte transepithelial migration upon influenza virus infection: impact of chemokines and adhesion molecules. 2006;177(3):1817-24.
172. Ancuta P, Weiss L, Haeffner-Cavaillon N. CD14+CD16++ cells derived in vitro from peripheral blood monocytes exhibit phenotypic and functional dendritic cell-like characteristics. European journal of immunology. 2000;30(7):1872-83.
173. McGovern N, Schlitzer A, Gunawan M, Jardine L, Shin A, Poyner E, et al. Human dermal CD14^{+} cells are a transient population of monocyte-derived macrophages. Immunity. 2014;41(3):465-77.
174. Thomas GD, Hamers AA, Nakao C, Marcovecchio P, Taylor AM, McSkimming C, et al. Human blood monocyte subsets: a new gating strategy defined using cell surface markers identified by mass cytometry. 2017;37(8):1548-58.
175. Yang J, Zhang L, Yu C, Yang XF, Wang H. Monocyte and macrophage differentiation: circulation inflammatory monocyte as biomarker for inflammatory diseases. Biomarker research. 2014;2(1):1.
176. Schmidl C, Renner K, Peter K, Eder R, Lassmann T, Balwierz PJ, et al. Transcription and enhancer profiling in human monocyte subsets. 2014;123(17):e90-e9.
177. Wong KL, Yeap WH, Tai JJY, Ong SM, Dang TM, Wong SCJIr. The three human monocyte subsets: implications for health and disease. 2012;53(1-3):41-57.
178. Ziegler-Heitbrock L, Ancuta P, Crowe S, Dalod M, Grau V, Hart DN, et al. Nomenclature of monocytes and dendritic cells in blood. 2010;116(16):e74-e80.
179. Damjanovic D, Divangahi M, Kugathasan K, Small C-L, Zganiacz A, Brown EG, et al. Negative regulation of lung inflammation and immunopathology by TNF-α during acute influenza infection. The American journal of pathology. 2011;179(6):2963-76.
180. Herold S, Becker C, Ridge KM, Budinger GRS. Influenza virus-induced lung injury: pathogenesis and implications for treatment. European Respiratory Journal. 2015;45(5):1463.
181. Tate MD, Pickett DL, van Rooijen N, Brooks AG, Reading PC. Critical Role of Airway Macrophages in Modulating Disease Severity during Influenza Virus Infection of Mice. Journal of Virology. 2010;84(15):7569.
182. Kim HM, Kang YM, Ku KB, Park EH, Yum J, Kim JC, et al. The severe pathogenicity of alveolar macrophage-depleted ferrets infected with 2009 pandemic H1N1 influenza virus. Virology. 2013;444(1):394-403.
183. Kim HM, Lee Y-W, Lee K-J, Kim HS, Cho SW, van Rooijen N, et al. Alveolar Macrophages Are Indispensable for Controlling Influenza Viruses in Lungs of Pigs. Journal of Virology. 2008;82(9):4265.
184. Aegerter H, Kulikauskaite J, Crotta S, Patel H, Kelly G, Hessel EM, et al. Influenza-induced monocyte-derived alveolar macrophages confer prolonged antibacterial protection. Nature Immunology. 2020;21(2):145-57.
185. Beaty SR, Rose CE, Jr., Sung SS. Diverse and potent chemokine production by lung CD11bhigh dendritic cells in homeostasis and in allergic lung inflammation. J Immunol. 2007;178(3):1882-95.
186. Chen K, Wang JM, Yuan R, Yi X, Li L, Gong W, et al. Tissue-resident dendritic cells and diseases involving dendritic cell malfunction. Int Immunopharmacol. 2016;34:1-15.
187. Alvarez D, Vollmann EH, von Andrian UH. Mechanisms and consequences of dendritic cell migration. Immunity. 2008;29(3):325-42.
188. Haist KC, Carpentier KS, Davenport BJ, Morrison TE. Plasmacytoid DCs mediate control of Ross River virus infection via a type I IFN-dependent, MAVS-independent mechanism. J Virol. 2020.
189. Sallusto F, Lanzavecchia A. The instructive role of dendritic cells on T-cell responses. Arthritis Research & Therapy. 2002;4(3):S127.
190. Ng SL, Teo YJ, Setiagani YA, Karjalainen K, Ruedl C. Type 1 Conventional CD103+ Dendritic Cells Control Effector CD8+ T Cell Migration, Survival, and Memory Responses During Influenza Infection. 2018;9(3043).

191. Shin J-Y, Wang C-Y, Lin C-C, Chu C-L. A recently described type 2 conventional dendritic cell (cDC2) subset mediates inflammation. Cellular & Molecular Immunology. 2020;17(12):1215-7.
192. Gillespie L, Roosendahl P, Ng WC, Brooks AG, Reading PC, Londrigan SL. Endocytic function is critical for influenza A virus infection via DC-SIGN and L-SIGN. Scientific reports. 2016;6:19428-.
193. Waithman J, Mintern JD. Dendritic cells and influenza A virus infection. Virulence. 2012;3(7):603-8.
194. Zhao Y, Lin L, Xiao Z, Li M, Wu X, Li W, et al. Protective Role of γδ T Cells in Different Pathogen Infections and Its Potential Clinical Application. Journal of immunology research. 2018;2018:5081634.
195. Krangel MS. Mechanics of T cell receptor gene rearrangement. Curr Opin Immunol. 2009;21(2):133-9.
196. Miles JJ, Douek DC, Price DA. Bias in the αβ T-cell repertoire: implications for disease pathogenesis and vaccination. Immunology and cell biology. 2011;89(3):375-87.
197. von Boehmer H, Fehling HJ. STRUCTURE AND FUNCTION OF THE PRE-T CELL RECEPTOR. Annual Review of Immunology. 1997;15(1):433-52.
198. Alcover A, Alarcón B, Di Bartolo V. Cell Biology of T Cell Receptor Expression and Regulation. Annu Rev Immunol. 2018;36:103-25.
199. Klein L, Kyewski B, Allen PM, Hogquist KA. Positive and negative selection of the T cell repertoire: what thymocytes see (and don't see). Nature reviews Immunology. 2014;14(6):377-91.
200. Chu ND, Bi HS, Emerson RO, Sherwood AM, Birnbaum ME, Robins HS, et al. Longitudinal immunosequencing in healthy people reveals persistent T cell receptors rich in highly public receptors. BMC Immunology. 2019;20(1):19.
201. Halle S, Halle O, Förster R. Mechanisms and Dynamics of T Cell-Mediated Cytotoxicity In Vivo. Trends in Immunology. 2017;38(6):432-43.
202. Stinchcombe JC, Griffiths GMJARCDB. Secretory mechanisms in cell-mediated cytotoxicity. 2007;23:495-517.
203. Basu R, Whitlock BM, Husson J, Le Floc'h A, Jin W, Oyler-Yaniv A, et al. Cytotoxic T Cells Use Mechanical Force to Potentiate Target Cell Killing. Cell. 2016;165(1):100-10.
204. Beuneu H, Lemaître F, Deguine J, Moreau HD, Bouvier I, Garcia Z, et al. Visualizing the functional diversification of CD8+ T cell responses in lymph nodes. Immunity. 2010;33(3):412-23.
205. Trandem K, Zhao J, Fleming E, Perlman S. Highly activated cytotoxic CD8 T cells express protective IL-10 at the peak of coronavirus-induced encephalitis. Journal of immunology (Baltimore, Md : 1950). 2011;186(6):3642-52.
206. Koutsakos M, Illing PT, Nguyen THO, Mifsud NA, Crawford JC, Rizzetto S, et al. Human CD8(+) T cell cross-reactivity across influenza A, B and C viruses. Nat Immunol. 2019;20(5):613-25.
207. Kaech SM, Tan JT, Wherry EJ, Konieczny BT, Surh CD, Ahmed R. Selective expression of the interleukin 7 receptor identifies effector CD8 T cells that give rise to long-lived memory cells. Nat Immunol. 2003;4(12):1191-8.
208. Pearce EL, Shen H. Generation of CD8 T cell memory is regulated by IL-12. J Immunol. 2007;179(4):2074-81.
209. Sallusto F, Lenig D, Förster R, Lipp M, Lanzavecchia AJN. Two subsets of memory T lymphocytes with distinct homing potentials and effector functions. 1999;401(6754):708-12.
210. Martin MD, Badovinac VP. Defining Memory CD8 T Cell. 2018;9(2692).
211. Tian Y, Babor M, Lane J, Schulten V, Patil VS, Seumois G, et al. Unique phenotypes and clonal expansions of human CD4 effector memory T cells re-expressing CD45RA. Nature Communications. 2017;8(1):1473.
212. Mackay LK, Braun A, Macleod BL, Collins N, Tebartz C, Bedoui S, et al. Cutting edge: CD69 interference with sphingosine-1-phosphate receptor function regulates peripheral T cell retention. 2015;194(5):2059-63.

213. Mackay LK, Rahimpour A, Ma JZ, Collins N, Stock AT, Hafon M-L, et al. The developmental pathway for CD103+ CD8+ tissue-resident memory T cells of skin. 2013;14(12):1294-301.
214. Slütter B, Pewe LL, Kaech SM, Harty JTJI. Lung airway-surveilling CXCR3hi memory CD8+ T cells are critical for protection against influenza A virus. 2013;39(5):939-48.
215. Pizzolla A, Nguyen TH, Smith JM, Brooks AG, Kedzierska K, Heath WR, et al. Resident memory CD8 (+) T cells in the upper respiratory tract prevent pulmonary influenza virus infection. 2017.
216. Laidlaw BJ, Zhang N, Marshall HD, Staron MM, Guan T, Hu Y, et al. CD4+ T cell help guides formation of CD103+ lung-resident memory CD8+ T cells during influenza viral infection. 2014;41(4):633-45.
217. Zander R, Schauder D, Xin G, Nguyen C, Wu X, Zajac A, et al. CD4(+) T Cell Help Is Required for the Formation of a Cytolytic CD8(+) T Cell Subset that Protects against Chronic Infection and Cancer. Immunity. 2019;51(6):1028-42.e4.
218. Kumar BV, Connors TJ, Farber DL. Human T Cell Development, Localization, and Function throughout Life. Immunity. 2018;48(2):202-13.
219. Bonecchi R, Bianchi G, Bordignon PP, D'Ambrosio D, Lang R, Borsatti A, et al. Differential Expression of Chemokine Receptors and Chemotactic Responsiveness of Type 1 T Helper Cells (Th1s) and Th2s. Journal of Experimental Medicine. 1998;187(1):129-34.
220. Austrup F, Vestweber D, Borges E, Löhning M, Bräuer R, Herz U, et al. P- and E-selectin mediate recruitment of T-helper-1 but not T-helper-2 cells into inflammed tissues. Nature. 1997;385(6611):81-3.
221. Romagnani S. T-cell subsets (Th1 versus Th2). Annals of allergy, asthma & immunology : official publication of the American College of Allergy, Asthma, & Immunology. 2000;85(1):9-18; quiz , 21.
222. Wohlleben G, Müller J, Tatsch U, Hambrecht C, Herz U, Renz H, et al. Influenza A Virus Infection Inhibits the Efficient Recruitment of Th2 Cells into the Airways and the Development of Airway Eosinophilia. The Journal of Immunology. 2003;170(9):4601.
223. Nurieva RI, Chung Y, Martinez GJ, Yang XO, Tanaka S, Matskevitch TD, et al. Bcl6 mediates the development of T follicular helper cells. Science. 2009;325(5943):1001-5.
224. Graf D, Müller S, Korthäuer U, van Kooten C, Weise C, Kroczek RAJEjoi. A soluble form of TRAP (CD40 ligand) is rapidly released after T cell activation. 1995;25(6):1749-54.
225. Qin L, Waseem TC, Sahoo A, Bieerkehazhi S, Zhou H, Galkina EV, et al. Insights Into the Molecular Mechanisms of T Follicular Helper-Mediated Immunity and Pathology. 2018;9(1884).
226. Kroeger DR, Rudulier CD, Bretscher PA. Antigen Presenting B Cells Facilitate CD4 T Cell Cooperation Resulting in Enhanced Generation of Effector and Memory CD4 T Cells. PLOS ONE. 2013;8(10):e77346.
227. Forthal DN. Functions of Antibodies. Microbiol Spectr. 2014;2(4):1-17.
228. Pieper K, Grimbacher B, Eibel H. B-cell biology and development. The Journal of allergy and clinical immunology. 2013;131(4):959-71.
229. Hardy RR, Hayakawa K. B Cell Development Pathways. Annual Review of Immunology. 2001;19(1):595-621.
230. Schroeder HW, Jr., Cavacini L. Structure and function of immunoglobulins. The Journal of allergy and clinical immunology. 2010;125(2 Suppl 2):S41-S52.
231. Torres M, Casadevall A. The immunoglobulin constant region contributes to affinity and specificity. Trends in Immunology. 2008;29(2):91-7.
232. Stavnezer J, Guikema JEJ, Schrader CE. Mechanism and regulation of class switch recombination. Annual review of immunology. 2008;26:261-92.
233. Hiramoto E, Tsutsumi A, Suzuki R, Matsuoka S, Arai S, Kikkawa M, et al. The IgM pentamer is an asymmetric pentagon with an open groove that binds the AIM protein. Science Advances. 2018;4(10):eaau1199.
234. Minuzzo S, Indraccolo S, Tosello V, Piovan E, Cabrelle A, Trentin L, et al. Heterogeneous intracellular expression of B-cell receptor components in B-cell chronic

lymphocytic leukaemia (B-CLL) cells and effects of CD79b gene transfer on surface immunoglobulin levels in a B-CLL-derived cell line. 2005;130(6):878-89.
235. Shulman MJ, Collins C, Pennell N, Hozumi N. Complement activation by IgM: evidence for the importance of the third constant domain of the mu heavy chain. European journal of immunology. 1987;17(4):549-54.
236. Sharp TH, Boyle AL, Diebolder CA, Kros A, Koster AJ, Gros P. Insights into IgM-mediated complement activation based on in situ structures of IgM-C1-C4b. Proceedings of the National Academy of Sciences. 2019;116(24):11900.
237. Skountzou I, Satyabhama L, Stavropoulou A, Ashraf Z, Esser ES, Vassilieva E, et al. Influenza virus-specific neutralizing IgM antibodies persist for a lifetime. Clin Vaccine Immunol. 2014;21(11):1481-9.
238. Shen C, Zhang M, Chen Y, Zhang L, Wang G, Chen J, et al. An IgM antibody targeting the receptor binding site of influenza B blocks viral infection with great breadth and potency. Theranostics. 2019;9(1):210-31.
239. Baumgarth N, Herman OC, Jager GC, Brown L, Herzenberg LA, Herzenberg LAJPotNAoS. Innate and acquired humoral immunities to influenza virus are mediated by distinct arms of the immune system. 1999;96(5):2250-5.
240. Mankarious S, Lee M, Fischer S, Pyun KH, Ochs HD, Oxelius VA, et al. The half-lives of IgG subclasses and specific antibodies in patients with primary immunodeficiency who are receiving intravenously administered immunoglobulin. The Journal of laboratory and clinical medicine. 1988;112(5):634-40.
241. Yu X, Tsibane T, McGraw PA, House FS, Keefer CJ, Hicar MD, et al. Neutralizing antibodies derived from the B cells of 1918 influenza pandemic survivors. 2008;455(7212):532-6.
242. Xu R, Ekiert DC, Krause JC, Hai R, Crowe JE, Jr., Wilson IA. Structural basis of preexisting immunity to the 2009 H1N1 pandemic influenza virus. Science. 2010;328(5976):357-60.
243. Foote J, Eisen HN. Kinetic and affinity limits on antibodies produced during immune responses. Proceedings of the National Academy of Sciences. 1995;92(5):1254.
244. Moldoveanu Z, Clements M, Prince S, Murphy B, Mestecky JJV. Human immune responses to influenza virus vaccines administered by systemic or mucosal routes. 1995;13(11):1006-12.
245. Krammer F. The human antibody response to influenza A virus infection and vaccination. Nature Reviews Immunology. 2019;19(6):383-97.
246. Nachbagauer R, Choi A, Hirsh A, Margine I, Iida S, Barrera A, et al. Defining the antibody cross-reactome directed against the influenza virus surface glycoproteins. 2017;18(4):464.
247. Marklund E, Leach S, Axelsson H, Nyström K, Norder H, Bemark M, et al. Serum-IgG responses to SARS-CoV-2 after mild and severe COVID-19 infection and analysis of IgG non-responders. PLOS ONE. 2020;15(10):e0241104.
248. Wang J, Chen C, Li Q, Cai P, Wang Z, Wang L. COVID-19 confirmed patients with negative antibodies results. BMC Infectious Diseases. 2020;20(1):698.
249. Marcus N, Frizinsky S, Hagin D, Ovadia A, Hanna S, Farkash M, et al. Minor Clinical Impact of COVID-19 Pandemic on Patients With Primary Immunodeficiency in Israel. 2021;11(3505).
250. Quinti I, Lougaris V, Milito C, Cinetto F, Pecoraro A, Mezzaroma I, et al. A possible role for B cells in COVID-19? Lesson from patients with agammaglobulinemia. The Journal of allergy and clinical immunology. 2020;146(1):211-3.e4.
251. Ingulli E, Funatake C, Jacovetty EL, Zanetti M. Cutting edge: antigen presentation to CD8 T cells after influenza A virus infection. J Immunol. 2009;182(1):29-33.
252. Coro ES, Chang WL, Baumgarth N. Type I IFN receptor signals directly stimulate local B cells early following influenza virus infection. J Immunol. 2006;176(7):4343-51.
253. Palm A-KE, Henry C. Remembrance of Things Past: Long-Term B Cell Memory After Infection and Vaccination. 2019;10(1787).

254. Kuchipudi SV, Tellabati M, Sebastian S, Londt BZ, Jansen C, Vervelde L, et al. Highly pathogenic avian influenza virus infection in chickens but not ducks is associated with elevated host immune and pro-inflammatory responses. Veterinary Research. 2014;45(118).
255. Short KR, Veeris R, Leitjen LM, van den Brand JMA, Jong VL, Stittelaar KJ, et al. Proinflammatory Cytokine Responses in Extra-Respiratory Tissues During Severe Influenza. The Journal of Infectious Diseases. 2017;216:829-33.
256. Shinya K, Gao Y, Cilloniz C, Suzuki Y, Fuije M, Deng G, et al. Integrated Clinical, Pathologic, Virologic, and Transcriptomic Analysis of H5N1 Influenza Virus-Induced Viral Pneumonia in the Rhesus Macaque. Journal of Virology. 2012;86(11):6055-66.
257. Gao S, Kang Y, Yuan R, Ma H, Xiang B, Wang Z, et al. Immune Responses of Chickens Infected with Wild Bird-Origin H5N6 Avian Influenza Virus. Frontiers in Microbiology. 2017;8(1081).
258. Meliopoulos VA, Karlsson EA, Kercher L, Cline T, Freiden P, Duan S, et al. Human H7N9 and H5N1 Influenza Viruses Differ in Induction of Cytokines and Tissue Tropism. Journal of Virology. 2014;88(22):12982-91.
259. To KKW, Lau CCS, Woo PCY, Lau SKP, Chan JFW, Chan K-H, et al. Human H7N9 virus induces a more pronounced pro-inflammatory cytokine but an attenuated interferon response in human bronchial epithelial cells when compared with an epidemiologically-linked chicken H7N9 virus. Virology Journal. 2016;13(42).
260. Wu W, Shi D, Fang D, Guo F, Guo J, Huang F, et al. A new perspective on C-reactive protein in H7N9 infections. International Journal of Infectious Disease. 2016;44:31-6.
261. Zhao C, Qi X, Ding M, Sun X, Zhou Z, Zhang S, et al. Pro-inflammatory cytokine dysregulation is associated with novel avian influenza A (H7N9) virus in primary human macrophages. Journal of General Virology. 2016;97(2):299-305.
262. Nelli RK, Dunham SP, Kuchipudi SV, White GA, Baquero-Perez B, Chang P, et al. Mammalian Innate Resistance to Highly Pathogenic Avian Influenza H5N1 Virus Infection Is Mediated through Reduced Proinflammation and Infectious Virus Release. Journal of Virology. 2012;86(17):9201-10.
263. Turner MD, Nedjai B, Hurst T, Pennington DJ. Cytokines and chemokines: At the crossroads of cell signalling and inflammatory disease. BBA - Molecular Cell Research. 2014;1843:2563-82.
264. Boonnak K, Vogel L, Feldmann F, Feldmann H, Legge KL, Subbarao K. Lymphopenia associated with highly virulent H5N1 virus infection due to plasmocytoid dendritic cell mediated apoptosis of Tcells. The Journal of Immunology. 2014;192(12):5906-12.
265. Waring P, Müllbacher A. Cell death induced by the Fas/Fas ligand pathway and its role in pathology. Immunology and Cell Biology. 1999;77:312-7.
266. Chen Y, Liang W, Yang S, Wu N, Gao H, Sheng J, et al. Human infections with the emerging avian influenza A H7N9 virus from wet market poultry: clinical analysis and characterisation of viral genome. The Lancet. 2013;381:1916-25.
267. Uiprasertkul M, Kitphati R, Puthavathana P, Kriwong R, Kongchanagul A, Ungchusak K, et al. Apoptosis and Pathogenesis of Avian Influenza A (H5N1) Virus in Humans. Emerging Infectious Diseases. 2007;13(5):708-12.
268. Wang C, Yu H, Horby PW, Cao B, Wu P, Yang S, et al. Comparison of Patients Hospitalized With Influenza A Subtypes H7N9, H5N1, and 2009 Pandemic H1N1. Clinical Infectious Disease. 2014;58(8):1095-103.
269. Wang Z, Zhu L, Nguyen THO, Wan Y, Sant S, Quiñones-Parra S, et al. Clonally diverse CD38+HLA-DR+CD8+ T cells persist during fatal H7N9. Nature Communications. 2018;9(824).
270. Nichols JE, Niles JA, Roberts Jr. NJ. Human Lymphocyte Apoptosis after Exposure to Influenza A Virus. Journal of Virology. 2001;73(13):5921-9.
271. Herfst S, Imai M, Kawaoka Y, Fouchier RAM. Avian influenza virus transmission to mammals. Current Topics in Microbiology and Immunology. 2014;385:137-55.

272. Rogers GN, Pritchett TJ, Lane JL, Paulson JC. Differential sensitivity of human, avian, and equine influenza A viruses to a glycoprotein inhibitor of infection: selection of receptor specific variants. Virology. 1983;131(2):394-408.
273. de Vries RP, Peng W, Grant OC, Thompson AJ, Zhu X, Bouwman KM, et al. Three mutations switch H7N9 influenza to human-type receptor specificity. PloS Pathogens. 2017;13(6).
274. Dortmans JCFM, Dekkers J, Wickramasinghe INA, Verheije MH, Rottier PJM, van Kuppeveld FJM, et al. Adaptation of novel H7N9 influenza virus to human receptors. Scientific Reports. 2013;3(3058).
275. Chandrasekaran A, Srinivasan A, Raman R, Viswanathan K, Raguram S, Tumpey TM, et al. Glycan topology determines human adaptation of avian H5N1 virus hemagglutinin. Nature Biotechnology. 2008;26(1):107-13.
276. Chrzastek K, Lee D-H, Gharaibeh S, Zsak A, Kapczynski DR. Characterization of H9N2 avian influenza viruses from the Middle East demonstrates heterogeneity at amino acid position 226 in the hemagglutinin and potential for transmission to mammals. Virology. 2018;518:195-201.
277. Li X, Shi J, Guo J, Deng G, Zhang Q, Wang J, et al. Genetics, Receptor Binding Property, and Transmissibility in Mammals of Naturally Isolated H9N2 Avian Influenza Viruses. PloS Pathogens. 2014;10(11).
278. Watanabe Y, Arai Y, Daidoji T, Kawashita N, Ibrahim MS, El-Gendy EE-DM, et al. Characterization of H5N1 Influenza Virus varaints with Hemagglutinin Mutations Isolated from Patients. mBio. 2015;6(2).
279. Watanabe Y, Ibrahim MS, Ellakany HF, Kawashita N, Mizuike R, Hiramatsu H, et al. Acquisition of Human-Type Receptor Binding Specificity by New H5N1 Influenza Virus Sublineages during Their Emergence in Birds in Egypt. PloS Pathogens. 2011;7(5).
280. Steel J, Lowen AC, Mubareka S, Palese P. Transmission of Influenza Virus in a Mammalian Host Is Increased by PB2 Amino Acids 627K or 627E/701N. PloS Pathogens. 2009;5(1).
281. Labadie K, Afonso EDS, Rameix-Welti M-A, van der Werf S, Naffakh N. Host-range determinants on the PB2 protein of influenza A viruses control the interacion between the viral polymerase and nucleoprotein in human cells. Virology. 2007;362:271-82.
282. Chen G-W, Kuo S-M, Yang S-L, Gong Y-N, Hsiao M-R, Liu Y-C, et al. Genomic Signatures for Avian H7N9 Viruses Adapting to Humans. PLoS ONE. 2016;11(2).
283. Zhang H, Li X, Guo J, Li L, Chang C, Li Y, et al. The PB2 E627K mutation contributes to the high polymerase activity and enhanced replication of H7N9 influenza virus. Journal of General Virology. 2014;95:779-86.
284. Schrauwen EJA, Herfst S, Leitjen LM, van Run P, Bestebroer TM, Linster M, et al. The Multibasic Cleavage Site in H5N1 Virus Is Critical for Systemic Spread along the Olfactory and Hematogenous Routes in Ferrets. Journal of Virology. 2012;86(7):3975-84.
285. Suguitan AL, Matsuoka Y, Lau Y-F, Santos CP, Vogel L, Cheng LI, et al. The Multibasic Cleavage Site of Hemagglutinin of Highly Pathogenic A/Vietnam/1203/2004 (H5N1) Avian Influenza Virus Acts as a Virulence Factor in a Host-Specific Manner in Mammals. 86. 2012;5(2706-2714).
286. Stieneke-Gröber A, Vey M, Angliker H, Shaw E, Thomas G, Roberts C, et al. Influenza virus hemagglutinin with a multibasic cleavage site is activated by furin, a subtilisin-like endoprotease. The EMBO Journal. 1992;11(7):2407-14.
287. Hagag IT, Mansour SMG, Zhang Z, Ali AAH, Ismaiel E-BM, Salama AA, et al. Pathogenicty of Highly Pathogenic Avian Influenza Virus H5N1 in Naturally Infected Poultry in Egypt. PLoS ONE. 2015;10(5).
288. Berhane Y, Hisanaga T, Kehler H, Neufeld J, Manning L, Argue C, et al. Highly Pathogenic Avian Influenza Virus A (H7N3) in Domestic Poultry, Saskatchewan, Canada, 2007. Emerging Infectious Diseases. 2009;15(9):1492-5.
289. Killian ML, Kim-Torchetti M, Hines N, Yingst S, DeLiberto TJ, Lee D-H. Outbreak of H7N8 Low Pathogenic Avian Influenza in Commercial Turkeys with Spontaneous Mutation to Highly Pathogenic Avian Influenza. Genome Announcements. 2016;4(3).

290. Stech O, Veits J, Weber S, Deckers D, Schröer D, Vahlenkamp TW, et al. Acquisition of a Polybasic Hemagglutinin Cleavage Site by a Low-Pathogenic Avian Influenza Virus Is Not Sufficient for Immediate Transformation into a Highly Pathogenic Strain. Journal of Virology. 2009;83(11):5864-8.
291. Chen J, Zhang J, Zhu W, Zhang Y, Tan H, Liu M, et al. First genome report of chicken H7N9 influenza viruses with poly-basic amino acids insertion in the hemagglutinin cleavage site. Scientific Reports. 2017;7(9972).
292. Imai M, Watanabe T, Hatta M, Das SC, Ozawa M, Shinya K, et al. Experimental adaptation of an influenza H5 NA confers respiratory droplet transmission to a reassortant H5 HA/H1N1 virus in ferrets. Nature. 2012;486:420-8.
293. Qi X, Zhang H, Wang Q, Wang J. The NS1 protein of avian influenza virus H9N2 induces oxidative-stress-mediated chicken oviduct epithelial cells apoptosis. Journal of General Virology. 2016;97:3183-92.
294. Burggraaf S, Bingham J, Payne J, Kimpton WG, Lowenthal JW, Bean AGD. Increased Inducible Nitric Oxide Synthase Expression in Organs Is Associated with a Higher Severity of H5N1 Influenza Infection. PLoS ONE. 2011;6(1).
295. Jia D, Rahbar R, Chan RWY, Lee SMY, Chan MCW, Wang BX, et al. Influenza Virus Non-Structural Protein 1 (NS1) Disrupts Interferon Signalling. PLoS ONE. 2010;5(11).
296. Wang J, Zeng Y, Xu S, Yang J, Wang W, Zhong B, et al. A Naturally Occuring Deletion in the Effector Domain of H5N1 Swine Influenza Virus Nonstructural Protein 1 Regulates Viral Fitness and Host Innate Immunity. Journal of Virology. 2018.
297. Jiao P, Tian G, Li Y, Deng G, Jiang Y, Liu C, et al. A Single-Amino-Acid Substitution in the NS1 Protein Changes the Pathogenicity of H5N1 Avian Influenza Viruses in Mice. Journal of Virology. 2008;82(3):1146-54.
298. Wang L, Fu X, Zheng Y, Zhou P, Fang B, Huang S, et al. The NS1 protein of H5N6 feline influenza virus inhibits feline beta interfereon response by preventing NF-κB and IRF3 activation. Developmental & Comparative Immunology. 2017;74:60-8.
299. Thube MM, Shil P, Kasbe R, Patil AA, Pawar SD, Mullick J. Differences in Type I interferon response in human lung epithelial cells infected by highly pathogenic H5N1 and low pathogenic H11N1 avian influenza viruses. Virus Genes. 2018.
300. Ayllon J, Domingues P, Rajsbaum R, Miorin L, Schmolke M, Hale BG, et al. A Single Amino Acid Substitution in the Novel H7N9 Influenza A NS1 Protein Increases CPSF30 Binding and Virulence. Journal of Virology. 2014;88(20):12146-51.
301. Cheng VCC, Chan JFW, Wen X, Wu WL, Que TL, Chen H, et al. Infection of immunocompromised patients by avian H9N2 influenza A virus. Journal of Infection. 2011;62:394-9.
302. Law AH-Y, Lee DC-W, Yuen K-Y, Peiris JSM, Lau AS-Y. Cellular response to influenza virus infection: a potential role for autophagy in CXCL10 and interferon-alpha induction. Cellular & Molecular Immunolgy. 2010;7:263-70.
303. Nili H, Asasi K. Avian Influenza (H9N2) Outbreak in Iran. Avian Diseases. 2003;47(s3):828-31.
304. Nili H, Asasi K. Natural cases and an experimental study of H9N2 avian influenza in commercial broiler chickens of Iran. Avian Pathology. 2002;31(3):247-52.
305. Valkenburg SA, Josephs TM, Clemens EB, Grant EJ, Nguyen THO, Wang GC, et al. Molecular basis for universal HLA-A*0201-restricted CD8+ T-cell immunity against influenza viruses. PNAS. 2016;113(16):4440-5.
306. Quiñones-Parra S, Grant EJ, Loh L, Nguyen THO, Campbell K-A, Tong SYC, et al. Preexisting CD8+ T-cell immunity to the H7N9 influenza A virus varies across ethnicities. PNAS. 2014;111(3):1049-54.
307. Nguyen THO, Sant S, Bird NJ, Grant EJ, Clemens EB, Koutsakos M, et al. Perturbed CD8+ T cell immunity across universal influenza epitopes in the elderly. Journal of Leukocyte Biology. 2017;103(2):321-39.
308. Clemens EB, Grant EJ, Wang Z, Gras S, Tipping P, Rossjohn J, et al. Towards identification of immune and genetic correlates of severe influenza disease in Indigenous Australians. Immunology and Cell Biology. 2016;94(367-377).

309. Hertz T, Oshansky CM, Roddam PL, DeVincenzo JP, Caniza MA, Jojic N, et al. HLA targeting efficiency correlates with human T-cell response magnitude and with mortality from influenza A infection. PNAS. 2013;110(33):13492-7.
310. Liu R, Moise L, Tassone R, Gutierrez AH, Terry FE, Sangare K, et al. H7N9 T-cell epitopes that mimic human sequences are less immunogenic and may induce Treg-mediated tolerance. Human Vaccines & Immunotherapuetics. 2015;11(9):2241-52.
311. Hou Y, Guo Y, Wu C, Shen N, Jiang Y, Wang J. Prediction and Identification of T Cell Epitopes in the H5N1 Influenza Virus Nucleoprotein in Chicken. PLoS ONE. 2012;7(6).
312. Zhang W, Huang Q, Lu M, Zhu F, Huang Y-y, Yang S-h, et al. Exploration of the BF2*15 major histocompatability complex class I binding motif and identification of cytotoxic T lymphocyte epitopes from the H5N1 influenza virus nucleoprotein in chickens. Archives Of Virology. 2016;161:3081-93.
313. Fleming-Canepa X, Jensen SM, Mesa CM, Diaz-Satizabal L, Roth AJ, Parks-Dely JA, et al. Extensive Allelic Diversity of MHC Class I in Wild Mallard Ducks. The Journal of Immunology. 2016;197:783-94.
314. Wu Y, Wang J, Fan S, Chen R, Liu Y, Zhang J, et al. Structural Definition of Duck Major Histocompatibility Complex Class I Molecules That Might Explain Efficient Cytotoxic T Lymphocyte Immunity to Influenza A Virus. Journal of Virology. 2017;91(14).
315. Buehler DM, Verkuil YI, Tavares ES, Baker AJ. Characterization of MHC class I in a long-distance migrant shorebird suggests multiple transcribed genes and intergenic recombination. Immunogenetics. 2013;65:211-25.
316. Bailey CC, Kondur HR, Huang I-C, Farzan M. Interferon-induced Transmembrane Protein 3 is a Type II Transmembrane Protein. The Journal of Biological Chemistry. 2013;288(45):32184-93.
317. Bailey CC, Zhong G, Huang I-C, Farzan M. IFITM-Family Proteins: The Cell's First Line of Antiviral Defense. Annual Review of Virology. 2014;1:261-83.
318. Siegrist F, Ebeling M, Certa U. The Small Interferon-Induced Transmembrane Genes and Proteins. Journal of Interferon & Cytokine Research. 2010;31(1):183-97.
319. Smith SE, Gibson MS, Wash RS, Ferrara F, Wright E, Temperton N, et al. Chicken Interferon-Inducible Transmembrane Protein 3 Restricts Influenza Viruses and Lyssaviruses In Vitro. Journal of Virology. 2013;87(23):12957.
320. Weston S, Czieso S, White IJ, Smith SE, Kellam P, Marsh M. A Membrane Topology Model for Human Interferon Inducible Transmembrane Protein 1. PLOS ONE. 2014;9(8):e104341.
321. Hach JC, McMichael T, Chesarino NM, Yount JS. Palmitoylation on Conserved and Nonconserved Cysteines of Murine IFITM1 Regulates Its Stability and Anti-Influenza A Virus Activity. Journal of Virology. 2013;87(17):9923.
322. Narayana SK, Helbig KJ, McCartney EM, Eyre NS, Bull RA, Eltahla A, et al. The Interferon-induced Transmembrane Proteins, IFITM1, IFITM2, and IFITM3 Inhibit Hepatitis C Virus Entry. J Biol Chem. 2015;290(43):25946-59.
323. Feeley EM, Sims JS, John SP, Chin CR, Pertel T, Chen L-M, et al. IFITM3 Inhibits Influenza A Virus Infection by Preventing Cytosolic Entry. PloS Pathogens. 2011;7(10).
324. Brass AL, Huang I-C, Benita Y, John SP, Krishnan MN, Feeley EM, et al. The IFITM Proteins Mediate Cellular Resistance to Influenza A H1N1 Virus, West Nile Virus, and Dengue Virus. Cell. 2009;139:1243-54.
325. Jia R, Pan Q, Ding S, Rong L, Liu S-L, Geng Y, et al. The N-Terminal Region of IFITM3 Modulates Its Antiviral Activity by Regulating IFITM3 Cellular Localization. 86. 2012;24(13697-13707).
326. Wakim LM, Gupta N, Mintern JD, Villadangos JA. Enhanced survival of tissue-resident memory CD8+ T cells during infection with influenza virus due to selective expression of IFITM3. Nature Immunology. 2013;14(3):238-46.
327. Shi G, Kenney AD, Kudryashova E, Zani A, Zhang L, Lai KK, et al. Opposing activities of IFITM proteins in SARS-CoV-2 infection. The EMBO journal. 2020:e106501.

328. Wrensch F, Winkler M, Pöhlmann SJV. IFITM proteins inhibit entry driven by the MERS-coronavirus spike protein: evidence for cholesterol-independent mechanisms. 2014;6(9):3683-98.
329. Zhao X, Guo F, Liu F, Cuconati A, Chang J, Block TM, et al. Interferon induction of IFITM proteins promotes infection by human coronavirus OC43. 2014;111(18):6756-61.
330. Bozzo CP, Nchioua R, Volcic M, Krüger J, Heller S, Stürzel CM, et al. IFITM proteins promote SARS-CoV-2 infection and are targets for virus inhibition. bioRxiv : the preprint server for biology. 2020:2020.08.18.255935.
331. Yang X, Tan B, Zhou X, Xue J, Zhang X, Wang P, et al. Interferon-Inducible Transmembrane Protein 3 Genetic Variant rs12252 and Influenza Susceptibility and Severity: A Meta-Analysis. PLoS ONE. 2015;10(5).
332. Zhang Y-H, Zhao Y, Li N, Peng Y-C, Giannoulatou E, Jin R-H, et al. Interferon-induced transmembrane protein-3 genetic variant rs12252-C is associated with severe influenza in Chinese individuals. Nature Communications. 2013;4(1418).
333. Wang Z, Zhang A, Wan Y, Liu X, Qiu C, Xi X, et al. Early hypercytokinemia is associated with interferon-induced transmembrane protein-3 dysfunction and predictive of fatal H7N9 infection. PNAS. 2014;111(2):769-74.
334. Zhang Y, Qin L, Zhao Y, Zhang P, Xu B, Li K, et al. Interferon-Induced Transmembrane Protein 3 Genetic Variant rs12252-C Associated With Disease Severity in Coronavirus Disease 2019. J Infect Dis. 2020;222(1):34-7.
335. Williams DEJ, Wu W-L, Grotefend CR, Radic V, Chung C, Chung Y-H, et al. IFITM3 Polymorphism rs12252-C Restricts Influenza A Viruses. PLoS ONE. 2014;9(10).
336. Makvandi-Nejad S, Luaurenson-Schafer H, Wang L, Wellington D, Zhao Y, Jin B, et al. Lack of Truncated IFITM3 Transcripts in Cells Homozygous for the rs12252-C Variant That is Associated With Severe Influeza Infection. The Journal of Infectious Diseases. 2018;217(257-262).
337. Allen EK, Randolph AG, Bhangale T, Dogra P, Ohlson M, Oshansky CM, et al. SNP-mediated disruption of CTCF binding at the IFITM3 promoter is associated with risk of severe influenza in humans. Nature Medicine. 2017;23:975-83.
338. Nikoloudis D, Kountouras D, Hiona A. The frequency of combined IFITM3 haplotype involving the reference alleles of both rs12252 and rs34481144 is in line with COVID-19 standardized mortality ratio of ethnic groups in England. PeerJ. 2020;8:e10402.
339. Kim YC, Jeong BH. Strong Correlation between the Case Fatality Rate of COVID-19 and the rs6598045 Single Nucleotide Polymorphism (SNP) of the Interferon-Induced Transmembrane Protein 3 (IFITM3) Gene at the Population-Level. Genes. 2020;12(1).
340. Bailey CC, Huang IC, Kam C, Farzan M. Ifitm3 Limits the Severity of Acute Influenza in Mice. PLOS Pathogens. 2012;8(9):e1002909.
341. Yu M, Qi W, Huang Z, Zhang K, Ye J, Liu R, et al. Expression profile and histological distribution of IFITM1 and IFITM3 during H9N2 avian influenza virus infection in BALB/c mice. Medical Microbiology and Immunology. 2015;204:505-14.
342. Benfield CTO, Smith SE, Wright E, Wash RS, Ferrara F, Temperton NJ, et al. Bat and pig IFN-induced transmembrane protein 3 restrict cell entry by influenza virus and lyssavirus. Journal of General Virology. 2015;96:991-1005.
343. Smith SE, Gibson MS, Wash RS, Ferrara F, Wright E, Temperton NJ, et al. Chicken Interferon-Inducible Transmembrane Protein 3 Restricts Influenza Viruses and Lyssaviruses In Vitro. Journal of Virology. 2013;87(23):12957-66.
344. Cao Y, Huang Y, Xu K, Liu Y, Li X, Xu Y, et al. Differential responses of innate immunity triggered by different subtypes of influenza a viruses in human and avian hosts. BMC Medical Genomics. 2017;10(70).
345. Smith J, Smith N, Yu L, paton IR, Gutowska MW, Forrest HL, et al. A comparative analysis of host responses to avian influenza infection in ducks and chickens highlights a role for the interferon-induced transmembrane proteins in viral resistance. BMC Genomics. 2015;16(574).
346. Belser JA, Katz JM, Tumpey TM. The ferret as a model organism to study influenza A virus infection. Disease Models & Mechanisms. 2011;4(5):575.

347. Sweet C, Price GE, Fenton RJ. Chapter 119 - The Ferret as an Animal Model of Influenza Virus Infection. In: Zak O, Sande MA, editors. Handbook of Animal Models of Infection. London: Academic Press; 1999. p. 989-98.
348. Zitzow LA, Rowe T, Morken T, Shieh W-J, Zaki S, Katz JM. Pathogenesis of Avian Influenza A (H5N1) Viruses in Ferrets. Journal of Virology. 2002;76(9):4420.
349. Oh DY, Hurt AC. Using the Ferret as an Animal Model for Investigating Influenza Antiviral Effectiveness. Frontiers in microbiology. 2016;7:80-.
350. Maines TR, Lu XH, Erb SM, Edwards L, Guarner J, Greer PW, et al. Avian influenza (H5N1) viruses isolated from humans in Asia in 2004 exhibit increased virulence in mammals. Journal of virology. 2005;79(18):11788-800.
351. van Riel D, Munster VJ, de Wit E, Rimmelzwaan GF, Fouchier RAM, Osterhaus ADME, et al. Human and Avian Influenza Viruses Target Different Cells in the Lower Respiratory Tract of Humans and Other Mammals. The American Journal of Pathology. 2007;171(4):1215-23.
352. Xu S, Li X, Yang J, Wang Z, Jia Y, Han L, et al. Comparative Pathogenicity and Transmissibility of Pandemic H1N1, Avian H5N1, and Human H7N9 Influenza Viruses in Tree Shrews. Frontiers In Microbiology. 2019;10(2955).
353. Moore IN, Lamirande EW, Paskel M, Donahue D, Kenney H, Qin J, et al. Severity of clinical disease and pathology in ferrets experimentally infected with influenza viruses is influenced by inoculum volume. Journal of virology. 2014;88(23):13879-91.
354. Svitek N, Rudd PA, Obojes K, Pillet S, von Messling V. Severe seasonal influenza in ferrets correlates with reduced interferon and increased IL-6 induction. Virology. 2008;376(1):53-9.
355. Tumpey TM, Lu X, Morken T, Zaki SR, Katz JMJJov. Depletion of lymphocytes and diminished cytokine production in mice infected with a highly virulent influenza A (H5N1) virus isolated from humans. 2000;74(13):6105-16.
356. Szretter KJ, Gangappa S, Lu X, Smith C, Shieh W-J, Zaki SR, et al. Role of Host Cytokine Responses in the Pathogenesis of Avian H5N1 Influenza Viruses in Mice. Journal of Virology. 2007;81(6):2736.
357. Herlocher ML, Elias S, Truscon R, Harrison S, Mindell D, Simon C, et al. Ferrets as a transmission model for influenza: sequence changes in HA1 of type A (H3N2) virus. J Infect Dis. 2001;184(5):542-6.
358. Maher JA, DeStefano J. The ferret: an animal model to study influenza virus. Lab animal. 2004;33(9):50-3.
359. DiPiazza A, Richards K, Batarse F, Lockard L, Zeng H, García-Sastre A, et al. Flow Cytometric and Cytokine ELISpot Approaches To Characterize the Cell-Mediated Immune Response in Ferrets following Influenza Virus Infection. Journal of virology. 2016;90(17):7991-8004.
360. Ryan KA, Slack GS, Marriott AC, Kane JA, Whittaker CJ, Silman NJ, et al. Cellular immune response to human influenza viruses differs between H1N1 and H3N2 subtypes in the ferret lung. PLOS ONE. 2018;13(9):e0202675.
361. Music N, Reber AJ, Kim JH, York IA. Peripheral Leukocyte Migration in Ferrets in Response to Infection with Seasonal Influenza Virus. PLOS ONE. 2016;11(6):e0157903.
362. Layton DS, Xiao X, Bentley JD, Lu L, Stewart CR, Bean AGD, et al. Development of an anti-ferret CD4 monoclonal antibody for the characterisation of ferret T lymphocytes. Journal of Immunological Methods. 2017;444:29-35.
363. Haller O, Staeheli P, Schwemmle M, Kochs G. Mx GTPases: dynamin-like antiviral machines of innate immunity. Trends in microbiology. 2015;23(3):154-63.
364. Villalón-Letelier F, Brooks AG, Saunders PM, Londrigan SL, Reading PC. Host Cell Restriction Factors that Limit Influenza A Infection. Viruses. 2017;9(12).
365. Carolan LA, Butler J, Rockman S, Guarnaccia T, Hurt AC, Reading P, et al. TaqMan real time RT-PCR assays for detecting ferret innate and adaptive immune responses. Journal of Virological Methods. 2014;205:38-52.

366. Carolan LA, Rockman S, Borg K, Guarnaccia T, Reading P, Mosse J, et al. Characterization of the Localized Immune Response in the Respiratory Tract of Ferrets following Infection with Influenza A and B Viruses. Journal of Virology. 2016;90(6):2838.
367. Hatta Y, Boltz D, Sarawar S, Kawaoka Y, Neumann G, Bilsel P. Novel influenza vaccine M2SR protects against drifted H1N1 and H3N2 influenza virus challenge in ferrets with pre-existing immunity. Vaccine. 2018;36(33):5097-103.
368. Carter DM, Darby CA, Johnson SK, Carlock MA, Kirchenbaum GA, Allen JD, et al. Elicitation of Protective Antibodies against a Broad Panel of H1N1 Viruses in Ferrets Preimmune to Historical H1N1 Influenza Viruses. Journal of virology. 2017;91(24):e01283-17.
369. Forrest HL, Khalenkov AM, Govorkova EA, Kim J-K, Del Giudice G, Webster RG. Single- and multiple-clade influenza A H5N1 vaccines induce cross protection in ferrets. Vaccine. 2009;27(31):4187-95.
370. Pascua PNQ, Song M-S, Lee JH, Park KJ, Kwon H-I, Baek YH, et al. Evaluation of the efficacy and cross-protectivity of recent human and swine vaccines against the pandemic (H1N1) 2009 virus infection. PloS one. 2009;4(12):e8431-e.
371. Wong S-S, Duan S, DeBeauchamp J, Zanin M, Kercher L, Sonnberg S, et al. The immune correlates of protection for an avian influenza H5N1 vaccine in the ferret model using oil-in-water adjuvants. Scientific Reports. 2017;7(1):44727.
372. Middleton D, Rockman S, Pearse M, Barr I, Lowther S, Klippel J, et al. Evaluation of Vaccines for H5N1 Influenza Virus in Ferrets Reveals the Potential for Protective Single-Shot Immunization. Journal of Virology. 2009;83(15):7770.
373. Reed LJ, Muench H. A Simple Method of Estimating Fifty Per Cent Endpoints. American Journal of Epidemiology. 1938;27(3):493-7.
374. Laurie KL, Horman W, Carolan LA, Chan KF, Layton D, Bean A, et al. Evidence for Viral Interference and Cross-reactive Protective Immunity Between Influenza B Virus Lineages. J Infect Dis. 2018;217(4):548-59.
375. Butler J, Stewart CR, Layton DS, Phommachanh P, Harper J, Payne J, et al. Novel Reassortant H5N6 Influenza A Virus from the Lao People's Democratic Republic Is Highly Pathogenic in Chickens. PLOS ONE. 2016;11(9):e0162375.
376. Wibawa H, Bingham J, Nuradji H, Lowther S, Payne J, Harper J, et al. The pathobiology of two Indonesian H5N1 avian influenza viruses representing different clade 2.1 sublineages in chickens and ducks. Comparative Immunology, Microbiology and Infectious Diseases. 2013;36(2):175-91.
377. Yates AD, Achuthan P, Akanni W, Allen J, Allen J, Alvarez-Jarreta J, et al. Ensembl 2020. Nucleic Acids Research. 2020;48(D1):D682-D8.
378. Burge C, Karlin S. Prediction of complete gene structures in human genomic DNA. J Mol Biol. 1997;268(1):78-94.
379. Kumar S, Stecher G, Tamura K. MEGA7: Molecular Evolutionary Genetics Analysis Version 7.0 for Bigger Datasets. Mol Biol Evol. 2016;33(7):1870-4.
380. World Health Organization. Weekly epidemiological update - 23 February 2021: World Health Organisation; 2021 [Available from: https://www.who.int/publications/m/item/weekly-epidemiological-update---23-february-2021.
381. Draper SJ, Moore AC, Goodman AL, Long CA, Holder AA, Gilbert SC, et al. Effective induction of high-titer antibodies by viral vector vaccines. Nat Med. 2008;14(8):819-21.
382. Shi J, Wen Z, Zhong G, Yang H, Wang C, Huang B, et al. Susceptibility of ferrets, cats, dogs, and other domesticated animals to SARS–coronavirus 2. Science. 2020;368(6494):1016.
383. Schlottau K, Rissmann M, Graaf A, Schön J, Sehl J, Wylezich C, et al. SARS-CoV-2 in fruit bats, ferrets, pigs, and chickens: an experimental transmission study. The Lancet Microbe. 2020;1(5):e218-e25.
384. Kim YI, Kim SG, Kim SM, Kim EH, Park SJ, Yu KM, et al. Infection and Rapid Transmission of SARS-CoV-2 in Ferrets. Cell Host Microbe. 2020;27(5):704-9.e2.

385. Weiskopf D, Schmitz KS, Raadsen MP, Grifoni A, Okba NMA, Endeman H, et al. Phenotype and kinetics of SARS-CoV-2–specific T cells in COVID-19 patients with acute respiratory distress syndrome. Science Immunology. 2020;5(48):eabd2071.
386. Braun J, Loyal L, Frentsch M, Wendisch D, Georg P, Kurth F, et al. SARS-CoV-2-reactive T cells in healthy donors and patients with COVID-19. Nature. 2020.
387. Grifoni A, Weiskopf D, Ramirez SI, Mateus J, Dan JM, Moderbacher CR, et al. Targets of T Cell Responses to SARS-CoV-2 Coronavirus in Humans with COVID-19 Disease and Unexposed Individuals. Cell. 2020;181(7):1489-501.e15.
388. Habel JR, Nguyen THO, van de Sandt CE, Juno JA, Chaurasia P, Wragg K, et al. Suboptimal SARS-CoV-2-specific CD8(+) T cell response associated with the prominent HLA-A*02:01 phenotype. Proceedings of the National Academy of Sciences of the United States of America. 2020;117(39):24384-91.
389. Diao B, Wang C, Tan Y, Chen X, Liu Y, Ning L, et al. Reduction and Functional Exhaustion of T Cells in Patients With Coronavirus Disease 2019 (COVID-19). 2020;11(827).
390. Horman WSJ, Nguyen THO, Kedzierska K, Butler J, Shan S, Layton R, et al. The Dynamics of the Ferret Immune Response During H7N9 Influenza Virus Infection. Front Immunol. 2020;11(2199).
391. De Koker S, Van Hoecke L, De Beuckelaer A, Roose K, Deswarte K, Willart MA, et al. Inflammatory monocytes regulate Th1 oriented immunity to CpG adjuvanted protein vaccines through production of IL-12. Scientific Reports. 2017;7(1):5986.
392. Luger D, Yang Y-A, Raviv A, Weinberg D, Banerjee S, Lee M-J, et al. Expression of the B-cell receptor component CD79a on immature myeloid cells contributes to their tumor promoting effects. PloS one. 2013;8(10):e76115-e.
393. Dworzak MN, Fritsch G, Fröschl G, Printz D, Gadner H. Four-color flow cytometric investigation of terminal deoxynucleotidyl transferase-positive lymphoid precursors in pediatric bone marrow: CD79a expression precedes CD19 in early B-cell ontogeny. Blood. 1998;92(9):3203-9.
394. Lederer K, Castaño D, Gómez Atria D, Oguin TH, 3rd, Wang S, Manzoni TB, et al. SARS-CoV-2 mRNA Vaccines Foster Potent Antigen-Specific Germinal Center Responses Associated with Neutralizing Antibody Generation. Immunity. 2020;53(6):1281-95.e5.
395. Helmold Hait S, Vargas-Inchaustegui DA, Musich T, Mohanram V, Tuero I, Venzon DJ, et al. Early T Follicular Helper Cell Responses and Germinal Center Reactions Are Associated with Viremia Control in Immunized Rhesus Macaques. J Virol. 2019;93(4).
396. Bentebibel SE, Khurana S, Schmitt N, Kurup P, Mueller C, Obermoser G, et al. ICOS(+)PD-1(+)CXCR3(+) T follicular helper cells contribute to the generation of high-avidity antibodies following influenza vaccination. Sci Rep. 2016;6:26494.
397. Jiang W, Wong J, Tan H-X, Kelly HG, Whitney PG, Barr I, et al. Screening and development of monoclonal antibodies for identification of ferret T follicular helper cells. Scientific Reports. 2021;11(1):1864.
398. Jackson LA, Anderson EJ, Rouphael NG, Roberts PC, Makhene M, Coler RN, et al. An mRNA Vaccine against SARS-CoV-2 — Preliminary Report. New England Journal of Medicine. 2020;383(20):1920-31.
399. De Biasi S, Meschiari M, Gibellini L, Bellinazzi C, Borella R, Fidanza L, et al. Marked T cell activation, senescence, exhaustion and skewing towards TH17 in patients with COVID-19 pneumonia. Nat Commun. 2020;11(1):3434.
400. Sahin U, Muik A, Derhovanessian E, Vogler I, Kranz LM, Vormehr M, et al. COVID-19 vaccine BNT162b1 elicits human antibody and T(H)1 T cell responses. Nature. 2020;586(7830):594-9.
401. Lee ACY, Zhu H, Zhang AJX, Li C, Wang P, Li C, et al. Suboptimal Humoral Immune Response against Influenza A(H7N9) Virus Is Related to Its Internal Genes. Clinical and Vaccine Immunology. 2015;22(12):1235.
402. Zhu Z, Yang Y, Feng Y, Shi B, Chen L, Zheng Y, et al. Infection of inbred BALB/c and C57BL/6 and outbred Institute of Cancer Research mice with the emerging H7N9 avian influenza virus. Emerg Microbes Infect. 2013;2(1):1-7.

403. Boonnak K, Vogel L, Feldmann F, Feldmann H, Legge KL, Subbarao K. Lymphopenia associated with highly virulent H5N1 virus infection due to plasmacytoid dendritic cell-mediated apoptosis of T cells. Journal of immunology (Baltimore, Md : 1950). 2014;192(12):5906-12.
404. Wang Z, Wan Y, Qiu C, Quiñones-Parra S, Zhu Z, Loh L, et al. Recovery from severe H7N9 disease is associated with diverse response mechanisms dominated by CD8+ T cells. Nature communications. 2015;6:6833-.
405. Morrison J, Josset L, Tchitchek N, Chang J, Belser JA, Swayne DE, et al. H7N9 and Other Pathogenic Avian Influenza Viruses Elicit a Three-Pronged Transcriptomic Signature That Is Reminiscent of 1918 Influenza Virus and Is Associated with Lethal Outcome in Mice. Journal of Virology. 2014;88(18):10556-68.
406. Pero SC, Sun YJ, Shukla GS, Carman CL, Krag CC, Teuscher C, et al. Vaccine draining lymph nodes are a source of antigen-specific B cells. Vaccine. 2017;35(9):1259-65.
407. Rattan A, Richards KA, Knowlden ZAG, Sant AJ. Protein Vaccination Directs the CD4+ T Cell Response toward Shared Protective Epitopes That Can Be Recalled after Influenza Virus Infection. Journal of Virology. 2019;93(20):e00947-19.
408. de Alwis R, Chen S, Gan ES, Ooi EEJE. Impact of immune enhancement on Covid-19 polyclonal hyperimmune globulin therapy and vaccine development. 2020:102768.
409. Ewer KJ, Barrett JR, Belij-Rammerstorfer S, Sharpe H, Makinson R, Morter R, et al. T cell and antibody responses induced by a single dose of ChAdOx1 nCoV-19 (AZD1222) vaccine in a phase 1/2 clinical trial. Nature Medicine. 2020.
410. Neidleman J, Luo X, Frouard J, Xie G, Gurjot G, Stein ES, et al. SARS-CoV-2-specific T cells exhibit unique features characterized by robust helper function, lack of terminal differentiation, and high proliferative potential. 2020.
411. Zhao J, Zhao J, Mangalam AK, Channappanavar R, Fett C, Meyerholz DK, et al. Airway memory CD4+ T cells mediate protective immunity against emerging respiratory coronaviruses. 2016;44(6):1379-91.
412. Westmeier J, Paniskaki K, Karaköse Z, Werner T, Sutter K, Dolff S, et al. Impaired Cytotoxic CD8⁺ T Cell Response in Elderly COVID-19 Patients. mBio. 2020;11(5):e02243-20.
413. Huang J-L, Huang J, Duan Z-H, Wei J, Min J, Luo X-H, et al. Th2 predominance and CD8+ memory T cell depletion in patients with severe acute respiratory syndrome. Microbes Infect. 2005;7(3):427-36.
414. Jeyanathan M, Afkhami S, Smaill F, Miller MS, Lichty BD, Xing Z. Immunological considerations for COVID-19 vaccine strategies. Nature Reviews Immunology. 2020;20(10):615-32.
415. Rosenthal KS, Zimmerman DH. Vaccines: all things considered. Clin Vaccine Immunol. 2006;13(8):821-9.
416. Greinacher A, Thiele T, Warkentin TE, Weisser K, Kyrle PA, Eichinger S. Thrombotic Thrombocytopenia after ChAdOx1 nCov-19 Vaccination. New England Journal of Medicine. 2021;384(22):2092-101.
417. MacIntyre CR, Veness B, Berger D, Hamad N, Bari N. Thrombosis with Thrombocytopenia Syndrome (TTS) following AstraZeneca ChAdOx1 nCoV-19 (AZD1222) COVID-19 vaccination – A risk–benefit analysis for people < 60 years in Australia. Vaccine. 2021;39(34):4784-7.
418. Schmidt T, Klemis V, Schub D, Mihm J, Hielscher F, Marx S, et al. Immunogenicity and reactogenicity of heterologous ChAdOx1 nCoV-19/mRNA vaccination. Nature Medicine. 2021.
419. Brass AL, Huang IC, Benita Y, John SP, Krishnan MN, Feeley EM, et al. The IFITM Proteins Mediate Cellular Resistance to Influenza A H1N1 Virus, West Nile Virus, and Dengue Virus. Cell. 2009;139(7):1243-54.
420. Huang IC, Bailey CC, Weyer JL, Radoshitzky SR, Becker MM, Chiang JJ, et al. Distinct patterns of IFITM-mediated restriction of filoviruses, SARS coronavirus, and influenza A virus. PLoS pathogens. 2011;7(1):e1001258-e.

421. Wang Z, Zhang A, Wan Y, Liu X, Qiu C, Xi X, et al. Early hypercytokinemia is associated with interferon-induced transmembrane protein-3 dysfunction and predictive of fatal H7N9 infection. Proceedings of the National Academy of Sciences. 2014;111(2):769.
422. Schulien I, Kemming J, Oberhardt V, Wild K, Seidel LM, Killmer S, et al. Characterization of pre-existing and induced SARS-CoV-2-specific CD8(+) T cells. Nat Med. 2021;27(1):78-85.

Appendix

The following manuscripts have been generated which includes work conducted during the duration of this thesis.

frontiers in Immunology

REVIEW
published: 08 August 2018
doi: 10.3389/fimmu.2018.01812

The Drivers of Pathology in Zoonotic Avian Influenza: The Interplay Between Host and Pathogen

*William S. J. Horman[1,2], Thi H. O. Nguyen[1], Katherine Kedzierska[1], Andrew G. D. Bean[2] and Daniel S. Layton[2]**

[1] Department of Microbiology and Immunology, University of Melbourne at the Peter Doherty Institute for Infection and Immunity, Parkville, VIC, Australia, [2] Australian Animal Health Laboratory, Health and Biosecurity, Commonwealth Scientific and Industrial Research Organisation (CSIRO), East Geelong, VIC, Australia

The emergence of zoonotic strains of avian influenza (AI) that cause high rates of mortality in people has caused significant global concern, with a looming threat that one of these strains may develop sustained human-to-human transmission and cause a pandemic outbreak. Most notable of these viral strains are the H5N1 highly pathogenic AI and the H7N9 low pathogenicity AI viruses, both of which have mortality rates above 30%. Understanding of their mechanisms of infection and pathobiology is key to our preparation for these and future viral strains of high consequence. AI viruses typically circulate in wild bird populations, commonly infecting waterfowl and also regularly entering commercial poultry flocks. Live poultry markets provide an ideal environment for the spread AI and potentially the selection of mutants with a greater propensity for infecting humans because of the potential for spill over from birds to humans. Pathology from these AI virus infections is associated with a dysregulated immune response, which is characterized by systemic spread of the virus, lymphopenia, and hypercytokinemia. It has been well documented that host/pathogen interactions, particularly molecules of the immune system, play a significant role in both disease susceptibility as well as disease outcome. Here, we review the immune/virus interactions in both avian and mammalian species, and provide an overview or our understanding of how immune dysregulation is driven. Understanding these susceptibility factors is critical for the development of new vaccines and therapeutics to combat the next pandemic influenza.

Keywords: avian influenza virus, zoonosis, H7N9, H5N1, highly pathogenic avian influenza virus

OPEN ACCESS

Edited by:
Ding Oh,
Federation University, Australia

Reviewed by:
Alyson Ann Kelvin,
Dalhousie University, Canada
Elisa Vicenzi,
San Raffaele Hospital (IRCCS), Italy

***Correspondence:**
Daniel S. Layton
daniel.layton@csiro.au

Specialty section:
This article was submitted to Viral Immunology, a section of the journal Frontiers in Immunology

Received: *20 April 2018*
Accepted: *23 July 2018*
Published: *08 August 2018*

Citation:
Horman WSJ, Nguyen THO, Kedzierska K, Bean AGD and Layton DS (2018) The Drivers of Pathology in Zoonotic Avian Influenza: The Interplay Between Host and Pathogen. Front. Immunol. 9:1812. doi: 10.3389/fimmu.2018.01812

EMERGENCE OF AVIAN INFLUENZA (AI) VIRUS INFECTION IN HUMANS

Influenza A viruses have consistently posed a major threat to human health, both through seasonal infections and pandemic outbreaks (1). AI viruses have contributed significantly to this, and in recent years, highly pathogenic AI (HPAI) viruses have emerged as a major zoonotic threat. AI viruses naturally circulate in wild bird populations, including but not limited to, ducks and waterfowl, and can spill over to poultry birds such as chickens. Other than a few novel strains isolated in bats, all influenza A subtypes have been found in aquatic birds, which act as natural reservoirs for the viruses (2). These viruses typically replicate in the gastrointestinal and upper respiratory tract of both these natural hosts and chickens, and typically present as subclinical to mild disease (3, 4). Based on these clinical signs in chickens, these influenza viruses are classified as "low pathogenicity AI" (LPAI)

infections (5). Although many AI viruses circulate without causing serious disease, other viral subtypes can lead to more severe outbreaks within birds. Birds infected with these subtypes have more severe pathogenesis and rapid disease progression, often as the result of dissemination of the virus into tissues peripheral to the gastrointestinal and respiratory tracts. This type of infection in chickens defines the subtypes as HPAI (5). Highlighting the importance of HPAI viruses, recent outbreaks of HPAI H5N6 in China and the Philippines have caused approximately 37,000 bird deaths and 400,000 more culled at an economic cost of nearly $USD40 million (6, 7), and novel strains of H7 viruses such as H7N4 continue to cause sporadic outbreaks (8). While such outbreaks represent a significant economic burden to the poultry industry, of greater concern is the potential for HPAI viruses to cross the species barrier into mammals, especially humans.

Despite there being a broad range of AI subtypes, fortunately, only a very select subset of these have been shown to infect humans with highly pathogenic consequences (9). The first known HPAI infections in humans were highlighted by the outbreak of H5N1 avian-derived influenza in Hong Kong in 1997, leading to 6 deaths from 18 confirmed cases (10). Since then, sporadic outbreaks of H5N1 have had highly pathogenic consequences in humans, resulting in over 450 deaths from approximately 900 cases (11–13). The emergence of the avian-derived H7N9 strain infecting humans was first described in March 2013 in China's Yangtze River Delta, which has since caused 613 deaths out of 1,566 human cases throughout most of China as of January 2018 (14). This viral subtype is of a particular concern, as unlike H5N1, which is highly pathogenic in chickens and humans, H7N9 typically presents as an LPAI in chickens, but causes a high mortality rate in humans (40%), similar to that seen for H5N1 infections. H7N9 is one of several LPAI viruses in the H7 family capable of human infections, with viral transmission usually only acquired through close contact with host species (15–17). However, for reasons that are still unclear, H7N9 has greater transmissibility and more severe disease outcomes in humans than any other H7 viruses (18, 19). Thus, differences in clinical presentation across species, coupled with the potential of viruses such as H7N9 to cause a pandemic outbreak *via* evidence of human-to-human transmission (20), makes understanding the mechanisms by which these viruses cross the species barrier and become highly pathogenic in humans a critical area of investigation. Here, we discuss recent findings relating viral fitness to host susceptibility factors to understand how HPAI phenotypes are developed. We also outline how clinical manifestations following infection with LPAI or HPAI strains across different species provide further insights into the mechanisms underlying disease severity and susceptibility.

CLINICAL MANIFESTATIONS OF DISEASE IN DIFFERENT SPECIES

Human cases of AI infection have become increasingly common since outbreaks of H5N1 in the late 1990s and accentuated by a dramatic increase in H7N9 infections during the recent "fifth wave" of epidemic infections in China (21–23). These viruses were commonly contracted by people in regular close contact with live poultry markets (24, 25), where outbreaks of AI viruses in chickens can be common yet go largely unnoticed, especially in the case of H7N9 infections. Despite the vast diversity of AI viruses, predominantly only viruses from three hemagglutinin (HA) subtypes have been recorded to naturally infect humans: H5Nx viruses, most notably H5N1; H7Nx viruses such as H7N9; and H9Nx viruses, commonly H9N2. H9Nx strains present as LPAI infections in birds and have less severe symptoms in human hosts compared to H5 and H7 strains (26–29). Despite this, as H9N2 viruses are regularly found co-circulating with H5N1 and H7N9 with assortment frequently occurring between these viruses in poultry there is a real possibility of a novel HPAI strain emerging from these subtypes (30, 31). While there have been isolated cases of human infections with other subtypes, such as H10 (32), and H6 viruses which have been discussed as a potential precursor to H5N1 with pandemic potential (33–38), H5/H7/H9-subtypes of AI remain of greatest concern for human infections and potential pandemics. Thus, understanding the clinical manifestations of these viruses in avian hosts is needed for our understanding of why these viruses are considered such a threat.

In the case of LPAI, infections tend to localize in the mucosal surfaces of the gastrointestinal tract of infected birds and although often asymptomatic, chickens may present with mild clinical signs following infection. These include excess mucus and congested tracheae, watery droppings, and mild respiratory inflammation, with rarely any other signs of respiratory disease associated with influenza infections (3, 26, 39, 40). Highest viral titers typically occur 2–3 days after infection with limited gross lesions evident, allowing the virus to replicate and be excreted into the environment with little to no effect on the host animal (41, 42). Interestingly, ducks can exhibit even more limited clinical signs following LPAI infection than chickens (43). Thus, it is interesting to note that even in avian hosts, there is a range of clinical severity to LPAI viruses, with chickens showing more moderate/severe signs compared to waterfowl infected with LPAI.

In contrast to LPAI viruses, HPAI viruses have the ability to induce severe disease and cause devastating outbreaks with high mortality rates in poultry (44, 45). In chickens, H5N1 causes acute illness with high levels of viral shedding and clinical signs such as dehydration, nasal discharge, and lesions in many tissue types (46–48). While LPAI infections tend to remain within the fecal–oral tract of infected birds, HPAI infections are often identified by virus spreading systemically to multiple tissues (49). Suzuki and colleagues (50) described the pathology of H5N1 infections in chickens, finding that clinical signs progressed from milder signs such as feather ruffling and depression behavior, to the more severe outcomes of hemorrhaging and edema in multiple tissues. These birds also showed severe respiratory distress not seen in LPAI infections (50). By contrast, ducks can present with a wider range of symptoms following infection with HPAI H5N1, with experimentally infected ducks having clinical signs as mild as depressive behavior without any other complications (51). Ducks may also show severe signs such as those seen

in chickens, with common outcomes including neurological spread and hemorrhaging in the body extremities. In addition, Yamamoto and colleagues have also found that domestic ducks, unlike chickens, show corneal opacity following H5N1 infection and less severe hemorrhaging compared to chickens (52, 53). Likewise, wild ducks have been shown to exhibit less severe signs following H5N1 infection compared to other gallinaceous birds including domestic ducks, despite showing high levels of viral shedding consistent with an HPAI infection, which may suggest their role as a key reservoir species (48).

Avian influenza viruses also have the ability to infect pigs, which are housed in close proximity to human populations. Pigs often act as a "mixing vessel" for influenza viruses, which are able to reassort and thus infect humans (54, 55). While this is particularly the case for low pathogenicity viruses, there has been little evidence to suggest that pigs can contract highly pathogenic strains such as H5N1 and H7N9 to any great level, with H5N1 strains isolated from pigs in China found to be attenuated from the HPAI form (56). Although there have been no confirmed cases of H7N9 infection in pigs (57), H7N9 can replicate, cause pathology, and transmit among pigs during *in vivo* studies at low levels (58–60), as well as replicate in swine respiratory tissue *in vitro*, reinforcing the idea that pigs could still act as an important reservoir species for mammalian-adapted H7N9 (61). Of particular concern, reports of H7N2 infection in pigs (62) suggest that as the frequency of H7Nx cases increases, the likelihood of an H7N9 virus infecting pigs and potentially gaining stable mammalian transmissibility is a genuine possibility.

Studies in ferrets as a model for human infection have shown that mammalian-adapted AI viruses typically localize to the respiratory tract (63), however, these viruses have can have a limited ability to transmit *via* droplets (64–66). H5N1 viruses cause acute illness in the upper respiratory tract of ferrets with symptoms such as nasal discharge, high temperatures, and weight loss due to dehydration, and worsened pathogenesis, as highlighted by lung damage due to extensive infiltration of the lung tissue by inflammatory cells (18, 67, 68). H7N9 can also cause severe respiratory distress in this way, with lengthened time until viral clearance contributing to viral transmission and the substantial inflammation in the lungs of ferrets (69). Severe infections may cause complications such as viral pneumonia due to the breakdown of lung endothelial barriers, which contributes to this systemic spread and may lead to encephalitis or other neurological issues (18, 70). However, systemic spread to the central nervous system is more commonly associated with HPAI H5N1 than LPAI H7N9 (68).

Symptoms following human infection with AI are similar to those observed in the ferret model. Less severe cases present as more typical influenza infections, with symptoms such as fever and coughing among those commonly associated with influenza-related illness (16, 71). However, these viruses can cause severe respiratory illness following infection in the lungs, which may manifest as atypical viral pneumonia and acute respiratory distress syndrome, and often patients who have contracted these infections die from respiratory failure (72, 73). Furthermore, much like in birds, dissemination of the virus away from the site of infection leads to other complications such as organ failure, encephalitis, and internal bleeding due to tissue destruction (10, 71, 74), all of which contribute to the lethal nature of these viruses. A summary of the varying degrees of clinical manifestations between the different species is depicted in **Figure 1**. These trends, including the ability for an LPAI AI viruses such as H7N9 to cause severe fatal disease in humans, is therefore of great importance to understand the pathology driving the variable signs and symptoms of these infections across species to best combat future infections.

PATHOGENESIS OF HPAI INFECTIONS

Several factors appear to contribute to the worsened pathology observed in HPAI infections when compared with LPAI infections. One hallmark of HPAI pathogenesis is a rapid and robust cytokine response, often referred to as a "cytokine storm" or hypercytokinemia. This build-up of cytokines causes an inflammatory environment at the site of infection, leading to immune cell infiltration. In addition to the hypercytokinemia, there is a well-established loss of leukocytes, leading to the severe pathogenesis seen in these infections (75). Recently, the main factors associated with pathology were further described by Kuchipudi and colleagues (76). Following infection with H5N1 *in vitro*, chicken lung cells had increased expression of specific pro-inflammatory cytokines, particularly interleukins (IL)-6 and IL-8 when compared to cells infected with LPAI H2N3, suggesting that IL-6 and IL-8 may be key regulators leading to worsened pathology of HPAI compared to LPAI (76). IL-6 and IL-8 were also found to be significantly upregulated in the lungs of H5N1 infected ferrets, as well as in peripheral tissues, including the spleen, heart, and liver (77). Interestingly, this study also found that IL-6 and IL-8 were downregulated in the nasal turbinates following infection with pandemic H1N1 virus, which produced a less severe clinical infection compared to the H5N1 in ferrets (77). These findings were consistent with studies completed in rhesus macaques, which similarly showed upregulation of tumor necrosis factor α (TNFα), IL-6, and IL-8 in response to experimentally induced H5N1 infection, along with an increase in the antiviral interferons (IFNs), findings which correlate to the severe fever symptoms observed in the macaques at the peak of the fever response at day six post-infection (78). Moreover, infections with the recently emerged HPAI H5N6 in chickens, which caused human fatalities, was shown to have a very distinct immune response compared to other H5N6 strains by producing much higher levels of IL-6, IL-8, and other pro-inflammatory mediators such as TNFα compared to previously identified strains (79). While chickens and ferrets show similar pathogenesis, conversely, duck lung cells infected with the same viruses showed a decrease in IL-6 expression compared to the LPAI viruses, while IL-8 remained unchanged. It suggests that IL-6 may play a pivotal role in the regulation of AI pathology in birds and, as previously discussed, ducks typically show lessened disease severity following H5N1 infection compared to chickens (**Figure 1**). Moreover in humans, H5N1 elicits a similarly robust cytokine response, with the upregulation of IL-6, IL-10, and TNFα in response to H5N1 (80).

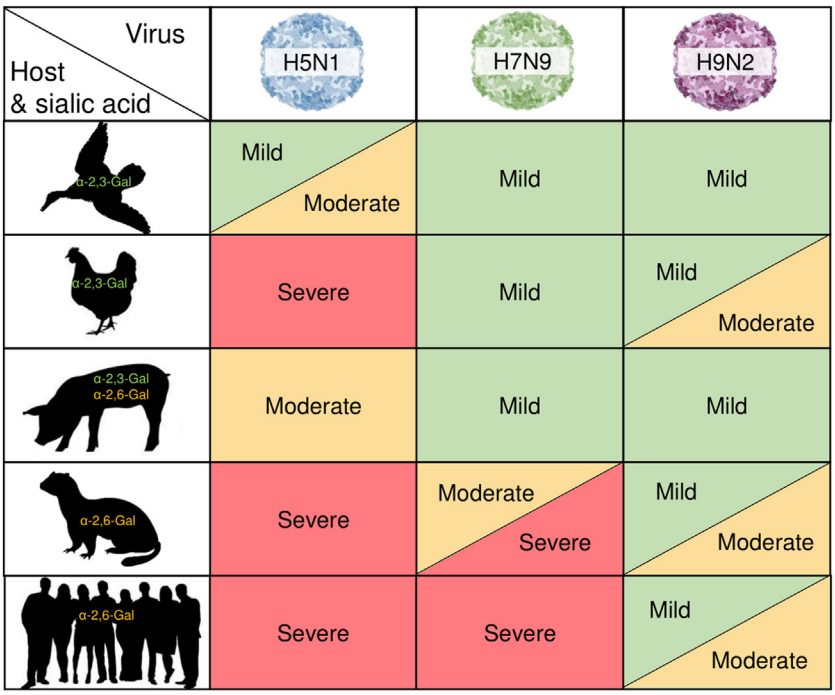

FIGURE 1 | Zoonotic influenza pathology is linked to host biology. H5N1, H7N9, and H9N2 avian influenza (AI) viruses causing varying degrees of clinical manifestations across different species is shown against different host and their sialic acid properties. AI viral hemagglutinin proteins selectively and preferentially bind to sialic residues with either an α-2,3-Gal or α-2,6-Gal terminating sequence on the host cell surface to allow for viral fusion and entry. This represents viral fitness and is a potential mechanism underlying the degree of disease severity and susceptibility in the different hosts.

As the H7N9 virus is classified as an LPAI in chickens, it is interesting to note that a similar trend was observed when H7N9 of human origin were shown to induce increased production of pro-inflammatory IL-6 and IL-8 cytokines when compared to H7N9 of chicken origin (81). In the same study, it was demonstrated that IFNλ1 production was reduced for the human isolate, suggesting a possible modulation of the immune response. In addition, Wu and colleagues also found that H7N9 patients had higher levels of C-reactive protein expression in their plasma compared to H1N1 patients, and as C-reactive protein is associated with broader inflammatory responses, it suggests that this may be yet another factor alongside these regulatory cytokines contributing to disease severity (82). A similar pro-inflammatory response was observed when alveolar macrophages were infected with H7N9, however, when compared to H5N1, this cytokine response was demonstrated to be milder (83). Downregulation of these inflammatory responses to infection confers a level of immunity to these viruses in pigs, which hints at how pigs can act as mixing vessel species for AI without succumbing to severe disease. Human lung epithelial cells can express 100-fold higher levels of TNFα compared to pig lung epithelia, with suppressor of cytokine signaling 3 (SOCS3) identified as a key factor in reducing levels of TNFα in pig cells (84).

The drivers of cytokine production are resident and infiltrating immune cells, which release these cytokines in response to the infection to recruit other immune cells and hinder viral replication. This occurs following cellular activation and results in further activation of leukocytes recruited to the area in a positive feedback loop (85). As pro-inflammatory molecules are associated with apoptotic pathways in humans, increased cytokine production is likely to be a contributing factor in the loss of immune cells, or leukopenia, observed in severe cases of HPAI infection (55). These pro-inflammatory regulators lead to upregulation of the death signaling molecule Fas-ligand on the infected host cell to initiate the caspase-mediated Fas-associated pathway, in which Fas receptors on the immune cell (part of the TNF-receptor family) bind to Fas-ligand and subsequently recruit the Fas-associated death domain (FADD) molecule (86). FADD interacts with caspase-8, which initiates a signaling cascade within the immune cell, resulting in the destruction of cellular components and thus cell death, which may be causative of the pathology seen in influenza patients (87). Indeed, both H5N1 and H7N9 have been observed to cause leukopenia in hospitalized patients (88–90). According to Boonnak and colleagues, $CD8^+$ T cells can be particularly affected by the Fas-ligand mediated pathway, where Fas-ligand was upregulated on plasmocytoid dendritic cells during lethal H5N1 infection in mice, which then lead to apoptosis of influenza-specific $CD8^+$ T cells in the lung draining lymph nodes (86). Furthermore, in hospitalized H7N9-infected patients during the emergence of H7N9 in 2013, the persistence of immune cell subsets within the blood contributed to disease severity and fatal outcomes, with the continuation of $CD38^+HLA\text{-}DR^+$ $CD8^+$ T cell responses shown to be predictive of fatal outcomes, possibly due to

longer-lasting inflammatory responses in the peripheral blood and lung (91). Loss of peripheral blood lymphocytes was also observed in human seasonal influenza A infections, with these cell subsets succumbing to apoptosis by the same apoptotic pathways described for AI viruses (92). In summary, LPAI versus HPAI viral strains differentially promote the induction of pro-inflammatory cytokines, which then alter disease outcomes in different species. The potential mechanisms by which certain HPAI AI viruses cause more severe disease will be further discussed in the following sections.

VIRAL FITNESS ACROSS SPECIES

In order for AI viruses to be capable of infecting multiple host species they require viral adaptations allowing replication in different host cells, which ultimately increase their genetic fitness and create a sustainably replicating and transmitting virus (93). It is well established that for zoonotic transmission of AI viruses, the virus needs to present the appropriate HA binding specificity to allow viral fusion and entry. AI virus HA proteins typically have a binding preference for sialic acid residues with an α-2,3-Gal terminating sequence found on the surface of avian cells (**Figure 1**), resulting in restriction to avian cells (63, 94). Therefore, for AI viruses to gain entry into human cells displaying an α-2,6-Gal terminating sequence, modifications to the HA binding site may be required to allow this new interaction.

One of the commonly associated amino acid substitutions for LPAI strains converting from avian to mammalian receptor-specificity is a HA Q226L substitution (58, 95–97). For example, LPAI H9N2 isolates from birds can adopt a Q226L substitution, which increases its mammalian receptor binding affinity and potentially infect mammalian hosts (98, 99). However, with regards to H7N9 human isolates, Belser and colleagues described the Q226 bearing Shanghai/1 and the L226 bearing Anhui/1 as binding to largely avian α-2,3-Gal receptor analogs and mixed α-2,3/α-2,6-Gal receptors, respectively (64). Despite these differences, infections with each isolate produced effective replication in the lower respiratory tract of ferrets, suggesting additional factors are involved in mammalian adaptation. Similarly, this Q226L mutation has not been commonly observed in the HA of H5N1 HPAI viruses (100, 101). However, alternative substitutions, HA Q192H and HA I151T, can confer increased ability for replication in human hosts. Moreover, Herfst and colleagues demonstrated a closely related change to the HA of H5N1, HA Q222L, conferring more efficient replication and transmission in the ferret model (66). Additional to this HA mutation, an E627K change in the polymerase basic 2 (PB2) protein in H5N1 HPAI was also shown to be critical for transmission in ferrets (64, 102–105).

In addition to HA-sialic acid binding, key to viral fitness is the presence of a multi-basic cleavage site (MBCS), which has been shown extensively with H5N1, that the presence of an MBCS often dictates the use of the term HPAI (106, 107). The presence of an MBCS in the HA of influenza A viruses allows HA cleavage by additional enzymes such as furin-like proteases, whereas without an MBCS, the virus relies on only trypsin-like proteases (108). This flexible range of enzyme activity results in the virus being able to infect a greater range of cells and can lead to systemic infection (106, 107, 109). Though commonly associated with H5N1, this motif is seen in other avian-infecting HPAI viruses such as H7N3, however, these strains are less frequently transmitted to humans (19, 110). Interestingly, LPAI can also acquire MBCS motifs, changing the pathogenicity of the virus from low to high, such as in the case of an H7N8 outbreak in Turkey in 2016, where an LPAI virus caused a severe outbreak in the poultry due to the spontaneous addition of an MBCS, leading to over 800 bird deaths (111). However, the addition of an MBCS does not guarantee an LPAI virus to increase its pathogenicity, as recombinant H5 and H7 viruses do not exhibit HPAI pathology in chickens specifically due to the addition of an MBCS (112), which suggests that these motifs are one of many factors contributing to HPAI pathogenesis. H7N9 has also been shown to be able to obtain an MBCS to become highly pathogenic in chickens (113). Imai and colleagues showed increased disease severity of an MBCS-containing H7N9 virus in the ferret model compared to an LPAI H7N9 virus (18). However, H7N9 will still cause severe disease without an MBCS in most human cases, highlighting how unique this virus is in the AI landscape for its ability to show HPAI-like symptoms in mammals, while maintaining low pathogenicity in birds. Similarly for H5Nx viruses, several additional changes in the H5 HA protein, such as an N158D mutation, also allow greater replication of the virus in ferrets without the need for an MBCS, which combined with reassortment with human-adapted H1N1 gene segments shows the potential for these viruses to not only cross into humans but also cause severe, sustained human infection without systemic spread (114). This, coupled with H7N9's ability to cause severe disease without the requirement of an MBCS, suggests that while the MBCS still acts as a key virulence factor for AI viruses, it is not a sole-determining factor for HPAI in humans.

A key interaction between host and viral proteins is the interplay between Mx GTPases and viral nucleoprotein (NP), which may be pivotal in determining viral fitness. Human MxA and murine Mx1 protein have been shown to confer antiviral protection against influenza A viruses by interfering with the ability of NP to localize to the nucleus, inhibiting the viral replication cycle (115). While many influenza viruses are susceptible to Mx restriction, changes in the NP have been shown to confer resistance to this form of protection, particularly in the case of AI viruses such as H5N1 which shows greater susceptibility to MxA inhibition than pandemic H1N1 (116, 117). Moreover, LPAI H7N9 viruses were similarly shown to be affected by Mx1 in infected mice compared to H5N1 by Deeg and colleagues, who showed that these viruses required human adaptive motifs in their NPs to evade Mx restriction (118). Interestingly, avian species such as chickens have been found to have an Mx that does not display strong antiviral properties, suggestive of why these avian viruses do not commonly have NP capable of MxA evasion (119, 120). Therefore, while these AI viruses often appear to cause worsened disease progression due to their differences to human-infecting strains, in the case of Mx restriction it is a lack of human adaptation that may provide a level of protection to mammalian hosts.

Another key virulence factor elucidated in recent years is the ability of the non-structural protein 1 (NS1) to aid viral escape in the host immune system. In avian hosts, NS1 has been associated with worsened pathology through increases in iNOS and oxygen-reactive species for both LPAI H9N2 (121) and HPAI H5N1 (122). However, in contrast in mammals, the NS1 protein has been more closely associated with inhibition of host IFN responses. Jia and colleagues (123) showed that the H5N1 NS1 protein inhibits IFN production through interference with the JAK/STAT pathway. They found that expression of NS1 in HeLa cells prevented STAT phosphorylation and upregulated inhibitors of this pathway to prevent expression of IFNAR and SOCS3 proteins, which generally upregulate IFN expression (123). Furthermore, a naturally occurring deletion in the H5N1 NS1 effector domain can attenuate the virulence of the virus in both chickens and mice, suggesting that this protein is critical in the ability of H5N1 to suppress host immune antiviral responses across hosts (124). The pathogenicity of H5N1 in mice is also affected by the NS1 protein, as a single mutation (P42S) conferred greater pathogenicity to the virus by preventing nuclear factor-κB (NF-κB) and interferon-regulatory factor 3 (IRF3) signaling, and thus inhibiting IFN responses (125). Interestingly, in cats the NS1 protein can be associated with blocking NF-κB and IRF3 signaling in response to the emerging HPAI H5N6 virus, with inhibition of the IFN-β promoter blunting the feline IFN response (126), suggesting that NS1 may have different ways of interacting with influenza hosts across species to produce similar immune suppression. On the other hand, Thube and colleagues investigated the IFN responses of HPAI H5N1 compared to LPAI H11N1 and suggested that decreased IFN signaling occurred independently of NS1, suggesting other viral elements can also induce a reduced antiviral state in cells (127). It is worth noting that while the NS1 of LPAI H7N9 is inefficient at binding to CPSF30 (involved in pre-mRNA processing), a single I106M mutation restores CPSF30 binding to NS1 thereby blocking the expression of host antiviral genes. This renders the virus more virulent than other LPAI infections (128), which may explain why H7N9 causes more severe disease in humans compared to other LPAIs. These results also highlight inhibition of IFN-activation pathways as an important viral factor in preventing host immune responses to infection, allowing for more productive infection and potentially more severe clinical outcomes.

HOST SUSCEPTIBILITY FACTORS

In addition to the ability of the virus to gain function through mutation, in recent years there has been an increasing focus on how host genetic factors can lead to changes in resistance or susceptibility to influenza A viruses. While many factors have been identified in preventing influenza A infection, a key which has come to light for AI host/pathogen interactions is the interferon-induced transmembrane (IFITM) protein family, which unlike other factors such as MxA seems to be predominantly the host, rather than the virus, that seems to control whether the virus is able to replicate. IFITMs are family of transmembrane antiviral proteins that are stimulated by the presence of elevated IFN levels, giving another reason why so many AI viruses attempt to quash the IFN response (129, 130). The IFITM proteins can interfere with viral entry to the cytosol *via* cell membranes (131), with Brass and colleagues showing that overexpression of human IFITMs 1, 2, and 3 effectively blocked infection with several influenza A pseudoviruses (retroviruses expressing influenza surface proteins), including those enveloped with H5 and H7 proteins (132). Moreover, IFITM3 specifically localizes to the endosomes due to phosphorylation of the Y20 tyrosine residue, enabling these proteins to intrinsically target pH-dependent viral pathways such as that seen with influenza A viruses (133).

The IFITM3 molecule can play a significant role in mice and human influenza infections. Mice inoculated with influenza antigen showing higher IFITM3 expression in the lungs developed a more robust lung tissue-resident memory $CD8^+$ T cell response as well as a longer duration of response even following reduction of IFN-α, suggestive of this molecule playing a role in not only innate immunity but also adaptive immunity as well (134). Of particular note, a single-nucleotide polymorphism (SNP) in the IFITM3 gene, *rs12252-C*, has been shown to strongly correlate to worsened disease progression, as this SNP leads to a truncated splice-variant that affects the protein's ability to localize to the membrane (135, 136). IFITM3 protein dysfunction can be associated with severe hypercytokinemia and worsened disease progression in H7N9-infected hospitalized patients. In support, Zhang and colleagues showed that the *rs12252-C* mutation correlated to severe seasonal H1N1 influenza cases in Chinese populations where the mutation appeared in higher frequencies (136, 137). However, studies have shown that while this SNP does affect IFITM3′s ability to localize, restriction of the virus may continue with the variant protein or with a Y20A mutation to affect the localization of the full protein (138). Furthermore, a recent study by Makvandi-Nejad and colleagues found that primary cell lines homozygous for the *rs12252-C* SNP expressed the non-truncated mRNA transcript and thus expressed the wild-type IFITM3 protein at levels greater than 99% when compared to the truncated versions (139), which may provide insights into why the *rs12252-C* mutation appears not to act as a significant risk factor in Caucasian populations, but perhaps in the Chinese patients. Moreover, an additional SNP has recently been identified, *rs34481144-A,* which affects the promoter for the *IFITM3* gene, resulting in lower IFITM3 expression compared to hosts without the mutation. Interestingly, both the *rs12252-C* and *rs34481144-A* mutation were found to be non-overlapping, as the risk allele for one was inherited with the protective allele of the other, suggesting a multifaceted IFITM response to influenza A viruses (140).

IFITM1 and IFITM3 distribution in mice has been investigated in the context of H9N2 infection, with the distribution of these proteins correlating with increased restriction of the virus' entry into host tissues, due to upregulation in the lungs and peripheral tissues of BALB/c mice following inoculation. Interestingly, when infected with a H9N2 strain with higher pathogenicity and ability for systemic spread due to a K627E mutation (rV_{K627E}) in the viral PB2 protein, compared to the wild-type strain, IFITM3 was upregulated accordingly in the

brain of rV_{K627E}-infected mice to combat this virus' ability to cause viral encephalitis (141). IFITM3 responses to H5 and H7 proteins have also been assessed in pigs and bats, with both these HA subtypes showing restricted entry due to the action of these IFITM3 proteins (142), suggestive of the broad action of IFITM molecules across species known to contract and potentially disseminate AI viruses. That IFITMs restrict AI viruses in "mixing vessel" species (i.e., pigs and bats) suggests that these proteins may have a key role in preventing the spread of human-infecting AI viruses through these routes, as well as contributing to these species showing lessened pathology compared to other mammalian species.

The role of IFITMs against AI viruses in avian species has not been clearly defined, though a study by Smith and colleagues has shown that chicken IFITM3 (which is "human IFITM1-like") similarly restricts H5 and H7 expressing viruses (143). However, when chickens were infected with H5N1, expression of IFITM molecules was not highly upregulated compared to other human-infecting seasonal strains such as H1N1, with IFITMs showing the weakest inhibiting effect against H7N9 (144). Hence, IFITM expression in chickens appears to be limited and does not vary greatly whether the virus is of low or high pathogenicity. Conversely, the IFITM expression profile observed in ducks is far more robust and variable between viral strains, whereby infection with LPAI H5N2 virus was reported to consistently cause a 3-fold increase in IFITM1, 2, and 3 expression levels in the lungs and ileum on day one post-inoculation, while infection with the HPAI H5N1 virus caused up to a 93-fold increase in IFITM3 expression in the lungs in a similar time frame (145). Therefore, understanding the differences in variable IFITM expression, and the reasons why chickens mount a lesser IFITM response to influenza viruses, may prove pivotal in understanding why some birds succumb to HPAI infection while others survive.

In addition to specific IFITM mutations, broad immunodeficiency can lead to worsened pathology and disease outcomes in humans and animals. For example, immunocompromised patients who contract LPAI viruses such as H9N2 suffer severe respiratory distress, and though many of these LPAI remain mild even in immunocompromised patients, H9N2 induces stronger cytokine responses than seasonal influenza viruses (146, 147). These trends are also observed in avian hosts, in which Nili and Asasi found that chickens co-infected with other pathogens such as *M. gallisepticum* showed worsened clinical signs such as severe necrotizing tracheitis, leading to a 19% mortality in the flock (148, 149). Therefore, it is apparent that both the host and pathogen can contribute to perturbed inflammation and severe disease outcomes. In addition, in humans, more severe AI subtypes have been associated with mortalities in very distinct age demographics when compared to seasonal influenza (**Figure 2**), and often manifest in age groups not commonly associated with immunodeficiency. Fatal cases in children (0–9 years) and younger adults (10–19 years) were predominantly caused by HPAI H5N1 infection, with 80.3% of H5N1 fatal cases seen in people aged 35 or under (12). Interestingly, a similar trend was observed with the pandemic [pdmH1N1(2009)] strain, which led to increased infection in younger age groups compared to other seasonal strains circulating at the same time (150). An interesting observation from the 2009 pandemic, however, was that disease outcomes were more mild in newly weaned ferrets infected with pdmH1N1(2009) as well as in younger children, suggesting the immune response in younger individuals may have a protective response to this strain (151, 152). Conversely, seasonal strains of influenza disproportionately impact older ferrets infected, which display a greater degree of morbidity and reduced HA and T cell responses (153). This is also true of human patients also whereby older patients (>60 years of age) are most susceptible to seasonal influenza strains (80% of mortality cases). With regards to H7N9 LPAI infections, the highest mortality was also skewed toward older people, which is likely due to the propensity for H7N9 cases to be found in live poultry farmers, typically older men (154, 155). This emphasizes the dynamic relationship between the pathogen and the human host, and how different strains of influenza viruses can lead to differential fatal outcomes across different ages, a concept further explored by Gostic and colleagues who suggest that pre-immunity to these viruses may confer differing levels of protection to AI based on whether they have been exposed to the viral HA class while still young (156).

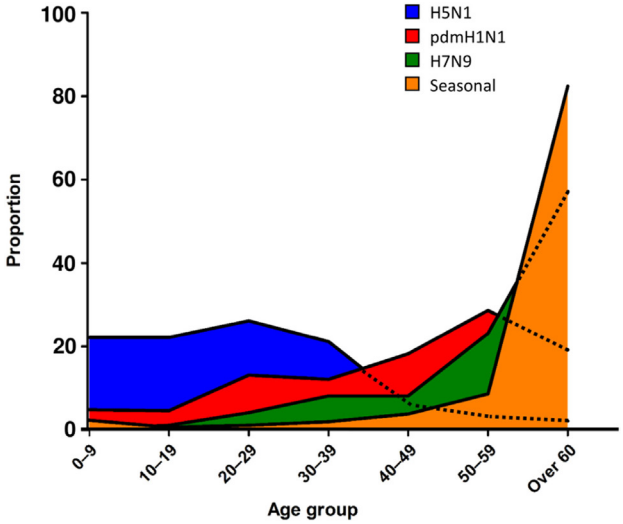

FIGURE 2 | Age-related mortality trends highlight impact of host–pathogen relationships. Frequency of age groups of patients who succumb to different strains of influenza is graphed as a proportion of total fatalities for a given strain. When we assessed the age of patients who succumb to different strains of influenza, as a proportion of the total mortalities for a given strain, trends emerge as to the host susceptibilities. For seasonal influenza, older patients (>60 years old) were the most susceptible, however, for a variation on seasonal influenza, pdmH1N1 2009, the age of patients who succumbed was reduced and included significant mortalities between 20 and 59 years old. Interestingly, the highly pathogenic AI H5N1 was predominantly fatal in those under 40 years old, whereas H7N9, a low pathogenicity AI strain, followed a similar trend to seasonal influenza.

While IFITM proteins aim to restrict viral entry, the interaction between influenza virus peptides and major histocompatibility complex (MHC) molecules is a key host–pathogen interaction affecting the outcome of disease following initial

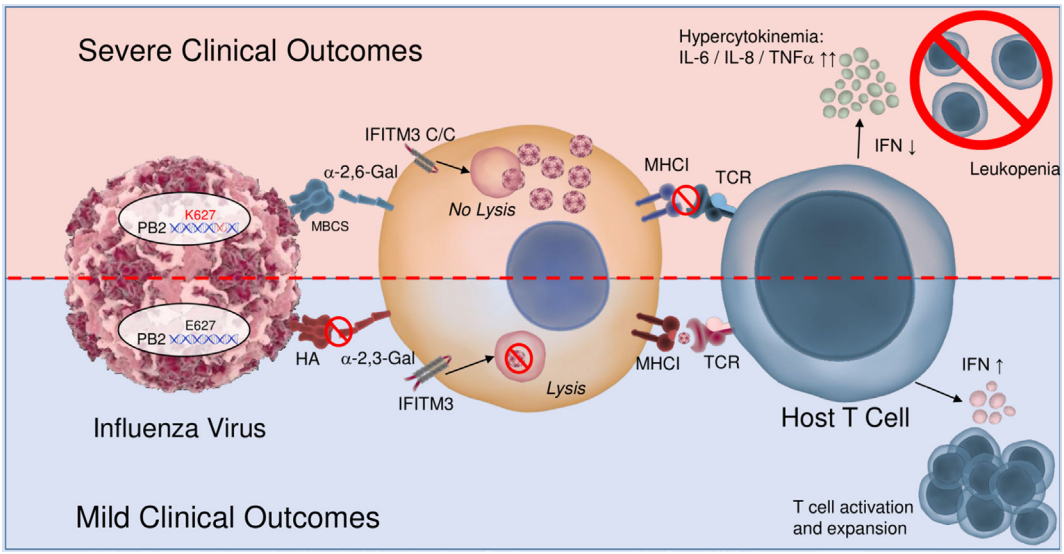

FIGURE 3 | Mechanisms leading to severe clinical outcomes involve both host and pathogen elements. A number of factors have been elucidated to contribute to the severity of influenza disease outcomes. This include viral fitness elements, such as the presence of a multi-basic cleavage site (MBCS), mutations to the polymerase basic 2 (PB2) genes, as well as the presentation of hemagglutinin (HA) protein capable of binding to human sialic acids. These viral fitness elements work in concert with host factors such as modified interferon-induced transmembrane (IFITM) proteins, with reduced ability to combat the virus and MHCI diversity which can or cannot present the antigen appropriately and efficiently to host T cells. Ultimately, these and other elements lead to changes in production of key cytokines as well as cellular activation that drives inflammation, cell death, and clinical manifestation of disease.

infection. In humans, MHC molecules are encoded for by the human leukocyte antigen (HLA) system, with a vast array of alleles in the genes encoding for the molecules responsible for the recognition of antigenic peptides. As such, different HLA subtypes confer different levels of susceptibility to influenza A viruses, as not all HLA subtypes respond to influenza peptides in the same way. For example, human populations expressing HLA-A*02:01 can elicit strong, cross-protective $CD8^+$ T cell responses following presentation of the internally conserved $M1_{58-66}$ epitope (157–160); this epitope is one of the most immunogenic influenza peptides observed in humans with HLA-A*02:01 being the most common HLA alleles expressed worldwide (157). Moreover, individuals lacking common HLA alleles may be at greater risk of influenza A infections, such as those carrying the HLA-A*24:02 allele, associated with increased mortality in individuals infected with pandemic H1N1 virus (161). Indigenous populations in particular are susceptible to influenza A due to a lowered prevalence of protective HLA variants toward these viruses (160). Wang and colleagues suggest that for AI viruses such as H7N9, MHC-interactions with internally conserved epitopes from other influenza A strains, such as pandemic H1N1, may explain why some populations show greater immunity through cross-reactive $CD8^+$ T cell responses than others (72). However, some H7N9 peptides may have cross-conservation with human host proteins that the immune system recognizes as "self," leading to an attenuated immune response to the virus and thus worsened disease progression due to T cell-mediated tolerance (162).

Interestingly, chickens show a restricted repertoire of MHC alleles compared to other species, and these haplotypes themselves are poorly characterized. As such, a few studies have been conducted into characterizing T cell epitopes in response to H5N1 infections, one such study predicting 25 potential T cell epitopes in the NP of H5N1 in four haplotypes (163). More recently, experiments into epitopes of a specific haplotype, BF2*15, further characterized NP epitopes that may lead to protective immunity against H5N1 (164). This limited repertoire may explain why chickens show more severe clinical outcomes due to HPAI such as H5N1 compared to waterfowl, as ducks show extensive diversity in their MHC class I alleles which allows the immune system greater coverage for viral variation (165). A recent investigation into duck MHC class I molecules found that the duck *Anpl*-UAA*01 complex showed similar peptide binding properties to HLA-A*02:01 in humans and as such appears to cover a greater array of influenza A virus epitopes compared to similar chicken MHC molecules such as BF2*2101 (166). Furthermore, migratory shorebirds which act as reservoirs for AI viruses (in particular LPAI H9N2) show increased diversity in their MHC alleles, likely as a mechanism for protecting against foreign pathogens that may be encountered during migration. A study in red knots found high MHC diversity with 36 alleles detected across eight birds, which when correlated to their low prevalence of shed AI virus and high antibody titers to AI viruses, they could mount effective immune responses toward these viruses, possibly *via* cytotoxic T lymphocyte responses recognizing novel peptide/MHC complexes (167). Based on a culmination of human and animal evidence, the interactions between the various pathogen and host factors contributing to human influenza severity are summarized in **Figure 3**.

CONCLUSION

The emergence of AI viruses is of major concern to the avian and human population. The lack of pre-existing antibody immunity and their ability to cause severe disease through multiple host and viral mechanisms makes these viruses difficult to counter. Currently, these viruses are yet to effectively replicate and transmit between humans, however, experiments in ferrets show that only a few mutations are needed for H5N1 and H7N9 viruses to quickly adapt and become a major pandemic threat (114, 168). Their ability to pass from birds to mammals commonly in contact with humans requires constant surveillance across all known bird reservoirs to limit the potential threat of an AI-derived pandemic. Characterization of the interactions between AI viruses and their hosts and how they illicit different degrees of clinical manifestations across species is of utmost importance. Here, we extend our current knowledge of the "cytokine storm" model of AI pathogenesis and delve into more complex underlying viral and host genetic factors that may also contribute greatly to disease severity and susceptibility outcomes.

AUTHOR CONTRIBUTIONS

WH and DL wrote and edited the manuscript. AB, TN, and KK edited the manuscript.

FUNDING

KK is supported by a NHMRC SRF Level B Fellowship #APP1102792. WH is supported by CSIRO and The University of Melbourne 'One Health PhD Scholarship'.

REFERENCES

1. Ehrhardt C, Seyer R, Hrincius ER, Eierhoff T, Wolff T, Ludwig S, et al. Interplay between influenza A virus and the innate immune signalling. *Microbes Infect* (2010) 12:81–7. doi:10.1016/j.micinf.2009.09.007
2. Tong S, Zhu X, Li Y, Shi M, Zhang J, Bourgeois M, et al. New world bats harbor diverse influenza A viruses. *PLoS Pathog* (2013) 9(10):e1003657. doi:10.1371/journal.ppat.1003657
3. Xing Z, Cardona CJ, Li J, Dao N, Tran T, Andrada J. Modulation of the immune response in chickens by low-pathogenicity avian influenza virus H9N2. *J Gen Virol* (2008) 89(5):1288–99. doi:10.1099/vir.0.83362-0
4. Daoust PY, Kibenge FS, Fouchier RA, van de Bildt MW, van Riel D, Kuiken T. Replication of low pathogenic avian influenza virus in naturally infected mallard ducks (*Anas platyrhynchos*) causes no morphologic lesions. *J Wildl Dis* (2011) 42(2):401–9. doi:10.7589/0090-3558-47.2.401
5. Alexander DJ. An overview of the epidemiology of avian influenza. *Vaccine* (2007) 25:5637–44. doi:10.1016/j.vaccine.2006.10.051
6. Du Y, Chen M, Yang J, Jia Y, Han S, Holmes EC, et al. Molecular evolution and emergence of H5N6 avian influenza virus in central China. *J Virol* (2017) 91(12):e00143-17. doi:10.1128/JVI.00143-17
7. Visperas E, Simeon LM. *First Bird Flu Outbreak: 400,000 to Be Culled*. Manila: The Philippine Star (2017).
8. World Health Organization. *Influenza at the Human-Animal Interface: Summary and Assessment, 26 January to 2 March 2018*. Geneva: World Health Organization (2018).
9. Wang Z, Loh L, Kedzierski L, Kedzierska K. Avian influenza viruses, inflammation, and CD8+ T cell immunity. *Front Immunol* (2016) 7:60. doi:10.3389/fimmu.2016.00060
10. Claas EC, Osterhaus AD, van Beek R, De Jong JC, Rimmelzwaan GF, Senne DA, et al. Human influenza A H5N1 virus related to a highly pathogenic avian influenza virus. *Lancet* (1998) 351:472–7. doi:10.1016/S0140-6736(97)11212-0
11. World Health Organization. *Cumulative Number of Confirmed Human Cases for Avian Influenza A(H5N1) Reported to WHO, 2003–2017*. Geneva: World Health Organization (2017). Available from: http://www.who.int/influenza/human_animal_interface/2017_10_30_tableH5N1.pdf?ua=1 (Accessed: March 21, 2018).
12. Lai S, Qin Y, Cowling BJ, Ren X, Wardrop NA, Gilbert M, et al. Global epidemiology of avian influenza A H5N1 virus infection in humans, 1997–2015: a systematic review of individual case data. *Lancet Infect Dis* (2016) 16:e108–18. doi:10.1016/S1473-3099(16)00153-5
13. World Health Organization. *Influenza at the Human-Animal Interface: Summary and Assessment, 28 September to 30 October 2017*. Geneva: World Health Organization (2017). Available from: http://www.who.int/influenza/human_animal_interface/Influenza_Summary_IRA_HA_interface_10_30_2017.pdf (Accessed: March 21, 2018).
14. World Health Organization. *Influenza at the Human-Animal Interface: Summary and Assessment, 8 December 2017 to 25 January 2018*. Geneva: World Health Organization (2018). Available from: http://www.who.int/influenza/human_animal_interface/Influenza_Summary_IRA_HA_interface_25_01_2018_FINAL.pdf?ua=1 (Accessed: March 21, 2018).
15. Teng Y, Bi D, Guo X, Hu D, Feng D, Tong Y. Contact reductions from live poultry market closures limit the epidemic of human infections with H7N9 influenza. *J Infect* (2018) 76:295–394. doi:10.1016/j.jinf.2017.12.015
16. Zaman M, Gasimov V, Oner AF, Dogan N, Adisasmito W, Coker R, et al. Recognizing true H5N1 infections in humans during confirmed outbreaks. *J Infect Dev Ctries* (2014) 8:202–7. doi:10.3855/jidc.3329
17. Farooqui A, Liu W, Zeng T, Liu Y, Zhang L, Khan A, et al. Probable hospital cluster of H7N9 influenza infection. *N Engl J Med* (2016) 374(6):596–8. doi:10.1056/NEJMc1505359
18. Imai M, Watanabe T, Kiso M, Nakajima N, Yamayoshi S, Iwatsuki-Horimoto K, et al. A highly pathogenic avian H7N9 influenza virus isolated from a human is lethal in some ferrets infected via respiratory droplets. *Cell Host Microbe* (2017) 22(5):615–26.e8. doi:10.1016/j.chom.2017.09.008
19. Lopez-Martinez I, Balish A, Barrera-Badillo G, Jones J, Nuñez-García TE, Jang Y, et al. Highly pathogenic avian influenza A(H7N3) virus in poultry workers, Mexico, 2012. *Emerg Infect Dis* (2013) 19(9):1531–4. doi:10.3201/eid1909.130087
20. Watanabe T, Kiso M, Fukuyama S, Nakajima N, Imai M, Yamada S, et al. Characterisation of H7N9 influenza A viruses isolated from humans. *Nature* (2013) 501(7468):551–5. doi:10.1038/nature12392
21. Huo X, Chen L, Qi X, Huang H, Dai Q, Yu H, et al. Significantly elevated number of human infections with H7N9 in Jiangsu in eastern China, October 2016 to January 2017. *Euro Surveill* (2017) 22(13):30496. doi:10.2807/1560-7917.ES.2017.22.13.30496
22. Su S, Gu M, Liu D, Cui J, Gao GF, Zhou J, et al. Epidemiology, evolution, and pathogenesis of H7N9 influenza viruses in five epidemic waves since 2013 in China. *Trends Microbiol* (2017) 25(9):713–28. doi:10.1016/j.tim.2017.06.008
23. Zhou L, Ren R, Yang L, Bao C, Wu J, Wang D, et al. Sudden increase in human infection with avian influenza A(H7N9) virus in China, September–December 2016. *Western Pac Surveill Response J* (2017) 8(1):6–14. doi:10.5365/WPSAR.2017.8.1.001
24. Pinsent A, Pepin KM, Zhu H, Guan Y, White MT, Riley S. The persistance of multiple strains of avian influenza in live bird markets. *Proc Biol Sci* (2017) 284(1868):20170715. doi:10.1098/rspb.2017.0715
25. Wan XF, Dong L, Lan Y, Long LP, Xu C, Zou S, et al. Indications that live poultry markets are a major source of human H5N1 influenza virus infection in China. *J Virol* (2011) 85(24):13432–8. doi:10.1128/JVI.05266-11
26. Bano S, Naeem K, Malik SA. Evaluation of pathogenic potential of avian influenza virus serotype H9N2 in chickens. *Avian Dis* (2003) 47(817):817–22. doi:10.1637/0005-2086-47.s3.817

27. Kalaiyarasu S, Kumar M, Senthil Kumar D, Bhatia S, Dash SK, Bhat S, et al. Highly pathogenic avian influenza H5N1 virus induces cytokine dysregulation with suppressed maturation of chicken monocyte-derived dendritic cells. *Microbiol Immunol* (2016) 60:687–93. doi:10.1111/1348-0421.12443
28. Huang Y, Li X, Zhang H, Chen B, Jiang Y, Yang L, et al. Human infection with an avian influenza A (H9N2) virus in the middle region of China. *J Med Virol* (2015) 87:1641–8. doi:10.1002/jmv.24231
29. Butt KM, Smith GJ, Chen H, Zhang LJ, Leung YH, Xu KM, et al. Human infection with an avian H9N2 influenza A virus in Hong Kong in 2003. *J Clin Microbiol* (2005) 43(11):5760–7. doi:10.1128/JCM.43.11.5760-5767.2005
30. Naguib MM, Arafa AS, El-Kady MF, Selim AA, Gunalan V, Maurer-Stroh S, et al. Evolutionary trajectories and diagnostic challenges of potentially zoonotic avian influenza viruses H5N1 and H9N2 co-circulating in Egypt. *Infect Genet Evol* (2015) 34:278–91. doi:10.1016/j.meegid.2015.06.004
31. Yu X, Jin T, Cui Y, Pu X, Li J, Xu J, et al. Influenza H7N9 and H9N2 viruses: coexistence in poultry linked to human H7N9 infection and genome characteristics. *J Virol* (2014) 88(6):3423–31. doi:10.1128/JVI.02059-13
32. Chen H, Yuan H, Gao R, Zhang J, Wang D, Xiong Y, et al. Clinical and epidemiological characteristics of a fatal case of avian influenza A H10N8 virus infection: a descriptive study. *Lancet* (2014) 383:714–21. doi:10.1016/S0140-6736(14)60111-2
33. Yuan J, Zhang L, Kan X, Jiang L, Yang J, Guo Z, et al. Origin and molecular characteristics of a novel 2013 avian influenza A(H6N1) virus causing human infection in Taiwan. *Clin Infect Dis* (2013) 57:1367–8. doi:10.1093/cid/cit479
34. Wei S-H, Yang JR, Wu HS, Chang MC, Lin JS, Lin CY, et al. Human infection with avian influenza A H6N1 virus: an epidemiological analysis. *Lancet Respir Med* (2013) 1(10):771–8. doi:10.1016/S2213-2600(13)70221-2
35. Ni F, Konrashkina E, Wang Q. Structural and functional studies of influenza virus A/H6 hemagglutinin. *PLoS One* (2015) 10(7):e0134576. doi:10.1371/journal.pone.0134576
36. Xin L, Bai T, Zhou JF, Chen YK, Li XD, Zhu WF, et al. Seropositivity for avian influenza H6 virus among humans, China. *Emerg Infect Dis* (2015) 21(7):1267–9. doi:10.3201/eid2107.150135
37. Hoffmann E, Stech J, Leneva I, Krauss S, Scholtissek C, Chin PS, et al. Characterization of the influenza A virus gene pool in avian species in Southern China: was H6N1 a derivative or a precursor of H5N1? *J Virol* (2000) 74(14):6309–15. doi:10.1128/JVI.74.14.6309-6315.2000
38. Chin PS, Hoffmann E, Webby R, Webster RG, Guan Y, Peiris M, et al. Molecular evolution of H6 influenza viruses from poultry in Southeastern China: prevalence of H6N1 influenza viruses possessing seven A/Hong Kong/156/97 (H5N1)-like genes in poultry. *J Virol* (2002) 76(2):507–16. doi:10.1128/JVI.76.2.507-516.2002
39. Lu H, Castro AE, Pennick K, Liu J, Yang Q, Dunn P, et al. Survival of avian influenza virus H7N2 in SPF chickens and their environments. *Avian Dis* (2003) 47(s3):1015–21. doi:10.1637/0005-2086-47.s3.1015
40. Gharaibeh S. Pathogenicity of an avian influenza serotype H9N2 in chickens. *Avian Dis* (2008) 52(1):106–10. doi:10.1637/8108-090907-Reg
41. França M, Stallknecht DE, Poulson R, Brown J, Howerth EW. The pathogenesis of low pathogenic avian influenza in mallards. *Avian Dis* (2012) 56:976–80. doi:10.1637/10153-040812-ResNote.1
42. Curran JM, Robertson ID, Ellis TM, Selleck PW, O'Dea MA. Variation in the responses of wild species of duck, gull, and wader to inoculation with a wild-bird-origin H6N2 low pathogenicity avain influenza virus. *Avian Dis* (2013) 57(3):581–6. doi:10.1637/10458-112712-Reg.1
43. Wang J, Li CC, Diao YX, Sun XY, Hao DM, Liu X, et al. Different outcomes of infection of chickens and ducks with duck-origin H9N2 influenza A virus. *Acta Virol* (2014) 58:223–30. doi:10.4149/av_2014_03_223
44. Aly MM, Arafa A-SA, Hassan MK. Epidemiological findings of outbreaks of disease caused by highly pathogenic H5N1 avian influenza virus in poultry in Egypt during 2006. *Avian Dis* (2008) 52(2):269–77. doi:10.1637/8166-103007-Reg.1
45. Perkins LEL, Swayne DE. Pathobiology of A/Chicken/Hong Kong/220/97 (H5N1) avian influenza virus in seven gallinaceous species. *Vet Pathol* (2001) 38(2):149–64. doi:10.1354/vp.38-2-149
46. Bingham J, Green DJ, Lowther S, Klippel J, Burggraaf S, Anderson DE, et al. Infection studies with two highly pathogenic avian influenza strains (Vietnamese and Indonesian) in Pekin ducks (*Anas platyrhynchos*), with particular reference to clinical disease, tissue tropism and viral shedding. *Avian Pathol* (2009) 38(4):267–78. doi:10.1080/03079450903055371
47. Acland HM, Silverman Bachin LA, Eckroade RJ. Lesions in broiler and layer chickens in an outbreak of highly pathogenic avian influenza virus infection. *Vet Pathol* (1984) 21:564–9. doi:10.1177/030098588402100603
48. Keawcharoen J, van Riel D, van Amerongen G, Bestebroer T, Beyer WE, van Lavieren R, et al. Wild ducks a long-distance vectors of highly pathogenic avian influenza virus (H5N1). *Emerg Infect Dis* (2008) 14(4):600–7. doi:10.3201/eid1404.071016
49. Pantin-Jackwood MJ, Swayne DE. Pathobiology of Asian highly pathogenic avian influenza H5N1 virus infections in ducks. *Avian Dis* (2007) 51(s1):250–9. doi:10.1637/7710-090606R.1
50. Suzuki K, Okada H, Itoh T, Tada T, Mase M, Nakamura K, et al. Association of increased pathogenicity of Asian H5N1 highly pathogenic avian influenza viruses in chickens with highly efficient viral replication accompanied by early destruction of innate immune responses. *J Virol* (2009) 83(15):7475–86. doi:10.1128/JVI.01434-08
51. Jeong O-M, Kim MC, Kim MJ, Kang HM, Kim HR, Kim YJ, et al. Experimental infection of chickens, ducks and quails with highly pathogenic H5N1 avian influenza virus. *J Vet Sci* (2009) 10(1):53–60. doi:10.4142/jvs.2009.10.1.53
52. Yamamoto Y, Nakamura K, Yamada M, Mase M. Corneal opacity in domestic ducks experimentally infected with H5N1 highly pathogenic avian influenza virus. *Vet Pathol* (2016) 53(1):65–76. doi:10.1177/0300985815591077
53. Yamamoto Y, Nakamura K, Yamada M, Mase M. Comparative pathology of chickens and domestic ducks experimentally infected with highly pathogenic avian influenza viruses (H5N1) isolated in Japan in 2007 and 2008. *Jpn Agric Res Q* (2010) 44(1):73–80. doi:10.6090/jarq.44.73
54. Ito T, Couceiro JN, Kelm S, Baum LG, Krauss S, Castrucci MR, et al. Molecular basis for the generation in pigs of influenza A viruses with pandemic potential. *J Virol* (1998) 72(9):7367–73.
55. Lipatov AS, Kwon YK, Sarmento LV, Lager KM, Spackman E, Suarez DL, et al. Domestic pigs have low susceptibility to H5N1 highly pathogenic avian influenza viruses. *PLoS Pathog* (2008) 4(7):e1000102. doi:10.1371/journal.ppat.1000102
56. Zhu Q, Yang H, Chen W, Cao W, Zhong G, Jiao P, et al. A naturally occurring deletion in its NS gene contributes to the attenuation of an H5N1 swine influenza virus in chickens. *J Virol* (2008) 82(1):220–8. doi:10.1128/JVI.00978-07
57. Zhou P, Hong M, Merrill MM, He H, Sun L, Zhang G. Serological report of influenza a (H7N9) infections among pigs in Southern China. *BMC Vet Res* (2014) 10:203. doi:10.1186/s12917-014-0203-x
58. Liu Q, Zhou B, Ma W, Bawa B, Ma J, Wang W, et al. Analysis of recombinant H7N9 wild-type and mutant viruses in pigs shows that the Q226L mutation in HA Is important for transmission. *J Virol* (2014) 88(14):8153–65. doi:10.1128/JVI.00894-14
59. Balzli C, Lager K, Vincent A, Gauger P, Brockmeier S, Miller L, et al. Susceptibility of swine to H5 and H7 low pathogenic avian influenza viruses. *Influenza Other Respi Viruses* (2016) 10(4):346–52. doi:10.1111/irv.12386
60. Yum J, Park EH, Ku KB, Kim JA, Oh SK, Kim HS, et al. Low infectivity of novel avian-origin H7N9 influenza virus in pigs. *Arch Virol* (2014) 159:2745–9. doi:10.1007/s00705-014-2143-y
61. Jones JC, Baranovich T, Zaraket H, Guan Y, Shu Y, Webby RJ, et al. Human H7N9 influenza A viruses replicate in swine respiratory tissue explants. *J Virol* (2013) 87(22):12496–8. doi:10.1128/JVI.02499-13
62. Kwon TY, Lee SS, Kim CY, Shin JY, Sunwoo SY, Lyoo YS. Genetic characterization of H7N2 influenza virus isolated from pigs. *Vet Microbiol* (2011) 153(3-4):393–7. doi:10.1016/j.vetmic.2011.06.011
63. van Riel D, Munster VJ, de Wit E, Rimmelzwaan GF, Fouchier RA, Osterhaus AD, et al. H5N1 virus attachment to lower respiratory tract. *Science* (2006) 312(5772):399. doi:10.1126/science.1125548
64. Belser JA, Gustin KM, Pearce MB, Maines TR, Zeng H, Pappas C, et al. Pathogenesis and transmission of avian influenza A (H7N9) virus in ferrets and mice. *Nature* (2013) 501:556–60. doi:10.1038/nature12391
65. Zhang Q, Shi J, Deng G, Guo J, Zeng X, He X, et al. H7N9 influenza viruses are transmissible in ferrets by respiratory droplet. *Science* (2013) 341(6144):410–4. doi:10.1126/science.1240532

66. Herfst S, Schrauwen EJ, Linster M, Chutinimitkul S, de Wit E, Munster VJ, et al. Airborne transmission of influenza A/H5N1 virus between ferrets. *Science* (2012) 336:1534–41. doi:10.1126/science.1213362
67. Zaraket H, Baranovich T, Kaplan BS, Carter R, Song MS, Paulson JC, et al. Mammalian adaptation of influenza A(H7N9) virus is limited by a narrow genetic bottleneck. *Nat Commun* (2015) 6:6553. doi:10.1038/ncomms7553
68. Edenborough KM, Lowther S, Laurie K, Yamada M, Long F, Bingham J, et al. Predicting disease severity and viral spread of H5N1 influenza virus in ferrets in the context of natural exposure routes. *J Virol* (2015) 90(4): 1888–97. doi:10.1128/JVI.01878-15
69. Zhu H, Wang D, Kelvin DJ, Li L, Zheng Z, Yoon SW, et al. Infectivity, transmission, and pathology of human-isolated H7N9 influenza virus in ferrets and pigs. *Science* (2013) 341(6142):183–6. doi:10.1126/science.1239844
70. Tundup S, Kandasamy M, Perez JT, Mena N, Steel J, Nagy T, et al. Endothelial cell tropism is a determinant of H5N1 pathogenesis in mammalian species. *PLoS Pathog* (2017) 13(3):e1006270. doi:10.1371/journal.ppat.1006270
71. Gao R, Cao B, Hu Y, Feng Z, Wang D, Hu W, et al. Human infection with a novel avian-origin influenza A (H7N9) virus. *N Engl J Med* (2013) 368(20):1888–97. doi:10.1056/NEJMoa1304459
72. Wang Z, Wan Y, Qiu C, Quiñones-Parra S, Zhu Z, Loh L, et al. Recovery from severe H7N9 disease is associated with diverse response mechanisms dominated by CD8+ T cells. *Nat Commun* (2015) 6:6833. doi:10.1038/ncomms7833
73. Hu Y, Lu S, Song Z, Wang W, Hao P, Li J, et al. Association between adverse clinical outcome in human disease caused by novel influenza A H7N9 virus and sustained viral shedding and emergence of antiviral resistance. *Lancet* (2013) 381(9885):2273–9. doi:10.1016/S0140-6736(13)61125-3
74. Zhang Z, Zhang J, Huang K, Li KS, Yuen KY, Guan Y, et al. Systemic infection of avian influenza A virus H5N1 subtype in humans. *Hum Pathol* (2009) 40:735–9. doi:10.1016/j.humpath.2008.08.015
75. To KF, Chan PK, Chan KF, Lee WK, Lam WY, Wong KF, et al. Pathology of fatal human infection associated with avian influenza A H5N1 virus. *J Med Virol* (2001) 63:242–6. doi:10.1002/1096-9071(200103)63:3<242::AID-JMV1007>3.0.CO;2-N
76. Kuchipudi SV, Tellabati M, Sebastian S, Londt BZ, Jansen C, Vervelde L, et al. Highly pathogenic avian influenza virus infection in chickens but not ducks is associated with elevated host immune and pro-inflammatory responses. *Vet Res* (2014) 45:118. doi:10.1186/s13567-014-0118-3
77. Short KR, Veeris R, Leijten LM, van den Brand JM, Jong VL, Stittelaar K, et al. Proinflammatory cytokine responses in extra-respiratory tissues during severe influenza. *J Infect Dis* (2017) 216:829–33. doi:10.1093/infdis/jix281
78. Shinya K, Gao Y, Cilloniz C, Suzuki Y, Fujie M, Deng G, et al. Integrated clinical, pathologic, virologic, and transcriptomic analysis of H5N1 influenza virus-induced viral pneumonia in the rhesus macaque. *J Virol* (2012) 86(11):6055–66. doi:10.1128/JVI.00365-12
79. Gao S, Kang Y, Yuan R, Ma H, Xiang B, Wang Z, et al. Immune responses of chickens infected with wild bird-origin H5N6 avian influenza virus. *Front Microbiol* (2017) 8:1081. doi:10.3389/fmicb.2017.01081
80. Meliopoulos VA, Karlsson EA, Kercher L, Cline T, Freiden P, Duan S, et al. Human H7N9 and H5N1 influenza viruses differ in induction of cytokines and tissue tropism. *J Virol* (2014) 88(22):12982–91. doi:10.1128/JVI.01571-14
81. To KK, Lau CC, Woo PC, Lau SK, Chan JF, Chan KH, et al. Human H7N9 virus induces a more pronounced pro-inflammatory cytokine but an attenuated interferon response in human bronchial epithelial cells when compared with an epidemiologically-linked chicken H7N9 virus. *Virol J* (2016) 13:42. doi:10.1186/s12985-016-0498-2
82. Wu W, Shi D, Fang D, Guo F, Guo J, Huang F, et al. A new perspective on C-reactive protein in H7N9 infections. *Int J Infect Dis* (2016) 44:31–6. doi:10.1016/j.ijid.2016.01.009
83. Zhao C, Qi X, Ding M, Sun X, Zhou Z, Zhang S, et al. Pro-inflammatory cytokine dysregulation is associated with novel avian influenza A (H7N9) virus in primary human macrophages. *J Gen Virol* (2016) 97(2):299–305. doi:10.1099/jgv.0.000357
84. Nelli RK, Dunham SP, Kuchipudi SV, White GA, Baquero-Perez B, Chang P, et al. Mammalian innate resistance to highly pathogenic avian influenza H5N1 virus infection is mediated through reduced proinflammation and infectious virus release. *J Virol* (2012) 86(17):9201–10. doi:10.1128/JVI.00244-12
85. Turner MD, Nedjai B, Hurst T, Pennington DJ. Cytokines and chemokines: at the crossroads of cell signalling and inflammatory disease. *Biochim Biophys Acta* (2014) 1843:2563–82. doi:10.1016/j.bbamcr.2014.05.014
86. Boonnak K, Vogel L, Feldmann F, Feldmann H, Legge KL, Subbarao K. Lymphopenia associated with highly virulent H5N1 virus infection due to plasmocytoid dendritic cell mediated apoptosis of T cells. *J Immunol* (2014) 192(12):5906–12. doi:10.4049/jimmunol.1302992
87. Waring P, Müllbacher A. Cell death induced by the Fas/Fas ligand pathway and its role in pathology. *Immunol Cell Biol* (1999) 77:312–7. doi:10.1046/j.1440-1711.1999.00837.x
88. Chen Y, Liang W, Yang S, Wu N, Gao H, Sheng J, et al. Human infections with the emerging avian influenza A H7N9 virus from wet market poultry: clinical analysis and characterisation of viral genome. *Lancet* (2013) 381:1916–25. doi:10.1016/S0140-6736(13)60903-4
89. Uiprasertkul M, Kitphati R, Puthavathana P, Kriwong R, Kongchanagul A, Ungchusak K, et al. Apoptosis and pathogenesis of avian influenza A (H5N1) virus in humans. *Emerg Infect Dis* (2007) 13(5):708–12. doi:10.3201/eid1305.060572
90. Wang C, Yu H, Horby PW, Cao B, Wu P, Yang S, et al. Comparison of patients hospitalized with influenza A subtypes H7N9, H5N1, and 2009 pandemic H1N1. *Clin Infect Dis* (2014) 58(8):1095–103. doi:10.1093/cid/ciu053
91. Wang Z, Zhu L, Nguyen THO, Wan Y, Sant S, Quiñones-Parra SM, et al. Clonally diverse CD38+HLA-DR+CD8+ T cells persist during fatal H7N9. *Nat Commun* (2018) 9:824. doi:10.1038/s41467-018-03243-7
92. Nichols JE, Niles JA, Roberts NJ Jr. Human lymphocyte apoptosis after exposure to influenza A virus. *J Virol* (2001) 73(13):5921–9. doi:10.1128/JVI.73.13.5921-5929.2001
93. Herfst S, Imai M, Kawaoka Y, Fouchier RA. Avian influenza virus transmission to mammals. *Curr Top Microbiol Immunol* (2014) 385:137–55. doi:10.1007/82_2014_387
94. Rogers GN, Pritchett TJ, Lane JL, Paulson JC. Differential sensitivity of human, avian, and equine influenza A viruses to a glycoprotein inhibitor of infection: selection of receptor specific variants. *Virology* (1983) 131(2): 394–408. doi:10.1016/0042-6822(83)90507-X
95. de Vries RP, Peng W, Grant OC, Thompson AJ, Zhu X, Bouwman KM, et al. Three mutations switch H7N9 influenza to human-type receptor specificity. *PLoS Pathog* (2017) 13(6):e1006390. doi:10.1371/journal.ppat.1006390
96. Dortmans JC, Dekkers J, Wickramasinghe IN, Verheije MH, Rottier PJ, van Kuppeveld FJ, et al. Adaptation of novel H7N9 influenza virus to human receptors. *Sci Rep* (2013) 3:3058. doi:10.1038/srep03058
97. Chandrasekaran A, Srinivasan A, Raman R, Viswanathan K, Raguram S, Tumpey TM, et al. Glycan topology determines human adaptation of avian H5N1 virus hemagglutinin. *Nat Biotechnol* (2008) 26(1):107–13. doi:10.1038/nbt1375
98. Chrzastek K, Lee DH, Gharaibeh S, Zsak A, Kapczynski DR. Characterization of H9N2 avian influenza viruses from the Middle East demonstrates heterogeneity at amino acid position 226 in the hemagglutinin and potential for transmission to mammals. *Virology* (2018) 518:195–201. doi:10.1016/j.virol.2018.02.016
99. Li X, Shi J, Guo J, Deng G, Zhang Q, Wang J, et al. Genetics, receptor binding property, and transmissibility in mammals of naturally isolated H9N2 avian influenza viruses. *PLoS Pathog* (2014) 10(11):e1004508. doi:10.1371/journal.ppat.1004508
100. Watanabe Y, Arai Y, Daidoji T, Kawashita N, Ibrahim MS, El-Gendy E-D, et al. Characterization of H5N1 influenza virus variants with hemagglutinin mutations isolated from patients. *MBio* (2015) 6(2):e00081-15. doi:10.1128/mBio.00081-15
101. Watanabe Y, Ibrahim MS, Ellakany HF, Kawashita N, Mizuike R, Hiramatsu H, et al. Acquisition of human-type receptor binding specificity by new H5N1 influenza virus sublineages during their emergence in birds in Egypt. *PLoS Pathog* (2011) 7(5):e1002068. doi:10.1371/journal.ppat.1002068

102. Steel J, Lowen AC, Mubareka S, Palese P. Transmission of influenza virus in a mammalian host is increased by PB2 amino acids 627K or 627E/701N. *PLoS Pathog* (2009) 5(1):e1000252. doi:10.1371/journal.ppat.1000252
103. Labadie K, Dos Santos Afonso E, Rameix-Welti MA, van der Werf S, Naffakh N. Host-range determinants on the PB2 protein of influenza A viruses control the interaction between the viral polymerase and nucleoprotein in human cells. *Virology* (2007) 362:271–82. doi:10.1016/j.virol.2006.12.027
104. Yu K, Liu X, Qi T, Yang H, Whitfield DM, Y Chen Q, et al. General low-temperature reaction pathway from precursors to monomers before nucleation of compound semiconductor nanocrystals. *Nat Commun* (2016) 7:12223. doi:10.1038/ncomms12223
105. Zhang H, Li X, Guo J, Li L, Chang C, Li Y, et al. The PB2 E627K mutation contributes to the high polymerase activity and enhanced replication of H7N9 influenza virus. *J Gen Virol* (2014) 95:779–86. doi:10.1099/vir.0.061721-0
106. Schrauwen EJ, Herfst S, Leijten LM, van Run P, Bestebroer TM, Linster M, et al. The multibasic cleavage site in H5N1 virus is critical for systemic spread along the olfactory and hematogenous routes in ferrets. *J Virol* (2012) 86(7):3975–84. doi:10.1128/JVI.06828-11
107. Suguitan AL, Matsuoka Y, Lau YF, Santos CP, Vogel L, Cheng LI, et al. The multibasic cleavage site of hemagglutinin of highly pathogenic A/Vietnam/1203/2004 (H5N1) avian influenza virus acts as a virulence factor in a host-specific manner in mammals. *J Virol* (2012) 86(5):2706–14. doi:10.1128/JVI.05546-11
108. Stieneke-Gröber A, Vey M, Angliker H, Shaw E, Thomas G, Roberts C, et al. Influenza virus hemagglutinin with a multibasic cleavage site is activated by furin, a subtilisin-like endoprotease. *EMBO J* (1992) 11(7):2407–14.
109. Hagag IT, Mansour SM, Zhang Z, Ali AA, Ismaiel el-BM, Salama AA, et al. Pathogenicty of highly pathogenic avian influenza virus H5N1 in naturally infected poultry in Egypt. *PLoS One* (2015) 10(5):e0120061. doi:10.1371/journal.pone.0120061
110. Berhane Y, Hisanaga T, Kehler H, Neufeld J, Manning L, Argue C, et al. Highly pathogenic avian influenza virus A (H7N3) in domestic poultry, Saskatchewan, Canada, 2007. *Emerg Infect Dis* (2009) 15(9):1492–5. doi:10.3201/eid1509.080231
111. Killian ML, Kim-Torchetti M, Hines N, Yingst S, DeLiberto T, Lee DH. Outbreak of H7N8 low pathogenic avian influenza in commercial Turkeys with spontaneous mutation to highly pathogenic avian influenza. *Genome Announc* (2016) 4(3):e00457-16. doi:10.1128/genomeA.00457-16
112. Stech O, Veits J, Weber S, Deckers D, Schröer D, Vahlenkamp TW, et al. Acquisition of a polybasic hemagglutinin cleavage site by a low-pathogenic avian influenza virus is not sufficient for immediate transformation into a highly pathogenic strain. *J Virol* (2009) 83(11):5864–8. doi:10.1128/JVI.02649-08
113. Wang QM, Liu SL, Chen EF. [Advances on epidemiological research of human infections with novel avian influenza A (H7N9) virus]. *Zhonghua Yu Fang Yi Xue Za Zhi* (2017) 51(2):183–7. doi:10.3760/cma.j.issn.0253-9624.2017.02.017
114. Imai M, Watanabe T, Hatta M, Das SC, Ozawa M, Shinya K, et al. Experimental adaptation of an influenza H5 haemagglutinin (HA) confers respiratory droplet transmission to a reassortant H5 HA/H1N1 virus in ferrets. *Nature* (2012) 486:420–8. doi:10.1038/nature10831
115. Haller O, Gao S, von der Malsburg A, Daumke O, Kochs G. Dynamin-like MxA GTPase: structural insights into oligomerization and implications for antiviral activity. *J Biol Chem* (2010) 285(37):28419–24. doi:10.1074/jbc.R110.145839
116. Zimmermann P, Mänz B, Haller O, Schwemmle M, Kochs G. The viral nucleoprotein determines Mx sensitivity of influenza A viruses. *J Virol* (2011) 85(16):8133–40. doi:10.1128/JVI.00712-11
117. Mänz B, Dornfeld D, Götz V, Zell R, Zimmermann P, Haller O, et al. Pandemic influenza A viruses escape from restriction by human MxA though adaptive mutations in the nucleoprotein. *PLoS Pathog* (2013) 9(3):e1003279. doi:10.1371/journal.ppat.1003279
118. Deeg CM, Hassan E, Mutz P, Rheinemann L, Götz V, Magar L, et al. In vivo evasion of MxA by avian influenza viruses requires human signature in the viral nucleoprotein. *J Exp Med* (2017) 214(5):1239–48. doi:10.1084/jem.20161033
119. Schusser B, Reuter A, von der Malsburg A, Penski N, Weigend S, Kaspers B, et al. Mx Is dispensable for interferon-mediated resistance of chicken cells against influenza A virus. *J Virol* (2011) 85(16):8307–15. doi:10.1128/JVI.00535-11
120. Benfield CTO, Lyall JW, Tiley LS. The cytoplasmic location of chicken Mx is not the determining factor for its lack of antiviral activity. *PLoS One* (2010) 5(8):e12151. doi:10.1371/journal.pone.0012151
121. Qi X, Zhang H, Wang Q, Wang J. The NS1 protein of avian influenza virus H9N2 induces oxidative-stress-mediated chicken oviduct epithelial cells apoptosis. *J Gen Virol* (2016) 97:3183–92. doi:10.1099/jgv.0.000625
122. Burggraaf S, Bingham J, Payne J, Kimpton WG, Lowenthal JW, Bean AG. Increased inducible nitric oxide synthase expression in organs is associated with a higher severity of H5N1 influenza infection. *PLoS One* (2011) 6(1):e14561. doi:10.1371/journal.pone.0014561
123. Jia D, et al. Influenza virus non-structural protein 1 (NS1) disrupts interferon signalling. *PLoS One* (2010) 5(11):e13927. doi:10.1371/journal.pone.0013927
124. Wang J, Zeng Y, Xu S, Yang J, Wang W, Zhong B, et al. A naturally occurring deletion in the effector domain of H5N1 swine influenza virus nonstructural protein 1 regulates viral fitness and host innate immunity. *J Virol* (2018) 92(11):e00149-18. doi:10.1128/JVI.00149-18
125. Jiao P, Tian G, Li Y, Deng G, Jiang Y, Liu C, et al. A single-amino-acid substitution in the NS1 protein changes the pathogenicity of H5N1 avian influenza viruses in mice. *J Virol* (2008) 82(3):1146–54. doi:10.1128/JVI.01698-07
126. Wang L, Fu X, Zheng Y, Zhou P, Fang B, Huang S, et al. The NS1 protein of H5N6 feline influenza virus inhibits feline beta interfereon response by preventing NF-κB and IRF3 activation. *Dev Comp Immunol* (2017) 74:60–8. doi:10.1016/j.dci.2017.04.003
127. Thube MM, Shil P, Kasbe R, Patil AA, Pawar SD, Mullick J. Differences in Type I interferon response in human lung epithelial cells infected by highly pathogenic H5N1 and low pathogenic H11N1 avian influenza viruses. *Virus Genes* (2018) 54(3):414–23. doi:10.1007/s11262-018-1556-1
128. Ayllon J, Domingues P, Rajsbaum R, Miorin L, Schmolke M, Hale BG, et al. A single amino acid substitution in the novel H7N9 influenza A NS1 protein increases CPSF30 binding and virulence. *J Virol* (2014) 88(20):12146–51. doi:10.1128/JVI.01567-14
129. Bailey CC, Kondur HR, Huang IC, Farzan M. Interferon-induced transmembrane protein 3 is a type II transmembrane protein. *J Biol Chem* (2013) 288(45):32184–93. doi:10.1074/jbc.M113.514356
130. Bailey CC, Zhong G, Huang IC, Farzan M. IFITM-family proteins: the cell's first line of antiviral defense. *Annu Rev Virol* (2014) 1:261–83. doi:10.1146/annurev-virology-031413-085537
131. Feeley EM, Sims JS, John SP, Chin CR, Pertel T, Chen LM, et al. IFITM3 inhibits influenza A virus infection by preventing cytosolic entry. *PLoS Pathog* (2011) 7(10):e1002337. doi:10.1371/journal.ppat.1002337
132. Brass AL, Huang IC, Benita Y, John SP, Krishnan MN, Feeley EM, et al. The IFITM proteins mediate cellular resistance to influenza A H1N1 virus, West Nile virus, and dengue virus. *Cell* (2009) 139:1243–54. doi:10.1016/j.cell.2009.12.017
133. Jia R, Pan Q, Ding S, Rong L, Liu SL, Geng Y, et al. The N-terminal region of IFITM3 modulates its antiviral activity by regulating IFITM3 cellular localization. *J Virol* (2012) 86(24):13697–707. doi:10.1128/JVI.01828-12
134. Wakim LM, Gupta N, Mintern JD, Villadangos JA. Enhanced survival of tissue-resident memory CD8+ T cells during infection with influenza virus due to selective expression of IFITM3. *Nat Immunol* (2013) 14(3):238–46. doi:10.1038/ni.2525
135. Yang X, Tan B, Zhou X, Xue J, Zhang X, Wang P, et al. Interferon-inducible transmembrane protein 3 genetic variant rs12252 and influenza susceptibility and severity: a meta-analysis. *PLoS One* (2015) 10(5):e0124985. doi:10.1371/journal.pone.0124985
136. Zhang YH, Zhao Y, Li N, Peng YC, Giannoulatou E, Jin RH, et al. Interferon-induced transmembrane protein-3 genetic variant rs12252-C is associated with severe influenza in Chinese individuals. *Nat Commun* (2013) 4:1418. doi:10.1038/ncomms2433
137. Wang Z, Zhang A, Wan Y, Liu X, Qiu C, Xi X, et al. Early hypercytokinemia is associated with interferon-induced transmembrane protein-3

dysfunction and predictive of fatal H7N9 infection. *Proc Natl Acad Sci U S A* (2014) 111(2):769–74. doi:10.1073/pnas.1321748111
138. Williams DE, Wu WL, Grotefend CR, Radic V, Chung C, Chung YH, et al. IFITM3 polymorphism rs12252-C restricts influenza A viruses. *PLoS One* (2014) 9(10):e110096. doi:10.1371/journal.pone.0110096
139. Makvandi-Nejad S, Laurenson-Schafer H, Wang L, Wellington D, Zhao Y, Jin B, et al. Lack of truncated IFITM3 transcripts in cells homozygous for the rs12252-C variant that is associated with severe influenza infection. *J Infect Dis* (2018) 217:257–62. doi:10.1093/infdis/jix512
140. Allen EK, Randolph AG, Bhangale T, Dogra P, Ohlson M, Oshansky CM, et al. SNP-mediated disruption of CTCF binding at the IFITM3 promoter is associated with risk of severe influenza in humans. *Nat Med* (2017) 23:975–83. doi:10.1038/nm.4370
141. Yu M, Qi W, Huang Z, Zhang K, Ye J, Liu R, et al. Expression profile and histological distribution of IFITM1 and IFITM3 during H9N2 avian influenza virus infection in BALB/c mice. *Med Microbiol Immunol* (2015) 204:505–14. doi:10.1007/s00430-014-0361-2
142. Benfield CTO, Smith SE, Wright E, Wash RS, Ferrara F, Temperton NJ, et al. Bat and pig IFN-induced transmembrane protein 3 restrict cell entry by influenza virus and lyssavirus. *J Gen Virol* (2015) 96:991–1005. doi:10.1099/vir.0.000058
143. Smith SE, Gibson MS, Wash RS, Ferrara F, Wright E, Temperton N, et al. Chicken interferon-inducible transmembrane protein 3 restricts influenza viruses and lyssaviruses in vitro. *J Virol* (2013) 87(23):12957–66. doi:10.1128/JVI.01443-13
144. Cao Y, Huang Y, Xu K, Liu Y, Li X, Xu Y, et al. Differential responses of innate immunity triggered by different subtypes of influenza a viruses in human and avian hosts. *BMC Med Genomics* (2017) 10:70. doi:10.1186/s12920-017-0304-z
145. Smith J, Smith N, Yu L, Paton IR, Gutowska MW, Forrest HL, et al. A comparative analysis of host responses to avian influenza infection in ducks and chickens highlights a role for the interferon-induced transmembrane proteins in viral resistance. *BMC Genomics* (2015) 16:574. doi:10.1186/s12864-015-1778-8
146. Cheng VC, Chan JF, Wen X, Wu WL, Que TL, Chen H, et al. Infection of immunocompromised patients by avian H9N2 influenza A virus. *J Infect* (2011) 62:394–9. doi:10.1016/j.jinf.2011.02.007
147. Law AH, Lee DC, Yuen KY, Peiris M, Lau AS. Cellular response to influenza virus infection: a potential role for autophagy in CXCL10 and interferon-alpha induction. *Cell Mol Immunol* (2010) 7:263–70. doi:10.1038/cmi.2010.25
148. Nili H, Asasi K. Avian influenza (H9N2) outbreak in Iran. *Avian Dis* (2003) 47(s3):828–31. doi:10.1637/0005-2086-47.s3.828
149. Nili H, Asasi K. Natural cases and an experimental study of H9N2 avian influenza in commercial broiler chickens of Iran. *Avian Pathol* (2002) 31(3):247–52. doi:10.1080/03079450220136567
150. Simonsen L, Spreeuwenberg P, Lustig R, Taylor RJ, Fleming DM, Kroneman M, et al. Global mortality estimates for the 2009 influenza pandemic from the GLaMOR project: a modeling study. *PLoS Med* (2013) 10(11):e1001558. doi:10.1371/journal.pmed.1001558
151. Huang SS, Banner D, Degousee N, Leon AJ, Xu L, Paquette SG, et al. Differential pathological and immune responses in newly weaned ferrets are associated with a mild clinical outcome of pandemic 2009 H1N1 infection. *J Virol* (2012) 86(24):13187–201. doi:10.1128/JVI.01456-12
152. Helferty M, Vachon J, Tarasuk J, Rodin R, Spika J, Pelletier L. Incidence of hospital admissions and severe outcomes during the first and second waves of pandemic (H1N1) 2009. *CMAJ* (2010) 182(18):1981–7. doi:10.1503/cmaj.100746
153. Paquette SG, Huang SSH, Banner D, Xu L, León A, Kelvin AA, et al. Impaired heterologous immunity in aged ferrets during sequential influenza A H1N1 infection. *Virology* (2014) 46(4–465):177–83. doi:10.1016/j.virol.2014.07.013
154. Zhou L, Tan Y, Kang M, Liu F, Ren R, Wang Y, et al. Preliminary epidemiology of human infections with highly pathogenic avian influenza A(H7N9) virus, China, 2017. *Emerg Infect Dis* (2017) 23(8):1355–9. doi:10.3201/eid2308.170640
155. Mackay IM. *Influenza A(H7N9) Virus: Detection Numbers and Graphs….* VDU's blog (2014).
156. Gostic KM, Ambrose M, Worobey M, Lloyd-Smith JO. Potent protection against H5N1 and H7N9 influenza via childhood hemagglutinin imprinting. *Science* (2016) 354(6313):722–6. doi:10.1126/science.aag1322
157. Valkenburg SA, Josephs TM, Clemens EB, Grant EJ, Nguyen TH, Wang GC, et al. Molecular basis for universal HLA-A*0201-restricted CD8+ T-cell immunity against influenza viruses. *Proc Natl Acad Sci U S A* (2016) 113(16):4440–5. doi:10.1073/pnas.1603106113
158. Quiñones-Parra S, Grant E, Loh L, Nguyen TH, Campbell KA, Tong SY, et al. Preexisting CD8+ T-cell immunity to the H7N9 influenza A virus varies across ethnicities. *Proc Natl Acad Sci U S A* (2014) 111(3):1049–54. doi:10.1073/pnas.1322229111
159. Nguyen THO, Sant S, Bird NL, Grant EJ, Clemens EB, Koutsakos M, et al. Perturbed CD8+ T cell immunity across universal influenza epitopes in the elderly. *J Leukoc Biol* (2017) 103(2):321–39. doi:10.1189/jlb.5MA0517-207R
160. Clemens EB, Grant EJ, Wang Z, Gras S, Tipping P, Rossjohn J, et al. Towards identification of immune and genetic correlates of severe influenza disease in Indigenous Australians. *Immunol Cell Biol* (2016) 94:367–77. doi:10.1038/icb.2015.93
161. Hertz T, Oshansky CM, Roddam PL, DeVincenzo JP, Caniza MA, Jojic N, et al. HLA targeting efficiency correlates with human T-cell response magnitude and with mortality from influenza A infection. *Proc Natl Acad Sci U S A* (2013) 110(33):13492–7. doi:10.1073/pnas.1221555110
162. Liu R, Moise L, Tassone R, Gutierrez AH, Terry FE, Sangare K, et al. H7N9 T-cell epitopes that mimic human sequences are less immunogenic and may induce Treg-mediated tolerance. *Hum Vaccin Immunother* (2015) 11(9):2241–52. doi:10.1080/21645515.2015.1052197
163. Hou Y, Guo Y, Wu C, Shen N, Jiang Y, Wang J. Prediction and identification of T cell epitopes in the H5N1 influenza virus nucleoprotein in chicken. *PLoS One* (2012) 7(6):e39344. doi:10.1371/journal.pone.0039344
164. Zhang W, Huang Q, Lu M, Zhu F, Huang YY, Yang SH, et al. Exploration of the BF2*15 major histocompatibility complex class I binding motif and identification of cytotoxic T lymphocyte epitopes from the H5N1 influenza virus nucleoprotein in chickens. *Arch Virol* (2016) 161:3081–93. doi:10.1007/s00705-016-3013-6
165. Fleming-Canepa X, Jensen SM, Mesa CM, Diaz-Satizabal L, Roth AJ, Parks-Dely JA, et al. Extensive allelic diversity of MHC class I in wild mallard ducks. *J Immunol* (2016) 197:783–94. doi:10.4049/jimmunol.1502450
166. Wu Y, Wang J, Fan S, Chen R, Liu Y, Zhang J, et al. Structural definition of duck major histocompatibility complex class I molecules that might explain efficient cytotoxic T lymphocyte immunity to influenza A virus. *J Virol* (2017) 91(14):e02511-16. doi:10.1128/JVI.02511-16
167. Buehler DM, Verkuil YI, Tavares ES, Baker AJ. Characterization of MHC class I in a long-distance migrant shorebird suggests multiple transcribed genes and intergenic recombination. *Immunogenetics* (2013) 65:211–25. doi:10.1007/s00251-012-0669-2
168. Watanabe T, Zhong G, Russell CA, Nakajima N, Hatta M, Hanson A, et al. Circulating avian influenza viruses closely related to the 1918 virus have pandemic potential. *Cell Host Microbe* (2014) 15:692–705. doi:10.1016/j.chom.2014.05.006

Conflict of Interest Statement: The authors declare that the research was conducted in the absence of any commercial or financial relationships that could be construed as a potential conflict of interest.

npj | Vaccines

www.nature.com/npjvaccines

ARTICLE OPEN

Check for updates

ChAdOx1 nCoV-19 (AZD1222) vaccine candidate significantly reduces SARS-CoV-2 shedding in ferrets

Glenn A. Marsh[1,4], Alexander J. McAuley[1,4], Gough G. Au[1], Sarah Riddell[1], Daniel Layton[1], Nagendrakumar B. Singanallur[1], Rachel Layton[1], Jean Payne[1], Peter A. Durr[1], Hannah Bender[1], Jennifer A. Barr[1], John Bingham[1], Victoria Boyd[1], Sheree Brown[1], Matthew P. Bruce[1], Kathie Burkett[1], Teresa Eastwood[1], Sarah Edwards[1], Tamara Gough[1], Kim Halpin[1], Jenni Harper[1], Clare Holmes[1], William S. J. Horman[1], Petrus Jansen van Vuren[1], Suzanne Lowther[1], Kate Maynard[1], Kristen D. McAuley[1], Matthew J. Neave[1], Timothy Poole[1], Christina Rootes[1], Brenton Rowe[1], Elisha Soldani[1], Vittoria Stevens[1], Cameron R. Stewart[1], Willy W. Suen[1], Mary Tachedjian[1], Shawn Todd[1], Lee Trinidad[1], Duane Walter[1], Naomi Watson[1], Trevor W. Drew[1], Sarah C. Gilbert[2], Teresa Lambe[2] and S. S. Vasan[1,3]✉

Vaccines against SARS-CoV-2 are likely to be critical in the management of the ongoing pandemic. A number of candidates are in Phase III human clinical trials, including ChAdOx1 nCoV-19 (AZD1222), a replication-deficient chimpanzee adenovirus-vectored vaccine candidate. In preclinical trials, the efficacy of ChAdOx1 nCoV-19 against SARS-CoV-2 challenge was evaluated in a ferret model of infection. Groups of ferrets received either prime-only or prime-boost administration of ChAdOx1 nCoV-19 via the intramuscular or intranasal route. All ChAdOx1 nCoV-19 administration combinations resulted in significant reductions in viral loads in nasal-wash and oral swab samples. No vaccine-associated adverse events were observed associated with the ChAdOx1 nCoV-19 candidate, with the data from this study suggesting it could be an effective and safe vaccine against COVID-19. Our study also indicates the potential for intranasal administration as a way to further improve the efficacy of this leading vaccine candidate.

npj Vaccines (2021)6:67 ; https://doi.org/10.1038/s41541-021-00315-6

INTRODUCTION

In December 2019, an outbreak of the severe respiratory disease was first reported in Wuhan, China. The causative agent of this outbreak was rapidly identified as a novel coronavirus and denoted severe acute respiratory syndrome coronavirus-2 (SARS-CoV-2), responsible for COVID-19 disease[1–3]. In less than 12 months since its identification, SARS-CoV-2 has spread around the world and has been responsible for over 64 million infections and 1.5 million deaths worldwide as of December 2020[4]. Safe and effective vaccines and therapeutics will be essential for mitigating viral spread and for bringing the pandemic under control. Of the vaccines currently in development for COVID-19, the adenovirus vector-based candidate, ChAdOx1 nCoV-19 (AZD1222), is in late-stage clinical development, with Phase III trials in multiple countries currently underway[5]. As of January 2021, this vaccine has been approved by regulatory agencies in the UK and India for emergency use in humans[6].

ChAdOx1 nCoV-19 is based upon the Jenner Institute's adenovirus vaccine platform that utilises a replication-deficient Simian adenovirus vector engineered to express an antigen of interest[7]. This virus vector-based approach has been successfully used previously to generate several vaccine candidates against other infectious diseases including Middle-East respiratory syndrome coronavirus (MERS-CoV). A single dose of ChAdOx1 MERS was capable of protecting Rhesus macaques from infection and reducing MERS-CoV shedding in camels[8,9]. Phase I clinical trials of this vaccine candidate demonstrated the induction of robust antibody and T-cell responses[10].

The ChAdOx1 nCoV-19 vaccine encodes the SARS-CoV-2 Spike protein, the main protein found on the surface of the virus, and after immunisation is subsequently expressed as an immunogen[11]. Administration of ChAdOx1 nCoV-19 to Rhesus macaques following a prime or prime-boost regimen induced a balanced humoral and cellular immune response. Following the challenge, vaccinated animals had a lack of pneumonia and a reduction in virus load in bronchioalveolar lavage fluid and the lower respiratory tract when compared to unvaccinated macaques[12]. Clinical trials have shown the vaccines to have an acceptable safety profile and are capable of inducing both humoral and cellular immune responses with recent data demonstrating efficacy[5,11].

SARS-CoV-2 infection in ferrets most closely models asymptomatic or mild infection in humans. Infection of these animals is associated with the shedding of virus from the upper respiratory tract, with viral RNA detected in clinical samples taken up to day 9 post challenge[13–18]. The ferret model is considered to be a relevant animal model for testing SARS-CoV-2 vaccine candidate safety, immunogenicity, and efficacy by assessing the level of viral shedding and the determination of immune responses[19].

We used the ferret model to assess the safety and efficacy of ChAdOx1 nCoV-19 against SARS-CoV-2 challenge. Ferrets received prime or prime-boost administrations of ChAdOx1 nCoV-19 as either an intramuscular injection or intranasal inoculation. Assessment of the immune response was performed post-vaccination, pre- and post challenge, and the ability to reduce viral shedding was also monitored.

RESULTS

Immunogenicity of ChAdOx1 nCoV-19 in ferrets

Eight animals per group (four male and four female) were administered ChAdOx1 nCoV-19 using a prime-only regimen (28-days pre-challenge) or a prime-boost regimen (56- and 28-days

[1]CSIRO Australian Centre for Disease Preparedness, Geelong, VIC, Australia. [2]Jenner Institute, Nuffield Department of Medicine, University of Oxford, Oxford, UK. [3]Department of Health Sciences, University of York, York, UK. [4]These authors contributed equally: Glenn A. Marsh, Alexander J. McAuley. ✉email: vasan.vasan@csiro.au

Published in partnership with the Sealy Institute for Vaccine Sciences

npj nature partner journals

utmb Health Sealy Institute for Vaccine Sciences

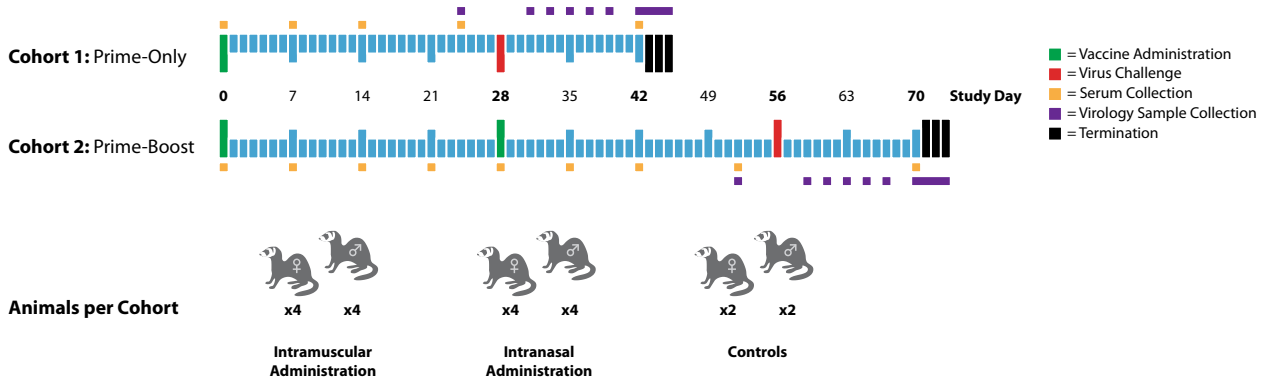

Fig. 1 Study Outline. Groups of eight ferrets (four male, four female) received either a single (prime) or two (prime-boost) doses of ChAdOx1 nCoV-19 via the intramuscular or intranasal route. An additional four ferrets (two male, two female) were included as mock (PBS) vaccinated control animals. Samples were collected from all of the animals at the timepoints highlighted.

pre-challenge) either intramuscularly or intranasally with 2.5×10^{10} ChAdOx1 nCoV-19 virus particles per dose, which is half of the standard human dose (Fig. 1). As controls, four animals were administered phosphate-buffered saline (PBS) intramuscularly on days 56 and 28 pre-challenge (two male and two female) with an additional four animals (two male and two female) on day 28 pre-challenge. No adverse events or effects on the ferrets' health were observed following ChAdOx1 nCoV-19 administration.

To measure antibody levels induced by the vaccine candidate, serum samples were collected on a weekly basis and neutralising antibody levels assessed using a standard virus microneutralisation assay. This assay assessed the ability of the samples to neutralise 100 $TCID_{50}$ of SARS-CoV-2 virus. No virus-neutralising antibodies were detected in control animals (Fig. 2a, b).

Prime-only intramuscular administration of ChAdOx1 nCoV-19 reliably induced detectable neutralising antibodies prior to challenge, which was boosted by the challenge. Prime-only intranasal administration did not reliably induce detectable neutralising antibodies in the serum prior to challenge and, following challenge, only 75% of animals had measurable neutralising antibodies (Fig. 2b).

Administration of a boost dose of ChAdOx1 nCoV-19 by either route led to a sharp increase in neutralising antibody levels in all ferrets 7 days after the second vaccination, which then declined prior to the challenge. Integrated analysis of the neutralisation data demonstrated that the administration of a boost dose of ChAdOx1 nCoV-19 increased the overall neutralisation levels in a similar manner regardless of the administration route (Fig. 2c).

Consistent with McAuley et al.[24], six serum samples per administration route were selected from available pre-challenge samples collected on study days 35 and 42 from the prime-boost animals. Each serum sample came from a different animal. Triplicate virus microneutralisation assays were performed with each serum sample against three Australian SARS-CoV-2 virus isolates: VIC01, SA01 and VIC31. Compared to the reference sequence for SARS-CoV-2 (Wuhan-Hu-1; NC_045512.2), these isolates have the following mutations in S: VIC01—S247R; SA01—no mutations; VIC31—D614G. Analysis of the results by route of administration revealed that neutralisation titres were greater in the animals that had received two doses of ChAdOx1 nCoV-19 via the intramuscular route (overall median titre 320) compared to those who received doses via the intranasal route (overall median titre 160; $P < 0.001$) (Fig. 3).

A mean neutralisation titre was calculated for each serum/isolate combination from the $\log_2$-transformed data. For animals that received intramuscular administration of ChAdOx1 nCoV-19, the overall mean neutralisation titres (blue bar) were within twofold of one another for each virus isolate, whilst for animals that received the intranasal administration, the overall mean neutralisation titre (red bar) was approximately 2.3-fold lower against the D614-containing SA01 isolate than the D614-containing VIC01 or the G614-containing VIC31 (Fig. 3). The mean neutralising titre against SA01 was significantly lower ($P < 0.01$) for each administration route. The reason for this variability is unclear, but we conclude that it is not directly due to the D614G mutation in the Spike protein given the similarity of neutralisation titres against VIC01 and VIC31.

Peripheral blood mononuclear cells (PBMCs) were isolated from the blood of ferrets on days −4 and 5, relative to virus challenge (study days 24 and 33 for prime-only animals; study days 52 and 61 for prime-boost animals). Due to an unexpected reaction at virus challenge, resulting in the euthanasia of two prime-only control ferrets (described in more detail below), values for only two prime-only control animals were obtained. Circulating interferon-gamma (IFNγ)-producing leukocytes were measured by IFNγ ELISpot (Fig. 4). None of the study groups had a significant change in IFNγ-positive PBMC levels between pre- and post-challenge samples. At day 5 post challenge, a significantly higher number of IFNγ-producing cells were observed in the intramuscular prime-boost group compared to the equivalent prime-only animals ($P < 0.01$). No other significant differences were observed.

Clinical signs following challenge

No clinical signs attributable to viral infection were observed following intranasal challenge with 3×10^4 $TCID_{50}$ SARS-CoV-2 VIC01. None of the animals showed signs of fever (determined by subcutaneous transponder temperature readings) or weight loss, with ferrets remaining bright, alert and responsive throughout the course of the study. Haematological and clinical chemistry analysis of pre- and post-challenge samples revealed no values outside expected ranges. Importantly, no evidence of immune enhancement was observed in either the prime-only or prime-boost animals for either route of administration.

On day 28, immediately following the virus challenge of the prime-only animals, two control animals that received a single PBS placebo vaccination were euthanised due to a severe unexpected reaction. On day 56, during the challenge of prime-boost animals, acute unexpected reactions were observed in several animals, one of which was severe enough to warrant euthanasia. Affected ferrets showed varying degrees of respiratory distress, and necropsies were performed on euthanised animals. Histopathological assessment of respiratory tissues suggested an underlying allergic process. Root cause analysis identified the challenge inoculum as the triggering agent, with a commercial canine vaccine (Protech® C3) administered to the ferrets as husbandry prophylaxis against canine distemper virus identified as the priming agent. Further analysis suggested an active immune response to a component(s) of FBS contained in both the C3

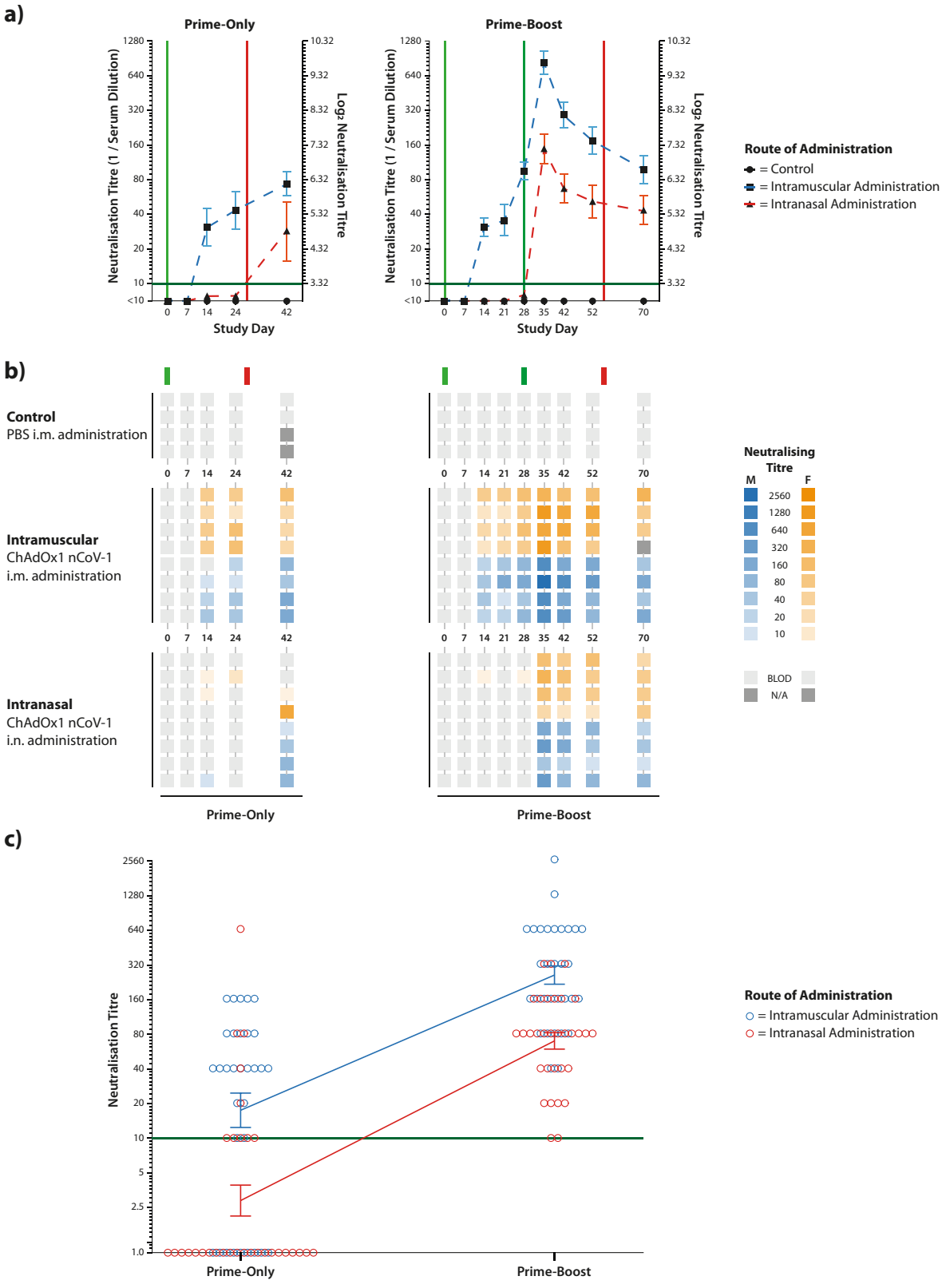

vaccine and the SARS-CoV-2 challenge inoculum[20]. The investigation found that the ChAdOx1 nCoV-19 vaccine candidate was not implicated in the unexpected reaction, and the observed reaction did not affect the study outcomes for the remaining ferrets.

Virus shedding following challenge

Nasal wash, rectal and oral swab samples were collected at the prescribed time points of the study (Fig. 1). None of the samples collected pre-challenge (study day 24 for prime-only animals; day

Fig. 2 Serum virus-neutralisation titres against SARS-CoV-2. Individual ferret serum samples were tested using a virus microneutralisation assay with a twofold dilution series starting at 1:10, with the neutralisation titre stated as the highest dilution of serum leading to 100% virus neutralisation. **a** Mean titres were calculated for each study group from log_2-transformed data and plotted with SEM. Green vertical lines represent dates of ChAdOx1 nCoV-19 administration, whilst red vertical lines represent virus challenge at study day 28 or 56 for the two cohorts, respectively. The dark green horizontal line represents the limit of detection of the assay. **b** Neutralising titres for individual ferrets were presented in a heatmap with vaccine administration and challenge dates represented with green and red lines, respectively. **c** Integrated analysis of neutralisation titres from prime-only and prime-boost administrations. Neutralisation titres from prime-only animals were combined from study days 7, 14, 24 and 40, whilst neutralisation titres from prime-boost animals were combined from study days 35, 42, 52 and 70. These represent the same timeframe relative to the challenge date. For both intramuscular and intranasal administration of ChAdOx1 nCoV-19, the increase in neutralisation titre from a boost dose is similar, as indicated by the almost-parallel linking lines. The vertical lines with error bars represent the mean and standard error of the mean (SEM) from log_2-transformed data.

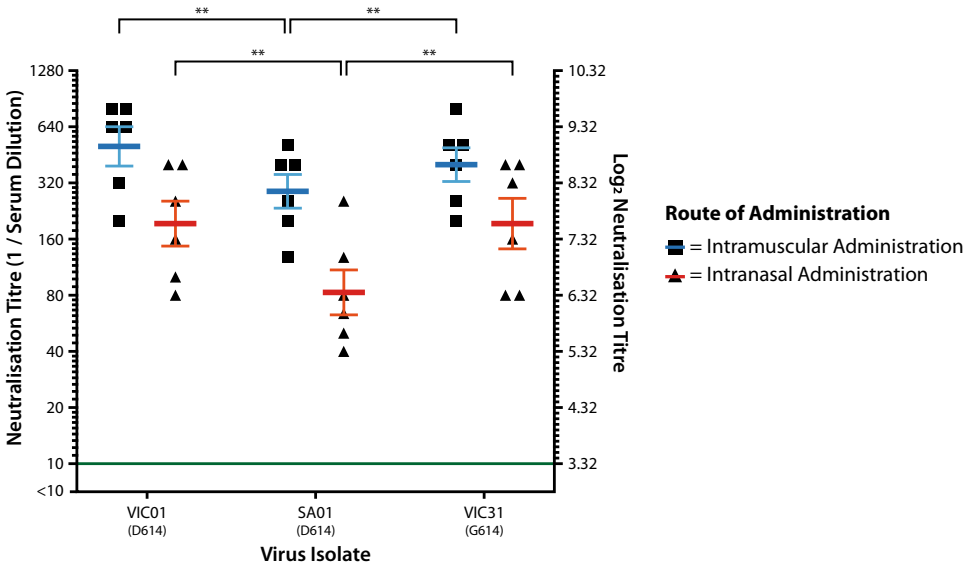

Fig. 3 Comparative neutralisation of D614- and G614-containing isolates. Six serum samples from prime-boost animals were selected from study day 35 and 42 samples per administration route. Microneutralisation assays were performed for each sample using three Australian virus isolates containing D614 (VIC01, SA01) or G614 (VIC31) in the Spike protein. Triplicate titres were obtained for each serum/isolate combination, with log_2-transformed mean values plotted as individual data points. Mean titres were calculated for each isolate/route of administration based upon log_2-transformed data, which were plotted as blue or red lines, depending on the route of administration. Error bars represent SEM, $^{**}P < 0.01$.

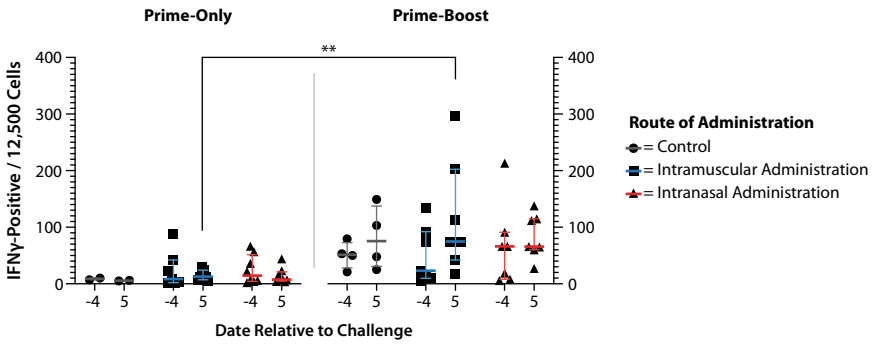

Fig. 4 IFNγ-producing PBMC levels pre- and post challenge. PBMCs were isolated from blood samples taken on days −4 and 5, relative to challenge, for quantification of circulating IFNγ-producing cells by ELISpot assay. Prime-only animals had few IFNγ-producing cells, whilst prime-boost animals had greater numbers. Comparison of intramuscular prime-boost with prime-only post-challenge results demonstrated statistical significance ($^{**}P < 0.01$). Horizontal lines represent mean and SEM.

52 for prime-boost animals) had detectable levels of SARS-CoV-2 E RNA, as determined by RT-qPCR.

Viral RNA loads (log_{10} SARS-CoV-2 E copies/mL) for each sample collected post challenge are presented in Fig. 5 for days 3, 5, 7 and 9 post challenge. These time points correspond to study days 31, 33, 35 and 37 for prime-only animals, and study days 59, 61, 63 and 65 for prime-boost animals. No virus shedding was detected in any ferret samples collected on day 11 or 14 post challenge (study days 39 and 42 for prime-only animals; study days 67 and 70 for prime-boost animals; data not shown).

Compared to the control animals, average levels of virus shedding (as determined by RT-qPCR) in nasal-wash and oral swab samples were lower for each ChAdOx1 nCoV-19 Study Group. These reductions were statistically significant ($P < 0.05$) in nasal-

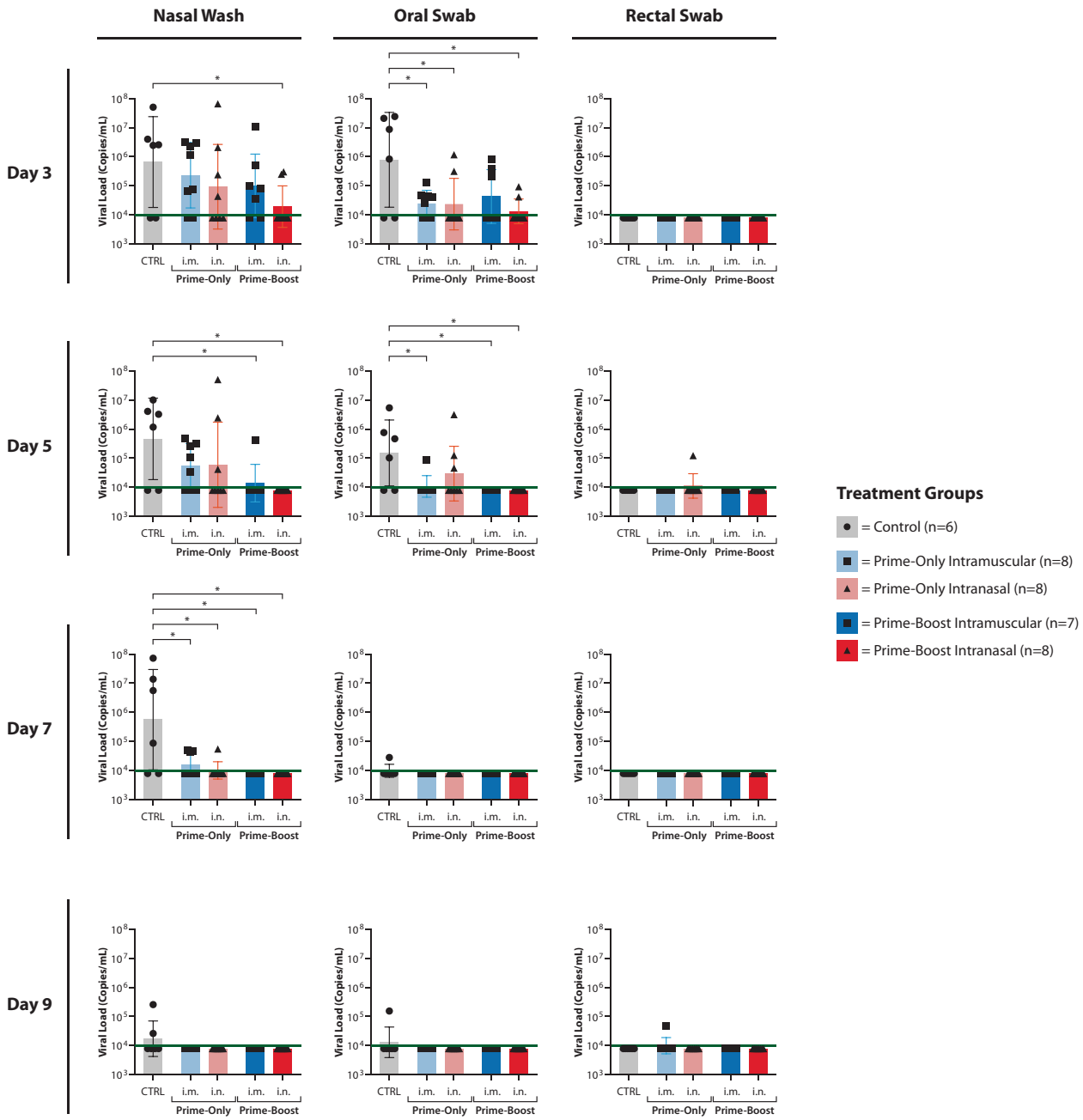

Fig. 5 Viral load in nasal-wash and rectal and oral swab fluids as determined by RT-qPCR. RNA was extracted from samples collected on days 3, 5, 7 and 9 post challenge (study days 31, 33, 35 and 37 for prime-only animals; days 59, 61, 63 and 65 for prime-boost animals), and was analysed in duplicate using RT-qPCR assay detecting SARS-CoV-2 E RNA. Black points represent mean RNA copy number of the duplicate reactions for individual ferrets. The columns represent mean RNA copy numbers for each group, error bars represent SEM and the green lines are the limit-of-detection for the assay. Where no viral RNA was detected by RT-qPCR, a data point has been plotted at 3.9. Statistical analysis was performed by one-tailed *t* test, with statistical significance indicated by an asterisk ($P < 0.05$).

wash samples on days 3, 5 and 7 post challenge, and oral swab samples on days 3 and 5 post challenge (Fig. 5). Administration of both prime and boost doses of ChAdOx1 nCoV-19 demonstrated a trend towards lower levels of shedding than prime-only administration, however, this trend was not statistically significant.

Virus isolation was attempted on PCR-positive samples, with only a single day 3 post-challenge nasal-wash sample from a prime-only, intranasal administration ferret positive for infectious virus. The infectious virus load in this sample was too low for a $TCID_{50}$/mL titre to be calculated.

Histopathological assessment of tissues

No evidence of viral-induced disease associated with the SARS-CoV-2 challenge was detected in any of the ferrets at the end of the trial. Moreover, no SARS-CoV-2 antigen labelling was detected by immunohistochemistry in the tissues examined (lung, spleen, tongue, nasal turbinate, pharynx, trachea, heart and retropharyngeal lymph nodes; data not shown as all negative). Minimal-to-moderate neutrophilic infiltrates were frequently present in the tracheal epithelium, bronchi, and terminal bronchioles of ferrets from all groups (including controls) and were considered incidental.

Small numbers of ferrets had minimal-to-moderate eosinophilic infiltration of the tracheal mucosa and peribronchial interstitium. This change was present in animals from all groups and was unrelated to ChAdOx1 nCoV-19 administration. In animals euthanised immediately following unexpected reactions, eosinophilic airway inflammation was associated with pronounced mucosal oedema, implicating an acute allergic or anaphylactic response to the virus inoculum. No evidence of a reaction to either intramuscular or intranasal vaccine administration was observed in any animal.

DISCUSSION

Safe, effective and widely available vaccines will be instrumental in managing the ongoing SARS-CoV-2 pandemic. As of February 2021, there are over 240 COVID-19 vaccine candidates in development, with 63 undergoing clinical evaluation[21]. ChAdOx1 nCoV-19 has previously been tested in a rhesus macaque model of SARS-CoV-2 infection, where vaccination was demonstrated to prevent pneumonia but not nasal shedding of the virus[12]. The objective of this study was to use a second animal model of SARS-CoV-2 infection and further evaluate the safety and efficacy of ChAdOx1 nCoV-19. Importantly, this study was the first to propose and investigate an alternative COVID-19 vaccination route (intranasal) which is of relevance given SARS-CoV-2 is a respiratory pathogen, and the results from this study have led to subsequent human clinical trials for this candidate[22].

All vaccine treatment groups presented statistically significant reductions in virus loads in nasal-wash and oral swab samples compared to control animals, demonstrating a vaccine-induced reduction in viral shedding. Animals that received prime-boost administration regimens had no statistically significant reductions in viral loads compared to animals that received prime-only administration of ChAdOx1 nCoV-19. This observation is in agreement with the previous studies investigating ChAdOx1 nCoV-19 efficacy in rhesus macaques[12].

Neutralising antibody titres were generally higher in prime-boost animals and animals that received intramuscular administration of ChAdOx1 nCoV-19, which is to be expected as these studies measured serum neutralising antibody titres. Indeed, pre-challenge neutralising antibody titres were very similar between the prime-only animals and prime-boost animals that had received only a single dose. The Challenge of prime-only animals led to a boost-effect in neutralising antibodies, whilst this effect was not observed following the challenge of prime-boost animals. This would suggest that the third dose of ChAdOx1 nCoV-19 would likely not further-increase neutralising antibody levels, at least in the ferret model.

The lower serum neutralising titres measured in animals that received intranasally administered ChAdOx1 nCoV-19 compared to intramuscular administration can likely be explained through the induction of a more localised mucosal immune response compared to the systemic response induced by peripheral inoculation, as previously demonstrated with influenza vaccines[23]. Future studies (such as ref. [22]) to look at the induction of mucosal immune responses following intranasal administration are strongly recommended, as only 25% (2/8) of animals that received prime-boost intranasal administration of ChAdOx1 nCoV-19 had detectable viral RNA in nasal-wash and oral swab samples on day 3 post challenge (compared to 75% (6/8) and 43% (3/7) positivity, respectively, in samples from prime-boost intramuscular-administered animals). Moreover, there no detectable viral RNA in any of the wash or swab samples for animals in the intranasal group on subsequent days.

The neutralising ability of vaccine-induced antibodies following intramuscular or intranasal prime-boost administration appeared not to be substantially affected by the D614G mutation that has arisen in the SARS-CoV-2 Spike protein. This is in agreement with studies looking at other vaccine candidates and post-challenge immune sera[24–26]. Whether vaccine efficacy will be affected by emerging mutations within neutralising epitopes in the receptor-binding domain remain to be determined.

ELISpot analysis of IFNγ-producing cells pre- and post challenge demonstrated that only the intramuscular prime-boost animals demonstrated a post-challenge increase compared to both prime-only groups, with no groups presenting significant change post challenge compared to pre-challenge levels.

Overall, ChAdOx1 nCoV-19 induced effective immune responses capable of reducing viral load in nasal-wash and oral swab samples. No unexpected reactions were observed following vaccination by either route. The results of this study complement and support parallel preclinical investigations in non-human primates and have supported regulatory applications for human clinical trials where preclinical evaluation in two animal models is expected[5,12]. The demonstration of a greater reduction in viral shedding following intranasal administration of ChAdOx1 nCoV-19 warrants further clinical investigation.

MATERIALS AND METHODS

Cells and viruses

The SARS-CoV-2 isolates hCoV-19/Australia/VIC01/2020 (VIC01), hCoV-19/Australia/SA01/2020 (SA01) and hCoV-19/Australia/VIC31/2020 (VIC31) were obtained as Passage 1 material from the Victorian Infectious Diseases Reference Laboratory (VIDRL; Melbourne, VIC, Australia)[27]. The SA01 isolate was made available courtesy of SA Pathology (Adelaide, SA, Australia). Virus propagation was performed in Vero E6 cells from BEI Resources (Manassas, VA, USA) for VIC01 and the European Collection of Animal Cell Cultures (ECACC; Porton Down, UK) for SA01 and VIC31, with cells grown in DMEM supplemented with 2% foetal bovine serum (FBS), 10 mM HEPES, 100 U/mL penicillin, 100 µg/mL streptomycin, and 250 ng/mL amphotericin B (all from Thermo Fisher Scientific; Scoresby, VIC, Australia). The virus stocks were characterised and demonstrated to have >99.9% sequence identity to the Wuhan-Hu-1 reference sequence (GenBank NC_045512.2), with no significant contaminants detected.

Approval for animal studies

This study was reviewed and approved by the Animal Ethics Committee (AEC) at the CSIRO Australian Centre for Disease Preparedness (AEC 2004), in compliance with Australian national and state legislation pertaining to the use of animals in research. Challenge of animals with SARS-CoV-2 was performed under physical containment (PC)-4 conditions.

Study design

This was a randomised, placebo-controlled study assessing ChAdOx1 nCoV-19 as a vaccine candidate against SARS-CoV-2 compared to a control (PBS). ChAdOx1 nCoV-19 was assessed by two different routes of administration, intranasal (i.n.) and intramuscular (i.m.). The study was carried out as a block design with two sex-matched cohorts of 20 outbred ferrets of ~4 months of age (total of 40 animals, 20 male and 20 female) that had previously received prime and boost doses of the canine C3 vaccine (Protech C3; Boehringer Ingelheim, Ingelheim am Rhein, Germany) as part of prescribed prophylaxis against canine distemper virus infection.

Prior to administration of ChAdOx1 nCoV-19, ferrets were implanted with a LifeChip Bio-Thermo transponder (Destron Fearing; Eagan, MN, USA). Subcutaneous temperature, rectal temperature and body weight was recorded for each animal, and pre-challenge serum samples were obtained.

On vaccination days, ChAdOx1 nCoV-19 stocks were diluted with sterile PBS to a concentration of 2.5×10^{10} virus particles per 100 µL. Sterile PBS was used as a placebo for unvaccinated control animals. The prepared material was then administered as either an intramuscular injection into the rear thigh muscle or dropwise to alternating nares, 100 µL per animal. Ferrets were monitored daily for 3 days post-administration for any reaction to ChAdOx1 nCoV-19. Following ChAdOx1 nCoV-19 administration, the ferrets were anaesthetised on a weekly basis to allow for the collection of serum samples to assess antibody responses (study days 0, 7, 14 and 24 for prime-only animals; study days 0, 7, 14, 21, 28, 35, 42 and 52 for prime-boost animals).

At challenge (study day 28 for prime-only animals; study day 56 for prime-boost animals), all animals were intranasally-exposed to a target dose of 3×10^4 50% Tissue Culture Infectious Dose ($TCID_{50}$) of SARS-CoV-2 VIC01. Following the challenge, the ferrets were assessed at least once-per-day (twice daily for days 2–12 post challenge) for the presence of clinical signs, such as reduced interaction, fever (microchip temperature) and respiratory disease. On days 3, 5, 7, 9 and 11 post challenge (study days 31, 33, 35, 37 and 39 for prime-only animals; study days 59, 61, 63, 65 and 67 for prime-boost animals), ferrets were anaesthetised for collection of nasal wash, oral and rectal swab samples, as well as for the measurement of rectal temperature and body weight.

On study day 42 (for prime-only animals) or study day 70 (for prime-boost animals), ferrets were bled and had shedding samples collected, representative of day 14 post challenge. Over the following 3 days for each group of animals, ferrets were euthanised, and samples of the lung, spleen, tongue, nasal turbinate, pharynx, trachea, heart, and retropharyngeal lymph nodes were collected at necropsy for analysis.

Determination of viral RNA load in samples

RNA was isolated from tissue, swab and nasal-wash samples using a MagMAX-96 Viral RNA Isolation Kit (Thermo Fisher Scientific) on a Kingfisher Flex instrument (Thermo Fisher Scientific). SARS-CoV-2 RNA load was determined by a quantitative real-time polymerase chain reaction (RT-qPCR), with each sample tested in duplicate using a modified assay targeting the viral E gene: forward primer 5′-AGTACGAACTTATGTACTC ATTCGTT-3′; probe and reverse primer from Cormann et al.[28]. Copy numbers for individual samples were calculated using cycle threshold (C_T) values as SARS-CoV-2 E gene copies per mL or per g, with an equation established from standard curve data using a synthetic DNA standard of known copy number.

Virus-neutralisation assay

All serum samples were heat-inactivated (56 °C ± 2 °C for 30–35 min), then tested as a single replicate using a virus microneutralisation assay (VNT). Twofold dilutions of each serum sample were prepared in DMEM and 100 $TCID_{50}$ SARS-CoV-2 VIC01 was added. After 1 h incubation at 37 °C/5% CO_2, the virus:serum mixtures were combined with Vero E6 cells (ECACC) and returned to the incubator. At 3 days post-infection, cytopathogenic effects were assessed. The virus-neutralisation titre was expressed as the reciprocal value of the highest dilution of the serum that showed 100% inhibition of virus replication.

For the comparison of neutralisation titres against D614- and G614-containing SARS-CoV-2 isolates, six serum samples each were selected at random from the intramuscular and intranasal prime-boost animals collected at study day 35 or 42. No animal provided more than one serum sample. Each serum/isolate combination was tested in triplicate in a VNT as described above. A mean neutralisation titre was calculated for each of the combinations based upon the triplicate values using log_2-transformed values.

ELISpot assay

Blood was collected in lithium heparin tubes at time points pre- and post challenge (study days 24 and 33 for prime-only animals; study days 52 and 61 for prime-boost animals). Red blood cells were lysed using an ammonium chloride-based red blood cell lysis buffer. The remaining cells were washed with PBS and counted using a Miltenyi Scepter 2.0 with a 60-µm tip (Miltenyi Biotech; Bergisch Gladbach, Germany). Ferret IFNγ ELISpot plates (Mabtech; Stockholm, Sweden) were prepared following the manufacturer's instructions. Briefly, plates were washed with sterile PBS five times and 200 µL DMEM containing 10% FBS was added to the required wells. The plates were incubated at 37 °C/5% CO_2 for 30 min, followed by removal of the medium and addition of 200 µL cell suspension (1.25×10^4 cells/well) to each of the required wells. The plate was then sealed and incubated at 37 °C for 24 h. At the end of the incubation, cells were removed and the plates were washed five times with 200 µL sterile PBS. Detection antibody and streptavidin-ALP were separately diluted 1:1000 in PBS with 0.05% FBS. In total, 100 µL detection antibody was added to each well and was incubated at room temperature for 2 h. The samples were washed five times with 200 µL sterile PBS, and 100 µL streptavidin-ALP was added per well. The plate was incubated at room temperature for 1 h. At the end of the incubation, the samples were again washed five times with 200 µL sterile PBS per well, and 100 µL substrate solution was added. The plate was incubated at room temperature until distinct spots emerged on the membrane. Once spots were clear, the plates were washed extensively with tap water to remove the substrate solution and halt the reaction. The plate was left to dry at room temperature for 30 min before being read using an AID vSPOT Spectrum ELISpot Reader (Autoimmun Diagnostika; Straßberg, Germany).

Histology

Samples for histological and immunohistochemical analysis were collected into 10% neutral-buffered formalin and processed by routine histological methods. Tissue sections of 4 µm were stained with haematoxylin and eosin for histological assessment. On consecutive sections, antigen retrieval for immunohistochemistry was performed using the Dako PT Link (Agilent Technologies; Glostrup, Denmark) and Dako EnVision FLEX Target retrieval solution, pH 9 (Agilent Technologies). For retrieval, tissues were heated at 97 °C for 20 min, followed by cooling to 65 °C. Endogenous peroxidases were quenched using a 3% H_2O_2 solution. The sections were then incubated for 60 min with a polyclonal rabbit antibody against SARS-CoV-2 nucleocapsid protein (Sino Biological; Beijing, China) at a 1:8000 dilution, then with EnVision FLEX horseradish peroxidase-labelled secondary antibody and 3-amino-9-ethylcabazole (AEC) chromogen (Agilent Technologies). Sections were rinsed between each step with Tris buffer, pH 7.6. Slides were counterstained with Lillie-Mayer haematoxylin.

Statistical analysis

To assess the effect of the D614G mutation and the two vaccine administration routes on the log_2 neutralisation titre, a two-way mixed-effects analysis of variance (ANOVA) was performed, with the three test replicates being treated as a random effect. For the post hoc analysis to detect significant factor-level differences, pairwise comparisons were performed using Tukey's adjustment. These analyses were performed in R 4.0, using the *nlme v3.1* package for the mixed-effects ANOVA modelling, and *multicomp v1.4* for post hoc comparisons.

Analysis of statistical significance in the ELISpot and viral shedding data was performed using Student's *T* test in GraphPad Prism v9.0.0.

Reporting summary

Further information on research design is available in the Nature Research Reporting Summary linked to this article.

DATA AVAILABILITY

The data that support the findings of this study are available from the corresponding author upon reasonable request.

Received: 12 January 2021; Accepted: 12 March 2021;
Published online: 10 May 2021

REFERENCES

1. Zhou, P. et al. A pneumonia outbreak associated with a new coronavirus of probable bat origin. *Nature* **579**, 270–273 (2020).
2. Gorbalenya, A. E. et al. The species severe acute respiratory syndrome-related coronavirus: classifying 2019-nCoV and naming it SARS-CoV-2. *Nat. Microbiol.* **5**, 536–544 (2020).
3. Zhu, N. et al. A novel coronavirus from patients with pneumonia in China, 2019. *N. Engl. J. Med.* **382**, 727–733 (2020).
4. CSSE. COVID-19 Dashboard by the Center for Systems Science and Engineering (CSSE) at Johns Hopkins University. https://coronavirus.jhu.edu/map.html (2020).
5. Ramasamy, M. N. et al. Safety and immunogenicity of ChAdOx1 nCoV-19 vaccine administered in a prime-boost regimen in young and old adults (COV002): a single-blind, randomised, controlled, phase 2/3 trial. *Lancet* https://doi.org/10.1016/S0140-6736(20)32466-1 (2020).
6. ABC. Oxford-AstraZeneca, local COVID vaccines given urgent approval in India. https://www.abc.net.au/news/2021-01-03/oxford-astrazeneca,-local-covid-vaccines-given-urgent-approval/13028808 (2021).
7. Dicks, M. D. J. et al. A novel chimpanzee adenovirus vector with low human seroprevalence: improved systems for vector derivation and comparative immunogenicity. *PLoS ONE* **7**, e40385 (2012).
8. van Doremalen, N. et al. A single dose of ChAdOx1 MERS provides protective immunity in rhesus macaques. *Sci. Adv.* **6**, eaba8399–eaba8399 (2020).

9. Alharbi, N. K. et al. Humoral immunogenicity and efficacy of a single dose of ChAdOx1 MERS vaccine candidate in dromedary camels. *Sci. Rep.* **9**, 16292 (2019).
10. Folegatti, P. M. et al. Safety and immunogenicity of a candidate Middle East respiratory syndrome coronavirus viral-vectored vaccine: a dose-escalation, open-label, non-randomised, uncontrolled, phase 1 trial. *Lancet Infect. Dis.* **20**, 816–826 (2020).
11. Folegatti, P. M. et al. Safety and immunogenicity of the ChAdOx1 nCoV-19 vaccine against SARS-CoV-2: a preliminary report of a phase 1/2, single-blind, randomised controlled trial. *Lancet* **396**, 467–478 (2020).
12. van Doremalen, N. et al. ChAdOx1 nCoV-19 vaccine prevents SARS-CoV-2 pneumonia in rhesus macaques. *Nature* **586**, 578–582 (2020).
13. Shi, J. et al. Susceptibility of ferrets, cats, dogs, and other domesticated animals to SARS–coronavirus 2. *Science* **368**, 1016 (2020).
14. Kim, Y.-I. et al. Infection and rapid transmission of SARS-CoV-2 in ferrets. *Cell Host Microbe* **27**, 704–709.e702 (2020).
15. Richard, M. et al. SARS-CoV-2 is transmitted via contact and via the air between ferrets. *Nat. Commun.* **11**, 3496 (2020).
16. Schlottau, K. et al. SARS-CoV-2 in fruit bats, ferrets, pigs, and chickens: an experimental transmission study. *Lancet Microbe* **1**, e218–e225 (2020).
17. Park, S.-J. et al. Antiviral efficacies of FDA-approved drugs against SARS-CoV-2 infection in ferrets. *mBio* **11**, e01114–01120 (2020).
18. Ryan, K. A. et al. Dose-dependent response to infection with SARS-CoV-2 in the ferret model: evidence of protection to re-challenge. *Nat. Commun.* **12**, 81 (2021).
19. Wu, S. et al. A single dose of an adenovirus-vectored vaccine provides protection against SARS-CoV-2 challenge. *Nat. Commun.* **11**, 4081 (2020).
20. Layton, D. et al. Type I hypersensitivity in ferrets following exposure to SARS-CoV-2 inoculum: lessons learned. *ILAR J.* https://doi.org/10.1093/ilar/ilab019 (accepted 16 Apr 2021) (2021). in press.
21. WHO. Draft landscape of COVID-19 candidate vaccines—02 February 2021. https://www.who.int/publications/m/item/draft-landscape-of-covid-19-candidate-vaccines (2021).
22. O'Hare, R. Landmark coronavirus study to trial inhaled imperial and Oxford vaccines. https://www.imperial.ac.uk/news/203653/landmark-coronavirus-study-trial-inhaled-imperial/ (2020).
23. Dhakal, S. et al. Mucosal immunity and protective efficacy of intranasal inactivated influenza vaccine is improved by chitosan nanoparticle delivery in pigs. *Front. Immunol.* **9**, https://doi.org/10.3389/fimmu.2018.00934 (2018).
24. McAuley, A. J. et al. Experimental and in silico evidence suggests vaccines are unlikely to be affected by D614G mutation in SARS-CoV-2 spike protein. *npj Vaccines* **5**, 96 (2020).
25. Plante, J. A. et al. Spike mutation D614G alters SARS-CoV-2 fitness. *Nature* https://doi.org/10.1038/s41586-020-2895-3 (2020).
26. Klumpp-Thomas, C. et al. D614G spike variant does not alter IgG, IgM, or IgA spike seroassay performance. *J. Infect. Dis.* https://doi.org/10.1093/infdis/jiaa743 (2020).
27. Caly, L. et al. Isolation and rapid sharing of the 2019 novel coronavirus (SARS-CoV-2) from the first patient diagnosed with COVID-19 in Australia. *Med J. Aust.* **212**, 459–462 (2020).
28. Corman, V. M. et al. Detection of 2019 novel coronavirus (2019-nCoV) by real-time RT-PCR. *Eurosurveillance* **25**, 2000045 (2020).

ACKNOWLEDGEMENTS

The authors would like to thank all our colleagues at the Australian Centre for Disease Preparedness who have supported these studies during challenging times, particularly Emma Allnutt, Christopher Morrissy, Debbie Eagles, Julia Marsh, Prasad Paradkar, Patricia Vietheer and Wilna Vosloo. We would also like to thank the staff at VIDRL, particularly Julian Druce and Mike Catton, for their efforts in virus diagnosis and isolation and SA Pathology, particularly Lex Leong, for providing SA01. We would like to thank StellaMay Gwini from Monash University and Barwon Health for statistical analysis support. This work was conducted with funding to the CSIRO from the Coalition for Epidemic Preparedness Innovations (CEPI) and the Australian Department of Finance, and we are especially grateful to Amy Shurtleff for her support and comments.

AUTHOR CONTRIBUTIONS

G.A.M. and A.J.M. contributed equally to this work. G.A.M., A.J.M., G.G.A. and S.S.V. designed the study. G.A.M., A.J.M., G.G.A., S.R., D.L., N.B.S., S.B., R.L., J.P., P.A.D., H.B., J.A.B., J.B., V.B., M.P.B., K.B., T.E., S.E., T.G., K.H., J.H., C.H., W.S.J.H., P.J.v.V., S.L., K.M., K.D.M., M.J.N., T.P., C.R., B.R., E.S., V.S., C.R.S., W.S., M.T., S.T., L.T., D.W. and N.W. performed the experiments and analysed the data. G.A.M., A.J.M., H.B. and P.A.D. prepared the paper. N.S.B., J.B., S.L., W.W.S., T.W.D., T.L., S.C.G. and S.S.V. provided feedback and corrections. All authors reviewed the paper. S.S.V. conceived the project and obtained funding.

COMPETING INTERESTS

Oxford University has entered into a partnership with AstraZeneca for further development of ChAdOx1 nCoV-19. S.C.G. is a co-founder of Vaccitech (collaborators in the early development of this vaccine candidate) and named as an inventor on a patent covering the use of ChAdOx1-vectored vaccines and a patent application covering this SARS-CoV-2 vaccine (PCT/GB2012/000467). T.L. is named as an inventor on a patent application covering this SARS-CoV-2 vaccine and was a consultant to Vaccitech for an unrelated project, during the conduct of the study. The remaining authors declare no competing interests.

ADDITIONAL INFORMATION

Supplementary information The online version contains supplementary material available at https://doi.org/10.1038/s41541-021-00315-6.

Correspondence and requests for materials should be addressed to S.S.V.

Reprints and permission information is available at http://www.nature.com/reprints

Publisher's note Springer Nature remains neutral with regard to jurisdictional claims in published maps and institutional affiliations.